PHOSPHATE UPTAKE IN *RHIZOBIUM MELILOTI*

By

SYLVIE D. BARDIN, M.Sc.

A Thesis

Submitted to the School of Graduate Studies

in Partial Fulfilment of the Requirements

for the Degree

Doctor of Philosophy

McMaster University

PHOSPHATE UPTAKE IN *RHIZOBIUM MELILOTI*

DOCTOR OF PHILOSOPHY (1997) McMaster University
(Biology) Hamilton, Ontario

TITLE: Phosphate uptake in *Rhizobium meliloti*

AUTHOR: Sylvie D. Bardin, M.Sc. (Geneva University, Switzerland)

SUPERVISOR: Professor T.M. Finan

NUMBER OF PAGES: xv, 260.

ABSTRACT

The soil bacterium *Rhizobium meliloti* fixes dinitrogen when associated with root nodules formed on its plant host *Medicago sativa* (alfalfa). A previously identified locus in *R. meliloti* 1021, *ndvF*, is required for nodule invasion and N_2-fixation. Genetic analysis of the locus revealed the presence of four genes, *phoCDET* which encode an ABC-type phosphate transport system. The transporter had a high affinity for phosphate (Km: 0.2μM) and took up phosphate with low velocity (Vmax: 6.7nmol/min/mg protein). It also showed a low specificity for phosphate as it likely transports phosphonate compounds as well. Expression of transcriptional *lacZ* fusions to *phoD* and *phoE* revealed that these genes were induced upon phosphate limitation and required a functional PhoB protein for their expression. *phoCDET* mutants grew poorly in MOPS-buffered minimal media containing 2mM Pi as sole phosphorus source, and failed to transport phosphate at concentrations usually found in the soil (1-10μM). This suggested that the symbiotic phenotype associated with mutation in this locus was the result of poor growth in this environment.

Analysis of two classes of mutation that suppressed the Fix^- phenotype of *phoCDET* mutants confirmed the function of this Pi transporter and provided insides into its regulation. Sequence analysis of the ClassI (*sfx1*) suppressor

locus revealed the presence of two genes *orfA* and *pit* which likely form an operon. While *orfA* did not share any significant homology with proteins found in the Data Bank, *pit* showed homology to phosphate transport systems of various organisms, including the *pit* gene of *Escherichia coli*. The *sfx1* mutation appeared to be a thymidine deletion in a hepta-thymidine sequence located 80 nucleotides upstream of *orfA*. *orfA pit* expression increased in a *sfx1* background (compared to the wild type) leading us to hypothesize that suppression by *sfx1* occurred by increasing Pi uptake by the Pit (OrfA) phosphate transport system.

The class II suppression mutations (*sfx2* and *sfx3* alleles) were unable to express the alkaline phosphatase enzyme (AP) suggesting that the mutations probably affect the Pho regulatory genes of *R. meliloti*. Three AP^- Tn*5*-132 mutants linked in transduction to *sfx2* were isolated. Sequence analysis of the DNA flanking these insertions revealed that they were located within the *phoU* and *phoB* genes of *R. meliloti*. These *phoU* and *phoB* mutations were able to suppress all the phenotypes associated with *phoCDET* mutations in a manner similar to *sfx2*. PhoB was also shown to be required for the uptake and/or metabolism of phosphonate compounds and activation of *phoCDET* expression. On the other hand, the product of the *phoB* gene, either directly or indirectly, negatively regulated *pit* expression in a phosphate dependent manner (i.e. repression under low phosphate conditions and in the phosphate starved environment of *phoCDET* mutant strains). Suppression of the symbiotic defect of

phoCDET mutants by *phoUB* (*sfx2*) mutations appeared then to occur by derepressing the *pit* system of *R. meliloti*, allowing increased phosphate uptake via this transporter.

ACKNOWLEDGMENTS

I thank Dr. Finan for allowing me to do my Ph.D. in his laboratory.

I also thank the under-graduate and graduate students, the post-doc and the technicians that worked with me in the laboratory for their friendship and support. Many thanks to Pat Hayward, Marg Biggs and all the secretaries for their availability, help and kindness.

A Special thanks to Paul and my family for their love and emotional support.

TABLE OF CONTENTS

LIST OF FIGURES

LIST OF TABLES

LIST OF ABBREVIATIONS

AEP	aminoethylphosphonate
AMP	aminomethylphosphonate
Ap	ampicillin
AP	alkaline phosphatase
ARA	acetylene reduction activity
Cm	chloramphenicol
EP	ethylphosphonate
EPS	exopolysaccharide
G3P	glycerol-3-phosphate
Glc6P	glucose-6-phosphate
Gm	gentamicin
kb	kilobase pairs of DNA
Km	kanamycin
MP	methylphosphonate
min	minute(s)
Nm	neomycin
NPP	*p*-nitrophenyl phosphate
OD	optical density
ONPG	*o*-nitrophenyl-β-D-galactopyranoside
ORF	open reading frame
Ot	oxytetracycline
P	phosphorus
P0	no phosphate added
Pi	inorganic phosphate
PSer	phosphoserine
RT	room temperature
SE	standard error
Sm	streptomycin
Sp	spectinomycin
Tc	tetracycline
Rif	rifampicin
sec	second (s)
vol	volume
XGal	5-bromo-4-chloro-3-indolyl-β-D-galactoside
X-Phos	5-bromo-4-chloro-3-indolyl phosphate

CHAPTER I

Introduction

A- The *Rhizobium*-legume symbiosis

Although gaseous nitrogen (N_2) constitutes 80% of our atmosphere, its inert nature makes it unavailable to eukaryotic organisms. The reduction of nitrogen gas to ammonia, known as nitrogen fixation, is however widely distributed among eubacteria and archaebacteria. Depending on the organism, nitrogen fixation occurs either in free-living state or in association with an eukaryotic organism such as in the *Rhizobium*/legume symbiosis. This symbiotic interaction between microorganism and eukaryotic host is agronomically important as it enables the plant host to grow in a nitrogen limited environment, thus reducing the requirement for nitrogen fertilizer.

This section reviews the different steps leading to the establishment of an effective symbiosis between *Rhizobium* bacteria and legume plant, focusing on the contribution of the bacterial symbiont.

All steps of nodule (plant organ in which the symbiosis takes place) development involve the expression of nodule-specific plant genes called nodulins (van Kammen, 1984). The early nodulin genes encode products that are expressed before the onset of nitrogen fixation and are involved in infection and nodule development. The products of the late nodulin genes are involved in the interaction with the symbiont and the metabolic specialization of the nodules (Nap and Bisseling, 1990). Analysis of the plant genes involved in root-nodule development was recently reviewed by Franssen et al. (1995) and will not be described in this literature review.

I) *Rhizobium* classification

Nitrogen-fixing, legume root nodule bacteria are gram-negative soil bacteria classified in the alpha subdivision of Proteobacteria (Holt et al., 1994). They are currently classified into three genera: *Rhizobium* ("fast grower"), *Bradyrhizobium* ("slow growers") and *Azorhizobium* ("stem nodulating") which so far has one characterized species that forms nodules on the stems of *Sesbania* (Dreyfus et al., 1988). *Bradyrhizobium* has just one named species as well; isolates that nodulate soybean (*Glycine max*) are called *Bradyrhizobium japonicum* whereas those that do not are known as *Bradyrhizobium* sp. followed by the host genus.

The named species of *Rhizobium* are *R. leguminosarum*, *R. meliloti*, *R. loti* (Jarvis et al., 1982), *R. fredii* (Scholla and Elkan, 1984) and *R. galegae* (Lindström, 1989). *R. leguminosarum* has been divided into three groups to reflect the host specificity (or biovar) defined by the plasmid carried (Jordan, 1984). The groups are clover (bv. *trifolii*), bean (bv. *phaseoli*) and pea, vetche and lentil (bv. *viciae*). *R. meliloti* strains, separated into two distinct genetic groups, nodulate alfalfa (*Medicago sativa*) and related legumes (Eardly et al., 1990).

The use of molecular techniques such as 16S ribosomal DNA comparisons, gene sequences analysis, DNA hybridization etc., showed that *Rhizobium* and *Bradyrhizobium* are not closely related (Young, 1992); *Rhizobium* resembles the plant tumor-inducing *Agrobacterium* more than it does *Bradyrhizobium* and *Bradyrhizobium* is phylogenetically related to the phototropic *Rhodospeudomonas palustris*. *Azorhizobium* is closer to *Bradyrhizobium* than to *Rhizobium* and is closely related to *Xanthobacter*. These data are supported by biochemical and physiological characteristics such as: in *Rhizobium* and in the closely related *Agrobacterium*, the nature of the plant interaction is determined by plasmid-borne genes, while in *Bradyrhizobium* and *Azorhizobium* there is no evidence for plasmids carrying symbiotic genes. Both *Bradyrhizobium* and *Azorhizobium* are able to fix nitrogen asymbiotically (Dreyfus et al., 1988).

II) Infection and nodulation

1- The Nod factors

The Rhizobium signal molecules which play a key role in the induction of the initial stages of nodulation are lipochito-oligosaccharides known as Nod factors. The *nod* genes involved in the synthesis of Nod factors are not expressed in free-living state bacteria with the exception of *nodD*, which is expressed constitutively. Upon binding to specific flavonoids secreted by the root of the plant host (Goethals et al., 1992), NodD activates transcription of the other *nod* genes (Fisher and Long, 1992). The structure of the major Nod factor of *Rhizobium meliloti* was determined by Lerouge et al. (1990) as a 6-*O*-sulfated *N*-($C_{16:2}$) acyl-tri-*N*-acetyl-β-1,4-D-glucosamine tetrasaccharide. In general, Nod factors consist of a backbone of three to five β-1,4-linked N-acetylglucosamines bearing a fatty acid on the non-reducing sugar residue, the synthesis of which is catalyzed by the products of the *nodABC* locus. The backbone is further modified by the action of other Nod proteins that synthesize or add various substituents. These substituents determine host specificity as well as the biological activity of the molecules (for detailed information on Nod factor structures and biosynthesis see Dénarié and Cullimore, 1993; Carlson et al., 1995). *Rhizobium meliloti* interacts with only a limited number of plant hosts and thus produces only a few different Nod factors (Truchet et al., 1991). In contrast,

Rhizobium NGR234, which can nodulate various tropical legumes, secretes 18 different Nod factors (Price et al., 1992).

Purified Nod factors were shown to induce root hair deformation at concentrations as low as 10^{-12}M (Lerouge et al., 1990; Spaink et al., 1991; Price et al., 1992; Sanjuan et al., 1992; Schultze et al., 1992; Mergaert et al., 1993; Heidstra et al., 1994). Nod factors also induce the expression of certain plant genes encoding early nodulins (Horvath et al., 1993; Jourmet et al., 1994; Cook et al., 1995).

2- Infection

After attachment of rhizobia to the root hair tips (Smit et al., 1992), the tips curl tightly and bacteria become "entrapped" within the curls. A local hydrolysis of the plant cell wall takes place in the curled region (Van Spronsen et al., 1994), the plasma membrane invaginates and new plant cell wall material (probably containing some nodulins) is deposited. This forms a tubular structure, the infection thread, by which the bacteria enter the plant (see Kijne, 1992 for review).

Simultaneously with infection thread formation, some cortical cells are mitotically reactivated and form the nodule primordium (Kijne, 1992). Nod factors are sufficient to induce this mitotic reactivation (Spaink et al., 1991; Truchet et al., 1991) probably by changing the phytohormone (auxin/cytokinin) balance

(Long, 1996; Copper and Long, 1994; Hirsch et al., 1989) via the induction of yet unidentified early nodulin genes. Infection threads grow toward this primordium and once they reach the cortical cells, bacteria are released into the cytoplasm.

Lipopolysaccharides of *R. leguminosarum bv. trifolii* (Dazzo et al., 1991) and exopolysaccharide of *R. meliloti* (Dylan et al., 1986; Niehaus et al., 1993) appear to be required for the formation of the infection thread.

Beside infection through root hairs, which is the most widely studied and the one observed when *R. meliloti* infects its plant hosts, rhizobia can also enter through cracks in the epidermis (i.e. symbiosis between *A. caulinodans*/*Sesbania rostrata*; Dreyfus and Dommergues, 1981; Ndoye et al., 1994; *Bradyrhizobium* sp./*Parasponia andersonii*; Trinick, 1988) or at the junction of epidermal cells (route of entry of rhizobia in *Mimosa scabrella*; de Faria et al., 1988).

3- The nodule

The infection route as well as the structural and developmental characteristics of an efficient nodule are determined by the plant host (Rolfe and Gresshoff, 1988; Dénarié et al., 1992) with two types of legume nodules distinguished; indeterminate and determinate (Newcomb, 1981). Both types possess peripheral vascular bundles and a central tissue which contains infected and uninfected cells. Indeterminate nodules can be divided into specific zones which characterize a certain developmental stage from the distal meristematic

zone to the proximal senescence zone (Vasse et al., 1990). The meristem is followed by the prefixation zone, where infection takes place, the zone III, containing the differentiated, nitrogen-fixing bacteroids, and the senescence zone where bacteria are degraded by the plant. Thus in these cigar-shaped nodules, growth and functioning occur simultaneously and all stages of differentiation can be observed in a single longitudinal section. In determinate nodules, bacteria infect the meristematic cells. The nodule meristem ceases to divide at an early stage of development so that all the cells of the central tissue differentiate simultaneously to form a nitrogen fixing tissue (Newcomb, 1981). In this case, nodule growth and function are dissociated, the nodules are round shaped and only a single stage of bacterial differentiation can be observed at any given time.

4- Metabolite exchange between plant and microsymbiont

Upon release from the infection thread, the bacteria become internalized by a process resembling endocytosis. The microsymbiont is surrounded by a membrane derived from the host plasma membrane, referred to as the peribacteroid membrane (PBM). The PBM has phospholipid and protein compositions that are different from the plasma membrane (Perotto et al., 1995; Verma, 1992). It also contains several nodulins as well as rhizobial proteins (Verma and Hong, 1996; Fortin et al., 1985). Because the PBM constitutes the

interface between bacteroids and the plant host, it plays an important role in controlling the exchange of metabolites. These include ammonium, the product of nitrogen fixation (O'Gara and Shanmugan, 1976) which is exported from the bacteroid to the host cytoplasm, while the host supplies the bacteroid with dicarboxylic acids as carbon source (Ronson et al., 1981; Yarosh et al., 1989; Werner, 1992) which are derived from the sucrose synthesized in the plant leaves (Hawker, 1985). It was speculated that the heme prosthetic group of leghemoglobin was synthesized by the bacteria and exported to the plant host. Recent work however suggested that heme was synthesized by the plant (for review see O'Brian, 1996). The form in which nitrogen is transported depends upon the plant: legumes forming determinate nodules import ureides, whereas legumes forming indeterminate nodules import amides after the ammonium is assimilated in the cytoplasm of nodule cells via the glutamine synthetase/glutamate synthase pathway (Schubert, 1986).

5- Nitrogen fixation

Symbiotic nitrogen fixation in bacteroids is catalyzed by the nitrogenase enzyme following the reaction:

$$N_2 + 8H^+ + 8e^- + 16\text{Mg-ATP} \rightarrow 2NH_3 + H_2 + 16\text{Mg-ADP} + 16\text{Pi}$$

Nitrogenase consists of two components, the homodimeric Fe protein, encoded by *nifH*, and the tetrameric molybdenum-iron (MoFe) containing protein, encoded

by *nifD* and *nifK*. The MoFe cofactor is irreversibly denatured by oxygen, which makes nitrogenase highly sensitive to oxygen (Shaw and Brill, 1977). On the other hand, there is a high demand for oxygen in nodules as the large amount of energy required for the nitrogenase reaction is generated by oxidative processes. In legume nodules, the low oxygen tension in the central part of the nodule is achieved by a combination of a high metabolic activity and an oxygen barrier in the periphery of the nodule (i.e. the nodule parenchyma; Witty et al., 1986). In the infected cells the oxygen carrier leghemoglobin facilitates oxygen diffusion.

The *nif* genes encoding enzymes, involved in the nitrogen fixation process, are suddenly induced in the interzone II-III of the nodule. From extensive studies on *nif* gene regulation, it is found that these genes are induced under microaerobic conditions (Fischer, 1994; Soupène et al., 1995). Low oxygen is sensed by FixL in *R. meliloti* which activates the FixJ protein by phosphorylation upon microaerobiosis. Phosphorylated FixJ, in turn induces the transcription of *nifA* and *fixK* (Galinier et al., 1994; Reyrat et al., 1993). Both genes encode transcriptional activators of *nif* and *fix* genes, the products of the latter genes being involved in biochemical functions associated with nitrogen fixation (Cebolla and Palomares, 1994).

III) *Rhizobium meliloti*

Rhizobium meliloti strains form nitrogen-fixing nodules on species of only three genera: *Medicago*, *Melilotus* and *Trigonella*. *R. meliloti* possess two large extrachromosomal replicons, referred to as megaplasmids. The presence of the two megaplasmids of 1200 to 1700kb in size appear to be a general feature among *R. meliloti* strains (Banfalvi et al., 1985; Bromfield et al., 1987; Burkhardt and Burkhardt, 1984; Burkhardt et al., 1987; Hynes et al., 1986; Finan et al., 1986; Rosenberg et al., 1982). In R. meliloti SU47, the two megaplasmids have been designated pRmeSU47a and pRmeSU47b. Both plasmids contain genes required for efficient nitrogen fixation; megaplasmid pRmeSU47a carries the *nod* genes and some *nif* and *fix* genes involved in nodule induction and nitrogen fixation (David et al., 1987; Debelle et al., 1986; Banfalvi et al., 1981; Rosenberg et al., 1981) whereas the larger megaplasmid pRmeSU47b carries genes involved in exopolysaccharide and thiamine biosynthesis (Finan et al., 1986; Glazebrook and Walker, 1989; Zhan et al., 1989; Glucksmann et al., 1993), dicarboxylic acid transport (Finan et al., 1988; Watson et al., 1988) as well as genes required for lactose (Charles et al., 1990), dulcitol, melibiose, raffinose, β-hydroxybutyrate, acetoacetate, protocatechuate and quinate utilization (Charles and Finan, 1991). Defined deletions of megaplasmid pRmeSU47b allowed the isolation of a new symbiotic locus, initially designated *fix-114* (Charles and Finan,

1991). Analysis of this locus constitutes the subject of the work presented here and will be discussed in greater detail later in this literature review.

B- Phosphate uptake in microorganisms

I) In *Escherichia coli*

Escherichia coli possesses two major inorganic phosphate (Pi) transporters; the Phosphate Specific Transporter (Pst) and the Phosphate Inorganic Transporter (Pit). Pst, a high affinity low-velocity system (Km: 0.4μM and Vmax: 15.9 nmol of Pi per min per mg of protein) is induced under conditions of phosphate limitation (Willsky and Malamy, 1980a). In contrast, Pit is a low affinity, high-velocity system (Km: 38.2μM and Vmax: 55 nmol of Pi per min per mg protein) and is constitutively expressed. In addition, two organophosphate transport systems (GlpT and UhpT) as well as the phosphonate transport system (PhnCDE) are capable of taking up phosphate as a secondary substrate (Ambudkar et al., 1986a; Metcalf and Wanner, 1991).

1- The Pst system

The Pst system is part of the Pho regulon. Its expression is inhibited when the preferred P source, Pi, is in excess and is induced 100 fold (or more) when the environmental Pi has been exhausted (Wanner, 1996). This transport system is a periplasmic protein-dependent transporter belonging to the superfamily of ABC (ATP-binding cassette) transport systems which are also called traffic ATPases. These type of transporters are present in a wide variety of organisms

including mammals (Higgins, 1992). The Pst system is composed of two integral membrane channel proteins PstA and PstC, PstB, a membrane bound ATPase protein believed to be active as a dimer (Chan and Torriani, 1996) and PstS the periplasmic phosphate-binding protein. Genes of the Pst components are arranged in an operon along with a protein called PhoU; the *pstSCAB-phoU* operon (Surin et al., 1985). PhoU, a peripheral cytoplasmic protein, has no effect on Pi uptake but may be involved in the overall process of Pi assimilation via the Pst system. Steed and Wanner (1993) observed that the low growth phenotype associated with a Δ*phoU* mutation was alleviated in a Δ*pstB-phoU* or Δ*pstSCAB-phoU* mutation, suggesting that the accumulation of Pi taken up by the Pst transport system in the absence of PhoU led to growth inhibition. In addition, both PstSCAB and PhoU are required for repression of the Pho regulon under phosphate sufficient conditions. The "repression function" of the PstSCAB complex is independent of its transport function (Cox et al., 1988). The mechanism of phosphate transport via the Pst system has been studied using site directed PstA, PstC and PstS mutants. The proposed model is as follows: the PstS protein, highly specific for phosphate, sequesters the monovalent or divalent phosphate anions from the periplasmic space and transfers it to the first membrane protein-binding site upon interaction of PstS with PstA and PstC. The transfer of phosphate to the second membrane protein-binding site and its subsequent release into the cytoplasm occurs as a result of conformational

changes energized by ATP hydrolysis which is catalyzed by the PstB subunits (see Webb and Cox, 1994 for review).

2- The Pit system

Pit is a single-component proton motive force-driven transporter analogous to LacY (Kaback, 1990), also called chemiosmotic carrier. Van Veen et al. (1994b) demonstrated that the substrate for the Pit system reconstituted in proteoliposomes was not inorganic phosphate but rather a neutral metal phosphate ($MeHPO_4$) chelate, formed by Pi complexing with divalent metal ions (such as Mn^{2+}, Mg^{2+}, Ca^{2+}, Co^{2+}). A homologous transport mechanism was also characterized for the second Pi transport system of *Acinetobacter johnsonii* (Van Veen et al., 1993b). Besides uptake of metal phosphate, Pit also mediates efflux and homologous exchange of metal phosphate in the absence of a driving force (Van Veen et al., 1994b). The fact that Pit (1) utilizes $MeHPO_4$ as a substrate, (2) is not required for growth with Pi as sole phosphorus source and is not involved in the Pho regulon control, raises questions about the physiological role of the Pit system. Pit may actually be a divalent metal transporter for which Pi is an effective anion (Van Veen et al., 1994b).

Genetic analysis of the *pit* locus is just beginning. Cells with a functional Pit protein were shown to be arsenate sensitive, due to the fact that arsenate is a substrate for this transporter. Using this phenotype *pit* mutants were isolated as

arsenate resistant (Willsky and Malamy, 1980b). All known *pit* mutations are mapped within the same locus (77 min) of the *E. coli* chromosome. The Pit locus has been cloned (Elvin et al., 1986) and its sequence contains a single open reading frame that encodes a 499 amino acid polypeptide (Sofia et al., 1994).

3- The organophosphate uptake systems

Like Pit, GlpT and UhpT are chemiosmotic carriers. The GlpT transport system is very similar to the UhpT transporter both at the amino acid sequence level of the proteins and transport mechanism (Eiglmeier et al., 1987; Ambudkar et al., 1986a). GlpT is part of the *glp* regulon which is induced by the presence of glycerol-3-phosphate (G3P) and repressed by GlpR (Larson et al., 1987; Lin and Iuchi, 1991). *glpT* and *glpQ* (encoding a periplasmic phosphodiesterase (Lin, 1976)) constitute an operon which maps near min 49 on the chromosomal map of *Escherichia coli*. The induction of *uhpT* transcription, in response to extracellular hexose-phosphate such as glucose-6-phosphate (Glc6P) (Dietz, 1976), is regulated by the *uhpABC* genes. These genes are located immediately upstream of *uhpT* at 82.1 min on the *E. coli* genetic map (Weston and Kadner, 1988). Both GlpT and UhpT accumulate G3P and sugar-phosphate, respectively, in exchange for internal phosphate. These systems are then capable of heterologous (G3P:Pi), (Glc6P:Pi) exchanges as well as homologous (Pi:Pi) exchanges, with Pi acting as competitive inhibitor for the uptake of the

organophosphates (Ambudkar et al., 1986a; Maloney et al., 1990). Whether the GlpT and UhpT system contribute to Pi uptake under conditions of Pi limitation has not been examined. Net Pi uptake by these anion exchangers may result from modification of the stoichiometric exchange between the organophosphate compound and Pi in response to intra or extracellular environment. This was observed for glucose 6-phosphate uptake in an analogous transporter of *Streptococcus lactis* (Ambudkar et al., 1986b).

G3P can also be taken up by the Ugp system (uptake of glycerol phosphate) in response to phosphate limitation (Argast and Boos, 1980). The Ugp system is a periplasmic binding protein-dependent transporter specific for G3P and glycerol phosphoryl phosphodiesters, (deacylation products of phospholipids; Argast, 1978). G3P transported by the Ugp system can only be used as phosphorus source in contrast to the G3P transported by GlpT system which can be used as both carbon and phosphorus source. G3P taken up by the Ugp system is not utilized by a specific pathway, it simply enters the common G3P pool with a rapid incorporation into phospholipids as well as proteins (Schweizer et al., 1982). The inability of G3P to serve as carbon source when transported by the Ugp system appears to be the result of uptake inhibition of this transporter by internal Pi accumulation as a result of G3P metabolism (Xavier et al., 1995).

4- The phosphonate transport system

Phosphonates (Pn) are organophosphorus compounds with a direct carbon-phosphorus bond. They can be found in various organisms (see Jiang et al., 1995 for review) as constituents of glycolipids, glycoproteins, polysaccharides or phosphonolipids. Industry also introduces synthetic phosphonates to the environment such as the herbicide glyphosate. Bacteria have evolved two pathways for uptake and degradation of phosphonates in order to use these compounds as sole phosphorus sources. These pathways utilize different mechanisms of C-P bond fission. The phosphonatase pathway is specific for phosphonates in which one hydrogen on the second carbon of the molecule has been substituted (such as 2-amino-ethylphosphonate) while the C-P lyase pathway has a broad substrate specificity. A given organism may have one or both pathways: *E. coli* for example has only the C-P lyase pathway (Wanner and Boline, 1990), *Salmonella typhimurium* carries genes for the phosphonatase pathway only (Jiang et al., 1995) while *Enterobacter aerogenes* carries genes for both pathways (Lee et al., 1992).

The genes encoding the C-P lyase pathway proteins of *E. coli* are organized in a single operon made of 14 genes (*phnC* to *phnP*) (Metcalf and Wanner, 1993). The *phnCDE* genes probably encode a binding protein-dependent (ABC type) Pn transporter with PhnD as the periplasmic binding protein, PhnE an integral membrane protein and PhnC the ATPase component

of the transport system. *phnF* and *phnO* appear to encode regulatory proteins while genes *phnG* to *phnN* probably encode proteins required for cleavage of the C-P bond (see Wanner, 1996 for review). Results from growth studies with various mutants suggested that Pi as well as phosphoserine are taken up by the PhnCDE transporter as non-specific substrates (Metcalf and Wanner, 1991). Recently, a global analysis of proteins synthesized from cells grown in the presence of phosphonates as sole phosphorus source revealed the induction of 227 proteins and the repression of 30 (out of 816 proteins monitored). 137 of these 227 proteins were also regulated by Pi limitation (118 induced, 19 repressed; VanBogelen et al., 1996).

5- The Pho regulon

Genes induced under Pi limitation and transcriptionally activated by the PhoB protein constitute the phosphate (Pho) regulon. In *Escherichia coli* more than 30 genes belonging to this regulon have been cloned and sequenced. They are arranged as eight separate transcriptional units and are involved in the uptake and assimilation of phosphorus compounds from the environment. In addition to the *pst-phoU*, *ugp*, and *phn* operons described above, the Pho regulon includes the following genes: The Pho regulatory genes, *phoBR* (Makino et al., 1986a and b); *phoA* which encodes a periplasmic alkaline phosphatase enzyme (AP) involved in the hydrolysis of organophosphates (Coleman, 1992);

phoE which encodes an outer membrane porin (Overbeeke et al., 1983); and *phoH* which encodes an ATP-binding protein whose function *in vivo* is yet to be characterized (Kim et al., 1993). A recent study, analyzing proteins synthesized during phosphorus limiting condition (using two-dimensional (2-D) polyacrylamide gel electrophoresis) suggested that 413 proteins out of the 816 studied were induced (208 proteins) or repressed (205 proteins) when the cells were grown under phosphate limitation (VanBogelen et al., 1996). This result is in fact not surprising if we consider phosphate as being a central component in many metabolic pathways. Analysis of these proteins will also probably lead to the discovery of new genes belonging to the Pho regulon.

a) Pi-dependent control of the Pho regulon

The primary control of the Pho regulon is the Pi concentration of the media. The work of Rao et al. (1993) suggested that it is the external phosphate concentration that regulates the Pho regulon and not the cytoplasmic Pi concentration. ^{31}P-NMR measurements revealed that the intracellular Pi concentration of 9 to 13mM, when extracellular Pi is in excess, remains high (about 7mM) during derepression of the Pho regulon (i.e. when the cells are grown under phosphate limitation; Rao et al., 1993).

Pi control of the Pho regulon involves two processes: Pho activation when Pi is limited and Pho inhibition when Pi is in excess.

Activation of the Pho regulon occurs via a two-component regulatory system (Parkinson, 1993) consisting of the transmembrane sensor histidine kinase, PhoR, and the transcriptional activator PhoB. When the external phosphate concentration falls below 4μM, PhoR undergoes autophosphorylation on a histidine residue using ATP as the phospho-donor. It then promotes PhoB phosphorylation on an aspartate residue (Makino et al., 1989) via its kinase activity. Phosphorylation of PhoB enhances its binding activity to the Pho Box, an 18 nucleotide sequence [5'-CT(T/G)TCATA(A/T)A(T/A)CT(T/G)TCA(C/T)-3'] consisting of two direct repeats of 5'-CT(T/G)TCAT-3' that flank a A+T-rich 4bp spacer. The Pho Box is located 10 nucleotides upstream from the putative -10 region in the promoter of the genes activated by PhoB (Wanner, 1996). No sequences homologous to the -35 region has been found in these promoters. Pho boxes are tandemly repeated twice and 3.5 times in the regulatory region of *pstS* and *ugpB*, respectively (Wanner, 1993). Mutational analysis of the *pstS* promoter region indicates that each Pho Box is functional (Kimura et al., 1989).

Inhibition of the Pho regulon requires, a high external phosphate concentration, the PhoU protein, an intact (although not necessary able to transport phosphate) Pst system, the phosphate specific transporter, and PhoR. PhoR is believed to dephosphorylate phospho-PhoB when the external Pi concentration increases above 4μM. As a small region of the PhoR protein is exposed to the periplasmic space (Scholten and Tommassen, 1993), sensing of

the external phosphate signal may be mediated by Pst and PhoU. Excess phosphate in the media may lead to the formation of a "repression complex" in which the PhoR phosphatase activity is induced. When the external Pi concentration decreases, the low Pi occupancy of PstS (or PhoR) may provoke conformational changes in the Pst complex and /or PhoU leading to the release of PhoR. PhoR then is activated by autophosphorylation which enhanced its kinase activity and thus phosphorylates PhoB (see model Fig. 1-1).

i) The PhoB protein

The PhoB protein is a cytoplasmic protein composed of 229 amino acids containing at least three domains: I- phosphorylation domain; II- DNA-binding domain (that recognizes the Pho Box); and III- domain that interacts with the RNA polymerase holoenzyme (Wanner, 1996). Truncated PhoB and point mutants were used to identify these domains (Makino et al., 1989; 1994 and 1996). Domain I is located in the N-terminal 127 amino acids with Asp-53 as the phospho-accepting residue and Thr-83 that appears to play an important role in the phosphate transfer reaction. The C-terminal 90 amino acids of PhoB constitutively activate transcription from the Pho genes suggesting that both domain II and III are located in this area of the protein. It is not known whether domain III is physically separable from domain II or overlaps it. Analysis of *rpoD* mutants (encoding the σ^{70} subunit of RNA polymerase), that are specifically

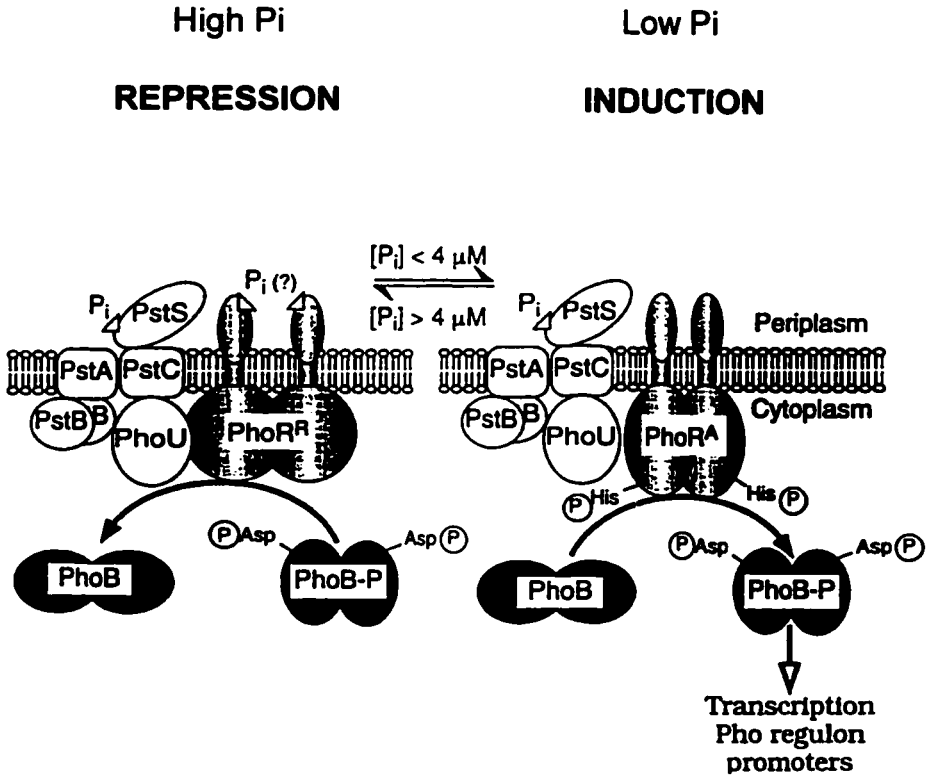

Transmembrane signal transduction by environmental P_i. Notation: PhoB, response regulator; PhoB-P, phospho-PhoB; $PhoR^A$, PhoR activation (autophosphorylated) form; $PhoR^R$, PhoR repression (inhibition) form; PhoU, *phoU* gene product; PstA and PstC, integral membrane channel proteins of Pst transporter; PstB, traffic ATPase of transporter; PstS, periplasmic P_i-binding protein; small triangles, P_i binding site on PstS and a hypothetical P_i regulatory site on PhoR.

Fig. 1-1: Phosphate regulation of the Pho regulon of *E. coli* as proposed by Wanner (1996).

defective in the expression of the pho genes, suggests that PhoB directly interacts with the first helix of the putative helix-turn-helix motif in the C-terminal region (region 4.2) of σ^{70} (Makino et al., 1993). σ^{70} likely contacts four amino acids of the PhoB protein located around the turn connecting α-helix 2 (amino acids 176 to 187) and 3 (amino acids 189 to 207), helices as deduced from their homology with the histone H5 structure (Makino et al., 1996). It was then proposed that the PhoB/σ^{70} interaction permits the RNA polymerase to enter the *pho* promoters for initiation of transcription. A recent study showed that a region around amino acids 87-97 of PhoB may be critical for interactions with histidine kinases (Haldimann et al., 1997).

ii) The PhoR protein

The PhoR protein is composed of 431 amino acids. Membrane topology studies, using *phoR-phoA* fusions and deletion mutants, suggested that PhoR is anchored to the cytoplasmic membrane by two transmembrane domains (N-terminus of the protein) (Scholten and Tommassen, 1993). PhoR exerts both positive and negative regulation of the Pho regulon. The positive regulation is due to its kinase activity, demonstrated *in vitro*, that leads to PhoB phosphorylation (Makino et al., 1989). The negative regulation is believed to occur by dephosphorylation of PhoB by PhoR; however the phosphatase activity of PhoR is yet to be demonstrated. Isolation of mutants constitutive for either

activation or repression of the Pho regulon suggests that the two activities are separable from one another. Since the two types of mutations were generally mapped in close proximity and intermixed locally, the functional elements should be intimately interacting with each other to allow reversible functional changes. The histidine His-213 is conserved among histidine kinases. Moreover, constitutive repression of the Pho regulon by point mutation (H213Y) strongly suggests His-213 to be the site of autophosphorylation in PhoR (Makino et al., 1992).

b) Pi-independent control of the Pho regulon

The Pho regulon is subject to multiple positive controls due to the fact that once Pi is taken up by the cells it can be incorporated into ATP via several central pathways. These pathways include: oxidative phosphorylation (via the ATP synthase enzyme), glycolysis (via the glyceraldehyde-3-phosphate dehydrogenase and the phosphoglycerate kinase enzymes), tricarboxylic acid cycle (via the succinyl coenzyme A synthetase) and mixed-acid fermentation (via the phosphotransacetylase/acetate kinase pathways).

At least two Pi-independent controls act on the Pho regulon in the absence of PhoR. CreC (formerly PhoM) a protein kinase, like PhoR, phosphorylates PhoB as well as CreB a transcriptional activator that regulates the expression of unknown genes (Amemura et al., 1990). The other Pi-

independent control requires acetyl phosphate which may directly phosphorylate the PhoB protein (Wanner, 1992).

Evidence for activation of the Pho regulon by the CreC protein was provided by the isolation of mutants in a *phoR*$^-$ background that completely abolished Pi control of the Pho regulon. Mutation in *creC* led to a 400-fold induction in alkaline phosphatase (AP) synthesis. This level was however lower than the level of AP synthesized in the presence of PhoR during phosphate limitation (1000-fold induction) (Wanner et al., 1988). This induction was abolished in a *phoR creC* double mutant suggesting that CreC was responsible for the induction.

The discovery of acetyl phosphate as an effector of the Pho regulon arose with the isolation of AP$^+$ revertants from a *phoR creC* double mutant. These pseudorevertants carried mutations in the *ackA* gene (for acetate kinase) that led to accumulation of acetyl phosphate. Because of severe growth defects, the triple mutants rapidly reverted to AP$^-$ through mutations in the *pta* gene (phosphotransacetylase) (Wanner and Wilmes-Riesenberg, 1992). Acetyl phosphate is an intermediate of the phosphotransacetylase-acetate kinase (Pta-AckA) pathway. Acetyl phosphate is made from acetyl-CoA and Pi by Pta and degraded into acetate and ATP by AckA. Mutations or growth conditions leading to increased levels of acetyl phosphate synthesis, either directly (i.e. growth on

pyruvate as carbon source) or indirectly, led to activation of the Pho regulon (Wanner and Wilmes-Riesenberg, 1992).

It is interesting that an intermediate in Pi metabolism (incorporation of Pi into ATP) seems to be involved in Pho regulon control probably via the [ATP] / [acetyl phosphate] ratio, with a lowered ratio causing induction. By extension, Pi-independent control by the CreC protein may be coupled to a different central pathway of carbon and energy metabolism (for entry of Pi into ATP). Such controls may provide a basal level of expression of the Pho regulon when the system is Pi repressed which could be especially important in wild-type strains undergoing shifts of carbon and energy sources.

II) Phosphate uptake in other micro-organisms

1- In *Pseudomonas aeruginosa*

In *Pseudomonas aeruginosa*, Pi limitation results in the synthesis of several proteins, including alkaline phosphatase (AP), an outer membrane protein P, as well as a hemolytic and nonhemolytic phospholipase C (Hancock et al., 1990; Shortridge et al., 1992). Pi transport in *P. aeruginosa* occurs with biphasic kinetics, suggesting the involvement of both a high affinity (*pst*-like) with an apparent Km of 0.46 ± 0.1μM and a low-affinity (*pit*-like) transporter with a Km of 12.0 ± 1.6μM (Poole and Hancock, 1984). The nucleotide sequence of the

phosphate-transport system was recently determined and revealed the presence of four open reading frames, *pstC*, *pstA*, *pstB* and *phoU* that probably constitute an operon (Nikata et al., 1996). The *pst* operon was Pho-regulated as indicated by the presence of a well conserved Pho Box preceding *pstC* and the 25 fold induction in level of expression in the presence of a functional PhoB protein. The deduced PstC and PstA proteins are both larger than their *E. coli* homologues with an additional hydrophilic domain in the N-terminal part of the protein. The most striking difference with the *pst* operon of *E. coli* is the absence of the *pstS* gene, which encodes the periplasmic Pi-binding protein. A Pi-binding protein required for Pi uptake via the high-affinity transport system has been purified (Poole and Hancock, 1984), suggesting the gene encoding this protein is not part of the *pst* operon in *P. aeruginosa*. Under phosphate limitation, *P. aeruginosa* shows a chemotactic response towards Pi (Kato et al., 1992) which may be important for scavenging Pi under these growth conditions. Both PstB and PhoU (but not PstC and PstA) are essential to repress Pi taxis and alkaline phosphatase under conditions of Pi excess (Nikata et al., 1996) but unlike AP expression, Pi taxis does not require the *phoB* and *phoR* gene products for regulation (Kato et al., 1994, Nikata et al., 1996).

2- In *Acinetobacter johnsonii*

Acinetobacter johnsonii 210A accumulates excessive amounts of phosphate as polyphosphate (polyP) under aerobic conditions. Pi is taken up by two phosphate transport systems similar to the high- (*pst*) and the low-affinity (*pit*) systems of *E. coli*. The high affinity transport system of *A. johnsonii* belongs to the group of ATP-driven binding protein-dependent transport systems. It is induced 6-10 fold by Pi limitation and has a Km value of 0.7 ± 0.2μM. The low-affinity uptake system is constitutively expressed, is inhibited by uncouplers and has a Km of 9 ± 1μM (Van Veen et al., 1993a). In *A. johnsonii*, Pi uptake is monophasic (over time) in contrast to the biphasic uptake of Pi in *E. coli* (Medveczky and Rosenberg, 1971), *P. aeruginosa* (Poole and Hancock, 1984) and *Bacillus cereus* (Rosemberg at al., 1969). Biphasic uptake is explained by the presence of two transport systems, with the high affinity transport system subject to inhibition when a primary pool of Pi within the cells is filled. This prevents accumulation of the solute to unacceptably high internal levels. Because Pi taken up by *A. johnsonii* is rapidly converted into polyphosphate, a low internal phosphate concentration can be maintained and Pi uptake remains linear until a maximum level is reached. Metal-phosphates ($MeHPO_4$; with Me being divalent cations such as Mg^{2+}, Ca^{2+}, Mn^{2+} and Co^{2+}) rather than Pi is transported by the secondary phosphate transport system, while the primary Pi transporter mediates the uptake $H_2PO_4^-$ and HPO_4^{2-} only (Van Veen et al.,

1994a). Stoichiometric studies suggest that the translocation of a (neutral) metal-phosphate together with one proton occurs via an electrogenic mechanism (Van Veen et al., 1993b). Anaerobic conditions lead to polyphosphate degradation in *A. johnsonii* followed by excretion of $MeHPO_4$ via the secondary transporter that was also shown to mediate $MeHPO_4$ efflux under these conditions. The two Pi transporters of *A. johnsonii* therefore evolved to allow the organism to efficiently use the predominant Pi species available. Genetic study of the Pi transport systems of *A. johnsonii* has yet to be reported.

3- In *Bacillus subtilis*

In the framework of the *Bacillus subtilis* genome sequencing project, genes homologous to the *pst* transporter of *E. coli* were characterized (Takemaru et al., 1996). The deduced amino acid sequence of the five ORFs of the *pst* locus of *B. subtilis* are similar to *pstS*, *pstC*, *pstA* and *pstB*. The fifth gene is also homologous to *pstB* so that two *pstB* genes (58% identity) are tandemly repeated while no *phoU* gene is present. These five genes likely form an operon. The presence of two Pho Boxes upstream of *pstS* suggests that these genes are under Pho regulation. The primary Pho regulon regulatory proteins, encoded by the *phoP* and *phoR* genes, constitute a two component regulatory system (response regulator and histidine kinase, respectively) similar to the PhoB and PhoR proteins of *E. coli* (Seki et al., 1987; 1988). The operon shows low level of

expression during vegetative growth and is induced during phosphate limitation. The Pho regulon of *B. subtilis* is also regulated by two other pairs of two-component regulatory systems. The *resD/E*, which affects respiratory-enzyme induction, is part of the Pho regulon and is also required for full induction of the *phoPR operon*. On the onset of sporulation, the response regulator encoded by *spoA* represses the Pho regulon via the AbrB protein probably by acting on the *phoPR* transcription (Hulett, 1995).

Phosphate transport systems have also been described in *Streptococcus lactis* (Poolman et al., 1987), *Streptococcus faecalis* (Harold et al., 1965; Harold and Banda, 1966; Harold and Spitz, 1975), *Micrococus lyzodeikticus* (Friedberg, 1977), *Bacillus cereus* (Rosenberg et al., 1969) and *Anabaena variabilis* (Thiel, 1988).

III) Phosphorus in *Rhizobium spp.*

Several studies have shown that *Rhizobium* and *Bradyrhizobium* species as well as their serotypes vary greatly in their tolerance to low levels of phosphate, their ability to store polyphosphates during growth under phosphate sufficient conditions and the utilization of these reserves for subsequent growth (Beck and Munns, 1984; Smart et al., 1984 (b); Cassman et al., 1981(a)). Delayed growth was observed when these cells were grown in a low phosphate

environment. Many rhizobial strains are, however, able to grow at nearly normal growth rates with phosphate concentrations commonly found in soils (0.1 to 10μM; Bieleski, 1973; Cassman et al., 1981b). It is interesting that many *R. meliloti* strains require a high calcium concentration in soil to grow at the low P levels found in soil solution (Beck and Munns, 1984; 1985).

Growth in a low phosphate soil environment suggests that Rhizobium strains evolved very efficient phosphate transport systems (Cassman et al., 1981b; Smart et al., 1984b). In this respect, Smart et al. (1984a) analyzed the effect of P nutrition on phosphate uptake in seven rhizobial and bradyrhizobial strains. They observed that phosphate-limited cells took up phosphate 10 to 180-fold faster than phosphate-sufficient cells. The apparent Km value for the phosphate uptake system was similar in all strains ranging from 1.6μM to 6.0μM phosphate with a Vmax from 17.2 to 126 nmol min^{-1} (mg dry weight of cells)$^{-1}$. Phosphate uptake in all strains was inhibited by carbonyl cyanide m-chlorophenyl hydrazone (CCCP) and these transporters failed to catalyze exchange or efflux of phosphate. The authors concluded that these strains carried a single, repressible, unidirectional and energy-dependent phosphate transport system. Alkaline phosphatase (AP) activity was strongly induced in *Rhizobium* strains in response to limiting phosphate and repressed under phosphate-sufficient conditions. No AP activity was detected in several *Bradyrhizobium* strains regardless of the P-status of the environment (Smart et

al., 1984a and b), suggesting that this may be a general phenomenon amongst bradyrhizobia.

Plants dependent on nitrogen fixation have a higher P requirement for optimum nitrogen accumulation than those utilizing combined nitrogen (Israel, 1987). The growing nodule is a major phosphate reservoir in the plant with P concentrations in the millimolar range (Mosse et al., 1976). This is probably due to the very high demand for ATP of the nitrogenase enzyme and the higher P content of the microbial tissue than plant cells. Even under phosphate limitation, the nodule remains the plant organ with the highest phosphate content. Using ^{31}P NMR spectroscopy, Rolin et al. (1989) showed that Pi and P metabolites were not uniformly distributed in the different cell types of soybean nodules. Phosphate deficiency often limits dinitrogen fixation of legume-*Rhizobium* interactions due to reduction in both nodule numbers and mass. However, the roles of P in nodulation and nodule activity remain unclear. Sa and Israel (1991) and Israel (1993) suggested that the decrease in N_2 fixation resulting from P deficiency was both a direct effect on nodule metabolism and an indirect effect due to growth reduction of the plant host.

P deficiency does not significantly alter the number of bacteroids per unit of nodule mass, but does decrease the bacteroid dry mass per unit of nodule dry mass (due to either decrease in cell size or density) and their nitrogen content (probably due to the inhibition of protein synthesis) (Sa and Israel, 1991). These

authors also observed that under P deficiency the adenylate energy charge (defined as ([ATP] + ½ [ADP]) / ([ATP] + [ADP] + [AMP])) and the ATP concentration were decreased in plant nodule cells but not in the bacteroids. In addition, the acetylene reduction activity (ARA) per nodule mass was not reduced (Ribet and Drevon, 1995a) and the ratio of total nitrogen fixed relative to nodule mass was not affected by P deficiency (Pongsakul and Jensen, 1991). This suggests that P deficiency limits total nitrogen fixation by inhibiting energy-dependent reaction(s) in the plant cells of the nodules rather than directly inhibiting nitrogenase activity.

Earlier papers (Bethenfalvay and Yoder, 1981; Robson et al., 1981; Jakobsen, 1985; Sa and Israel, 1991; Israel, 1993) mentioned a decrease in nitrogenase activity upon phosphorus limitation. This discrepancy with Ribet and Drevon's results was explained by the different procedure used for the acetylene reduction assay (open-flow assays on whole plants that was less disturbing to the system than detopped root systems), and the assumption made by the earlier authors that the acetylene-induced decline (AID) in ethylene production rate (Minchin et al., 1986) was the same under all growth conditions. Ribet and Drevon (1995b), however, recently demonstrated that AID increases with P deficiency thus leading to a reduced ARA for P deficient compared to P sufficient plants.

Upon alleviation of phosphorus deficiency, the rapid phosphate increase in the shoots and the nodules occurs nearly simultaneously (Israel, 1993). This is followed by an increase in nodule growth indicated by nodule mass and ARA, which coincides with increase in the nitrogen content of these two plant organs. So, enhanced acetylene reduction upon alleviation of phosphorus deficiency may be associated with both increased carbohydrate supply from the leaves (photosynthesis was reduced under phosphate deficient conditions (Clarkson et al., 1983)) and/or enhanced carbohydrate utilization within the nodules. Nitrogen concentration in the stems and roots increases after delay followed by an increase in plant dry weight.

Delayed nodulation is observed when Pi-starved cells and cells with lower tolerance to phosphate limiting conditions are used to inoculate their host plants (Mullen et al., 1988; Leung and Bottomley, 1987). This delay may primarily be the result of a reduction in bacterial density in the rhizosphere of the plant root. However growth per se may not be the determining factor for successful nodulation. McKay and Djordjevic (1993) observed that excretion (rather than production) of Nod factors in *R. leguminosarum* was decreased under low phosphate conditions and that the extent of this decrease was strain dependent. So growth efficiency and Nod factor excretion may not necessarily be related. Low external phosphate concentration was also responsible for reducing the attachment of *R. meliloti* to roots of annual medics (Howieson et al., 1993).

Several studies reported that phosphate limitation stimulates the biosynthesis and/or alters the structure of rhizobial cell surface carbohydrates such as exopolysaccharide II (Zhan et al., 1991) and cyclic β-(1,2)-glucans in *R. meliloti* (Breedveld et al., 1995) and lipopolysaccharide in *R. leguminosarum* (Tao et al., 1992). As these compounds are required for effective symbiosis, their modification, under phosphate limiting conditions, may have profound effects on the infection of the plant host.

C- Previous work on *ndvF* and *sfx*

I) The *ndvF* locus

Testing strains containing defined deletions of the pExo megaplasmid for their symbiotic phenotype on plants led to the identification of the symbiotic locus *ndvF* (formerly *fix114*; Charles and Finan, 1991; 1990; Fig. 1-2a). The two overlapping deletions of the megaplasmid carrying this locus, Δ5408 and ΔF114 which delete about 150kb, also remove a region known to carry the *exp* genes (involved in the biosynthesis of EPS-II) (Glazebrook and Walker, 1989) and a previously unidentified locus, *exoZ*, which is involved in the synthesis of the acidic exopolysaccharide succinoglycan (EPS-I) of *R. meliloti.* Neither the *exp* biosynthetic genes nor *exoZ* was associated with the symbiotic (Fix^-) phenotype of the deletions. Rm5408 and RmF114 as well as a 12kb deletion of *ndvF* and Tn*5* insertions in the locus, all induced small white nodules containing very few bacteria when inoculated on alfalfa plants, indicating that the infection is blocked at an early stage. This type of nodule is structurally similar to nodules formed by exopolysaccharides (*exo*) and β-(1,2)-glucans (*ndv*) mutants (Finan et al., 1986; Dylan et al., 1986), thus the designation *ndvF* for nodule development.

The *ndvF* locus was isolated after complementing the RmF114 Fix^- phenotype with a pLAFR1 cosmid clone bank carrying wild type *R. meliloti* DNA (Charles et al., 1991). Tn*5* mutagenesis of the complementing cosmid localized

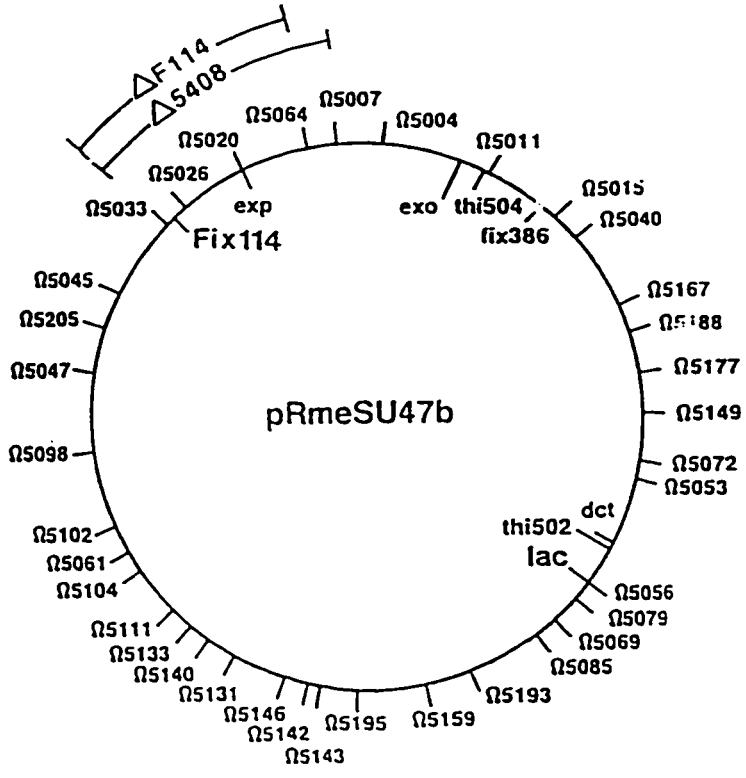

Fig. 1-2a: Figure adapted from Charles and Finan (1991) showing the genetic linkage map of pRmeSU47b of *R. meliloti* and the two overlapping deletions that delete the *ndvF* (Fix 114) locus.

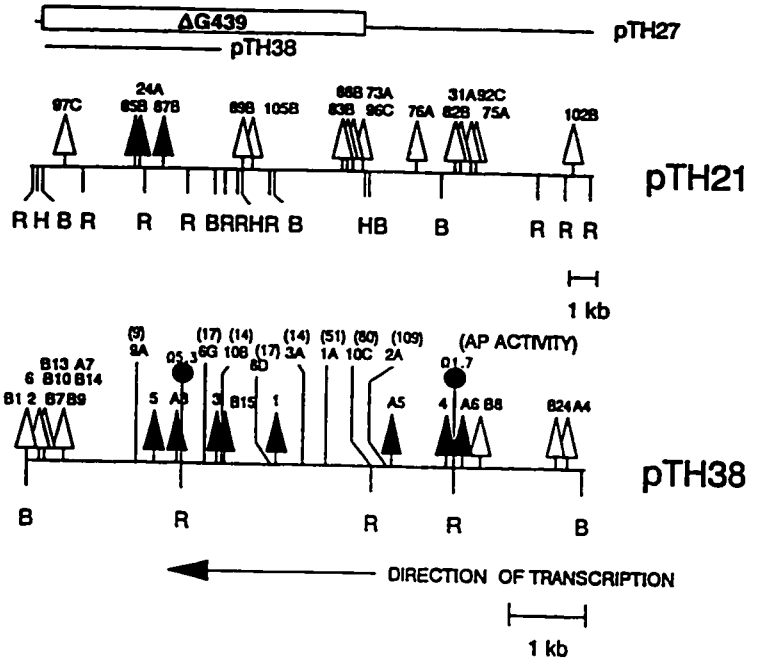

FIG. 2. Restriction map of pTH21 and pTH38 carrying *ndvF* and locations of transposon insertions. Restriction enzyme sites are designated B (*Bam*HI), H (*Hin*dIII), and R (*Eco*RI). Dark and light arrowheads indicate Tn*5* insertions that do and do not, respectively, abolish the ability of the complementing plasmid to restore RmF114 to Fix$^+$; dark circles indicate omega fragment insertions; vertical lines indicate representative *ndvF*::Tn*phoA* fusions. The alkaline phosphatase activities are for the LBmc-grown cells of the indicated pTH38-carried Tn*phoA* fusion in strain RmG173 (= PhoA$^-$ ΔF114). Also shown are the segments of pTH21 DNA that comprise pTH27 and pTH38, the extent of the deletion in strain RmG439, and the direction of transcription of *ndvF* as determined by the orientation of active Tn*phoA* fusions.

Fig. 1-2b: Restriction map of pTH21 and pTH38 carrying *ndvF* and locations of the transposon insertions; From Charles et al. (1991).

the *ndvF* locus to a 7.3kb *Bam*HI fragment. This fragment was subcloned into pRK7813 and the resulting plasmids pTH38 and pTH39 (two orientations of the insert) were able to restore a Fix^+ phenotype when transferred into *ndvF* deleted mutants. Southern blot hybridization revealed that fragments hybridizing to the 7.3kb *Bam*HI fragment were present in at least three other *R. meliloti* strains, suggesting that *ndvF* is conserved in *R. meliloti* (Charles et al., 1991). Subclones of pTH38 as well as the isolation of additional Tn*5* and Tn*phoA* insertions localized the *ndvF* locus to less than 5kb of this DNA. The isolation of active T*nphoA* fusions, which formed Fix^- nodules on alfalfa when recombined on the *R. meliloti* genome, suggests that the *ndvF* gene(s) encoded membrane anchored, periplasmic, or secreted protein(s). Each of these fusions were oriented in the same direction suggesting the direction of transcription of the *ndvF* gene(s) as indicated in Fig. 1-2b (Charles et al., 1991).

In addition to transposon insertions, Ω insertions and deletion mutants of the *ndvF* locus were created (Charles et al., 1991). Two Ω interposons were cloned in the first and the third *Eco*RI sites of pTH38 and recombined into a wild type strain to obtain the *ndvF* mutant strains RmG490 (Rm1021 *ndvF-1.7*::Ω) and RmG491 (Rm1021 *ndvF-5.3*::Ω). The RmG439 deletion mutant strain was made by replacing a 12kb *Hin*dIII fragment which encompasses the 7.3kb *Bam*HI fragment, with the 3.3kb neomycin-kanamycin (Nm-Km) resistance *Hin*dIII fragment of Tn*5* and recombining the Nm^r marker to the *R. meliloti* wild type

genome. Both insertion and deletion constructs were confirmed by Southern blot analysis and were Fix$^-$ when inoculated in alfalfa plants (Charles et al., 1991). Nodule formation was delayed for 2 to 3 days when RmG439 was inoculated on alfalfa plants. The average nodule number per plant inoculated with RmG439 relative to Rm1021 varied. Oresnik et al. (1994) reported that the *ndvF* mutants exhibit an additional phenotype. When plated on low osmolarity media (GYM), plates on which *R. meliloti* β-1,2-glucan mutants were not able to grow (Dylan et al., 1990), *ndvF* mutant strains form colonies with mucoid morphology in contrast to the non-mucoid (dry) phenotype of the wild type strain. This phenotype, specific to *ndvF*, requires the synthesis of exopolysaccharide II (Esp II) and can be reversed by increasing the osmolarity of the media with the addition of 100mM of various salts. It is interesting that the genes required for exopolysaccharide II synthesis are expressed under phosphate-limiting conditions (Zhan et al., 1991). Increased synthesis of EspII in the *ndvF* mutants is however not responsible for the symbiotic phenotype of these mutants.

II) The *sfx* loci

Occasionally some pink Fix$^+$ nodules developed on plants inoculated with the *ndvF* mutant strains (Oresnik et al., 1994). Rhizobia isolated from these nodules retained the original *ndvF* mutations but had acquired an extragenic

mutation that fully suppressed the symbiotic deficiency caused by the *ndvF* mutations. Bacteria from Fix$^+$ nodules were isolated from five independent nodulation experiments and designated RmF263 (*sfx1*), RmF346 (*sfx2*), RmG203 (*sfx4*), RmG204 (*sfx5*) and RmG425 (*sfx3*) (Oresnik et al., 1994). Upon re-inoculation on alfalfa seedlings, all formed Fix$^+$ nodules with plant shoot dry weights similar to that of plants inoculated with the *R. meliloti* wild type strain. The "suppressor" mutations, however, only partially restored nitrogen fixation of *ndvF* mutants when inoculated on sweet clover (*M. alba* cv. Polara) (Oresnik et al., 1994). Also all suppressor mutations suppressed the mucoid phenotype of *ndvF* mutants when plated on GYM media.

Tn5 (and *Tn5* derivatives) insertions which were linked to the suppressor alleles were isolated. These insertions led to the distinction of two different classes of suppressors. Class I, represented by *sfx1*, *sfx4* and *sfx5*, are flanked by insertions Ω5122::Tn*5*-132 and Ω5117::Tn*5* while class II, represented by *sfx2* and *sfx3*, are not. In addition, only strains RmF346 (*sfx2*) and RmG425 (*sfx3*) show sensitivity to the antibiotic bacitracin and the detergents deoxycholate, sodium dodecyl sulfate and sarkosyl. This detergent sensitivity phenotype is only observed in strains lacking a gene designated *exoZ*. The altered sensitivities of these two strains suggest that *sfx2* and *sfx3* lead to changes in the permeability of the cell envelope. T*n5* and Tn*5*-233 insertions linked to sfx2 were isolated employing the deoxycholate sensitivity phenotype to

screen for the presence of the *sfx2* mutation. Insertion Ω5258::Tn*5* is 70% linked in transduction to the deoxycholate sensitivity of both RmF346 and RmG425, suggesting that *sfx2* and *sfx3* map to the same locus (Oresnik et al., 1994).

The *sfx1* locus was isolated from pink Fix$^+$ alfalfa nodules inoculated with RmF114 in which clones from a pRK7813 cosmid library made with partial *Bam*HI digested DNA from RmF263 (*sfx1*, Δ5408) were mated. This allowed for the isolation of two cosmids (pTH56 and pTH57) that carry a common 18kb *Bam*HI fragment. Both pTH56 and pTH57 suppress the Fix$^-$ phenotype when mated back into RmF114 and Rm5408 and direct evidence that pTH56 maps to the *sfx1* region was obtained from Southern blot analysis showing that two Tn*5*-233 insertions linked to *sfx1* lay within the pTH56 insert.

D- This Work

The goal of this work was to genetically characterize the two types of suppressor mutations in order to identify the symbiotic function(s) associated with the *ndvF* locus. In the first part of this work, we established that *ndvF* contains four genes *phoCDET* which encode a high affinity phosphate transport system. This was deduced from:

- Sequence homology with the phosphonate transport system in *E. coli* (sequencing of *ndvF* was performed by Shan Dan, MSc. student in the laboratory).
- Inability of *phoCDET* to grow in minimal media containing 2mM Pi as sole phosphorus source.
- Inability of the deleted mutant strain to transport phosphate.

Definite evidence that the symbiotic deficiency of *phoCDET* mutants resulted from the failure of these strains to assimilate Pi came from the genetic characterization of the suppressor mutations.

The *sfx1* mutation is located upstream of an operon in which the deduced protein of one gene shared homology with the low-affinity phosphate transport system (Pit) of *Escherichia coli*. Subsequent analysis revealed that *sfx1* suppression occurs by increasing expression of this locus, which probably results in increased phosphate transport via this alternative transporter.

The *sfx2* mutation was mapped to the Pho regulatory genes, encoded by *phoUB*. Evidence presented suggests that while PhoB is a positive regulator of *phoCDET*, it represses the expression of the *pit*-like transporter under phosphate limitation. Suppression of the symbiotic phenotype of *phoCDET* mutants by *sfx2* and *phoUB* mutations appears to occur by derepression of *pit* expression and consequently increased Pi transport via this system.

CHAPTER II

Material and Methods

A- Material

I) Strains, plasmids and transposons

The strains, plasmids and transposons used in this study are listed in table 2-1.

II) Media

All media were sterilized by autoclaving the solutions at 120°C for at least 20 minutes (18 p.s.i.). Solid media were prepared by adding 15g/l Difco Bacto agar to the media prior to being autoclaved. Heat sensitive solutions were filter-sterilized through 0.45μm filters.

Table 2-1: Strains, plasmids and transposons; Relevant characteristics; Source, reference or construction.

Strains, plasmids and transposons	Relevant characteristics	Source, reference or construction
Rhizobium meliloti		
SU47	wild type (strain RCR2011)	Laboratory collection
Rm1021	SU47 *str-21*	Meade et al. (1982)
Rm5000	SU47 *rif-5*	Finan et al. (1988)
Transposon insertion banks		
Bank MM1	ca. 6000 Tn*5* insertions in Rm1021 background (=Rm5354)	Laboratory collection
Bank GS2	ca. 2000 Tn*5*-233 insertions in Rm5000 background	Laboratory collection
Bank OT1	ca. 14000 Tn*5*-132 insertions in Rm1021 background (=Rm5353)	Laboratory collection
Rm1021 derivatives		
Rm5439	*pck-1*::Tn*V*	Finan et al. (1988)
Rm5408	ΔΩ5033-5007::Tn*5*-233; Fix$^-$	Charles and Finan (1991)
RmF114	ΔΩ5033-5064::Tn*5*-233; Fix$^-$	Charles and Finan (1991)
RmF222	(=Rm8002) Pho$^-$	Long et al.(1988)
RmF263	ΔΩ5033-5007::Tn*5*-233, *sfx1*; Fix$^+$	Oresnik et al. (1994)
RmF288	*ntrA*Ω76::Tn*5*	O. Yaroch
RmF346	ΔΩ5033-5064::Tn*5*-233, *sfx2*; Fix$^+$	Oresnik et al. (1994)
RmG203	ΔΩ5033-5007::Tn*5*-233, *sfx4*; Fix$^+$	Oresnik et al. (1994)
RmG212	Lac$^-$	J. Glazebrook
RmG204	ΔΩ5033-5064::Tn*5*-233, *sfx5*; Fix$^+$	Oresnik et al. (1994)
RmG425	ΔΩ5033-5064::Tn*5*-233, *sfx3*; Fix$^+$	Oresnik et al. (1994)
RmG439	ΔG439 (Δ*ndvF* *Hin*dIII::Nm (12kb)) = *ndvF*ΔG439; Fix$^-$	Charles et al. (1991)
RmG490	*ndvF-1.7*Ω Sp^r.= *phoC*Ω490; Fix$^-$	Charles et al. (1991)
RmG491	*ndvF-5.3*Ω Sp^r = *phoT*Ω491; Fix$^-$	Charles et al. (1991)
RmG479	Ω5025::Tn*5*, *sfx2*	Oresnik et al. (1994)

RmG497	Ω5033::Tn*5*-233, *sfx2*	Oresnik et al. (1994)
RmG514	*ndvF*ΔG439, *sfx2*, Ω5025::Tn*5*; Fix$^+$	Oresnik et al. (1994)
RmG549	ΔΩ5033-5064::Tn*5*-233, Ω5256:: Tn*5*	I. Oresnik
RmG551	ΔΩ5033-5064::Tn*5*-233, Ω5258:: Tn*5*	I. Oresnik
RmG552	ΔΩ5033-5064::Tn*5*-233, Ω5259:: Tn*5*	I. Oresnik
RmG591	*sfx1*	Oresnik et al. (1994)
RmG639	Ω5262::Tn*5*-233, *sfx2*	I. Oresnik
RmG640	Ω5263::Tn*5*-233, *sfx2*	I. Oresnik
RmG641	Ω5264::Tn*5*-233, *sfx2*	I. Oresnik
RmG702	*sfx1-orfA*Ω10A::Tn*5*	pTH56Ω10A::Tn*5*→(pPH1JI)→G591, Nm^r
RmG762	*phoC*Ω490, *sfx1*; Fix$^+$	ΦRmG490 → RmG591, Sp^r
RmG763	*phoT*Ω491, *sfx1*; Fix$^+$	ΦRmG491 → RmG591, Sp^r
RmG764	*sfx1*Ω2-2::Tn*5*	pTH90Ω2-2::Tn*5*→(pPH1JI)→G591, Nm^r
RmG765	*sfx1-orfA*Ω2-3::Tn*5*	pTH90Ω2-3::Tn*5*→(pPH1JI)→G591, Nm^r
RmG766	*sfx1-pit*Ω2-5::Tn*5*	pTH90Ω2-5::Tn*5*→(pPH1JI)→G591, Nm^r
RmG771	*sfx1-pit*Ω3-3::Tn*5*	pTH90Ω3-3::Tn*5*→(pPH1JI)→G591, Nm^r
RmG774	*sfx1-pit*Ω3-10::Tn*5*	pTH90Ω3-10::Tn*5*→(pPH1JI)→G591, Nm^r
RmG777	*sfx1-pit*Ω3-16::Tn*5*	pTH90Ω3-16::Tn*5*→(pPH1JI)→G591, Nm^r
RmG781	*sfx1*ΩE::Tn*5*	pTH90ΩE::Tn*5*→(pPH1JI)→G591, Nm^r
RmG783	*sfx1-pit*ΩJ::Tn*5*	pTH90ΩJ::Tn*5*→(pPH1JI)→G591, Nm^r
RmG821	*phoC*Ω490, *sfx1*Ω2-2::Tn*5*; Fix$^+$	ΦRmG764 → RmG762, Nm^r
RmG822	*phoC*Ω490, *sfx1-orfA*Ω2-3::Tn*5*; Fix$^-$	ΦRmG765 → RmG762, Nm^r
RmG823	*phoC*Ω490, *sfx1-pit*Ω2-5::Tn*5*; Fix$^-$	ΦRmG766 → RmG762, Nm^r
RmG827	*phoC*Ω490, *sfx1-pit*Ω3-3::Tn*5*; Fix$^-$	ΦRmG771 → RmG762, Nm^r
RmG830	*phoC*Ω490, *sfx1-pit*Ω3-10::Tn*5*; Fix$^-$	ΦRmG774 → RmG762, Nm^r
RmG833	*phoC*Ω490, *sfx1-pit*Ω3-16::Tn*5*; Fix$^-$	ΦRmG777 → RmG762, Nm^r
RmG837	*phoC*Ω490, *sfx1-pit*ΩJ::Tn*5*; Fix$^-$	ΦRmG783 → RmG762, Nm^r
RmG838	*phoC*Ω490, *sfx1-orfA*Ω10A::Tn*5*; Fix$^-$	ΦRmG702 → RmG762, Nm^r
RmH138	*ndvF*ΔG439, *sfx1*; Fix$^+$	ΦRmG439 → RmG591, Nm^r
RmH318	Ω5258:: Tn*5*, Ω5033::Tn*5*-233, *sfx2*	ΦRmG551 → RmG497, Nm^r Gm^r-Sp^r
RmH363	*phoC*Ω490, *sfx2*; Fix$^+$	ΦRmG490 → RmG479, Sp^r Nm^s
RmH392	Lac$^-$, *phoE*Ω19::Tn*5*B20	pTH21Ω19::Tn*5*B20→(pPH1JI)→G212, Nm^r
RmH393	Lac$^-$, Ω17::Tn*5*B20	pTH21Ω17::Tn*5*B20→(pPH1JI)→G212, Nm^r
RmH394	Lac$^-$, *phoD*Ω7A::Tn*5*B20	pTH21Ω7A::Tn*5*B20→(pPH1JI)→G212, Nm^r

RmH395	Lac$^-$, *phoT*Ω4B::Tn*5*B20	pTH21Ω4B::Tn*5*B20→(pPH1JI)→G212, Nm^r
RmH396	Ω*pho12*::Tn*5*-132, white on XPhos	This work
RmH397	Ω*pho12*::Tn*V*	Tn*V* replacement of RmH396, Ot^s Nm^r
RmH399	Ω*phoU10*::Tn*V*	Tn*V* replacement of RmH429, Ot^s Nm^r
RmH405	Ω*pho27*::Tn*5*, 100% linked to RmH396	This work
RmH406	Ω*phoB3*::Tn*5*-132, white on X-Phos, 66% linked to Ω5258::Tn*5*	This work
RmH407	Ω*phoB8*::Tn*5*-132, white on X-Phos, 64% linked to Ω5258::Tn*5*	This work
RmH428	Ω*phoB8*::Tn*V*	Tn*V* replacement of RmH407, Ot^s Nm^r
RmH429	Ω*phoU10*::Tn*5*-132, white on X-Phos, 60% linked to Ω5258::Tn*5*	This work
RmH430	Ω*phoB3*::Tn*V*	Tn*V* replacement of RmH406, Ot^s Nm^r
RmH541	Lac$^-$, Ω*pho28*::Tn*5*B20, 100% linked to RmH396	isolated by 3V03 student
RmH610	Ω*pho27*::Tn*V*	ΦRmH609 → Rm1021, Nm^r
RmH615	Lac$^-$, Ω*phoB3*::Tn*V*	ΦRmH430 → RmG212, Nm^r
RmH616	Lac$^-$, Ω*phoB8*::Tn*V*	ΦRmH428 → RmG212, Nm^r
RmH617	Lac$^-$, Ω*phoU10*::Tn*V*	ΦRmH429 → RmG212, Nm^r
RmH623	Ω*phoU10*::Tn*V*, *phoC*Ω490; Fix$^+$	ΦRmH429 → RmG490, Sp^r Nm^r
RmH624	Ω*phoB8*::Tn*V*, *phoC*Ω490; Fix$^+$	ΦRmH428 → RmG490, Sp^r Nm^r
RmH625	Ω*phoB3*::Tn*V*, *phoC*Ω490; Fix$^+$	ΦRmH430 → RmG490, Sp^r Nm^r
RmH627	*sfx1*Ω12A::Tn*phoA*	pTH276Ω12A::Tn*phoA*→(pPH1JI)→G591, Nm^r
RmH635	Lac$^-$, *sfx1-orfA*Ω2-3::Tn	ΦRmG822 → RmG212, Nm^r
RmH636	Lac$^-$, *sfx1-pit*Ω3-10::Tn*5*	ΦRmG830 → RmG212, Nm^r
RmH659	Lac$^-$, *ndvF*ΔG439	ΦRmG439 → RmG212, Nm^r
RmH661	Lac$^-$, *phoT*Ω491	ΦRmG491 → RmG212, Sp^r
RmH662	Lac$^-$, wild type promoter *pit*Ω::*lacZmob*Sp, ort I	ΦRmH657 → RmG212, Sp^r Tc^2
RmH667	Lac$^-$, *phoC*Ω490	ΦRmG490 → RmG212, Sp^r
RmH668	Lac$^-$, wild type promoter *pit*Ω::*lacZmob*Sp, ort II	ΦRmH658 → RmG212, Sp^r Tc^2
RmH689	*ndvF*ΔG439, *sfx1* promoter *pit*Ω::*lacZmob*Sp, ort II	pTH352 recombined onto RmH138, Nm^r Sp^r Tc^2
RmH692	Lac$^-$, Ω5258:: Tn*5*,	ΦRmH138 → RmG212, Nm^r
RmH693	Lac$^-$, Ω5258:: Tn*5*, *sfx2*	ΦRmH138 → RmG212, Nm^r
RmH695	Lac$^-$, *sfx1* promoter *pit*Ω::*lacZmob*Sp, ort II	ΦRmH689 → RmG212, Sp^r Tc^2
RmH753	*ndvF*ΔG439, *sfx1* promoter *pit*Ω::*lacZmob*Sp, ort I	pTH351 recombined onto RmH138, Nm^r Sp^r Tc^2
RmH754	Lac$^-$, wild type promoter *pit*Ω::*lacZmob*Sp, ort I; Ω*phoU10*::Tn*V*	ΦRmH399 → RmH662, Nm^r Sp^r Tc^2
RmH755	Lac$^-$, wild type promoter *pit*Ω::*lacZmob*Sp, ort I; Ω*phoB8*::Tn*V*	ΦRmH428 → RmH662, Nm^r Sp^r Tc^2
RmH756	Lac$^-$, wild type promoter *pit*Ω::*lacZmob*Sp, ort I; Ω*phoB3*::Tn*V*	ΦRmH430 → RmH662, Nm^r Sp^r Tc^2

RmH757	Lac$^-$, wild type promoter *pit*Ω::*lacZmob*Sp, ort II; Ω*phoU10*::Tn*V*	ΦRmH399 → RmH668, Nm^r Sp^r Tc^2
RmH758	Lac$^-$, wild type promoter *pit*Ω::*lacZmob*Sp, ort II; Ω*phoB8*::Tn*V*	ΦRmH428 → RmH668, Nm^r Sp^r Tc^2
RmH759	Lac$^-$, wild type promoter *pit*Ω::*lacZmob*Sp, ort II; Ω*phoB3*::Tn*V*	ΦRmH430 → RmH668, Nm^r Sp^r Tc^2
RmH765	Lac$^-$, wild type promoter *pit*Ω::*lacZmob*Sp, ort I; Ω5258:: Tn*5*, *sfx2*	ΦRmH318 → RmH662, Nm^r Sp^r Tc^2
RmH766	Lac$^-$, wild type promoter *pit*Ω::*lacZmob*Sp, ort I; Ω5258:: Tn*5*	ΦRmH318 → RmH662, Nm^r Sp^r Tc^2
RmH767	Lac$^-$, wild type promoter *pit*Ω::*lacZmob*Sp, ort II; Ω5258:: Tn*5*, *sfx2*	ΦRmH318 → RmH668, Nm^r Sp^r Tc^2
RmH768	Lac$^-$, wild type promoter *pit*Ω::*lacZmob*Sp, ort II; Ω5258:: Tn*5*	ΦRmH318 → RmH668, Nm^r Sp^r Tc^2
RmH769	Lac$^-$, wild type promoter *pit*Ω::*lacZmob*Sp, ort I; *ndvF*ΔG439	ΦRmG439 → RmH662, Nm^r Sp^r Tc^2
RmH770	Lac$^-$, wild type promoter *pit*Ω::*lacZmob*Sp, ort II; *ndvF*ΔG439	ΦRmG439 → RmH668, Nm^r Sp^r Tc^2
RmH771	Lac$^-$, *sfx1* promoter *pit*Ω::*lacZmob*Sp, ort I	ΦRmH753 → RmG212, Sp^r Tc^2
RmH785	Lac$^-$, *sfx1* promoter *pit*Ω::*lacZmob*Sp, ort I; *ndvF*ΔG439	ΦRmG439 → RmH771, Nm^r Sp^r Tc^2
RmH791	Lac$^-$, *phoC*Ω490; Ω*phoU10*::Tn*V*	ΦRmH399 → RmH667, Nm^r Sp^r
RmH792	Lac$^-$, *phoC*Ω490; Ω*phoB8*::Tn*V*	ΦRmH428 → RmH667, Nm^r Sp^r
RmH793	Lac$^-$, *phoC*Ω490; Ω*phoB3*::Tn*V*	ΦRmH430 → RmH667, Nm^r Sp^r
RmH794	Lac$^-$, *phoC*Ω490; Ω5258:: Tn*5*, *sfx2*	ΦRmH318 → RmH667, Nm^r Sp^r
RmH795	Lac$^-$, *phoC*Ω490; Ω5258:: Tn*5*	ΦRmH318 → RmH667, Nm^r Sp^r
RmH796	Lac$^-$, *sfx1* promoter *pit*Ω::*lacZmob*Sp, ort II, Ω*phoU10*::Tn*V*	ΦRmH399 → RmH695, Nm^r Sp^r Tc^2
RmH797	Lac$^-$, *sfx1* promoter *pit*Ω::*lacZmob*Sp, ort II, Ω*phoB8*::Tn*V*	ΦRmH428 → RmH695, Nm^r Sp^r Tc^2
RmH798	Lac$^-$, *sfx1* promoter *pit*Ω::*lacZmob*Sp, ort II, Ω*phoB3*::Tn*V*	ΦRmH430 → RmH695, Nm^r Sp^r Tc^2
RmH807	Lac$^-$, *sfx1* promoter *pit*Ω::*lacZmob*Sp, ort II, *ndvF*ΔG439	ΦRmG439 → RmH695, Nm^r Sp^r Tc^2
RmH808	Lac$^-$, *ntrA*Ω76::Tn*5*	ΦRmF288 → Rm1021, Nm^r
RmH836	Ω*phoU10*::Tn*V*	ΦRmH399 → Rm1021, Nm^r
RmH837	Ω*phoB8*::Tn*V*	ΦRmH428 → Rm1021, Nm^r
RmH838	Ω*phoB3*::Tn*V*	ΦRmH430 → Rm1021, Nm^r
RmH842	*phoC*Ω490, *sfx1*Ω12A::Tn*phoA*; Fix$^+$	ΦRmH627 → RmG762, Nm^r Sp^r
RmH850	Ω*phoU10*::Tn*5*-233	ΦRmH847 → Rm1021, Gm^r Sp^r
RmH851	Ω*phoB8*::Tn*5*-233	ΦRmH848 → Rm1021, Gm^r Sp^r
RmH852	Ω*phoB3*::Tn*5*-233	ΦRmH849 → Rm1021, Gm^r Sp^r
RmH859	Lac$^-$, *sfx1* promoter *pit*Ω::*lacZmob*Sp, ort I; Ω5258::Tn*5*	ΦRmH318 → RmH771, Nm^r Sp^r Tc^2
RmH860	Lac$^-$, *sfx1* promoter *pit*Ω::*lacZmob*Sp, ort I; Ω5258:: Tn*5*, *sfx2*	ΦRmH318 → RmH771, Nm^r Sp^r Tc^2
RmH861	Lac$^-$, *sfx1* promoter *pit*Ω::*lacZmob*Sp, ort I; Ω*phoU10*::Tn*V*	ΦRmH399 → RmH771, Nm^r Sp^r Tc^2
RmH862	Lac$^-$, *sfx1* promoter *pit*Ω::*lacZmob*Sp, ort I; Ω*pho B8*::Tn*V*	ΦRmH428 → RmH771, Nm^r Sp^r Tc^2
RmH863	Lac$^-$, *sfx1* promoter *pit*Ω::*lacZmob*Sp, ort I; Ω*pho B3*::Tn*V*	ΦRmH430 → RmH771, Nm^r Sp^r Tc^2

Rm5000 derivatives

RmH590	Ω*phoU10*::Tn*V*	ΦRmG429 → Rm5000, Rif^r Nm^r
RmH591	Ω*phoB8*::Tn*V*	ΦRmG428 → Rm5000, Rif^r Nm^r
RmH592	Ω*phoB3*::Tn*V*	ΦRmG430 → Rm5000, Rif^r Nm^r
RmH593	Ω*pho27*::Tn*5*	ΦRmG405 → Rm5000, Rif^r Nm^r
RmH598	Ω*pho27*::Tn*5*-233	Tn*5*-233 replacement of RmH593, Rif^r Gm-Sp^r
RmH609	Ω*pho27*::Tn*V*	Tn*V* replacement of RmH598, Rif^r Nm^r
RmH657	wild type promoter *pit*Ω::*lacZmob*Sp, ortI	pTH351 recombined onto Rm5000, Rif^r Sp^r Tc^2
RmH658	wild type promoter *pit*Ω::*lacZmob*Sp, ortII	pTH352 recombined onto Rm5000, Rif^r Sp^r Tc^2
RmH847	Ω*phoU10*::Tn*5*-233	Tn*5* replacement of RmH590, Rif^r Gm^r Sp^r
RmH848	Ω*phoB8*::Tn*5*-233	Tn*5* replacement of RmH591, Rif^r Gm^r Sp^r
RmH847	Ω*phoB3*::Tn*5*-233	Tn*5* replacement of RmH592, Rif^r Gm^r Sp^r

Escherichia coli

MM294A	*pro82 thi1 hsdR17 supE44 endA1*	Laboratory collection
MT607	MM294A *recA56*	Finan et al. (1986)
MT609	*thy36 polA1* Sp^r	T.M Finan
MT614	MT607 Ω::Tn*5*, Nm-Km^r	Finan et al. (1986)
MT616	MT607 (pRK600)	Finan et al. (1986)
MT621	MM294A *malF*::Tn*phoA*, Nm-Km^r	Yarosh et al. (1989)
G312	MT607 Ω5::Tn5B20, Nm-Km^r	B. Driscoll
HB101	*supE44 hsdS20 recA13 ara-14 proA2 lacY1 galK2 rpsK20 xyl-5 mtl-1 r$^-$ m$^-$*	Laboratory collection
DH5α	*endA1 hsdR17 supE44 thi-1 recA1 gyrA96 relA1* Δ(*argF-lacZYA*) U169 ϕ80d*lacZ*ΔM15	B.R.L. Inc.
XL1-Blue	*supE44 hsdR17 endA1 gyrA46 relA1 thi recA* [F' *proAB lacI^q Z*ΔM15 Tn*10* (Tc^r)]	Bullock et al. (1987)

Plasmids

pUC18,19	Cloning vector, ColE1 *oriV*, Ap^r	Yanisch-Perron et al. (1985)
pUC118, 119	pUC18/19 containing intergenic (IG) region of M13	Vieira and Messing (1987)
pRK2013	ColE1 replicon with RK2 transfer region, Nm-Km^r	Figurski and Helinski (1979)
pRK600	pRK2013 *npt*::Tn*9*; Cm^r, Nm-Km^s	Finan et al. (1986)
pRK602	pRK600::Tn*5*, Cm^r, Nm-Km^r	Finan et al. (1985)
pRK607	pRK2013::Tn*5*-233; Nm-Km^r Gm^r Sp^r	De Vos et al. (1986)
pRK7813	RK2 derivative carrying pUC9 polylinker and *cos* site, Tc^r	Jones and Gutterson (1987)
pLAFRI	IncP cosmid cloning vector, Tc^r	Friedman et al. (1982)
pGS220	Tn*5* in deletion derivative of pBR322, Ap^r Nm-Km^r	De Vos et al. (1986)
pPH1JI	IncP, Gm^r Sp^r Cm^r	Beringer et al. (1978)
pMP220	IncP, promoterless *lacZ*, Tc^r	Spaink et al. (1987)
pTF1	pBR322::Tn*V*; Ap^r, Nm-Km^r	Furuichi et al. (1985)
pLMS	pUC 18 containing the *lacZ* mob Sp^r cassette	M. Hynes
pTH21	pLAFR1 clone carrying Rm1021 *ndvF*	Charles et al. (1991)
pTH22	pLAFR1 clone carrying Rm1021 *ndvF*	Charles et al. (1991)
pTH38	7.3kb *Bam*HI subclone of pTH22 in pRK7813, carries *ndvF*	Charles et al. (1991)
pTH56	pRK7813 clone carrying *sfx1*	Oresnik et al. (1994)
pTH57	pRK7813 clone carrying *sfx1*	Oresnik et al. (1994)
pTH61	12kb *Hin*dIII fragment of pTH56 in pUC19, carrying *sfx1*	I. Oresnik
pTH90	12kb *Hin*dIII fragment of pTH61 in pRK7813, carrying *sfx1*	T.C. Charles
pTH191	2.1kb *Eco*RI fragment of pTH90 in pUC118; ort I; *orfA pit* region	This work
pTH192	2.1kb *Eco*RI fragment of pTH90 in pUC118; ort II. *orfA pit* region	This work
pTH270	pRK600 Ω5A::Tn*5*B20; Nm-Km^r	B. Driscoll
pTH276	4.8kb *Hin*dIII/*Sac*I fragment of pTH90 in pRK7813, carrying *orfA pit*	This work
pTH282	pLAFR1 cosmid clone restoring AP of RmH399; # 3	B. Schoeman
pTH284	pLAFR1 cosmid clone restoring AP of RmH399; # 7	B. Schoeman
pTH286	pLAFR1 cosmid clone restoring AP of RmH399; # 11	B. Schoeman
pTH287	*Sal*I ligation of RmH430 (*phoB3*::Tn*V*)	B. Schoeman
pTH292	*Sal*I ligation of RmH399 (*phoU10*::Tn*V*)	B. Schoeman
pTH304	2.6kb *Hin*dIII/*Sma*I fragment of pTH90 in pRK7813, *orfA pit* region	This work
pTH305	2.7kb *Hin*dIII/*Eco*RV fragment of pTH90 in pRK7813, carrying *orfA pit*	This work
pTH306	0.5kb *Eco*RI fragment of pTH90 in pUC118, ortI I, end of *pit*	This work

pTH310	2.6kb partial (2.1kb + 0.5kb) *Eco*RI fragment of pTH90 in pUC118, carrying *orfA pit*	This work
pTH311	SalI ligation of RmH428 (*phoB8*::Tn*V*)	B. Schoeman
pTH343	pTH306 in which the *Sac*II-*Pst*I fragment as been substituted by a 30 mer oligo (for construction of the chromosomal *lacZ* fusion)	This work
pTH344	*Pst*I/*Eco*RI fragment of pTH343 subcloned in pBR322	This work
pTH347	2.6kb partial *Eco*RI fragment of pTH90 in pRK7813 (ort I), carrying *orfA pit*	This work
pTH348	2.6kb partial *Eco*RI fragment of pTH90 in pRK7813 (ort II), carrying *orfA pit*	This work
pTH351	pTH344 containing the *lacZmob*Sp cassette of pUC18LMS subcloned as a *Sma*I fragment (ort I)	This work
pTH352	pTH344 containing the *lacZmob*Sp cassette of pUC18LMS subcloned as a *Sma*I fragment (ort II)	This work
pTH354	4.8kb *Hin*dIII/*Sac*I fragment isolated from wild type genomic DNA and containing the wild type *orfA pit* allele.	This work
pTH365	2.1kb *Eco*RI fragment of pTH90 in pMP220 (ort I); *sfx*1 promoter *pit-lacZ* fusion	This work
pTH367	pTH365 Δ *Sph*I; *sfx*1 promoter *orfB-lacZ* fusion	This work
pTH376	2.1kb *Eco*RI fragment of pTH354 in pMP220 (ort I); wild type promoter *pit-lacZ* fusion	This work
pTH378	pTH376 Δ *Sph*I; wild type promoter *orfB-lacZ* fusion	This work
pTH380	4.8kb *Hin*dIII/*Sac*I fragment of pTH90 in pUC118; carrying *orfA pit*	This work
pTH391	2.6kb partial *Eco*RI fragment of pTH354 in pRK7813 (ort II) carrying wild type *orfA pit* locus	This work
pTH396	0.9kb *Hin*dIII-*Xho*I fragment of pTH191 in *Hin*dIII-*Sal*I sites of pBR322, *orfA* promoter region	This work
pTH397	0.6kb *Hin*dIII-*Eco*RV fragment of pTH191 in *Hin*dIII-*Eco*RV sites of pBR322, *orfA* promoter region	This work

Plasmids and phage

M13K07	M13 derivative, helper phage	Vieira and Messing (1987)
ΦM12	*R. meliloti* bacteriophage	Finan et al. (1984)

Transposons

Tn*5*	Nm^r-Km^r Sm^r	Berg and Berg (1987)
Tn*5*-132	Ot^r	Berg and Berg (1987)
Tn*5*-233	Gm^r, Sp^r	De Vos et al. (1986)
Tn*V*	Tn*5* containing pSC101 *oriV*, Nm^r-Km^r	Furuichi et al. (1985)
Tn*phoA*	Tn*5* derivative generating AP translational fusion, Nm^r-Km^r	Manoil and Beckwith (1985)
Tn*5*B20	Tn*5* derivative generating *lacZ* transcriptional fusion, Nm^r-Km^r	Simon et al. (1989)

Abbreviations are as followed: Ap, ampicillin; AP, alkaline phosphatase; Cm, chloramphenicol; Gm, gentamicin; Km, kanamycin; Nm, neomycin; Ot, oxytetracycline; Sm, streptomycin; Sp, spectinomycin; Tc, tetracycline; Rif, rifampicin, Lac, lactose utilization genes; *mob*, mobilization region of RK2; ort I and II, orientation I and II; *oriT*, origin of transfer; *oriV*, origin of vegetative replication; X-Phos, 5-bromo-4-cholro-3-indolyl phosphate. ΦM12 transducing lysates are indicated by Φ followed by the strain number. For strain construction, an arrow indicates transduction from the indicated ΦM12 transducing lysates to the recipient strain. Homogenotizations followed by transduction of the insertion recombined back into the recipient strain are indicated by an arrow and parentheses enclosing the introduced incompatible plasmid pPH1JI.

- LB (Luria-Bertani) was prepared by dissolving 10g of tryptone, 5g of yeast extract and 5g sodium chloride per liter (l) of solution. 4ml/l sodium hydroxide (1M) was added to the broth while 1ml/l of sodium hydroxide and 15g/l of agar was added for the preparation of plates. 2.5mM of magnesium sulfate and calcium chloride were added to medium used for *Rhizobium* growth (LBmc).
- M9 minimal medium was prepared by dissolving 5.8g disodium hydrogen phosphate, 3g potassium dihydrogen phosphate, 0.5g sodium chloride and 1g of ammonium chloride per liter of solution (1x M9). The solution was autoclaved without agar or other supplement to prevent precipitation. To prepare M9 plates, sterile 2x M9 medium was mixed with an equal volume of sterile distilled water containing 30g/l agar. Filter sterilized solutions of magnesium sulfate, calcium chloride, biotin and D-glucose (or other carbon sources) were added to the autoclaved M9 media at final concentrations of 1mM, 0.25mM, 3μg/ml and 15mM, respectively.

For transduction experiments, ½ LB-½ 1x M9 agar plates were used. This media was prepared by mixing 150ml of the LB solution containing 30g/l agar with 150ml of 1x M9 solution.

- GYM media was made of 1mM sodium glutamate, 2.5mM mannitol, 1mM dipotassium hydrogen phosphate pH 6.8, 0.5mM magnesium sulfate, 0.5mM calcium chloride and 0.2% (w/v) yeast extract. GYM/NaCl was prepared by adding 100mM sodium chloride to the GYM media.
- MOPS-buffered minimal media was made of 40mM morpholinopropane sulfonic acid/20mM potassium hydroxide pH 7.4, 20mM ammonium chloride, 2mM magnesium sulfate, 1.2mM calcium chloride, 100mM sodium chloride, 3μg/ml biotin, 5ml/l of a partially purified factor isolated from yeast extract (provided by Dr. Watson) and 15mM glucose (or succinate) as carbon source. When required a phosphorus source was added at a final concentration of 2mM.

Note: The MOPS/KOH solution, the biotin and the carbon source were filter-sterilized through a 0.45μm filter and added after the rest of the ingredients were autoclaved. The glassware used was phosphate-free (rinsed in HNO_3 6M solution).

- Water containing 15g/l agar was used to prepare plates for the germination of plant seedlings.

III) Antibiotics and other additives

For the preparation of plates, antibiotics were added to the media at the following concentrations (in μg/ml): Neomycin (Nm) 200, Spectinomycin (Sp) 200, Gentamicin (Gm) 20, Oxytetracycline (Ot) 0.5, Kanamycin (Km) 20, Rifampicin (Rif) 20, Chloramphenicol (Cm) 10, Ampicillin (Ap) 100, Tetracycline (Tc) 10 and Streptomycin (Sm) 200. All antibiotics were dissolved in water (and filter sterilized through a 0.45μm filter) except for Ot and Tc that were dissolved in 95% ethanol, Cm dissolved in 50% ethanol and Rif dissolved in dimethylsulfoxide.

For liquid media or media containing more than one antibiotic, each antibiotic was used at half the concentration.

Other additives include (final concentration in μg/ml): thymidine 60, IPTG (isopropyl β-D-thiogalacto-pyranoside) 30, X-Gal (5-bromo-4-chloro-3-indolyl-β-D-galactopyranoside) 50 and X-Phos (5-bromo-4-chloro-3-indolyl phosphate) 60. The phosphorus sources used for the growth experiments in the MOPS-buffered minimal media included ethylphosphonate (EP; Aldrich), aminoethylphosphonate (AEP; Sigma), methylphosphonate (MP; Aldrich), aminomethylphosphonate (AMP; Aldrich), L-α-glycerophosphate (G3P; Sigma), glucose-6-phosphate (Glc6P; Sigma) and O-phospho-L-serine (PSer; Sigma).

B- Methods

I) Growth conditions

Rhizobium and *E. coli* strains were grown at 30°C and 37°C, respectively. Liquid cultures inoculated with a single colony were shaken to provide aeration.

For growth in the MOPS-buffered minimal media the following procedure was used: The cells were grown for 24 hours in LBmc, spun down, washed once with phosphate-free MOPS media (MOPS P0), and 5µl of cells resuspended in MOPS P0 was used to inoculate 5ml of MOPS media (1/1000 dilution). For the growth experiments over time, an additional step was added in order to reduce the polyphosphate content of the cells. This otherwise allowed significant growth in MOPS P0 media. The washed cells were inoculated in 5ml of MOPS P0 media (starting absorbency at OD_{600} was 0.05 approximately) and grown for 24 hours. The optical density of the cultures were diluted to an OD_{600} of 0.2 and 5µl was used to inoculate 5ml of MOPS media containing various phosphorus sources.

II) Genetic modification of a cell

1- Preparation of competent cells and transformation

This method was used to transfer plasmid DNA into competent *E. coli* cells. The cells were made competent using a calcium chloride solution as follows:

0.1ml of an overnight saturated culture was used to inoculate 100ml of LB broth. The cells were grown to an OD_{600} of 0.2-0.3 and centrifuged for 5 min at 4000rpm, 4°C. The subsequent steps were performed on ice. The pellet of cells was resuspended in 50ml of an ice cold solution of 50mM calcium chloride and 20mM potassium acetate (pH 6.2) and left on ice for one hour. After 10 min centrifugation at 4000rpm, 4°C the cells were resuspended in 10ml of the above solution containing 20% glycerol. 0.5ml aliquots were stored at -70°C.

For the transformation, 100µl of competent cells were thawed on ice then mixed with 1µg of plasmid DNA. The mixture was left on ice for an hour, heat shocked for 2 min at 37°C and put back on ice for 1 min. 1ml of LB was added to the cells and the cultures were grown for one hour before being pelleted, resuspended in about 200µl LB and plated on two LB plates containing antibiotic to select for the plasmid. Colonies appeared after 12 hours growth at 37°C.

2- Conjugal mating

The transfer of a foreign plasmid DNA into *R. meliloti* cell required mating between the plasmid donor strain (*E. coli*) and the recipient cell. Mating of mobilisable plasmids was facilitated by the presence of an *E. coli* strain, MT616, containing the "helper" plasmid pRK600 which supplied the RK2 transfer genes in trans. This procedure is referred to as triparental mating.

The strains involved in the mating were grown to late log phase in LB containing appropriate antibiotics for the *E. coli* strains (donor and helper) and in LBmc for the *Rhizobium* recipient strain. The *E. coli* cultures were spun down and resuspended in LB media to eliminate of the antibiotics. 20μl of each culture were mixed and the resulting 60μl was spotted on an LB plate. As controls, 20μl of each strain culture was spotted on their own on an LB plate. After 16 hours incubation at 30°C, the spots were resuspended in 1ml saline (0.85% sodium chloride) and 100μl of the suitable dilution was plated on LB containing antibiotics selecting for the plasmid mated and the recipient strain. Colonies appeared after 3-4 days incubation at 30°C.

3- Homogenotization

Insertions within genes cloned in the plasmid pRK7813 (IncP) were recombined onto the chromosome via homologous recombination. To select for homogenotes, the pRK7813 plasmid was cured by mating into the *Rhizobium*

strain a second plasmid (pPH1JI) of the same incompatibility group (IncP) and selecting for the second plasmid, the selective marker of the recombined insert, and the recipient cell. The procedure was as follows: An overnight culture of a purified *Rhizobium* transconjugant colony grown in LBmc Nm (50μg/ml) (to select for a Tn*5* insert, for example) was mixed with an equal volume (1ml) of a log phase culture of the *E. coli* J53 strain grown in LB Gm (10μg/ml) (Note: J53 contains pPH1JI a self-transmissible plasmid). The cells were pelleted, resuspended in 1ml LB and 100μl was spotted on an LB plate. After 16 hours incubation at 30°C the spot was resuspended in 1ml saline and 100μl was plated at 10^0 and 10^{-1} dilutions on LB Sm (100μg/ml) Nm (100μg/ml) and Gm (70μg/ml). Colonies appeared 3 to 5 days after incubation at 30°C. The colonies were purified 3 times by plating on the above selective media and the loss of the pRK7813 plasmid was confirmed by the sensitivity of single colonies on LB Tc (10μg/ml) plates. To eliminate of the incompatible plasmid (pPH1JI), the recombined insertion was transduced back into the recipient strain and the structure of the recombinants was checked by Southern blot (see below).

4- Generalized Transduction and Phage preparation

Generalized transduction involved the transfer of genomic DNA fragment from one strain to another via a transducing phage that is able to pack random

fragments of host DNA. The phage used for transduction in *R. meliloti* is ΦM12 (Finan et al., 1984).

a) To prepare a ΦM12 phage lysate, 5ml of an overnight culture grown in LBmc (the phage requires calcium for infection) was diluted to an OD_{675} of 0.4-0.5 in the same media. 100μl of Rm1021 lysate was added to the culture which was incubated on a 30°C rotating wheel for 12 hours to allow complete lysis of the cells. 200μl of chloroform was added to the lysate to kill any remaining viable cells. The lysate was vortexed briefly and the cell debris was allowed to settle at 4°C for at least one hour. The top 4ml of the lysate was transferred to a new tube and centrifuged for 5 min, at 4000rpm, 4°C. The lysate should give a titer of 10^{10}-10^{11} PFU/ml (PFU = plaque forming units) and can be stored at 4°C for several years.

b) To determine the phage titer, the lysate was diluted to 10^{-10} in LBmc. 0.1ml of the 10^{-8}, 10^{-9} and 10^{-10} dilutions was mixed with 0.1ml of overnight culture of Rm1021 grown in LBmc. Following incubation at room temperature for 15 min, 3ml of LBmc containing 0.5% agar (cooled to 50°C) was added. The mixture was poured onto an LBmc plate and after solidification of the soft agar, the plates were incubated overnight at 30°C. The PFU per ml was calculated by multiplying the number of plaques obtained by the dilution factor and dividing by 0.1.

c) Transduction of genetic markers from one strain to another was performed by mixing 1ml of 1/30 diluted lysate, made from the strain containing the marker to be transduced, with 1ml of the recipient culture (OD_{675} ~ 1). This gave a multiplicity of infection of ~ 0.5. The mixture was left on the bench for 20-25 min to allow adsorption. 2.5ml of saline was added and the cells were pelleted. The supernatant was removed and the cells were washed once with 2.5ml saline. The pellet of cells was resuspended in 1ml saline. 0.1ml was plated on ½ LB-½ 1x M9 agar plates supplemented with the antibiotic(s) selecting for the transduced marker. As a control, the diluted phage lysate and the recipient cells were plated on this selective media as well.

d) Linkage between two markers

To determine whether two markers (A and B) were linked (closely located), marker A was transduced into a strain containing a chromosomal insertion of marker B. The transductants, isolated by selecting for marker A, were checked for the presence of marker B by patching 50 to 100 colonies on media selecting for marker B. The percentage of transductants that have lost their resistance for marker B provided the % linkage between the two markers. The physical distance between two markers can be determined from the Wu equation (Wu, 1966): $c = (1-d/L)^3$, where c represents the cotransduction frequency, d the distance between markers (kb) and L the length of DNA in the transducing particle (160kb for ΦM12; Charles and Finan, 1990; Finan et al., 1984).

5- Tn*5*, Tn*5*-B20 and Tn*phoA* mutagenesis

Transposon Tn*5* is 5.7kb in size and carries genes encoding resistance for Nm-Km, bleomycin and Sm which are flanked by inverted repeats (IS50 elements). They can transpose from one replicon to another at a frequency of about 10^{-4} to 10^{-6} per recipient. Two techniques were used to create Tn*5* mutations:

a) Random mutagenesis

Random mutagenesis of *R. meliloti* genomic DNA was performed by introducing a suicide plasmid (plasmid that cannot replicate in *Rhizobium)* carrying Tn*5* or derivatives (such as pRK602 for Tn*5*; pTH270 for Tn*5*-B20) from an *E. coli* strain and selecting for the Nm^r recombinants.

b) Directed mutagenesis

In this case, Tn*5* insertions into cloned DNA fragment were isolated from an *E. coli* strain carrying a transposon on its chromosome (i.e. MT614 for Tn*5*; G312 for Tn*5*-B20; MT621 for Tn*phoA*). The cloned plasmid DNA was then transferred, by triparental mating, into another *E. coli* strain (MT609; Sp^r *polA*) by selecting for the plasmid (Tc^r) carrying the transposon (Km^r) .

c) Transposon replacements

The replacement of Tn*5*-132 (Ot^r) and Tn*5*-233 (Gm^r-Sp^r) insertions with Tn*V* was performed by homologous recombination between the flanking IS50 elements. Plasmid pTF1 from *E. coli* was mated to the *R. meliloti* (Sm^r) strains

carrying the insertions to be replaced. As pTF1 cannot replicate in *Rhizobium*, recombinants were selected as Sm^r-Nm^r strains and true replacements were obtained after screening for the loss of Ot or Gm-Sp resistance markers. To replace a Tn*5* insertion with Tn*5*-233, the Tn*5* marker was first transduced into the Rif^r strain Rm5000. The replacement was then performed by mating pRK607 into this strain, selecting for Rif^r Gm^r-Sp^r transconjugants and screening for the loss of the Nm marker.

III) DNA and RNA preparation

1- DNA preparation

a) Alkaline lysis

Mini- and large- scale plasmid DNA preparations (preps) were performed as described in Sambrook et al. (1989; second edition, vol. 1, pp. 1.38-39). For mini-preps (1.5ml of cells), 100µl of Solution I (50mM glucose, 25mM Tris-HCl pH 8, 10mM EDTA pH 8), 200µl Solution II (0.2N NaOH, 1% SDS) and 150µl Solution III (60ml 5M K-acetate, 11.5ml glacial acetic acid, 28.5ml H_2O) were used. Large scale preps were further purified using the LiCl; PEG/NaCl precipitation procedure described in Sambrook et al. (1989; pp. 1.41).

b) Single-stranded DNA

E. coli strains containing either pUC118 or pUC119 cloned DNA were grown in LB Ap^{50} to an OD_{600} of 0.1. 5µl of M13K07 helper phage (~ 10^{11} phage/ml) was added to the culture which was subsequently grown at 30°C for at least 8 hours. 1.5ml of culture was centrifuged at room temperature (RT) for 5 min (12,000rpm). The supernatant was transferred to a new tube, centrifuged a second time and transferred to a tube containing 250µl of PEG/NaCl (polyethylene glycol 6000/2.5M sodium chloride). The tubes were vortexed, left 10 min at RT to allow precipitation and centrifuged 10 min at 12,000rpm. The pellet was dissolved in 200µl TES (20mM Tris-HCl pH 7.4, 0.1mM EDTA, 10mM NaCl) and the phage proteins were extracted with phenol:chloroform (3:1; v:v) as follows: the mixture was vortexed for I min, left on ice for 5 min, vortexed again and centrifuged at RT for 5 min (12,000rpm). This extraction was repeated once followed by a chloroform extraction. The ssDNA was precipitated by adding 0.1 volume (vol) of 3M NH_4Ac and 2.5 vol of ethanol. After centrifugation the pellet was washed with ethanol 70% and dissolved in 20µl of $T_{10}E_1$. 5µl was checked on an agarose gel.

c) *R. meliloti* genomic DNA

5ml LBmc overnight cultures were centrifuged at RT for 5 min (5,000rpm). The pellets were washed once with 0.85% NaCl (saline), once with TES (10mM Tris-HCl pH 8, 25mM EDTA, 150mM NaCl) and were resuspended in 2.5ml of

$T_{10}E_{25}$ to which 250µl lysozyme (2mg/ml in $T_{10}E_{25}$) was added. The mixture was incubated 15 min at 37°C. 300µl of sarkosyl-protease solution (5mg/ml protease E (Sigma) was dissolved in $T_{10}E_{25}$ and incubated at 37°C for 2 hours. After this autolysis period, 10% sarkosyl was added. The solution was kept at -20°C) was then added and the incubation at 37°C was continued for another hour. The mixture was phenol extracted by adding 1.5ml of phenol, mixing gently by inversion, and centrifuging 20 min at 5,000rpm (RT). The aqueous (upper) layer was withdrawn very carefully avoiding interface and was re-extracted once with phenol and once with chloroform. The DNA was precipitated by adding 1 vol of isopropanol and mixing by inversion. The precipitated DNA was picked up with a glass pipette, washed once with 70% ethanol, once with 95% ethanol, air dried and dissolved in 300µl $T_{10}E_1$. 1µl of 100µg/ml RNAase was added to the dissolved DNA and the mixture was incubated for 30 min at 37°C. After phenol:chloroform and chloroform extractions, the DNA was precipitated by adding 0.1 vol of 3M NH_4Ac and 2 vol of ethanol. The precipitated DNA was picked up with a glass pipette, washed with 70% ethanol, then 95% ethanol, air dried for a 2 min and dissolved in 200µl $T_{10}E_1$. 5µl was checked on an agarose gel.

2- *R. meliloti* RNA preparation (using hot phenol)

When working with RNA, gloves were worn at all times and all the solutions were treated with diethylpyrocarbonate (DEPC) 0.1% (carcinogen) as follows: the DEPC was mixed well in the solutions; left overnight at room temperature and autoclaved.

To prepare RNA from *R. meliloti*, 100µl of saturated LBmc culture was used to inoculate 200 ml of LBmc. When an OD_{600} between 0.3-0.8 was reached, the cells were centrifuged for 5 min at 5,000rpm (RT), resuspended in 50 ml of TES (10mM Tris-HCl pH 7.5, 1mM EDTA, 100mM NaCl), centrifuged again as above and resuspended in 6ml of TES. 1.5 ml were dispensed into four eppendorf tubes that were kept on ice at all time from this point on. The tubes were centrifuged for 5 min at 12,000rpm (4°C) and the pellets were dissolved in 500µl of ice cold Extraction Buffer (10mM Tris-HCl pH 7.5, 5mM EDTA, 5% sucrose, 300mM CH_3COONa, 1% SDS and 1% β-mercaptoethanol). 300µl of hot phenol (90°C) were added to each tube. The tubes were mixed gently by inversion and 300µl of chloroform:iso-amyl-alcohol (24:1) were added. After vortexing the mixture, the tubes were centrifuged 10 min at 12,000rpm (4°C). The aqueous (upper) phase was transferred to a new tube and 2.5 vol of 95% ethanol was added. After precipitation, the pellets were dissolved in 50µl H_2O (treated with DEPC 0.1%). Two rounds of precipitation with 150µl of 4M NaAc, pH 7 (treated with DEPC) were performed. Both times, the RNA was allow to

precipitate for at least 16 hours at -20°C. After the second precipitation, the RNA was dissolved in 100µl H_2O (treated with DEPC 0.1%) and the remaining proteins were extracted once with phenol:chloroform (1:1) and once with chloroform. The RNA was precipitated by adding 1/10 volume of 3M NaAc pH 5 and 250µl 95% EtOH and centrifuged for 10 min at 12,000rpm (4°C). The pellet was dissolved in 100µl H_2O (DEPC treated). 250µl of 95% ethanol was added to the RNA which was stored at -20°C. When needed, the RNA was precipitated by adding 10µl of 3M NaAc pH 5 and after centrifugation, the RNA was dissolved in 100µl H_2O (DEPC treated). 5µl was checked on an 1.2% agarose gel.

IV) Southern blot and colony hybridization

1- Southern blot

Digested DNA fragments separated on an agarose gel were transferred to a nylon filter as follows: the gel, stained with ethidium bromide, was photographed (with a ruler beside the molecular weight markers) and the DNA was depurinated for 10 min in 0.25M HCl solution, denatured in 1.5M NaCl, 0.5M NaOH solution for 2x 15 min and neutralized in 1M Tris-HCl pH 7.4, 1.5M NaCl, solution for 2x 15 min. The gel was rinsed with water after each solution. The denatured DNA was transferred to nylon membrane by capillary as described in

Sambrook et al. (1989; pp. 9-34 and 9-38,40) using 5x SSC for the transfer (20x SSC pH 7: 175.3g/l NaCl; 88.5g/l trisodium citrate).

2- Colony hybridization

Nylon membranes, cut to match the size of a petri-dish, were placed on the colonies and left there for three min (to increase the transfer, the membrane can be pressed gently with a glass bar). The membrane and the petri-dish were both marked to be able to orient the membrane after hybridization. The membranes (colony side face up) were then transferred in petri-dishes containing whatman paper soaked with the following solutions; i) 0.2M NaCl, 1% SDS for 5 min; ii) 1.5M NaCl, 0.5M NaOH for 10 min; iii) 1M Tris-HCl pH 7.4, 1.5M NaCl, for 15 min and iv) 2x SSC for 5 min. The DNA was fixed to the membrane by UV irradiation (2 min). The membranes were then soaked in 2x SSC, 0.1% SDS for 5 min and the cell debris were gently removed with a Kimwipe.

3- Preparation of the Digoxigenin-probe

The DNA fragment used to make the probe was isolated from an agarose gel using the Geneclean II kit from Bio101 (cat # 001-400) and Digoxigenin (Dig)-labeled following the protocol of Boehringer Mannheim (Kit # 1093 657). About 10ng of DNA was denatured (10 min in boiling water followed by 3 min in an

ice/ethanol bath) and added to the following labeling mix from the kit: 4µl of hexanucleotide mix (random primer for DNA synthesis), 4µl dNTP mix (1mmol/l dATP, 1mmol/l dCTP, 1mmol/l dGTP, 0.65mmol/l dTTP, 0.35mmol/l digoxigenin-11-dUTP), 2µl (4U) Klenow DNA polymerase and water to a volume of 40µl. The reaction mixture was placed in a 37°C water bath overnight. The reaction was stopped by adding 2µl of 0.5M EDTA pH 8. The DNA-probe was precipitated by adding 5µl of 2.5M NaCl and 150µl ethanol and left at least 30 min at -70°C prior to centrifugation. The pellet was washed once with 70% ethanol, once with 95% ethanol, air dried and dissolved in 50µl $T_{20}E_1$.

4- Estimation of the yield of the Dig-labeled DNA probe

This was performed by comparing the labeled probe with dilutions of labeled control DNA of known concentration. The labeled DNA control (concentration of 5ng/µl) was diluted 5; 50; 500; 5000; 50000 times to give final concentrations of 1ng; 100pg; 10pg; 1pg; 0.1pg per µl. 1µl of each dilution was spotted onto a nylon membrane. 1µl of the undiluted probe and 1µl of the probe diluted 10; 100; 1000; 10000 times were also spotted on the nylon membrane beneath the control spots. The DNA was fixed to the membrane by UV irradiation (2 min) and the labeled DNA was detected as follows: The following steps were done under agitation and at room temperature. The membrane, wetted in Buffer 1 (100mM Tris-HCl pH 7.5, 150mM NaCl), was incubated i) in Buffer 2 (same as

Buffer 1 but containing 0.5% blocking reagent) for 15 min and ii) 15 min in the diluted Dig-antibody Solution (1:5000 in Buffer 1), which was washed off with Buffer 1 (2x 15 min). The membrane was then equilibrated at pH 9.5 by incubating it 2 min in Buffer 3 (100mM Tris-HCl pH 9.5, 100mM NaCl, 50mM $MgCl_2$) and after pouring off Buffer 3, 10ml of Color Substrate Solution (10ml Buffer 3 containing 45µl NBT and 35µl X-Phos) was added to the membrane. The color was allowed to develop in the dark at 37°C, without agitation. The NBT solution (nitroblue tetrazolium salt) was at a concentration of 75mg/ml in 70% dimethylformamide. The X-Phos solution (5-bromo-4-chloro-3-indolyl phosphate sodium salt) was dissolved in water at a concentration of 50mg/ml. The reaction was stopped by putting the membrane in water for 5 min, then allowed to air dry. The spot intensities of the sample were compared to the control to estimate the concentration of the probe.

5- Hybridization

The membrane was placed in a plastic box with 50ml prehybridization solution (5x SSC, 0.1% sarkosyl, 0.02% SDS, 5% blocking reagent and 50% deionized formamide) for 1 hour at 42°C. The prehybridization solution was replaced with 20ml of hybridization solution, prehybridization solution containing the denatured probe (see "preparation of the Dig-probe" for the denaturation of the probe), and incubated for 24 hours at 42°C. The hybridization solution was

poured off (and stored at -20°C for future use) and the membrane was washed 2x 5 min in wash 1 (2x SSC, 0.1% SDS) at room temperature and 2x 15 min in wash 2 (0.1x SSC, 0.1% SDS) at 42°C. The membrane was air dried or used immediately for detection.

6- Detection

The detection was performed as described in "Estimation of the yield of the Dig-labeled probe" (# 4) with the following modifications; the membrane was rehydrated in Buffer 1, incubated in Buffer 2 for 30 min and another 90 min in the diluted Dig-antibody Solution. The subsequent steps were identical to those described in "Estimation of the yield of the Dig-labeled probe".

7- Stripping of the probe

The membrane was not dried if it was to be stripped and reprobed. To remove the color precipitate the membrane was incubated in a glass plate containing dimethylformamide heated on a heater block to 50-60°C (No flame, dimethylformamide is flammable!!!; work in a fume hood). The dimethylformamide solution was changed several times until the blue color was removed. The membrane was then rinsed thoroughly in water. The probe was removed, by incubating the membrane 2x 10 min in the Alkaline Probe-Stripping

Solution (0.4M NaOH, 0.1% SDS) at 37°C and rinsing it in 2x SSC solution. The filters were reprobed by starting at the prehybridization step.

V) Plant growth

Plant growth experiments were performed in a nitrogen-free environment to determine the ability of mutant strains to nodulate and fix nitrogen. The plants were grown in Leonard jars containing Jensen's media.

1- Preparation of the Jars

Leonard assemblies consist of a plastic jar sitting inside a 250ml beaker with a cotton wick extending from a hole at the bottom of the jar. The jar was filled with a nitrogen-free sand/vermiculite (1:1) mixture and 250ml of 1x Jensen's media (1g/l $CaHPO_4$, 0.2g/l K_2HPO_4, 0.2g/l $MgSO_4.7H_2O$, 0.2g/l NaCl, 0.1g/l $FeCl_3$, and 1ml/l trace minerals. The trace minerals solution was composed of 1g/l H_3BO_3, 1g/l $ZnSO_4.7H_2O$, 0.5g/l $CuSO_4.5H_2O$, 0.5g/l $MnCl_2.4H_2O$, 1g/l $NaMoO_4.2H_2O$, 10g/l EDTA, 2g/l NaFe-EDTA and 0.4g/l Biotin). The whole apparatus was autoclaved for 2 hours.

2- Sterilization of the seeds

Alfalfa seeds (*Medicago sativa* cultivar Iroquois; 100 seeds weighting approximately 0.25g) were surface sterilized 5 min in 95% ethanol followed by 20 min in a 50% bleach solution (sodium hypochlorite). The seeds were then rinsed with sterile water at least 8 times over an hour and were spread on water agar plates (15g/l agar) using a flamed spatula. The plates were placed in the dark at room temperature until germination (2-3 days).

3- Inoculation of the seedlings

Ten germinated seedlings were transferred to an autoclaved Leonard jar assembly and put in the growth chamber (day = 18 hours, 21°C; night = 6 hours, 18°C). After 2 days, 0.1ml of a *R. meliloti* saturated cultures (OD_{600} 1 to 1.5) diluted in 10 ml of sterile water ($1x10^7$-$1x10^8$ cells) were used to inoculate a Leonard jar assembly containing emerging seedlings. Three jars were inoculated with the same bacterial strain (total of 30 seedlings). The plants were grown up to one month and were watered as needed with sterile distilled water.

4- Acetylene reduction assay

To determine the nitrogenase activity of the nodules, an acetylene reduction assay (ARA) was performed. The roots of three plants from each jar were inserted in a 30 ml bottle and sealed with a serum stopper. 3ml of

acetylene gas were injected in each bottle and the quantity of acetylene reduced (ethylene produced) after 15 min was monitored by injecting an 0.2ml sample into a Hewlett-Pakard 5890 gas chromatograph (GC; air 34psi, H_2 12psi, N_2 65psi). The ethylene peaks were integrated using the HP3365 Series II Chemstation computer program and the nmol of acetylene reduced per hour per plant was determined as follows:

Using the formula V = nRT/Pr and the fact that at standard temperature (T) and pressure (Pr), 1 mole of gas has a volume of 22.4l (= R), 1ml of gas then contains $1/2.24 \times 10^4$ moles. 1ml of 506ppm ethylene ($506 \text{ part}/10^6 = 5.06 \times 10^{-4}$) will have $5.06 \times 10^{-4}/2.24 \times 10^4 = 2.26 \times 10^{-8}$ moles and 0.2ml of 506ppm ethylene, $2.26 \times 10^{-8}/ 5 = 4.52$ nmol. By relating the unit peak area, when 0.2ml of a 506ppm ethylene standard was injected to the GC, to the number of mole, the number of mole per unit area can be determined (Znmol/unit). The acetylene reduction per plant per hour of the sample can then be calculated from the general formula (ARA =):

$$\frac{\text{\# area units of sample} \cdot \text{Znmol/unit} \cdot 150 \text{ (0.2ml is 1/150 the bottle volume)}}{\text{3 plants} \cdot \text{0.25 hours (= 15 min)}}$$

5- Determination of the plant dry weight

The plant shoots from each jar were cut and dried in a paper bag for one week in a 100°C oven. The dry weight (in mg per plant) was determined by weighting the dried plants of each bag and dividing by the number of shoots.

VI) Uptake experiments

1- Phosphate and succinate transport assays

Phosphate and succinate uptake experiments were done as described in Bardin et al. (1996) and Yarosh et al. (1989; see also Chapter III of this thesis). The inhibition experiments were performed by adding the inhibitors to the assay mixture 15 s prior to adding the ^{33}P-labeled phosphate.

2- Protein determination

Protein concentration was determined by the Bradford method using the Biorad protein assay dye (Coomassie blue; Bradford, 1976). The cells were solubilized by diluting them in 1N NaOH (1:1 ratio) and boiling them for 15 min. The protein concentration of a sample was determined from a bovine serum albumin (BSA) standard curve made using the microassay procedure (concentration from 0 to 10μg protein per ml of 0.5M NaOH). The procedure was as follows: 100μl of 0 to 100μg/ml BSA (or protein sample) in 0.5M NaOH were

added to 700µl water and 200µl of Biorad solution (undiluted). The solutions were vortexed, incubated 5 min at RT and the OD_{595} was determined.

3- Phosphate determination

The phosphate concentration of a solution was determined using the method of Martin and Tolbert (1983). The reagent (made fresh each time) was prepared by mixing 10 ml of water with 3ml of concentrated sulfuric acid (H_2SO_4) in which 0.25g of ammonium molybdate ($(NH_4)_6$ MoO_{24}) was dissolved. The volume of the solution was then brought to 50ml with water and 1g of ascorbic acid was added (yellow solution; if the solution turned blue this indicated that the water was contaminated with phosphate). A standard curve was prepared by mixing 500µl of the reagent with 500µl of a potassium phosphate solution with concentration ranging from 0 to 50µM. The mixtures were vortexed and incubated at 37°C for 90 min and the OD_{820} was measured. The phosphate concentration of samples was determined by mixing 500µl sample with 500µl reagent and comparing the optical densities obtained from the samples to those of the standard curve .

VII) Enzymatic assays

1- β-Galactosidase assay

0.5ml of overnight grown cells (for which OD_{600} was measured) was mixed with 0.5ml of Buffer Z (pH 7; 60mM $Na_2HPO_4.7H_2O$, 40mM $NaH_2PO_4.H_2O$, 10mM KCl anhydrous, 1mM $MgSO_4.7H_2O$ and 2.7ml/l of 2-mercaptoethanol added just before use); 20µl chloroform and 10µl SDS 0.1%. The tubes were vortexed and equilibrated at 30°C for 5 min. The reaction was started by adding 0.2ml of 4mg/ml O-nitrophenyl-β-D-galactoside (ONPG) dissolved in Buffer Z (at 37°C). When the solution turned yellow, the reaction was stopped by adding 0.5ml of 1M Na_2CO_3. The tubes were centrifuged 5 min at 12,000rpm and the optical density at 420nm (OD_{420}) was measured.

The β-Galactosidase activity, in Miller units was calculated using the following formula: $(1000 \cdot OD_{420}) / (OD_{600} \cdot \Delta T \cdot V)$

with ΔT: reaction time (min) and V: initial volume of culture used (ml).

2- Alkaline phosphatase assay

The alkaline phosphate (AP) activity was determined after the cells (to be assayed) were centrifuged and resuspended in a 1M Tris-HCl pH 8 buffer to an OD_{600} of approximately 0.1. The OD_{600} was precisely recorded for each tube. 3ml of the diluted cells were equilibrated at 30°C for 5 min and the reaction was started by adding 500µl of 4mg/ml nitrophenyl phosphate (NPP). After

development of a yellow coloration (or after 1 hour) the reaction was stopped by adding 600µl of 1M phosphate solution. The tubes were centrifuged 5 min at 12,000rpm and the OD_{420} was measured. The alkaline phosphatase activity was calculated using the following formula:

$$(1000 \cdot OD_{420}) / (OD_{600} \cdot \Delta T)$$

with ΔT: reaction time (min)

VIII) DNA Sequencing (see also chapter IV)

DNA sequencing was performed using single-stranded DNA, following the dideoxy chain termination method according to the protocol of United States Biochemicals for the Sequenase 2.0 enzyme and using [α-^{35}S]dATP. 7µl of single stranded DNA (about 1µg) was mixed with 1µl of primer (0.5pmol/µl) and 2µl of 5x Sequenase buffer. The mixture was incubated 2 min at 65°C and the tubes were allowed to cool down slowly to room temperature to allow annealing. Labeling of the reactions was performed by adding 1µl DTT, 2µl labeling mix (diluted 5x), 0.5µl [α-^{35}S]dATP (1000Ci/mmol) and 2µl Sequenase enzyme (diluted 8x) to the annealing mixture. The labeling mixture was incubated for 3 min at RT. The reactions were terminated by adding 3.5µl of the labeling mix to 2.5µl of each of the four dideoxy nucleotide Termination Mix (the ddA Termination Mix was a 50mM NaCl solution containing 80µM of each dGTP,

dCTP, dATP and dTTP in addition to 8μM ddATP) and incubating the reactions 5 min at 37°C. The reactions were stopped by adding 4μl of Stop solution (95% formamide, 20mM EDTA, 0.05% Bromophenol Blue and 0.05% Xylene Cyanol FF) and stored at -20°C for up to one week. The sequencing reactions (2μl) were run on a 6% denaturing polyacrylamide gel (acryl (19):bisacryl (1); 7M urea) after denaturing the samples by incubating them 2 min at 80°C followed by 1 min on ice. The gel was run at 2000 volts.

CHAPTER III

A phosphate transport system is required for symbiotic nitrogen fixation in *Rhizobium meliloti*

A- Introduction

This chapter presents the genetic characterization of the symbiotic locus, *ndvF*, identified on the second megaplasmid (pRmSU47b) of *Rhizobium meliloti* 1021 (Charles and Finan, 1991; Charles et al., 1991). The locus was located in a 5kb region within a 7.3kb *Bam*HI fragment. Isolation of active Tn*phoA* fusions to the locus indicated that *ndvF* encodes membrane anchored, periplasmic or secreted protein(s). Light microscopy of nodules elicited by *ndvF* mutant strains showed very few infected cortical cells, suggesting that nodule development is blocked early in the infection process (Charles et al., 1991).

The results reported here show that *ndvF* contains four genes (*phoCDET*) that together encode for an ABC-type transporter involved in the uptake of phosphate and possibly phosphonate (organophosphorus compounds with a direct C-P bond). The results are presented in the following publication:

Bardin, S.D., S. Dan, M. Osteras, and T.M. Finan. 1996. A phosphate transport system is required for symbiotic nitrogen fixation by *Rhizobium meliloti*. J. Bacteriol. **178**:4540-4547.

My contribution to the paper includes:

- Growth experiments in MOPS-buffered minimal media containing phosphate, phosphorus and phosphonate compounds.
- Phosphate and succinate uptake experiments.
- Participation in the primer extension experiments.

This chapter is completed with experiments investigating the affinity and specificity of the PhoCDET transporter for phosphate.

B- Results

1- A phosphate transport system is required for symbiotic nitrogen fixation by *Rhizobium meliloti*.

(see publication)

JOURNAL OF BACTERIOLOGY, Aug. 1996, p. 4540–4547
0021-9193/96/$04.00+0

Vol. 178, No. 15

A Phosphate Transport System Is Required for Symbiotic Nitrogen Fixation by *Rhizobium meliloti*

SYLVIE BARDIN, SHAN DAN, MAGNE OSTERAS,† AND TURLOUGH M. FINAN*

Department of Biology, McMaster University, Hamilton, Ontario L8S 4K1, Canada

Received 23 February 1996/Accepted 30 May 1996

The bacterium *Rhizobium meliloti* forms N_2-fixing root nodules on alfalfa plants. The *ndvF* locus, located on the 1,700-kb pEXO megaplasmid of *R. meliloti*, is required for nodule invasion and N_2 fixation. Here we report that *ndvF* contains four genes, *phoCDET*, which encode an ABC-type transport system for the uptake of P_i into the bacteria. The PhoC and PhoD proteins are homologous to the *Escherichia coli* phosphonate transport proteins PhnC and PhnD. The PhoT and PhoE proteins are homologous to each other and to the *E. coli* phosphonate transport protein PhnE. We show that the *R. meliloti phoD* and *phoE* genes are induced in response to phosphate starvation and that the *phoC* promoter contains two elements which are similar in sequence to the PHO boxes present in *E. coli* phosphate-regulated promoters. The *R. meliloti ndvF* mutants grow poorly at a phosphate concentration of 2 mM, and we hypothesize that their symbiotic phenotype results from their failure to grow during the nodule infection process. Presumably, the PhoCDET transport system is employed by the bacteria in the soil environment, where the concentration of available phosphate is normally 0.1 to 1 μM.

In the biogeochemical nitrogen cycle, much of the reduction of atmospheric N_2 to ammonia occurs in bacteria within plant root nodules. Molecular genetic studies of bacterial symbiotic mutants have resulted in the identification of nodulation (*nod*) and nitrogen fixation (*nif*) genes whose products are directly involved in the biochemical events which give rise to these nodules. The products of the bacterial *nod* genes synthesize lipooligosaccharide molecules which trigger the dedifferentiation of the plant root cortical cells destined to develop into the nodule primordia (30, 49). Many of the *nif* genes are involved in the regulation or synthesis of the N_2-fixing enzyme nitrogenase and its accessory proteins (17). The *nod* genes are induced in response to plant flavonoid signals (40), while in planta expression of the nitrogen fixation genes appears to be controlled by oxygen concentration (12, 48).

Mutants which are classified as defective in nodule development (*ndv*) have also been identified. In the alfalfa symbiont *Rhizobium meliloti*, *ndvA*, *ndvB*, *ndvF*, and *exo* mutants form "empty nodules" which contain very few infected cells and fail to fix N_2(Fix$^-$) (15, 19, 29). While the *ndvA* and *ndvB* gene products are involved in production of cyclic β-(1,2)-glucans and *exo* mutants lack a succinoglucan exopolysaccharide, the precise role(s) of these polysaccharides in nodule development remains unclear (14, 28). In *exoD* mutants, the symbiotic phenotype appears to result from an inability of these mutants to grow in planta during the nodule infection process (41).

R. meliloti contains two megaplasmids, pSYM and pEXO, which are 1,600 and 1,700 kb, respectively (7, 24, 25, 42). The *nod* and *nif* genes are located on pSYM, and we have previously reported the identification and cloning of the *ndvF* locus, which is located on the pEXO megaplasmid. Here we report results showing that *ndvF* contains four genes (*phoCDET*) which encode an ABC-type (periplasmic binding protein-dependent) transport system which transports phosphate (P_i), and likely alkylphosphonates, across the cytoplasmic membrane of *R. meliloti*. We hypothesize that the symbiotic phenotype of the *ndvF* mutants is a direct result of their failure to obtain sufficient phosphorus for growth during the infection process.

MATERIALS AND METHODS

Bacterial strains, plasmids, and media. Bacteria were grown on LB or LBmc medium with antibiotic concentrations as previously described (7). MOPS-minimal medium contained 40 mM morpholinopropanesulfonic acid (MOPS), 20 mM KOH, 20 mM NH_4Cl, 2 mM $MgSO_4$, 100 mM NaCl, 1.2 mM $CaCl_2$, and 0.3 μg of biotin per ml. Glucose or succinate was added as a carbon source to a final concentration of 15 mM. *R. meliloti* Rm 1021 is a streptomycin-resistant derivative of SU47. Strain Rm G439 is a strain Rm 1021 derivative in which the 12-kb *Hin*dIII fragment containing the *ndvF* locus was replaced with the internal neomycin resistance (Nm^r) *Hin*dIII fragment of Tn*5*; *R. meliloti* Rm G490 (*phoC490*) and Rm G491 (*phoT491*) are strain Rm 1021 derivatives in which an Ω Sp^r interposon was inserted in the first and third *Eco*RI sites within *ndvF*, respectively (8). pTH38 contains the complete *ndvF* locus cloned in a 7.3-kb *Bam*HI fragment in pRK7813, and pTH21 is a pLAFR1 cosmid clone carrying the complete *ndvF* locus within a 22-kb region (8).

Genetic techniques, DNA manipulations, and sequencing. Bacterial matings were performed as previously described (7). Tn*5*-B20 (45) insertions in *ndvF* were identified following mutagenesis of pTH21 by using *Escherichia coli* MT607::Tn*5*-B20 as transposon donor. Tn*5*-B20 insertions in the plasmid DNA were determined by restriction and DNA sequence analysis. Standard methods were used for plasmid DNA isolation, restriction digestion, agarose and polyacrylamide gel electrophoresis, ligations, and transformation (44).

Plasmids pTH38 and pTH38ΩB8::Tn*5* were used as the sources of material for DNA sequencing (Fig. 1). Restriction fragments were subcloned into pUC118 and pUC119 and used for construction of unidirectional nested deletions by exonuclease III treatment followed by S1 nuclease digestion (21). The nucleotide sequence was determined from single-stranded DNA obtained from host strain XL-1Blue (Stratagene) following infection with helper phage M13K07 (52). DNA sequencing was performed by dideoxy chain termination according to the protocol of United States Biochemicals for the Sequenase 2.0 enzyme, by using [α-^{35}S]ATP (NEN/DuPont) and 7-deaza dGTP (Pharmacia). Both strands of DNA were sequenced. Tn*phoA* insertion sites in pTH38 were sequenced directly from double-stranded DNA by using the *phoA*-specific primer (5′AATATCGC CCTGAGC-3′). Tn*5*-B20 insertion sites were sequenced by using the universal −20 (*lacZ*) primer (5′-GTAAAACGACGGCCAGT-3′). 7A, 19, 4B, and 17 had inserted at nucleotide positions 1792, 2862, 4481, and 5211, respectively (Fig. 1).

* Corresponding author. Mailing address: Dept. of Biology, McMaster University, 1280 Main St. West, Hamilton, Ontario L8S 4K1, Canada. Phone: (905) 525-9140, ext. 22932. Fax: (905) 522-6066. Electronic mail address: FINAN@MCMASTER.CA

† Present address: Laboratoire de Biologie, Végétale et Microbiologie, URA CNRS 1114, Université de Nice Sophia-Antipolis, Parc Valrose, 06108 Nice Cedex 02, France.

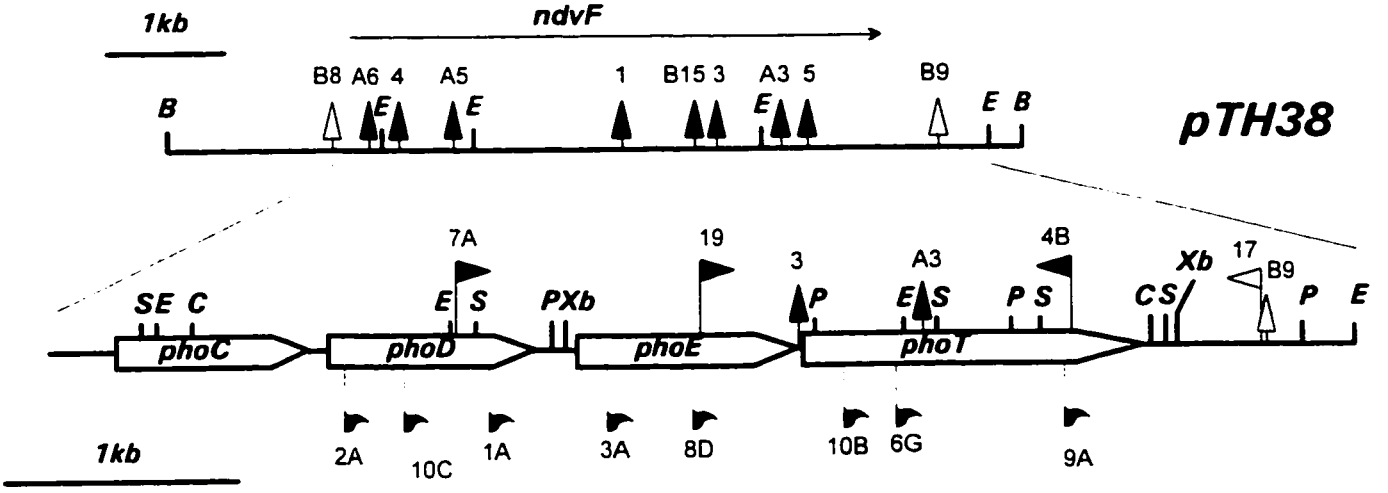

FIG. 1. (Top) Physical and genetic map of the *ndvF* locus of *R. meliloti* cloned in pTH38. The horizontal arrow above the pTH38 map shows the direction of transcription of *ndvF* as previously determined from the orientation of Tn*phoA* fusions. Filled (Fix$^-$) and open (Fix$^+$) arrows indicate locations of Tn*5* insertions that do and do not, respectively, abolish the ability of pTH38 to complement the Fix$^-$ phenotype of the *ndvF* deletion mutant RmF114 (8). (Bottom) The sequenced region (from insertion B8 to the indicated *Eco*RI site). The four ORFs, *phoC*, *phoD*, *phoE*, and *phoT*, are indicated. Also indicated are the locations of four Tn*5*-B20 insertions (flags facing up) and eight Tn*phoA* fusions (flags facing down). The direction of the flag points indicates the orientation of the *lacZ* and *phoA* genes. Restriction sites shown are *Bam*HI (B), *Cla*I (C), *Eco*RI (E), *Pst*I (P), *Sal*I (S), and *Xba*I (Xb).

DNA and derived protein sequences were analyzed with the PC Gene (Intelligenetics), Blast (2), CLUSTALV (23), and Top Pred II (10) software packages.

RNA extraction and primer extension. RNA was extracted from wild-type *R. meliloti* 1021 cultures as previously described (39). The purity and quality of the RNA were checked by electrophoresis through a 1.2% agarose gel with Tris-acetate-EDTA (TAE) running buffer. The contaminating DNA was removed by treatment with 270 U of RNase-free DNase (Boehringer-Mannheim) per ml for 30 min at 37°C in the presence of 6 U of RNase inhibitor (RNAguard; Pharmacia) per ml. This was followed by a phenol-chloroform-isoamyl alcohol (25:24:1) extraction and ethanol precipitation of the RNA.

To identify the transcription start site of the *phoC* mRNA, a specific oligonucleotide (5′GTCTTCTTGCCGAACTGGCGGGTTACGTTC3′) complementary to the beginning of the coding region of the gene was synthesized (Mobix; McMaster University). End labelling and extension of the primer with avian myeloblastosis virus reverse transcriptase were performed as previously described (39).

Transport and growth experiments. For phosphate transport assays, LBmc-grown cells were washed twice with MOPS-minimal medium, subcultured (1:50 dilution) into phosphate-free MOPS-minimal medium, and incubated with shaking (200 rpm) overnight at 30°C. Cells were harvested by centrifugation, washed at 4°C in MOPS minimal medium (without P [−P]), resuspended in the same medium to an optical density at 600 nm of 5, and stored at 4°C. For phosphate uptake assays, the cells were diluted 1:20 into MOPS minimal medium (−P) and incubated at 30°C for 5 min. A 12-μl volume of $^{33}P_i$ (60 μCi/μmol) was added to a final concentration of 10 μM. Aliquots (100 μl), removed at various times, were placed on a 0.45-μm-pore-size nitrocellulose filter (presoaked in 1 M K_2HPO_4) and immediately washed with MOPS minimal medium (−P). Filters were dried, placed in liquid scintillation vials with scintillation fluid, and counted in a scintillation spectrophotometer. For all experiments, we used chloroform-treated cells to determine the amount of background binding of $^{33}P_i$ to the bacterial cells. Succinate uptake experiments employing [^{14}C]succinate (2.5 μCi/μmol) at a final concentration of 40 μM were done as previously described (56).

To test strains for P utilization ability, cultures grown in LBmc were diluted 1:1,000 into 5 ml of MOPS-buffered minimal medium containing the indicated phosphorus sources at 2 mM. Cultures were grown with shaking at 30°C, and growth was monitored by measuring the optical density at 600 nm.

β-Galactosidase and alkaline phosphatase (AP) assays were performed with aliquots of cells from 5-ml cultures as previously described (39, 56).

Nucleotide sequence accession number. The nucleotide sequence (5,705 bp) of the *ndvF* locus of *R. meliloti* has been deposited in GenBank under accession number U59229.

RESULTS

Nucleotide sequence of the *ndvF* locus. The *ndvF* locus was previously localized to a 7.3-kb *Bam*HI fragment cloned in plasmid pTH38. Transposon Tn*5* insertion mutagenesis of pTH38 followed by complementation analysis further localized *ndvF* to a 5-kb region between the Fix$^-$ insertions B8 and B9 (Fig. 1). We have determined the nucleotide sequence for both strands of the 5,705-bp region from insertion B8 to the *Eco*RI site located 493 nucleotides beyond insertion B9 (Fig. 1). Analysis of this sequence revealed four nonoverlapping open reading frames (ORFs) encoding proteins of 270, 300, 320, and 505 amino acids, which we designated PhoC, PhoD, PhoE, and PhoT, respectively (Fig. 1). The four genes are transcribed in the direction predicted in a previous study employing AP gene fusions to the *ndvF* locus (8). A clear G+C bias was observed at the third nucleotide position of the codons within each ORF (79 to 83%), relative to the general G+C content (64%), and the results (not shown) of a codon preference plot employing an *R. meliloti* codon usage table suggested that the four predicted genes were expressed in *R. meliloti* (20). Putative ribosome-binding sites were identified for all ORFs, between 5 and 9 bp upstream of the ATG start codons ($AGGAAN_9ATG$, $GAGAAN_8ATG$, $CGGAAN_5ATG$, and $TAGGAN_7ATG$, respectively). The intergenic regions were 117 bp long between *phoC* and *phoD*, 172 bp long between *phoD* and *phoE*, and 9 bp between *phoE* and *phoT*. While it appears likely that these four genes compose an operon, further experiments are required to conclusively establish this supposition.

Characterization of the encoded proteins. A BLASTX search of GenBank revealed that the *ndvF*-encoded proteins were similar to the *E. coli phnC*, *phnD*, and *phnE* gene products (2, 9). The PhoC and PhoD proteins were homologous to PhnC and PhnD, respectively, while the PhoT and PhoE proteins were homologous to each other and to the *E. coli* PhnE protein. The *E. coli phn* genes are required for the transport and catabolism of phosphonates and are transcribed as an 11-kb operon (54). Phosphonates are organophosphorus compounds which have direct C-P bonds rather than the common C-O-P phosphodiester linkage. Sequence analysis and experimental evidence suggest that the *E. coli phnC*, *phnD*, and *phnE* genes encode a phosphonate and phosphate transport system of the ABC (ATP-binding cassette) class (54). In gram-negative bacteria, these transport systems are made up of a periplasmic binding protein, one or two integral membrane proteins, and a hydrophilic ATP-binding protein (13, 22).

CLUSTALV alignments of the *R. meliloti* Pho and *E. coli* Phn proteins are shown in Fig. 2. The PhoC and PhnC proteins are 43% identical. They are homologous to the highly conserved ATPase component of the ABC transport systems and contain the two Walker motifs associated with many nucleotide-binding proteins (residues 34 to 42 and 165 to 170) (Fig. 2; boxes A and B). The amino terminus of the PhoD protein has characteristics of an export signal sequence, such as a basic amino terminus, a hydrophobic core, and in this case two cleavage sites (amino acids 19/20 and 21/22) which conform to the (−3, −1) rule (37). This is in agreement with the periplasmic location of the substrate-binding protein present in all ABC transporters that mediate solute uptake (22). The *R. meliloti* PhoT protein contains 505 amino acid residues, and while it is much larger than the *R. meliloti* PhoE (320 amino acids) and *E. coli* PhnE (276 amino acids) proteins, its C-terminal 200 amino acids have a high level of homology with those two proteins (Fig. 2). This size difference is reminiscent of that found between the analogous integral membrane proteins MalF (514 amino acids) and MalG (296 amino acids) of the ABC-type maltose transport system of *E. coli* (11, 18).

Membrane topology of the PhoCDET proteins. In a previous study, we isolated mutants with *ndvF*::Tn*phoA* gene fusions which expressed AP activity (8). Such fusions are generally only active when AP is fused to an exported protein or to the external domain of a transmembrane protein (35). Analysis of the DNA sequence of the *ndvF*::Tn*phoA* fusion junctions (Fig. 1) revealed that all formed in-frame protein fusions between AP and the predicted PhoD, PhoE, and PhoT proteins. No Tn*phoA* insertions which expressed AP activity were located in the *phoC* gene. This is not surprising in view of the similarity between PhoC and the hydrophilic ATP-binding component of ABC transport systems; these proteins appear to be located in the cytoplasm, where they associate with the cytoplasmic membrane (22; see also reference 3). The three *ndvF*::Tn*phoA* insertions (2A, 10C and 1A, Fig. 1) which showed the highest level of AP activity were located in the *phoD* gene. Together with the predicted N-terminal secretory leader peptide of PhoD, these data are consistent with the proposed role of PhoD as a periplasmic binding protein.

Of the remaining five Tn*phoA* insertions, 3A and 8D fused AP to PhoE at amino acid residues 51 and 188, respectively, while 10B, 6G, and 9A fused AP to PhoT at amino acid residues 62, 239, and 397, respectively. Hydrophobicity plots of PhoE and PhoT revealed that each of these proteins contains four "certain" and two "putative" transmembrane domains (Fig. 2) (10). Consistent with the positive-inside rule (53), if we assume that there are six transmembrane domains and that the N termini are in the cytoplasm, we calculate a lysine-plus-arginine cytoplasmic-domain bias of 10 for PhoE and 8 for PhoT. AP fusion 3A in PhoE and fusions 10B and 6G in PhoT are located between the first and second predicted transmembrane domains (boxes 1 and 2 in Fig. 2). Therefore, for these fusions to be external, the N termini of the PhoE and PhoT proteins must be located in the cytoplasm. When this topology is extended across the protein, we note that insertion 9A in PhoT is located in the second predicted periplasmic domain (between boxes 3 and 4 in Fig. 2). Insertion 8D fuses AP to PhoE, 4 amino acids from the C-terminal end of the predicted third transmembrane domain; we assume that this fusion extends into the periplasm. In comparing the derived topologies of PhoE and PhoT, it is evident that much of the difference between these two proteins resides in the 258-amino-acid periplasmic loop of PhoT, which is very large in comparison with the equivalent 76-amino-acid loop of PhoE (see regions between boxes 1 and 2 in Fig. 2).

Phosphate and phosphonate phenotype of *ndvF* mutants. The above results prompted us to examine the ability of wild-type *R. meliloti* and three *ndvF* mutants to utilize various sources of phosphorus for growth in MOPS-buffered minimal medium. We compared the parental strain 1021 with the insertion mutants Rm G490 (*phoC490*) and Rm G491 (*phoT491*) and the deletion strain Rm G439, in which a 12-kb region including the *phoCDET* genes has been removed. Whereas the wild type and mutants grew well in media containing 2 mM glycerol-3-phosphate or aminoethylphosphonate as P sources, all three mutants grew very poorly in media containing 2 mM P_i as the P source (Fig. 3; data for *R. meliloti* Rm 490 and Rm 491 were similar). These results suggested that the mutant strains were defective in P_i assimilation.

The deletion strain, Rm G439, grew poorly with aminomethyl- or methylphosphonate as the P source, while growth of the *phoC* and *phoT* insertion mutants, Rm G490 and Rm G491, on these phosphonates was similar to that of the wild type (Fig. 3 and data not shown). Limited DNA sequencing of regions outside the *phoCDET* genes, but within the region deleted in strain Rm G439, has revealed a gene homologous to the *phnM* gene of *E. coli* (9); the *phnM* gene product is believed to be part of an enzyme complex (C-P lyase) which cleaves the C-P bond upon entry of the phosphonate into the cell. We assume that deletion of *phnM* (and perhaps other *phn* genes) in strain Rm G439 inactivates the C-P lyase with the result that Rm G439 cannot degrade or grow in media containing aminomethyl- and methylphosphonate as P sources. The growth of the *phoC* and *phoT* mutants with aminomethyl- and methylphosphonate suggests that these compounds can be transported by an alternate system in *R. meliloti*. It is not yet clear whether the PhoCDET proteins are involved in phosphonate uptake. In this respect, we note that *Enterobacter aerogenes* has two phosphonate degradative pathways (27).

To determine the nature of the phosphate utilization defect in the *ndvF* mutants, we examined phosphate-starved cells of the wild type and the *ndvF* mutant Rm G439 for their ability to take up $^{33}P_i$. As a positive control, we examined the ability of the same cells to transport [^{14}C]succinate (Fig. 4). Unlike the parent strain Rm 1021, the *ndvF* mutant failed to transport phosphate, whereas both strains transported succinate at similar rates. Together, the uptake, growth, and sequence homology data show that the *ndvF* locus encodes an uptake system which transports P_i, and possibly phosphonates, across the cytoplasmic membrane.

Phosphate control of *ndvF* expression. To determine whether expression of the *ndvF* locus responds to available phosphate, we employed Tn*5*-B20 (45) to generate transcriptional gene fusions between *lacZ* and *ndvF* on the cosmid pTH21. The DNA sequences of the fusion junctions of four Tn*5*-B20 insertions which lay within the 7.3-kb *Bam*HI restriction fragment were determined (Fig. 1). Insertions 7A and 19 were located in, and transcribed in the same direction as, the *phoD* and *phoE* genes, respectively. Insertion 4B was in the *phoT* gene, and the direction of transcription of *lacZ* was opposite to that of *phoT*. Insert 17 lay downstream of the *phoCDET* genes. Employing these plasmid-borne gene fusions in an *R. meliloti* Lac$^-$ background, we assayed for β-galactosidase activities in cells cultured in a MOPS-buffered minimal medium with added phosphate (2 mM) and without added phosphate (Fig. 5). We also measured AP activity, as this activity is known to be derepressed in P-limited cultures (46, 54). As expected, we observed high-level AP activities in all cells cultured in the absence of added P and low-level activity in cells grown in the media containing P (Fig. 5, open bars). The β-galactosidase activities of strains carrying insertion 4B

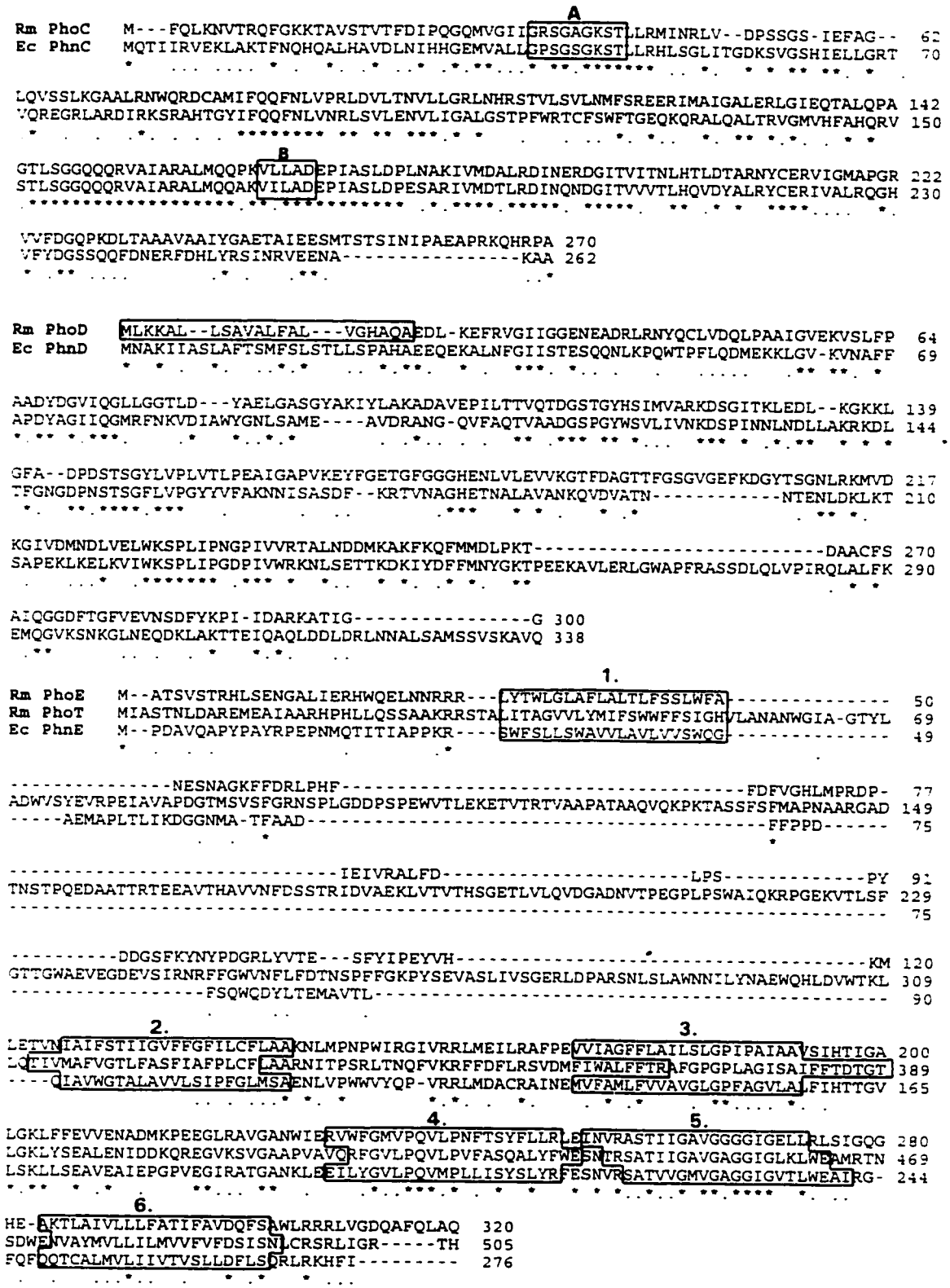

FIG. 2. Alignment of deduced amino acid sequences for *R. meliloti* (Rm) *phoC*, *phoD*, and *phoET* with the PhnC, PhnD, and PhnE proteins of *E. coli* (Ec) respectively. The * and . symbols below the sequences indicate residues which are identical and conserved, respectively, within the proteins. Boxes A and B in the *R. meliloti* PhoC-*E. coli* PhnC alignment indicate the conserved Walker motifs characteristic of many nucleotide-binding proteins. The N-terminal boxed region of *R. meliloti* PhoD indicates a potential secretory signal sequence. Boxed regions in the alignment between *R. meliloti* PhoE, *R. meliloti* PhoT, and *E. coli* PhnE indicate certain (boxes 1, 2, 3, and 6) and putative (boxes 4 and 5) membrane-spanning segments as predicted by Top Pred II (10).

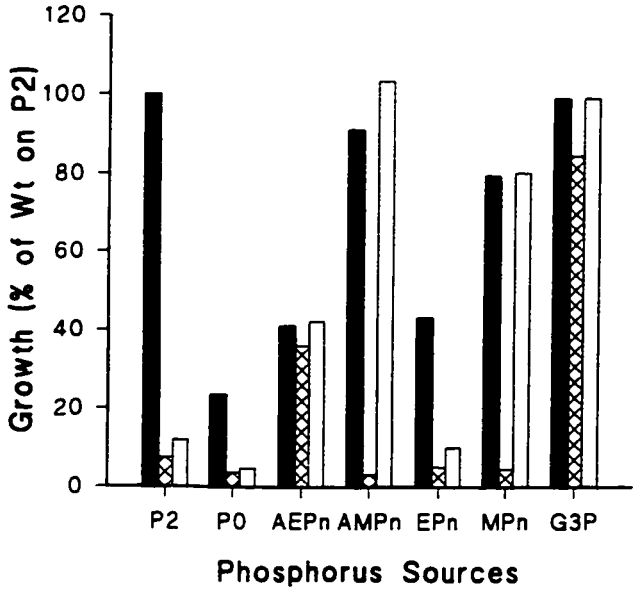

FIG. 3. Histogram representing the growth of wild-type *R. meliloti* Rm 1021 (black bars), the *phoCDET* deletion mutant, Rm G439 (cross-hatched bars), and the *phoC490* insertion mutant, Rm G490 (open bars), when supplied with various sources of P. MOPS-minimal medium contained no phosphate (P0), 2 mM P_i (P2), 2 mM aminoethylphosphonate (AEPn), 2 mM aminomethylphosphonate (AMPn), 2 mM methylphosphonate (MPn), 2 mM ethylphosphonate (EPn), or 2 mM glycerol-3-phosphate (G3P). The optical density at 600 nm (OD_{600}) measured after 60 h is reported as a percentage of the growth of strain 1021 in 2 mM P_i (OD_{600} = 0.8). Values are the means of triplicate determinations.

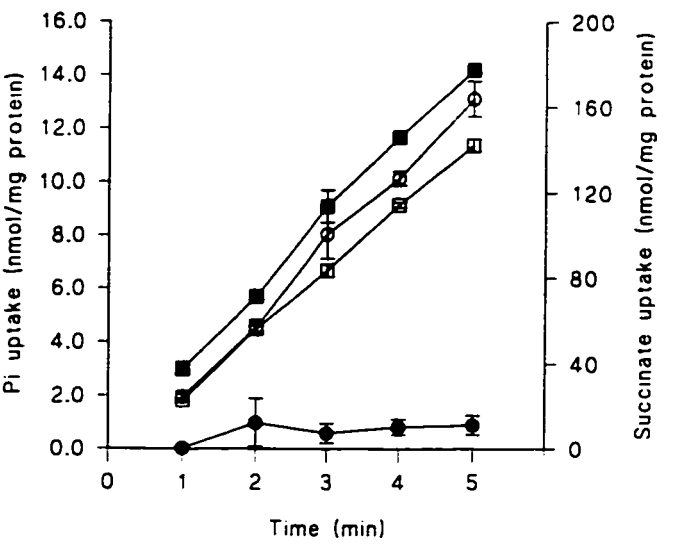

FIG. 4. Uptake of phosphate and succinate by phosphate-starved cells of strains Rm 1021 (■, □) and Rm G439 (●, ○). Closed symbols indicate phosphate uptake, and open symbols indicate succinate uptake. The cells were starved for 24 h in a phosphate-free MOPS medium containing 15 mM succinate and 15 mM glucose as carbon sources. The uptake experiment was performed in the same medium except that glucose was provided as an energy source. 10 μM $^{32}P_i$ and 40 μM [^{14}C]succinate were added to the medium for the phosphate and succinate uptake assays, respectively. Values are the means of triplicate determinations ± standard errors.

or 17 were similar under the two growth regimes; however, the *phoD* and *phoE* gene fusions 19 and 7A were induced 10- to 25-fold in response to phosphate starvation (Fig. 5, black bars). Thus, expression of *phoD* and *phoE* is derepressed in response to limiting phosphate. The substantially lower level of β-galactosidase activity detected from the strain with the *phoE* gene fusion (fusion 19) in comparison with that for the *phoD* fusion (fusion 7A) suggests that these genes may be differentially expressed. In agreement with this suggestion, we note that an examination of the previously reported AP activities derived from strains carrying the *pho*::Tn*phoA* insertions (Fig. 1) reveals that the levels of activity from strains with the *phoD* insertions (2A, 10C, and 1A) were at least three times higher than the activity from *phoE* or *phoT* insertion strains (3A, 8D, 10B, 6G, and 9A) (see Fig. 2 in reference 8). It is possible that the 172-bp *phoD-phoE* intergenic region has a role in regulating *phoE* and *phoT* expression.

To map the transcription start site of *phoC*, we extracted mRNA from cells grown in LBmc, as we have observed that the expression level of the *phoD* and *phoE lacZ* fusions (fusions 7A and 19) was high in LBmc-grown cells. In two separate experiments, we extended a primer from the 5′ end of *phoC* (see Materials and Methods) and observed one major transcript which started 40 bp upstream of the translational start codon (Fig. 6). Analysis of this region revealed a possible −10 region preceded by two tandem 18-bp sequences, located at bp −23 to −40 and −45 to −62 relative to the transcriptional start site, which share 12 and 11 identical nucleotides, respectively, with the PHO box consensus CTGTCATA(A,T)A(A,T)CTGTCA(C,T) of *E. coli* (33, 54).

DISCUSSION

The data in this paper demonstrate that the *ndvF* locus of *R. meliloti* consists of four genes, *phoCDET*, which together code for an ABC-type solute uptake system that transports phosphate, and possibly phosphonates, across the cytoplasmic membrane. *R. meliloti ndvF* mutants form root nodules which fail to fix N_2(Fix$^-$). In many of these mutant nodules, the infection process is blocked early, before release of the bacteria from the infection threads (8). Given that we now know that the *ndvF* locus encodes a phosphate transport system, and that *ndvF* mutants fail to grow in defined medium containing 2 mM $H_2PO_4^-$ as the sole P source, it seems likely that the Fix$^-$ symbiotic phenotype results from an inability of the mutants to

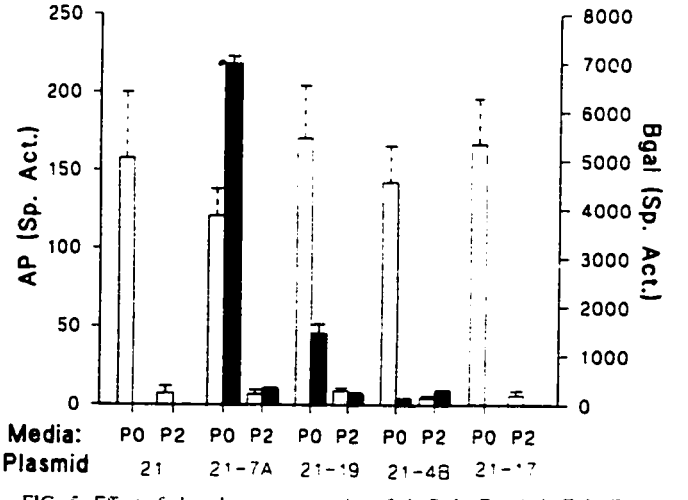

FIG. 5. Effect of phosphate on expression of *phoD::lacZ* and *phoE::lacZ* gene fusions. *R. meliloti* cells carrying Tn*5*-B20 insertions in plasmid pTH21 were cultured in MOPS-minimal medium containing no added P_i (P0) or 2 mM P_i (P2). Specific activities (Sp. Act.) for β-galactosidase (Bgal) (closed bars) and AP (open bars) were determined. Values are the means ± standard errors of the mean for triplicate assays.

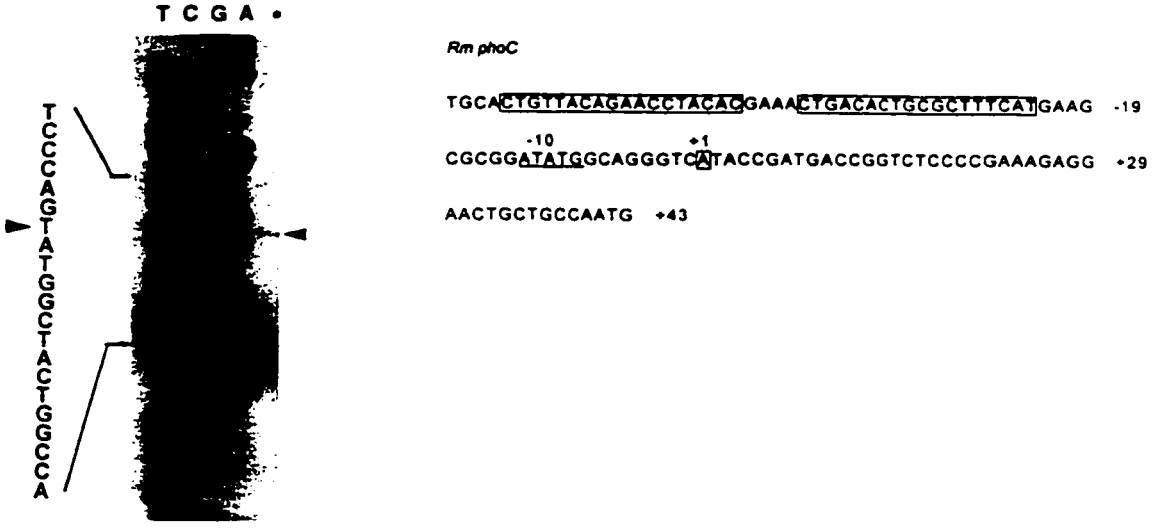

FIG. 6. Promoter analysis of *R. meliloti* (*Rm*) *phoC* gene. The autoradiograph contact print shows the primer extension product (lane +) (30 μg of RNA from LBmc-grown strain Rm 1021) and the products of sequencing reactions with the same primer. The relevant sequence is shown on the left of the gel, and the position of the extension product is indicated by an arrowhead. On the right is shown the promoter region of *R. meliloti phoC*. The transcription start site is indicated by +1, the −10 region is underlined, and the boxed sequences indicate the positions of the two putative PHO boxes.

grow during the infection process within the nodule. The *ndvF* mutants exhibit a delay in inducing root nodules in comparison with nodule development with the wild-type strain (8). This delay may also result from reduced bacterial growth, and thus requirement for a longer time period to reach a cell density such that sufficient Nod factor signal is synthesized to trigger root nodule formation (30). There are other possible explanations for the symbiotic phenotype of the *ndvF* mutants: for example, the P status of the bacteria may be involved in the regulation of other cellular processes involved in the symbiosis. In this respect, it is interesting that in the plant pathogen *Agrobacterium tumefaciens*, phosphate starvation increases the expression of the central virulence regulatory gene, *virG* (55). We are currently investigating the nature of the symbiotic defect by characterizing strains carrying second-site mutations which suppress the Fix$^-$ phenotype of the *ndvF* mutants (38). The elucidation of the biochemical mechanism of suppression will clarify the role of the *ndvF* locus in nodule development.

The conclusion that the *phoCDET* genes encode a periplasmic binding protein-dependent system for the transport of phosphate and likely phosphonates is based on (i) the high degree of homology of PhoC to the ATP-binding proteins of the ABC-type transport systems and the deduced topology of the PhoD, PhoE, and PhoT proteins; (ii) the fact that *phoCDET* mutants fail to grow in defined media containing 2 mM P_i; and (iii) the failure of the *phoCDET* deletion mutant, RmG439, to transport ^{33}P-labelled phosphate despite its ability to transport succinate at wild-type rates.

The inability of the *R. meliloti phoCDET* mutants to grow when P is supplied as 2 mM P_i suggests that the *phoCDET* genes encode the sole phosphate transport system in *R. meliloti*. Conversely, the growth of the *phoCDET* insertion and deletion mutants in media containing 2 mM glycerol-3-phosphate or aminoethylphosphonate indicates that there are separate uptake systems for these compounds in *R. meliloti*. The existence of distinct phosphate and glycerol-3-phosphate uptake systems in many bacterial species is well-known (e.g., see reference 26), and *E. aerogenes* probably has two separate phosphonate transporters capable of aminoethylphosphonate transport (27). Data from uptake experiments employing cells of various *Rhizobium* species grown under P-limiting and P-excess conditions also led other workers to conclude that rhizobia contain a single, repressible, energy-dependent phosphate transport system (47). However, bacterial phosphate transport is best characterized in *E. coli* and *Acinetobacter johnsonii*, and both of these organisms contain two major P_i transport systems: one is a low-affinity system (*pit*) which is believed to be constitutively expressed, and the other is a high-affinity, binding protein-dependent system (*pstSCAB*) which is expressed under phosphate-limiting conditions (43, 50, 51). We believe that it is premature to conclude that *R. meliloti* contains a single phosphate transport system, as we recently identified a *pit*-like gene, and the expression and regulation of this gene are currently under investigation (4). The PhoCDET proteins of *R. meliloti* are clearly similar to the phosphonate uptake proteins PhnCDE of *E. coli* (Fig. 2) rather than to the proteins of the *pstSCAB*-encoded high-affinity phosphate transport system of *E. coli*. The phosphonate transport genes are cryptic in *E. coli* K-12-derived strains (34); however, when this system is active, there is good evidence that it can transport P_i in addition to phosphonates (36). Further experiments are required to definitively establish that the *R. meliloti* PhoCDET system also transports phosphonates. In this respect, we note that in one study, all of the members of the family *Rhizobiaceae* examined were able to utilize methyl-, ethyl-, aminomethyl-, and aminoethylphosphonate as sole sources of P (32).

In view of the very low concentrations of soluble P_i in most soils (0.1 to 10 μM) (6), it is possible that the acquisition of phosphate plays an important role in the growth and survival of soil microorganisms. In this respect, it is interesting that Beck and Munns (5) found a large variation in the ability of strains from various *Rhizobium* species to grow and survive at very low phosphate concentrations. Moreover, Almendras and Bottomley (1) and Leung and Bottomley (31) have presented strong evidence to establish a link between the phosphate-sequestering abilities of *Rhizobium trifolii* strains and nodulation competition, as influenced by the addition of phosphate or lime to soil.

In *E. coli*, the PHO regulon consists of some 30 genes in

eight operons whose expression is derepressed under phosphate-limiting conditions (43, 54). Transcription of these operons is regulated by the PhoB protein, which binds to similar 18-bp sequences (PHO boxes) in the regions of their promoters from positions −22 to −42. We have identified two tandem PHO-box-like sequences, located at bp −23 to −40 and −45 to −62 relative to the transcriptional start site of the *R. meliloti phoC* gene (Fig. 6). The *pstS* and *ugpB* promoters in *E. coli* have similarly arranged PHO boxes also, with a 4-nucleotide gap between boxes. As expression of the *phoD* and *phoE* genes is induced over 10-fold in response to phosphate starvation (Fig. 5), it is likely that the two putative PHO boxes in the *phoC* promoter are functional. It is also likely that *phoCDET*, and the other genes which constitute the PHO regulon in *R. meliloti*, will be derepressed under the low-phosphate conditions found in soil.

The recognition that the *phoCDET* genes encode a phosphate transport system is also of interest, as this locus is located on the 1,700-kb pEXO megaplasmid of *R. meliloti*. As in the case of genes involved in thiamine biosynthesis and carbohydrate utilization, and the other genes located on this plasmid (7, 16), the *phoCDET* genes are likely to be important to the life of the bacteria in the soil environment; however, they are clearly not essential for growth of the bacteria under all culture conditions.

ACKNOWLEDGMENTS

This work was supported by NSERC Research and Strategic grants to T.M.F.

We are grateful to Brian Golding and Dick and Brian Morton for advice and assistance with DNA and protein sequence analysis, Kim Napper for technical assistance, and Brian Driscoll and Ralf Voegele for critical comments on the manuscript.

REFERENCES

1. **Almendras, A. S., and P. J. Bottomley.** 1987. Influence of lime and phosphate on nodulation of soil-grown *Trifolium subterraneum* L. by indigenous *Rhizobium trifolii*. Appl. Environ. Microbiol. **53**:2090–2097.
2. **Altschul, S. F., W. Gish, W. Miller, E. W. Myers, and D. J. Lipman.** 1990. Basic local alignment research tool. J. Mol. Biol. **215**:403–410.
3. **Baichwal, V., D. Liu, and G. Ames.** 1993. The ATP-binding component of a prokaryotic traffic ATPase is exposed to the periplasmic (external) surface. Proc. Natl. Acad. Sci. USA **90**:620–624.
4. **Bardin, S., and T. M. Finan.** Unpublished data.
5. **Beck, D. P., and D. N. Munns.** 1984. Phosphate nutrition of *Rhizobium* spp. Appl. Environ. Microbiol. **47**:278–282.
6. **Bieleski, R. L.** 1973. Phosphate pools, phosphate transport, and phosphate availability. Annu. Rev. Plant Physiol. **24**:225–252.
7. **Charles, T. C., and T. M. Finan.** 1991. Analysis of a 1600 kilobases *Rhizobium meliloti* megaplasmid using *in vivo* generated defined deletions. Genetics **127**:5–20.
8. **Charles, T. C., W. Newcomb, and T. M. Finan.** 1991. NdvF, a novel locus located on megaplasmid pRmeSU47b (pExo) of *Rhizobium meliloti*, is required for normal nodule development. J. Bacteriol. **173**:3981–3992.
9. **Chen, C. M., Q.-Z. Ye, Z. Zhu, B. L. Wanner, and C. T. Walsh.** 1990. Molecular biology of carbon-phosphorus bond cleavage. J. Biol. Chem. **265**: 4461–4471.
10. **Claros, M. G., and G. von Heijne.** 1994. TopPred II: an improved software for membrane protein structure predictions. Comput. Appl. Biosci. **10**:685–686.
11. **Dassa, E., and M. Hofnung.** 1985. Sequence of gene *malG* in *E. coli*: homologies between integral membrane components from binding protein-dependent transport systems. EMBO J. **4**:2287–2293.
12. **Ditta, G. R., E. Viris, A. Palomares, and C. H. Kim.** 1987. The *nifA* gene of *Rhizobium meliloti* is oxygen regulated. J. Bacteriol. **169**:3217–3223.
13. **Doige, C. A., and D. F.-L. Ames.** 1993. ATP-dependent transport systems in bacteria and humans: relevance to cystic fibrosis and multidrug resistance. Annu. Rev. Microbiol. **47**:291–319.
14. **Dylan, T., P. Nagpul, D. R. Helinski, and G. R. Ditta.** 1990. Symbiotic pseudorevertants of *Rhizobium meliloti ndv* mutants. J. Bacteriol. **172**:1409–1417.
15. **Finan, T. M., A. M. Hirsch, J. A. Leigh, E. Johansen, G. A. Kuldau, S. Deegan, G. C. Walker, and E. R. Signer.** 1985. Symbiotic mutants of *Rhizobium meliloti* that uncouple plant from bacterial differentiation. Cell **40**:869–877.
16. **Finan, T. M., B. Kunkel, G. F. DeVos, and E. R. Signer.** 1986. Second symbiotic megaplasmid of *Rhizobium meliloti* carrying exopolysaccharide and thiamine biosynthetic genes. J. Bacteriol. **167**:66–72.
17. **Fisher, H. M.** 1994. Genetic regulation of nitrogen fixation in rhizobia. Microbiol. Rev. **58**:352–386.
18. **Froshauer, S., and J. Beckwith.** 1984. The nucleotide sequence of the gene for the *malF* protein, an inner membrane component of the maltose transport system of *Escherichia coli*. J. Biol. Chem. **259**:10896–10903.
19. **Geremia, R. A., S. Cavaignac, A. Zorreguieta, N. Toro, J. Olivares, and R. A. Ugalde.** 1987. A *Rhizobium meliloti* mutant that forms ineffective pseudonodules in alfalfa produces exopolysaccharides but fails to form β-(1-2) glucan. J. Bacteriol. **169**:880–884.
20. **Gribskov, M., J. Devereux, and R. R. Burgess.** 1984. The codon preference plot: graphic analysis of protein coding sequences and prediction of gene expression. Nucleic Acids Res. **12**:539–548.
21. **Henikoff, S.** 1984. Unidirectional digestion with exonuclease III creates targeted breakpoints for DNA sequencing. Gene **28**:351–359.
22. **Higgins, C. F.** 1992. ABC transports: from microorganisms to man. Annu. Rev. Cell Biol. **8**:67–113.
23. **Higgins, D. G., A. J. Beasby, and R. Fuchs.** 1992. CLUSTALV: improved software for multiple alignment. Comput. Appl. Biosci. **8**:189–191.
24. **Honeycutt, R. J., M. McClelland, and B. W. Sobral.** 1993. Physical map of the genome of *Rhizobium meliloti* 1021. J. Bacteriol. **175**:6945–6952.
25. **Hynes, M., R. Simon, P. Muller, K. Niehaus, M. Labes, and A. Puhler.** 1986. The two megaplasmids of *Rhizobium meliloti* are involved in the effective nodulation of alfalfa. Mol. Gen. Genet. **202**:356–362.
26. **Larson, T., G. Schumacher, and W. Boos.** 1982. Identification of the *glpT*-encoded *sn*-glycerol-3-phosphate permease of *Escherichia coli*, an oligomeric integral membrane protein. J. Bacteriol. **152**:1008–1021.
27. **Lee, K., W. Metcalf, and B. Wanner.** 1992. Evidence for two phosphonate degradative pathways in *Enterobacter aerogenes*. J. Bacteriol. **174**:2501–2510.
28. **Leigh, J. A., and D. L. Coplin.** 1992. Exopolysaccharides in plant-bacterial interactions. Annu. Rev. Microbiol. **46**:307–346.
29. **Leigh, J. A., E. R. Signer, and G. C. Walker.** 1985. Exopolysaccharide deficient mutants of *Rhizobium meliloti* that form ineffective nodules. Proc. Natl. Acad. Sci. USA **82**:6231–6234.
30. **Lerouge, P., P. Roche, C. Faucher, F. Maillet, G. Truchet, J. C. Prome, and J. Denaire.** 1990. Symbiotic host specificity of *Rhizobium meliloti* is determined by a sulphated and acylated glucosamine oligosaccharide signal Nature (London) **344**:781–784.
31. **Leung, K., and P. J. Bottomley.** 1987. Influence of phosphate on the growth and nodulation characteristics of *Rhizobium trifolii*. Appl. Environ. Microbiol. **53**:2098–2105.
32. **Liu, C.-M., P. A. McLean, C. C. Sookdeo, and F. C. Cannon.** 1991. Degradation of the herbicide glyphosate by members of the family *Rhizobiaceae*. Appl. Environ. Microbiol. **57**:1799–1804.
33. **Makino, K., M. Amemura, S. Kim, A. Nakata, and H. Shinagawa.** 1994. Mechanism of transcriptional activation of the phosphate regulon in *Escherichia coli*. p. 5–12. *In* A. Torriani-Gorini, E. Yagil, and S. Silver (ed.), Phosphate in microorganisms. ASM Press, Washington, D.C.
34. **Makino, K., S. Kim, H. Shinagawa, M. Amemura, and A. Nakata.** 1991. Molecular analysis of the cryptic and functional *phn* operons for phosphonate use in *Escherichia coli* K-12. J. Bacteriol. **173**:2665–2672.
35. **Manoil, C., and J. Beckwith.** 1985. TnphoA, a transposon probe for protein export signals. Proc. Natl. Acad. Sci. USA **82**:8129–8133.
36. **Metcalf, W. W., and B. L. Wanner.** 1991. Involvement of the *Escherichia coli phn* (*psiD*) gene cluster in assimilation of phosphorus in the form of phosphonates, phosphite, P_i^* esters, and P_i. J. Bacteriol. **173**:587–600.
37. **Oliver, D.** 1985. Protein secretion in *Escherichia coli*. Annu. Rev. Microbiol. **39**:615–648.
38. **Oresnik, I. J., T. C. Charles, and T. M. Finan.** 1994. Second site mutations specifically suppress the Fix− phenotype of *Rhizobium meliloti* mutations on alfalfa: identification of a conditional ndvF-dependent mucoid colony phenotype. Genetics **136**:1233–1243.
39. **Osteras, M., B. T. Driscoll, and T. M. Finan.** 1995. Molecular and expression analysis of the *Rhizobium meliloti* phosphoenolpyruvate carboxykinase (*pckA*) gene. J. Bacteriol. **177**:1452–1460.
40. **Peters, N. K., J. W. Frost, and S. R. Long.** 1986. A plant flavone, luteolin, induces expression of *Rhizobium meliloti* nodulation genes. Science **233**:977–980.
41. **Reed, J. W., and G. C. Walker.** 1991. Acidic conditions permit effective nodulation of alfalfa by invasion-deficient *Rhizobium meliloti* exoD mutants. Genes Dev. **5**:2274–2287.
42. **Rosenberg, C., P. Boitard, J. Dénarié, and F. Casse-Delbart.** 1981. Genes controlling early and late functions in symbiosis are located on a megaplasmid in *Rhizobium meliloti*. Mol. Gen. Genet. **184**:326–333.
43. **Rosenberg, H.** 1987. Phosphate transport in prokaryotes. p. 205–248. *In* B. Rosen and S. Silver (ed.), Ion transport in prokaryotes. Academic Press, Inc., New York.
44. **Sambrook, J., E. F. Fritsch, and T. Maniatis.** 1989. Molecular cloning: a laboratory manual. 2nd ed. Cold Spring Harbor Laboratory, Cold Spring Harbor, N.Y.

45. **Simon, R., J. Quandt, and W. Klipp.** 1989. New derivatives of transposon Tn*5* suitable for mobilization of replicons, generation of operon fusions and introduction of genes in Gram-negative bacteria. Gene **80**:161–169.
46. **Smart, J. B., M. J. Dilworth, and A. D. Robson.** 1984. Effect of phosphorus supply on phosphate uptake and alkaline phosphatase activity in Rhizobia. Arch. Microbiol. **140**:218–286.
47. **Smart, J. B., A. D. Dobson, and M. J. Dilworth.** 1984. A continuous culture study of the phosphorus nutrition of *Rhizobium trifolii* WU95. *Rhizobium* NGR234 and *Bradyrhizobium* CB756. Arch. Microbiol. **140**:276–280.
48. **Soupène, E., M. Foussard, P. Boistard, G. Truchet, and J. Batut.** 1995. Oxygen as a key developmental regulator of *Rhizobium meliloti* N_2-fixation gene expression within the alfalfa root nodule. Proc. Natl. Acad. Sci. USA **92**:3759–3763.
49. **Spaink, H. P., D. M. Sheeley, A. A. van Brussel, J. Glushka, W. S. York, T. Tak, O. Geiger, E. P. Kennedy, V. N. Reinhold, and B. J. Lugtenberg.** 1991. A novel highly unsaturated fatty acid moiety of lipo-oligosaccharide signals determines host specificity of *Rhizobium*. Nature (London) **354**:125–130.
50. **van Veen, H. W., T. Abee, G. J. J. Kortstee, W. N. Konings, and A. J. B. Zehnder.** 1993. Mechanism and energetics of the secondary phosphate transport system of *Acinetobacter johnsonii 210A*. J. Biol. Chem. **268**:19377–19383.
51. **van Veen, H. W., T. Abee, G. J. J. Kortstee, W. N. Konings, and A. J. B. Zehnder.** 1994. Substrate specificity of the two phosphate transport systems of *Acinetobacter johnsonii 210A* in relation to phosphate speciation in its aquatic environment. J. Biol. Chem. **269**:16212–16216.
52. **Vieirra, J., and J. Messing.** 1987. Production of single-stranded plasmid DNA. Methods Enzymol. **153**:3–34.
53. **von Heijne, G.** 1986. The distribution of positively charged residues in bacterial inner membrane proteins correlates with the trans-membrane topology. EMBO J. **5**:3021–3027.
54. **Wanner, B. L.** 1993. Gene regulation by phosphate in enteric bacteria. J. Cell. Biochem. **51**:47–54.
55. **Winans, S.** 1990. Transcriptional induction of an *Agrobacterium* regulatory gene at tandem promoters by plant-released phenolic compounds, phosphate starvation, and acidic growth media. J. Bacteriol. **172**:2433–2438.
56. **Yarosh, O. K., T. C. Charles, and T. M. Finan.** 1989. Analysis of C4-dicarboxylate transport genes in *Rhizobium meliloti*. Mol. Microbiol. **3**:813–823.

2- Specificity of the phosphate transport system encoded by *phoCDET*.

To determine the affinity and the specificity of the PhoCDET phosphate transport system, kinetic constants were determined and competition studies were performed. Phosphate uptake over a 5 minute period showed that the *phoCDET* deletion mutant RmG439, starved for phosphate, was unable to transport phosphate (Pi) when 10μM ^{33}P-orthophosphate was provided in the medium (see Fig. 4; Bardin et al., 1996). The kinetic constants of the wild type strain Rm1021, grown under phosphate limitation, were then determined using concentrations of ^{33}P-labeled orthophosphate from 0.05 to 3μM. When the data was plotted using [S] versus v axes, a typical Michaelis-Menten curve was obtained (Fig. 3-1). A Km value of 0.21μM and a Vmax value of 6.7 nmol Pi/min/mg protein was determined using a Hanes-Woolf plot (Fig. 3-2). The very low Km value obtained for Pi uptake indicated that *phoCDET* encodes a high affinity phosphate transport system, similar to *pst*, the high affinity phosphate transport system of *E. coli* (Km: 0.4μM; Willsky and Malamy, 1980a).

The sequence homology between the phosphonate transport system of *E. coli* (*phnCDE*) and *phoCDET* indicates that *ndvF* may also be involved in phosphonate uptake (Bardin et al., 1996). The specificity of PhoCDET for phosphate was addressed by performing experiments investigating the inhibition of phosphate uptake by various phosphonate compounds. Inhibition experiments

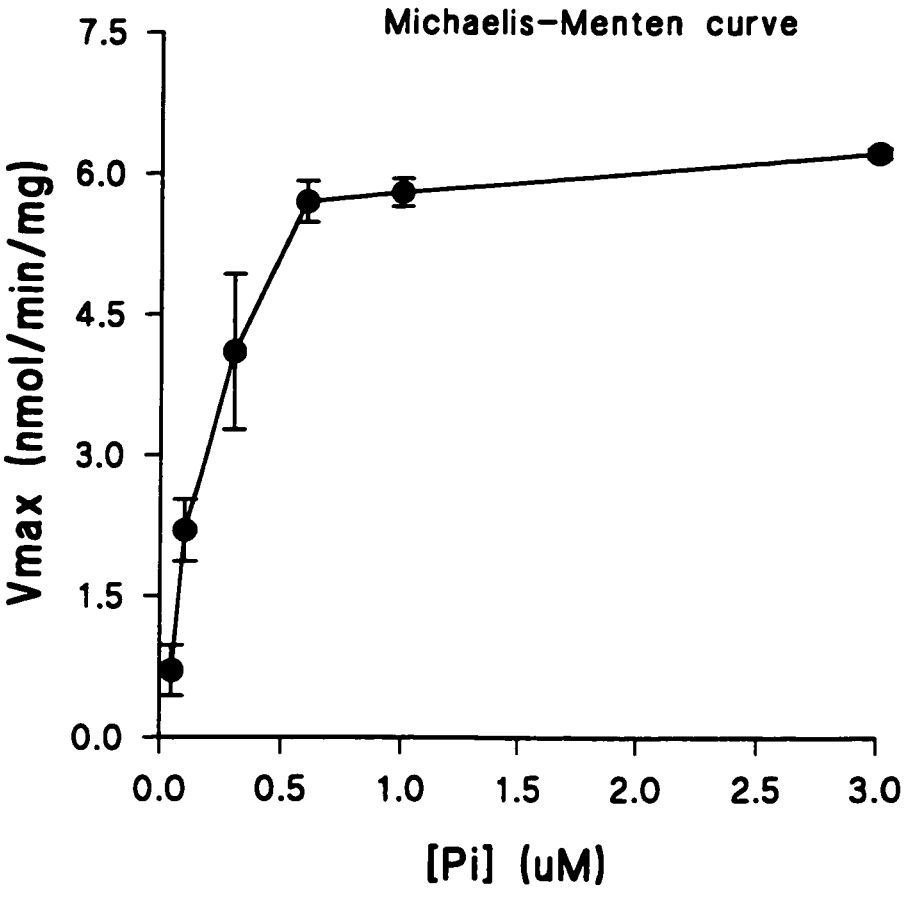

Fig. 3-1: Michaelis-Menten curve showing phosphate uptake of phosphate-starved wild type strain when concentrations between 0 and 3μM of ^{33}P-labeled phosphate were provided to the reaction mixture. Each point represents the average of triplicate value ± standard error (error bars).

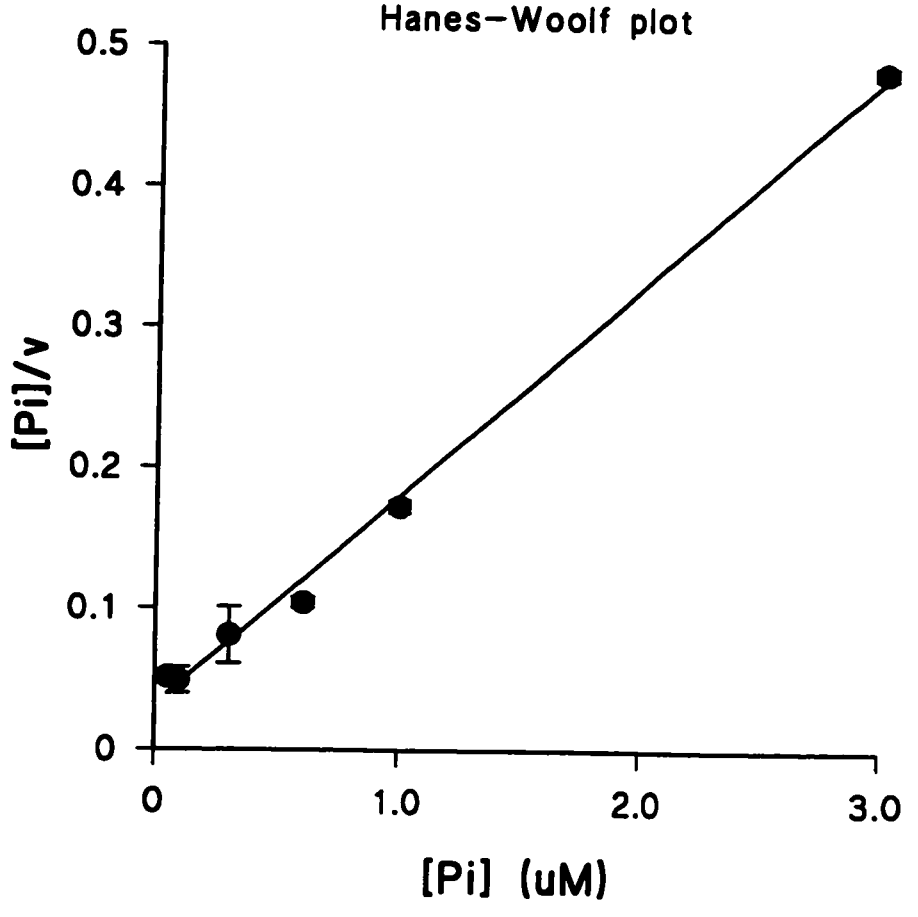

Fig. 3-2: Hanes-Woolf plot used to determine the kinetic values of phosphate uptake by the PhoCDET system. Each point represents the average of triplicate values. The linear regression was calculated to :
$Y = 0.148348 (X) + 0.031835$ with correlation coefficient of $r^2 = 0.996114$.

by arsenate were also performed as this phosphate analogue was shown to compete with phosphate for transport in many organisms such as *E. coli* (Bennett and Malamy, 1970), *Bacillus cereus* (Rosenberg et al., 1969), *Micrococcus lyzodeikticus* (Friedberg, 1977) and *Streptococcus faecalis* (Harold and Spitz, 1975). Inhibitors were provided at 5 (5μM) and 50 times (50μM) the concentration of labeled phosphate (1μM).

Cold phosphate at 5 times the labeled-phosphate concentration showed 82% uptake inhibition as expected (Table 3-1). Succinate was used as a negative control and showed no phosphate uptake inhibition. Ethylphosphonate (EP), aminoethylphosphonate (AEP) and methylphosphonate (MP) inhibited phosphate uptake to a greater extent than phosphate itself (88 to 96% phosphate uptake inhibition at 5 times the ^{33}Pi concentration). If this is due to competitive inhibitions, our results suggest that EP, AEP and MP have a higher affinity for PhoCDET than phosphate and may be transported into the cells by this transport system. Aminomethylphosphonate (AMP) showed less inhibition activity than the other phosphonates with 60% uptake inhibition when provided at 5 times the concentration of labeled-phosphate. This may be attributed to structural constraints of this compound on the binding site of the transporter. It was interesting that the phosphonate, glyphosate [*N*-(phosphonomethyl)glycine], the active ingredient in the herbicide Roundup, showed very little phosphate uptake inhibition even when provided at 50 times the concentration of labeled

% inhibition of Pi transport via PhoCDET

Competitors	Inhibitor concentrations 5μM	50μM
None	0.0	0.0
Pi	82.4 ± 1.6	97.9 ± 0.5
AEP	96.1 ± 1.3	98.3 ± 1.7
EP	94.5 ± 1.1	99.7 ± 0.3
AMP	57.8 ± 4.8	92.4 ± 0.9
MP	88.0 ± 2.7	99.7 ±0.3
glyphosate	7.8 ± 3.0	17.1 ± 0.6
arsenate	77.5 ± 1.9	98.4 ± 0.2
Succ	0.0	0.0

Phosphate uptake was performed at ^{33}Pi concentration of 1μM.
Rate of uptake with no inhibitor present was 5.5 ± 0.2 nmol/min/mg protein.

Table 3-1: Inhibition experiments investigating the specificity of PhoCDET for phosphate. The experiments were performed on phosphate starved cells and the numbers reported in the table express the percent inhibition when 1μM ^{33}P-labeled phosphate was provided to the medium. The inhibitors (at 5 or 50 times the concentration of ^{33}P-labeled phosphate) were added to the cells 15 sec prior to the addition of the radio-labeled compound. The inhibitors used were cold orthophosphate (Pi), ethylphosphonate (EP), aminoethylphosphonate (AEP), methylphosphonate (MP), aminomethylphosphonate (AMP), glyphosate, arsenate and succinate (Succ). The data were from a 1 min uptake experiment and the % inhibition, representing the average of three independent assays, was calculated from a Pi uptake rate of 5.5 nmol/min/mg protein obtained in the absence of inhibitors.

phosphate (17% inhibition). The ability to degrade glyphosate and the use of this compound as a phosphorus source was shown to be widespread in the Rhizobiaceae family (Liu et al., 1991). The inhibition experiments presented here as well as the ability of *R. meliloti* to grow in MOPS-buffered minimal media containing glyphosate as the sole phosphorus source (Liu et al., 1991) suggest that glyphosate uptake does not involve PhoCDET. Arsenate inhibited phosphate uptake similarly to cold phosphate (77% inhibition was observed when arsenate was provided at 5 times the labeled phosphate concentration) suggesting that this phosphorus analogue may be transported into the cell by the PhoCDET system with an affinity similar to that for phosphate.

C- Discussion

The *ndvF* locus is made up of four genes, *phoCDET* that together encode an ATP-binding-cassette dependent transport system responsible for the uptake of phosphate and possibly phosphonates. The presence of two Pho Boxes upstream of *phoC* and the 10- to 20-fold induction in level of expression of the system under phosphate deprivation suggest that this locus is part of a Pho regulon in *R. meliloti* similar to the Pho regulon described in *E. coli* (Wanner, 1993).

The kinetics of phosphate uptake into cells grown under phosphate limitating conditions indicate the presence of a single high affinity (Km: 0.2μM), low velocity (Vmax: 6.7 nmol Pi/min/mg protein) phosphate transport system. The Km value measured was significantly lower (8- to 30-fold) than the Km values for phosphate uptake reported for seven rhizobia/bradyrhizobia strains (Smart et al., 1984a) but was similar to the value of the high-affinity phosphate transport system (*pst*) of *E. coli* (Km: 0.4μM; Willsky and Malamy, 1980a), *Pseudomonas aeruginosa* (Km: 0.46μM; Poole and Hancock, 1984), and *Acinetobacter johnsonii* (Km: 0.7μM; Van Veen et al., 1993a). In the study of Smart et al. (1984a), the single strain of *R. meliloti* examined (RmWU3) had a Km of 6μM. This value is very similar to the Km value of the *pit*-like alternative phosphate transport system in *R. meliloti* 1021 (see Chapter IV; Dr. Voegele,

personal communication) and to the low-affinity Pit phosphate transport system of *E. coli*. In addition, although Pi uptake by RmWU3 was unidirectional, the system was not sensitive to osmotic shock suggesting that the phosphate transport system studied in RmWU3 was not a periplasmic binding protein-dependent transport system like the ABC-type transporter. These observations indicates that (a) *R. meliloti* WU3 strain only carried the low affinity-type phosphate transporter or (b) under the growth and transport assay conditions used by these authors, only the low-affinity phosphate transport system was expressed. The second proposition is favored as a fragment homologous to the 7.3kb *Bam*HI fragment (containing the *phoCDET* locus) of *R. meliloti* 1021 was found in at least three other *R. meliloti* strains (Charles et al., 1991), suggesting that *phoCDET* is conserved among *R. meliloti* strains.

The Vmax value of the PhoCDET system was low, even when compared to the low velocity of the *pst* system of *E. coli* (Vmax: 15.9 nmol Pi/min/mg protein; Willsky and Malamy, 1980a). This may be due to the slower growth rate of *R. meliloti* compared to *E. coli*. It is important to mention that slight variations in growth conditions lead to variations in the velocity of phosphate uptake. We observed variations from 3 to 6.7 nmol Pi/min/mg protein in the Vmax's determined from different experiments in which P starved cells were examined.

Phosphate uptake via the PhoCDET transport system was inhibited by the presence of arsenate and phosphonate compounds. These compounds may act

as competitors for phosphate uptake, either by binding to the periplasmic Pi-binding protein thus making it unavailable for phosphate uptake or by being transported into the cell by the PhoCDET transport system. The periplasmic Pi-binding protein of the PhoCDET system, encoded by *phoD*, may then have a broad specificity for various phosphorus compounds. This would then be in contrast with the Pst system of *E. coli* in which the periplasmic Pi-binding protein, encoded by *pstS*, is highly specific for phosphate and does not even recognize the phosphate analogue arsenate as a substrate (Bennett and Malamy, 1970; Medveczky and Rosenberg, 1971).

Appendix A

Further characterization of the growth of *phoCDET* mutants on phosphonate and phosphorus compounds.

Growth curves of the wild type strain (Rm1021, ■) and the three *phoCDET* mutants; RmG439 (*ndvF*Δ439, ▲), RmG490 (*phoC*Ω490, ●) and RmG491 (*phoT*Ω491, ◆) in phosphate-free MOPS-buffered minimal media (P0), and containing 2mM of, orthophosphate (Pi), aminoethylphosphonate (AEP), ethylphosphonate (EP), aminomethylphosphonate (AMP), methylphosphonate (MP), glycerol-3-phosphate (G3P), glucose-6-phosphate (Glc6P) or phosphoserine (PSer). The cells were inoculated in the various media after a 24 hour period of growth in MOPS P0.

Analysis of the results

- The four strains grew poorly in MOPS P0.
- In MOPS Pi, the wild type reached saturation after 65 hours growth (doubling time: 5 hours); The three *phoCDET* mutants behaved similarly with a slow but

constant growth (doubling time: 30 hours), reaching the wild type growth saturation level after 160 hours.

- In MOPS AEP, the four strains grew at similar rate.
- In MOPS EP, the wild type growth was delayed by 40 hours compared to its growth in MOPS Pi. The three mutants behaved similarly with a slow and constant growth similar to the one observed in MOPS Pi.
- In MOPS AMP and MP, RmG490 and RmG491 behaved similarly but were different from RmG439: RmG439 grew poorly in both media while both RmG490 and RmG491 grew as well as the wild type strain in MOPS AMP and reached the wild type level of growth after a 20 hours delay in MOPS MP.
- In MOPS G3P, Glc6P and PSer, the three *phoCDET* mutants grew at similar rate to that of the wild type. Growth of the wild type strain was delayed by 40 hours in MOPS Glc6P compared to its growth in MOPS Pi.

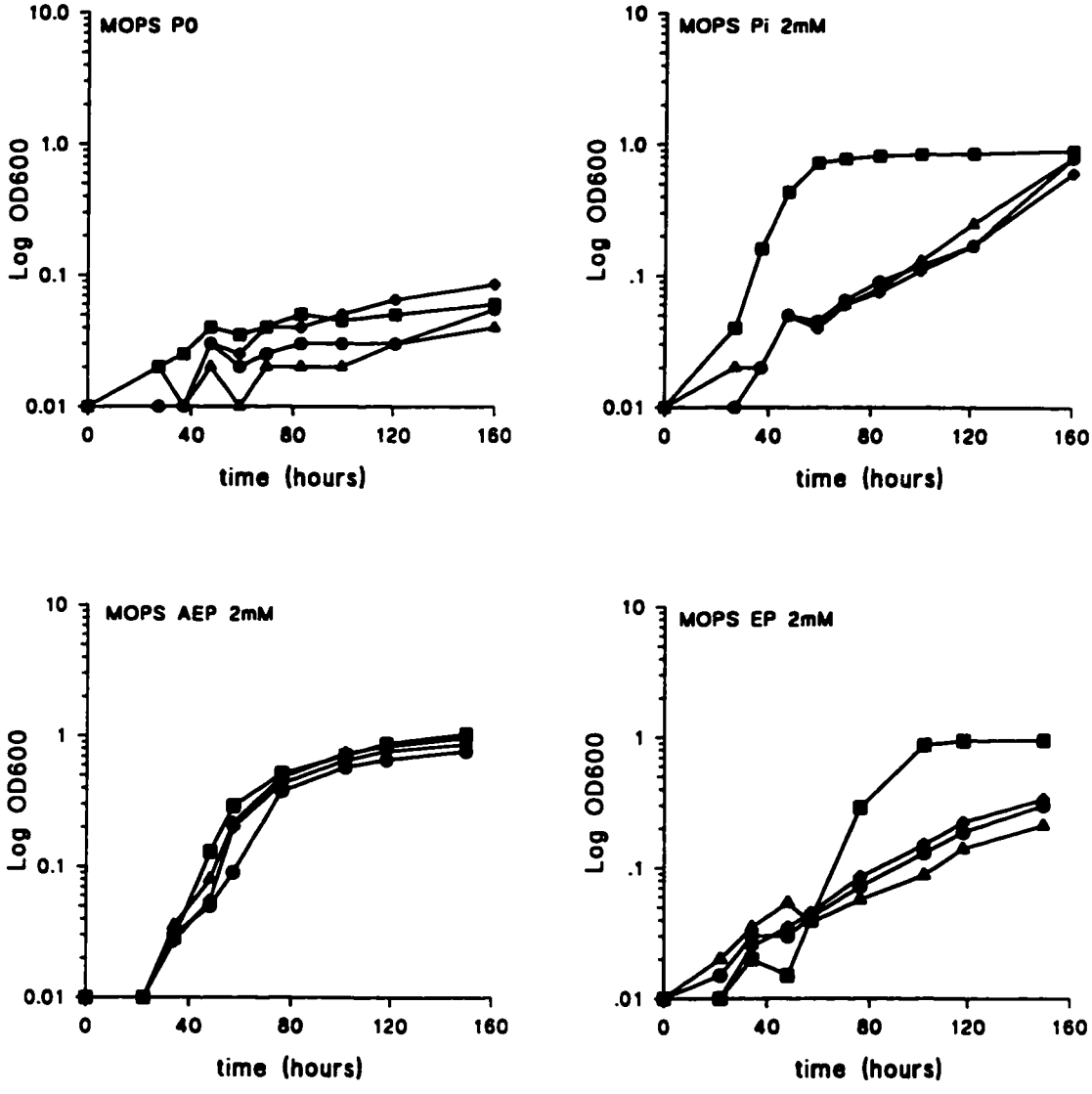
MOPS P0
Log OD600
10.0
1.0
0.1
0.01
0
40
80
120
160
time (hours)
MOPS Pi 2mM
Log OD600
10
1.0
.1
0.01
0
40
80
120
160
time (hours)
MOPS AEP 2mM
Log OD600
10
1
0.1
0.01
0
40
80
120
160
time (hours)
MOPS EP 2mM
Log OD600
10
1
.1
.01
0
40
80
120
160
time (hours)

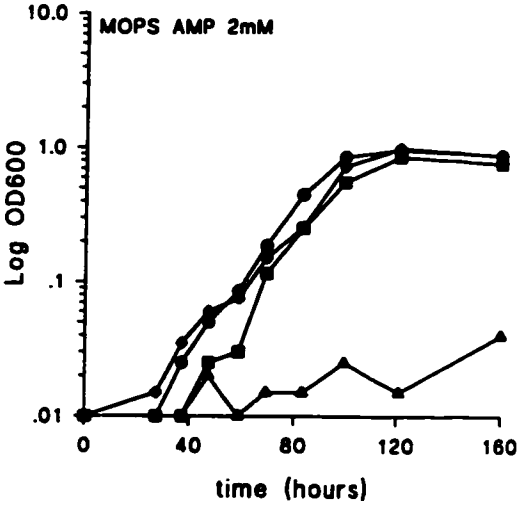
MOPS AMP 2mM
10.0
1.0
.1
.01
Log OD600
0
40
80
120
160
time (hours)

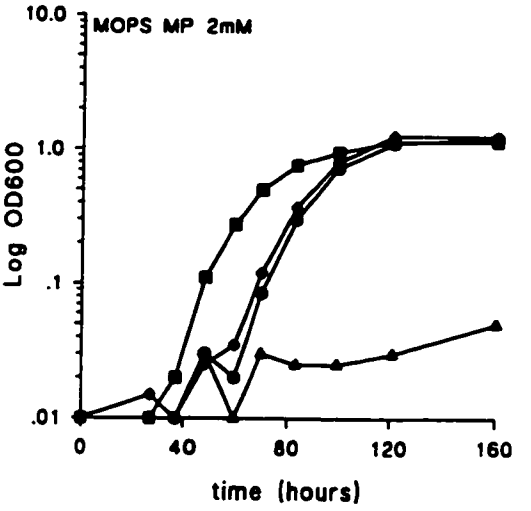
MOPS MP 2mM
10.0
1.0
.1
.01
Log OD600
0
40
80
120
160
time (hours)

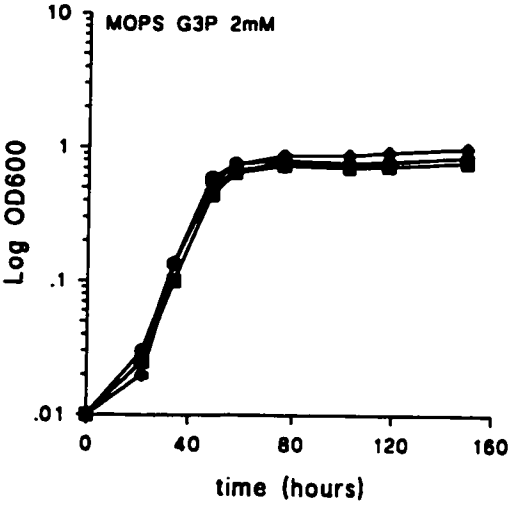
MOPS G3P 2mM
10
1
.1
.01
Log OD600
0
40
80
120
160
time (hours)

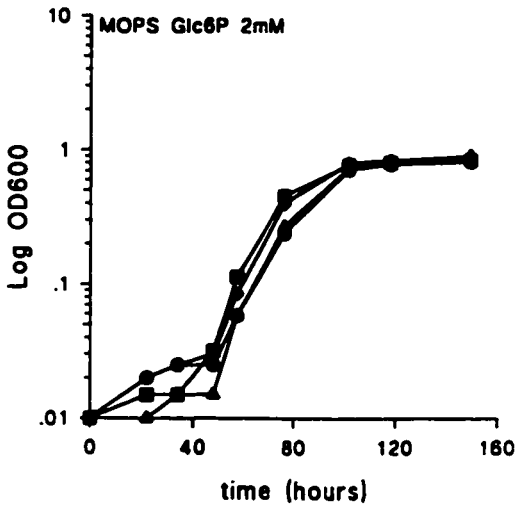
MOPS Glc6P 2mM
10
1
.1
.01
Log OD600
0
40
80
120
160
time (hours)

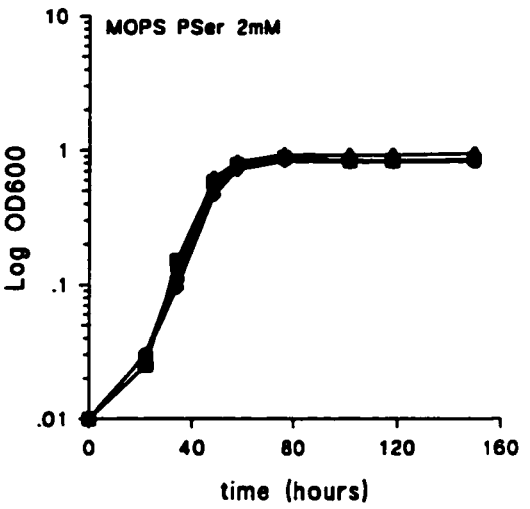
MOPS PSer 2mM
10
1
.1
.01
Log OD600
0
40
80
120
160
time (hours)

CHAPTER IV

Genetic characterization of the *sfx*1 locus

A- Introduction

The *ndvF* locus of *R. meliloti* contains four genes designated *phoCDET.* These genes were found to encode a phosphate transport system and the Fix$^-$ phenotype of *ndvF* mutants when inoculated on alfalfa plants was attributed to their inability to assimilate enough phosphate for growth during nodule formation process (Chapter III; Bardin et al., 1996). It was also observed that occasionally, plants inoculated with the Fix$^-$ *phoCDET* strains formed some pink Fix$^+$ nodules (Charles et al., 1991). Bacteria isolated from these nodules carried the original *phoCDET* mutations and genetic analysis revealed that these strains also carried second-site mutations (designated *sfx*) which suppressed the Fix$^-$ phenotype. The *sfx* mutations in five independent pseudorevertant strains were shown to map to two distinct loci (Oresnik et al., 1994). Class I suppressor mutations (*sfx1*, *sfx4* and *sfx5*) were tightly linked to the insertions Ω5117::Tn*5* and Ω5122::Tn*5*-132 while class II suppressor alleles *sfx2* and *sfx3* were not. The class II suppressor strains, but not class I, were sensitive to deoxycholate, sodium

dodecyl sulfate and sarkosyl as well as to the antibiotic bacitracin (Oresnik et al., 1994).

The *sfx1* locus was cloned from a pRK7813 cosmid library containing partial *Bam*HI DNA fragments from the class I suppressor strain RmF263 (*ndvF*, *sfx1*) (Oresnik et al., 1994). Cosmids pTH56 and pTH57 which suppressed the Fix$^-$ phenotype of *phoCDET* deletion mutants were isolated. Both cosmids shared an identical 18kb *Bam*HI fragment, and direct evidence that the insert DNA in pTH56 was collinear with the *sfx1* region was obtained by Southern blot analysis revealing that some transposon insertions linked in transduction to the *sfx1* region lay within the pTH56 insert DNA.

This chapter presents a molecular genetic characterization of the *sfx1* locus and presents data addressing the physiological mechanism through which *sfx1* suppresses the Fix$^-$ phenotype of *ndvF* mutants.

B- Material and methods

1- Construction of transcriptional *lacZ* fusions to *pit* and *orfA*

Plasmid-borne *lacZ* fusions to the *pit* open reading frame were made by subcloning the 2.1kb *Eco*RI fragments from pTH354 (wild type) and pTH380 (*sfx1*) into the *Eco*RI restriction site of the pMP220 vector (Spaink et al., 1987) to create plasmids pTH376 and pTH365. Fusions of the "*orfA*" open reading frame to *lacZ* were made by deleting the DNA between the *Sph*I site located in the *orfA* gene and the *Sph*I site of the pMP220 polylinker of plasmids pTH376 and pTH365 to create plasmids pTH378 and pTH367, respectively. The plasmid fusions were then mated into wild type and *phoC*Ω490, Lac$^-$ strains (RmG212 and RmH667, respectively).

Chromosomal *lacZ* gene fusions to *pit* in both wild type and *sfx1* backgrounds were constructed as outlined in Fig 4-1a. The *lacZ* cassette was inserted, in both orientations, immediately downstream of the *pit* translational stop codon so that the *pit* product would be functional. The resulting pBR322 based plasmids, pTH351 and pTH352, were recombined by a single crossover into the genome of wild type or *sfx1*, Lac$^-$ background strains. Spectinomycin resistant recombinants were checked for resistance to 2μg/ml Tc and by Southern blot using pTH276 as probe (Fig. 4-1b).

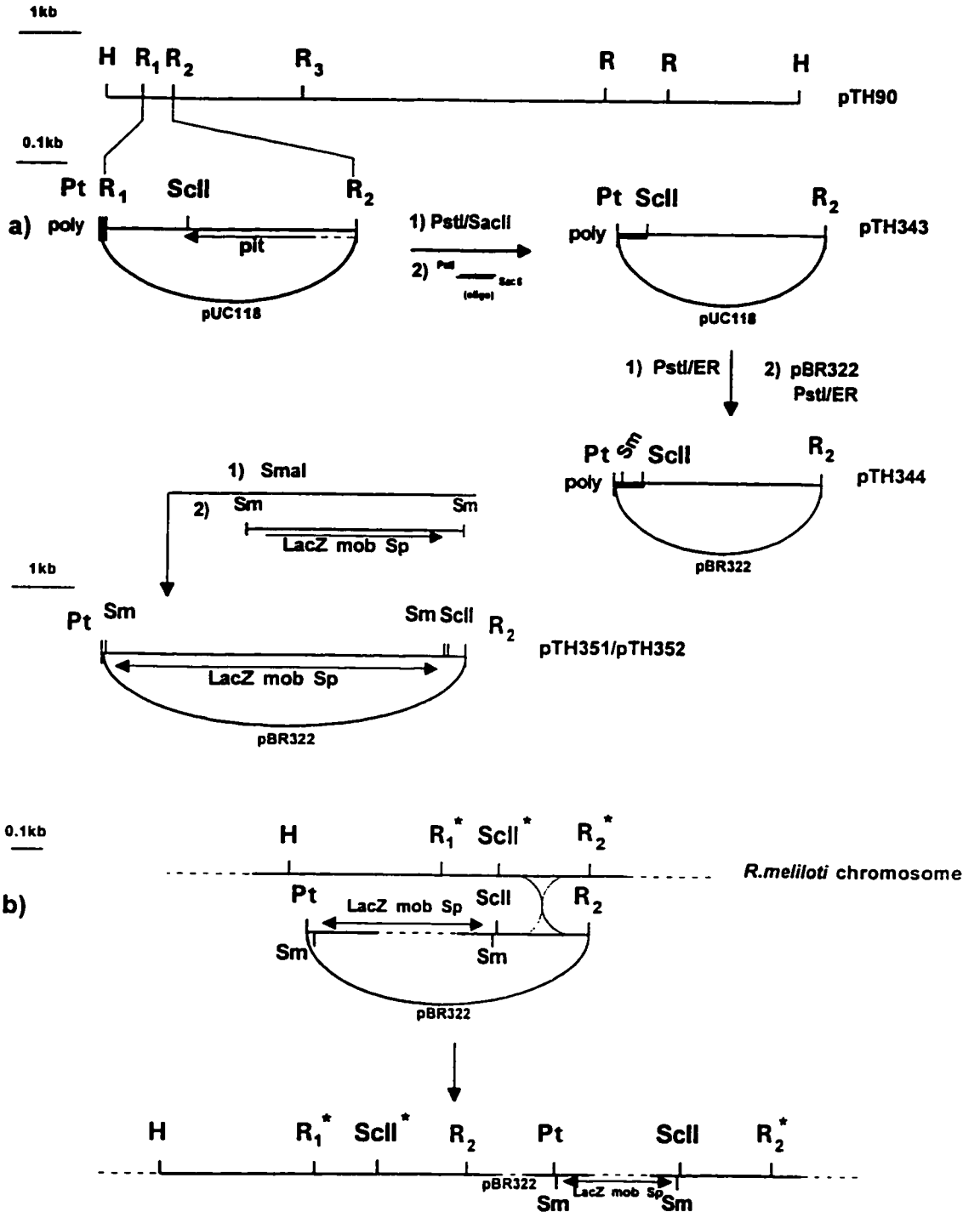
1kb
H R1 R2 R3 R R H
pTH90
0.1kb
Pt R1 SclI R2
a) poly
plt
pUC118
1) PstI/SacI
2)
Pt SclI R2
poly
pTH343
pUC118
1) PstI/ER
2) pBR322 PstI/ER
Pt Sm SclI R2
poly
pTH344
pBR322
1) SmaI
2) Sm Sm
LacZ mob Sp
1kb
Pt Sm Sm SclI R2
pTH351/pTH352
LacZ mob Sp
pBR322
0.1kb
b)
H R1* SclI* R2*
R.meliloti chromosome
Pt LacZ mob Sp SclI R2
Sm Sm
pBR322
H R1* SclI* R2 Pt SclI R2*
pBR322
LacZ mob Sp
Sm Sm

Fig. 4-1a: Construction of the *pit* chromosomal *lacZ* fusions was performed as follows:

a) The 0.5kb *Eco*RI fragment (R_1-R_2) of pTH90 (containing the 3'-end of *sfx1-pit*) was subcloned in pUC118 so that R_1 was on the polylinker side. The subclone was digested with *Sac*II (located 11 nucleotides upstream from the *pit* translational stop codon) and *Pst*I (located in the polylinker) and the fragment was replaced by a linker (with *Sac*II/ *Pst*I protruding ends) to create pTH343. The linker was constructed by hybridizing two complementary oligos. The two oligos (5'-GGACCTCGTCGCCTGACCCGGGCTGCA-3' and 5'- GCCCGGGTCAGGCG ACGAGGTCCGC-3') were synthesized so that the end of the *pit* gene was reconstituted (in order to obtain a functional gene). The translational stop codon was followed by a *Sma*I site used to clone the *lacZ* cassette. pTH343 was then digested with *Pst*I/ *Eco*RI and the fragment was cloned in pBR322 digested with the same enzymes to create pTH344. The *lacZ* cassette of the pLMS clone (pUC18 with the *lacZmob*Sp^r cassette) was subcloned as a *Sma*I fragment in pTH344 to create pTH351 and pTH352 with the *lacZ* gene in the same and opposite orientation as *pit*, respectively.

b) The plasmids were recombined into the chromosome of a wild type and a *sfx1* strain by single cross-over using homologous recombination of the 0.3kb *Sac*II/*Eco*RI(2) fragment.

Symbols used: poly: polylinker; H: *Hin*dIII; Pt: *Pst*I; R: *Eco*RI; ScII: *Sac*II; Sm: *Sma*I.

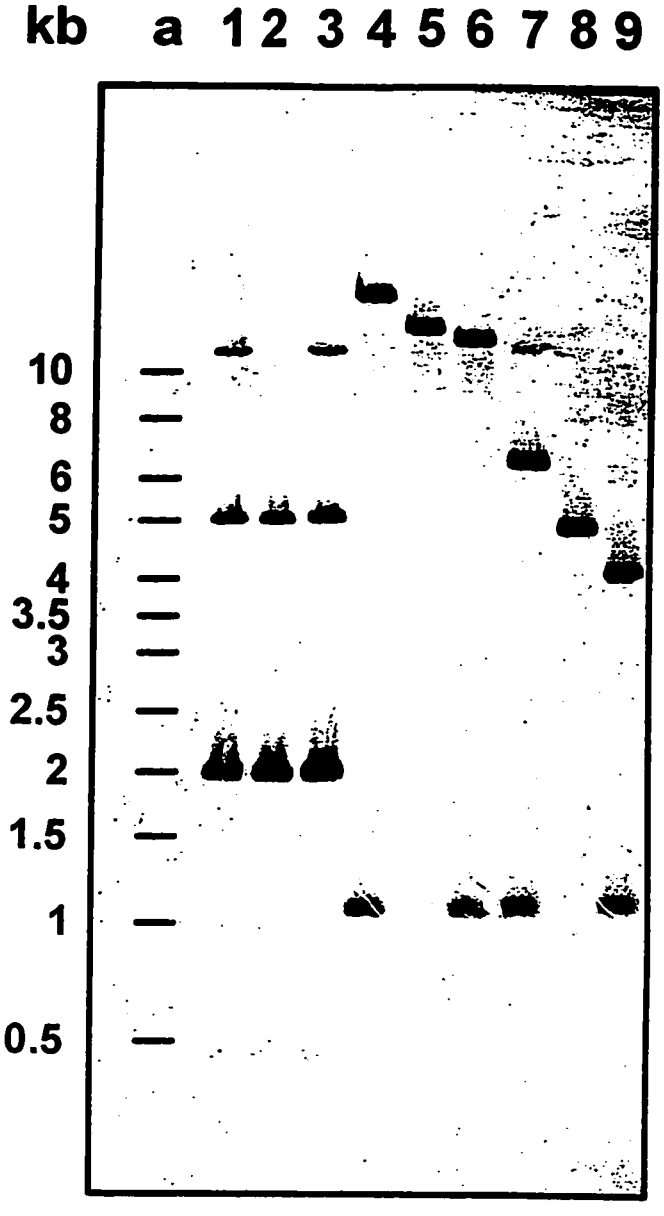

Fig. 4-1b: Southern blot of Rif^r Sp^r recombinants obtained following transfer of pTH351 and pTH352 into the wild type strain Rm5000 and probed with the pTH276 (*Hind*III/*Sac*I, 4.8kb) plasmid. Line 1, 4 and 7: Rm5000-pTH351 recombinant; Line 2, 5 and 8: Rm1021; Line 3, 6 and 9: Rm5000-pTH352 recombinant. Digestion with *Eco*RI (R): Line 1, 2 and 3; Digestion with *Hind*III (H): Line 4, 5 and 6; Digestion with *Sac*I/*Hind*III (Sc/H): Line 7, 8 and 9. Line a: 1kb ladder. The figure on the following page shows the fragments expected for each recombinant type as well as for the wild type strain.

Rm5000 - pTH351 recombinants

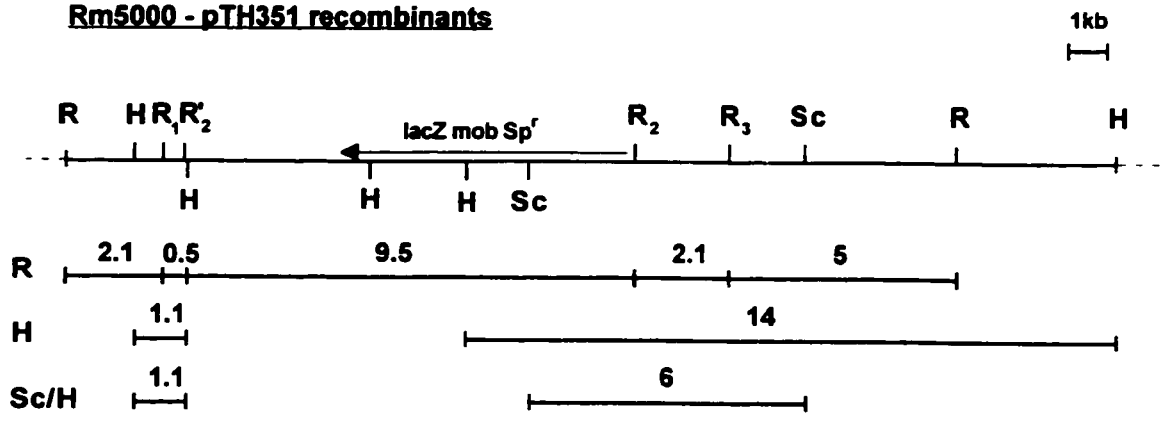

Wild type

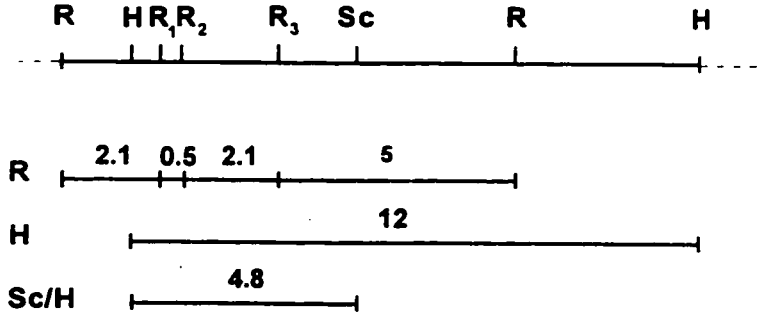

Rm5000 - pTH352 recombinants

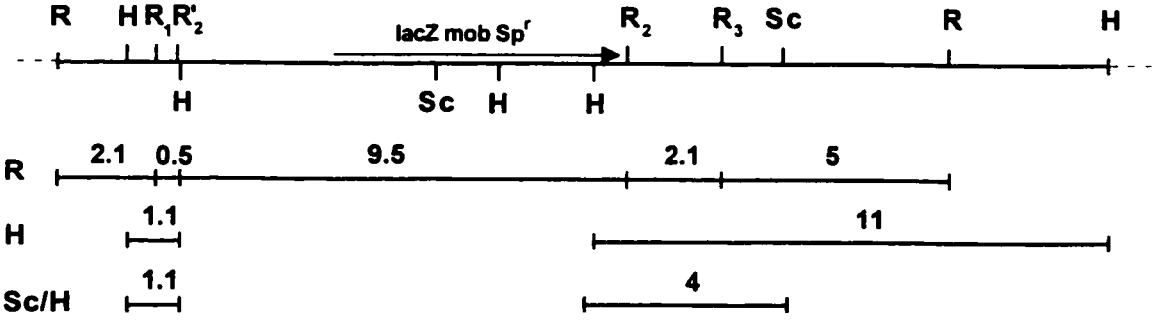

2- Construction of pTH396 and pTH397

These constructs were prepared to delineate the fragment in which the *sfx1* mutation was located. As the mutation was suspected to be in the promoter region of *orfA*, the 920bp *Xho*I/*Eco*RI(3) and 540bp *Eco*RV/*Eco*RI(3) fragments (see Fig. 4-4a) of pTH191 were subcloned as *Xho*I/*Hin*dIII and *Eco*RV/*Hin*dIII fragments (using the *Hin*dIII site of the polylinker) into the *Sal*I/*Hin*dIII and *Eco*RV/*Hin*dIII restriction sites of pBR322, respectively. The pBR322 vector was chosen because it is mobilized by pRK600 but cannot replicate in *Rhizobium meliloti*. To provide a selective marker to identify *R. meliloti* recombinants, the 3.4kb *Hin*dIII fragment of pGS220 containing the Km^R gene of Tn*5* (De Vos et al., 1986), was subcloned into the *Hin*dIII site of the two subclones.

3- DNA sequencing and sequence analysis

(see also material and methods)

DNA sequencing was performed on single-stranded DNA using the dideoxy chain termination method according to the protocol of United States Biochemicals for the Sequenase 2.0 enzyme and using [α-^{35}S] ATP (NEN/DuPont). Single stranded DNA was obtained from host strain XL-1Blue (Stratagene) following infection with the helper phage M13K07 (Vieira, and Messing, 1987). Both strands of DNA were sequenced using the -20 (*lacZ*) primer (5'-GTAAAACGACGGCCAGT-3') and the IS50 primer (5'-TCACATGGAA

GTCAGATCCT-3'). DNA and deduced protein sequences were analyzed with PC/Gene (Intelligenetics), Blast (Gish and States, 1993), CLUSTAL W (Thompson et al., 1994) and Top Pred II (Claros and von Heijne, 1994) software.

C- Results

1- *sfx*1 suppresses the growth phenotype of *phoCDET* mutants in 2mM Pi

To investigate whether *sfx1*-mediated suppression of the Fix$^-$ phenotype of *phoCDET* mutants was related to phosphate assimilation, *sfx1* was tested for its ability to suppress the poor growth phenotype of *phoCDET* mutants in MOPS-buffered minimal media containing 2mM phosphate (MOPS P2). An *sfx1* *phoC*Ω490 double mutant, strain RmG762, was constructed by transducing the ΩSp insertion from strain RmG490 (*phoC*Ω490) into strain RmG591 (*sfx1*). The growth of Rm1021 (wild type), RmG490 (*phoC*Ω490) and RmG762 (*phoC*Ω490, *sfx1*) in 2mM phosphate was monitored over a 160 hour time period and is presented in Fig. 4-2a. The wild type strain had a doubling time of 5.4 hours in the exponential phase of growth and reached the stationary phase 65 hours after inoculation. The *phoC*Ω490 mutant showed a slow but constant growth rate (doubling of 34.8 hours between OD_{600} of 0.1 to 0.6) and reached growth saturation 160 hours after inoculation. An identical growth pattern was obtained for the *phoCDET* deletion strain (*ndvF*ΔG439) and for *phoT* mutant (*phoT*Ω491) (see Appendix A). The presence of the *sfx1* mutation in the *phoC*Ω490 strain restored its growth rate to near the wild type (doubling time 6.6 hours). *sfx1*

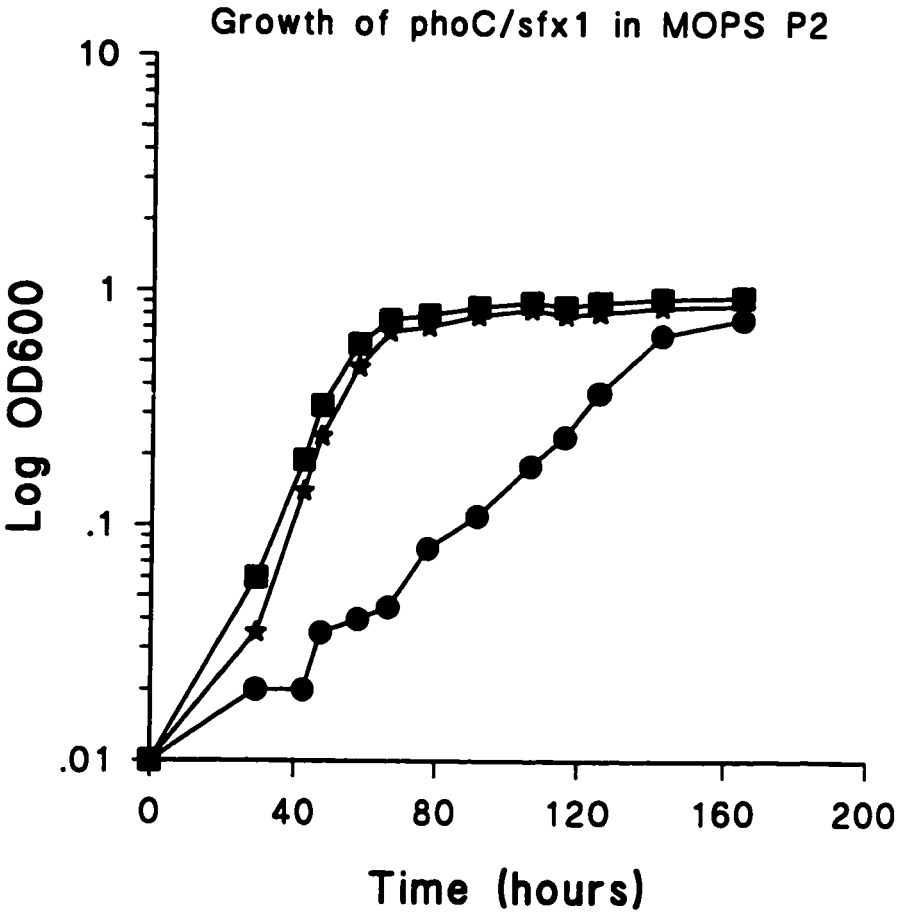

Fig. 4-2a: Growth of Rm1021 (wt, ■), RmG490 (*phoC*Ω490, ●) and RmG762 (*phoC*Ω490, *sfx1*, ★) in MOPS-buffered minimal media supplemented with 2mM Pi. Each time point represents the average of triplicate values.

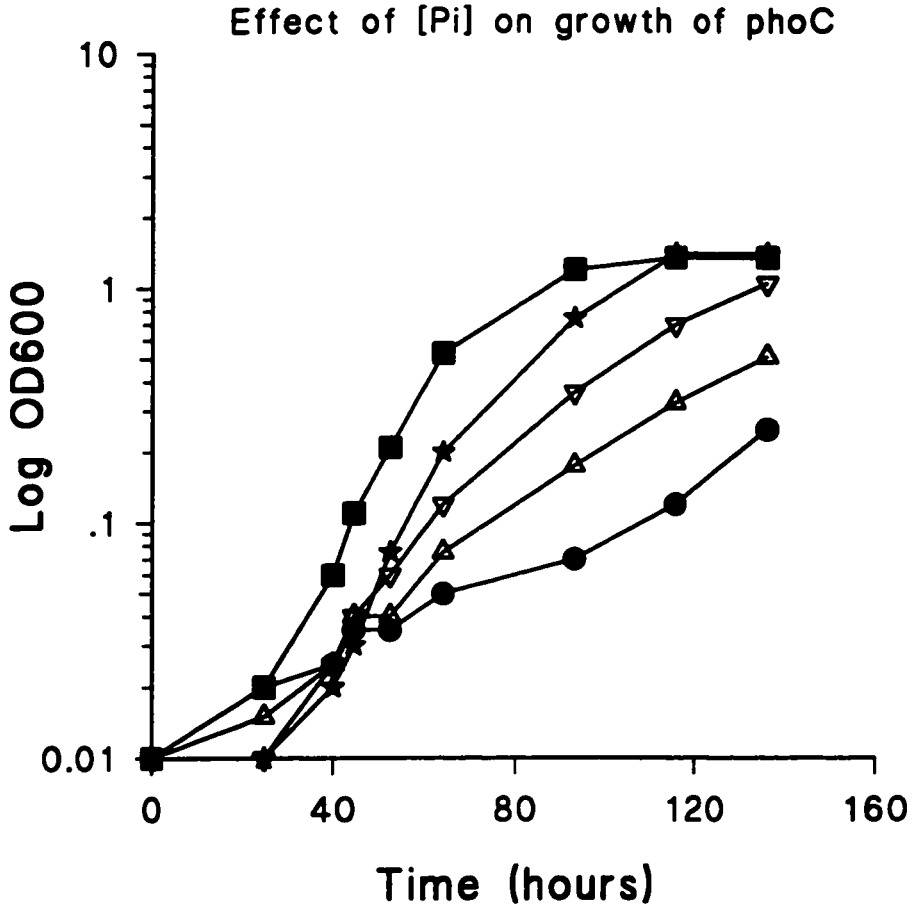

Fig. 4-2b: Growth of the wild type strain and the *phoC*Ω490 mutant when increasing phosphate concentrations were added to the media. The growth of Rm1021 was similar in every media (■). The growth of *phoC*Ω490 is reported as follows: 2mM (●), 10mM (Δ), 20mM (∇) and 60mM Pi (☆). Each time point represents the average of triplicate values.

was also able to suppress the growth phenotype of *ndvF*ΔG439 and *phoT*Ω491 in a similar manner (data not shown).

The *sfx1*-dependent suppression of the growth phenotype of *phoCDET* mutants in media containing 2mM Pi provided further evidence that the Fix$^-$ phenotype of these mutants was due to poor phosphate assimilation. Suppression by *sfx1* seems to occur by providing the mutant cells with an alternative and efficient way to assimilate phosphate. The slow growth of *phoCDET* mutants in MOPS media containing 2mM Pi suggests that an alternative transport system(s) with a low affinity for phosphate and independent from the *phoCDET* system is present in the cell.

When growth of the *phoC*Ω490 mutant in media containing increasing concentrations of phosphate was examined, the growth rate increased with increasing Pi; in 60mM Pi the mutant strain reached a doubling time in the exponential phase that was 80% of that of the wild type strain (Fig. 4-2b). Thus other transport systems able to transport phosphate appear to be present in *Rhizobium meliloti*. However the low affinity of such system(s) for phosphate suggests that they probably don't play an important role as phosphate transporter in a wild type cell.

2- Localization of *sfx*1 on pTH90

The *sfx1* locus was previously localized to an 18kb *Bam*HI fragment of the pTH56 cosmid (Oresnik et al., 1994). A 12kb *Hin*dIII fragment, internal to the 18kb *Bam*HI fragment of pTH56, was subcloned into pRK7813 to give pTH90. Transconjugants obtained following transfer of pTH90 into RmG490 (*phoC*Ω490) formed Fix^+ nodules and grew like the wild type strain in media containing 2mM phosphate (Fig. 4-3b, 4-3c). These data confirmed that pTH90 possessed the entire *sfx1* locus. A restriction map of pTH90 was constructed for the enzymes *Eco*RI, *Bgl*II and SacI. To localize the *sfx1* region 19 Tn*5* insertions which mapped within the 12kb insert of pTH90 were isolated (Fig. 4-3a). Using seven of these Tn5 insertions, we created defined deletions of pTH90 by removing DNA from the *Bam*HI restriction site within the polylinker to the *Bam*HI site within the Tn*5* insertions. The resulting plasmids were mated into RmG490 (*phoC*Ω490) and the Tc^r transconjugants were tested for suppression of the mucoid phenotype on low osmolarity media (GYM). Deletions removing any of the 7kb region up to insertion ΩE suppressed the mucoid phenotype of RmG490 while further deletions prevented suppression (Fig. 4-3b). In addition, while the Fix^- phenotype of the *phoC*Ω490 strain was suppressed by either pTH90 or pTH90ΔΩE, *phoC*Ω490 strains containing the pTH90 plasmids deleted up to insertion Ω2.3, Ω3.10 and Ω2.2 remained Fix^- (Fig. 4-3b). As these data suggested that the *sfx1* suppressor locus lay within the 4.8kb *Hin*dIII-*Sac*I

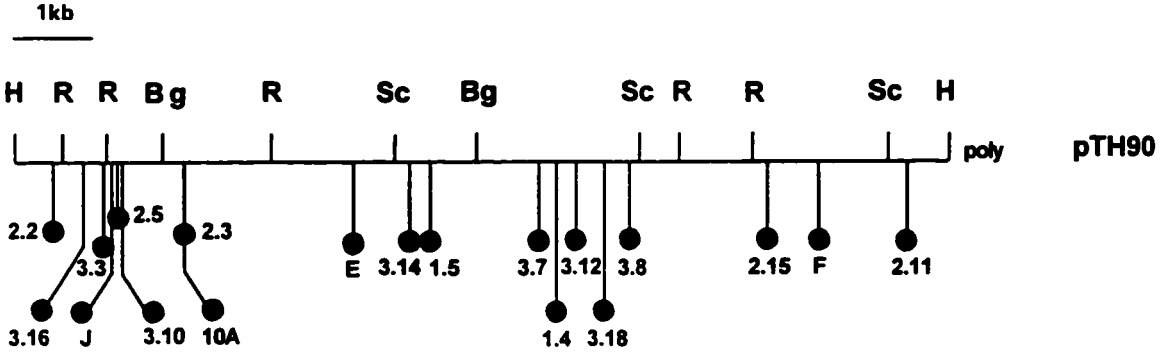

Fig. 4-3a: Restriction map of pTH90 showing the location of the restriction sites for Bg: *Bgl*II; H: *Hin*dIII; R: *Eco*RI and Sc: *Sac*I. Also shown are the locations of 19 Tn*5* insertions (●).

Fig. 4-3b: (next page) *Bam*HI (B) deletions of seven pTH90::Tn*5* insertions (Ω2.15; 1.4; 1.5; E; 2.3; 3.10 and 2.2). The table on the right side of the figure indicates the osmolarity on glutamate/yeast/mannitol (GYM) media and the Fix phenotypes of RmG490 (*phoC*Ω490) into which the truncated plasmids were mated. In GYM/NaCl, NaCl was supplemented at a concentration of 100mM. D and M indicate a dry and mucoid colony morphology types, respectively. The Fix phenotype was determined by the shoot dry weight in mg (average ± S.E. of 30 plants from 3 pots). The percent % dry weight was calculated in relation to that of Rm1021 (100%). + and - indicates effective and ineffective nitrogen fixation, respectively. UI: uninoculated, ND: not determined.

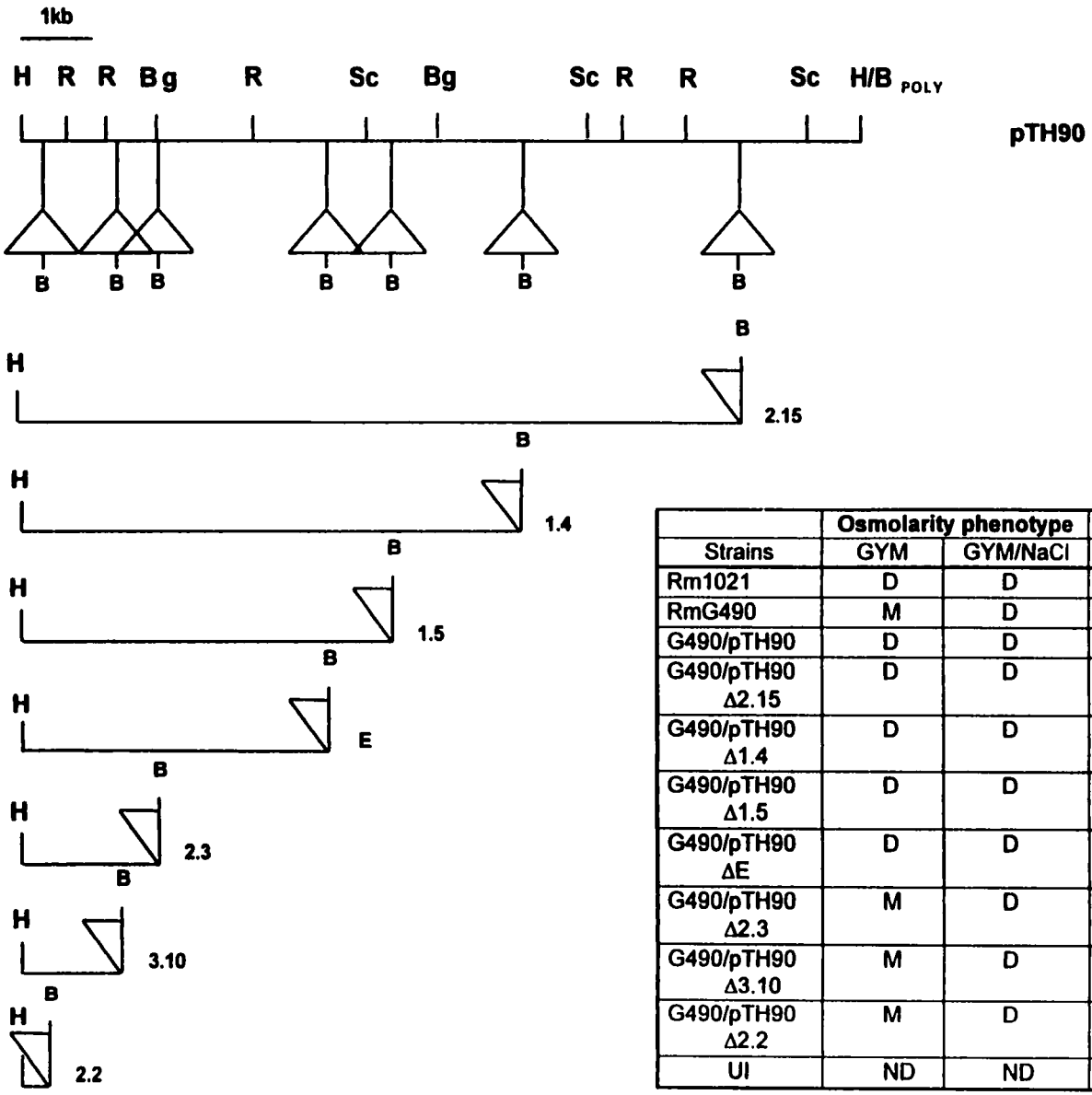

	Osmolarity phenotype		Fix phenotype		
Strains	GYM	GYM/NaCl	Dry Weight	%	Fix
Rm1021	D	D	14.5 ±1.0	100	+
RmG490	M	D	5.7 ±0.2	39.3	-
G490/pTH90	D	D	16.2 ±1.0	111.7	+
G490/pTH90 Δ2.15	D	D	ND		
G490/pTH90 Δ1.4	D	D	ND		
G490/pTH90 Δ1.5	D	D	ND		
G490/pTH90 ΔE	D	D	21.5 ±1.7	148.3	+
G490/pTH90 Δ2.3	M	D	5.7 ±0.4	39.3	-
G490/pTH90 Δ3.10	M	D	5.3 ±0.6	36.5	-
G490/pTH90 Δ2.2	M	D	4.9 ±0.2	33.8	-
UI	ND	ND	4.6 ±0.1	31.7	-

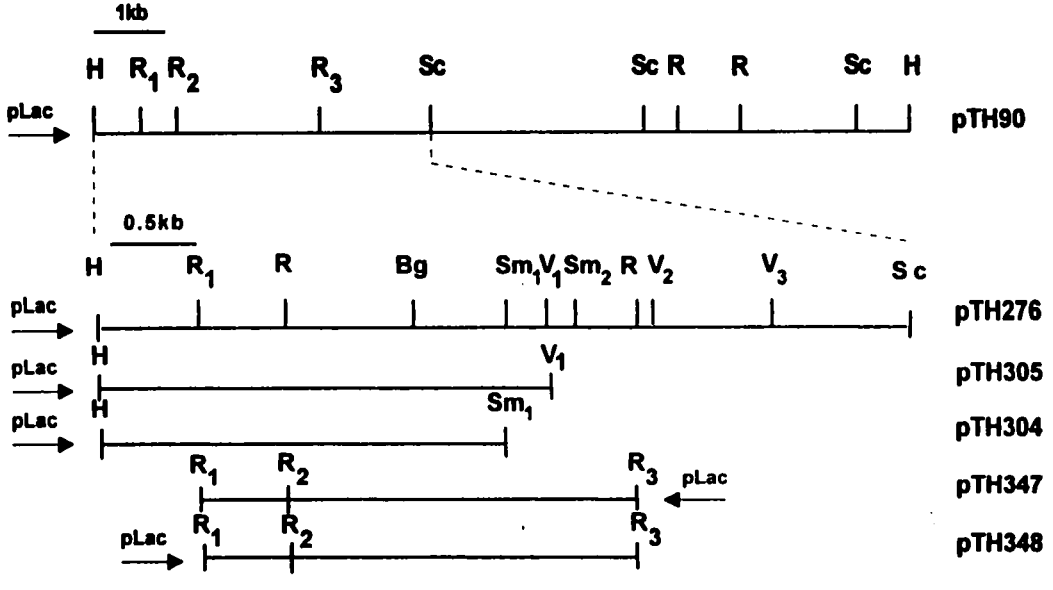

Strains	Phenotype	OD_{600} (after 60h growth)
Rm1021	wt	0.93 ±0.02
RmG490	phocΩ490	0.05 ±.005
RmH501	phocΩ490/pTH90	0.89 ±0.1
RmH315	phocΩ490/pTH276	0.94 ±0.2
RmH313	phocΩ490/pTH305	0.92 ±0.08
RmH305	phocΩ490/pTH304	0.055 ±0.005
RmH606	phocΩ490/pTH347	0.87 ±0.2
RmH607	phocΩ490/pTH348	0.93 ±0.1

Fig. 4-3c: Restriction map and subclones of pTH276. The restriction enzyme shown are Bg: *Bgl*II; C: *Cla*I; H: *Hin*dIII; R: *Eco*RI; Sc: *Sac*I; Sm: *Sma*I; Sp: *Sph*I; V: *Eco*RV and X: *Xho*I. Also indicated is the position of the pLac promoter of the vector relative to the orientation of the clones. The table on the right side of the figure indicates the growth (absorbance at OD600 after 60 hours growth) of the *phoCΩ490* strain containing the different plasmids in MOPS-buffered minimal media supplemented with 2mM Pi. The values represent an average of triplicate data ± S.E.

fragment, this fragment was subcloned into pRK7813 and a restriction map for the enzymes *Eco*RV and *Sma*I was determined (Fig. 4-3c). In addition, the 2.6kb *Hin*dIII-*Eco*RV(1), the 2.5kb *Hin*dIII-*Sma*I(1) and the partial 2.6kb *Eco*RI fragments were subcloned in pRK7813 to give the plasmids pTH305, pTH304, pTH347 and pTH348 with pTH347 and pTH348 representing the two orientations of the 2.6kb *Eco*RI fragment (Fig. 4-3c). Plasmids pTH276, pTH305, pTH347 and pTH348 but not pTH304 allowed *phoC*Ω490 to grow on media containing 2mM phosphate suggesting that the *sfx1* locus spanned the *Sma*I restriction site. From these data we deduced that the entire *sfx1* locus was located between the *Eco*RI(1) and *Eco*RV(1) sites.

Seven Tn*5* insertions and one Tn*phoA* insertion located in this area were recombined onto RmG762 (*phoC*Ω490, *sfx1*) (Fig. 4-4a). The recombinants, checked by Southern blot using pTH276 as probe, were assayed for growth in MOPS media containing 2mM Pi. Recombinants for insertions Ω2.2 and Ω12 grew in this media as well as the wild type and thus retained the suppressor phenotype (Fig. 4-4b). Ω3.16, 3.3, J, 2.5, 3.10, 2.3 or 10A recombinants failed to grow in the 2mM phosphate media and thus disrupted the suppressor locus. As expected, recombinants Ω3.10 and Ω2.3 were also unable to restore the symbiotic phenotype of *phoC*Ω490 when tested on alfalfa plants (data not shown). Together, these results indicates that *sfx1* is located between the *Eco*RI and the *Eco*RV(1) restriction sites.

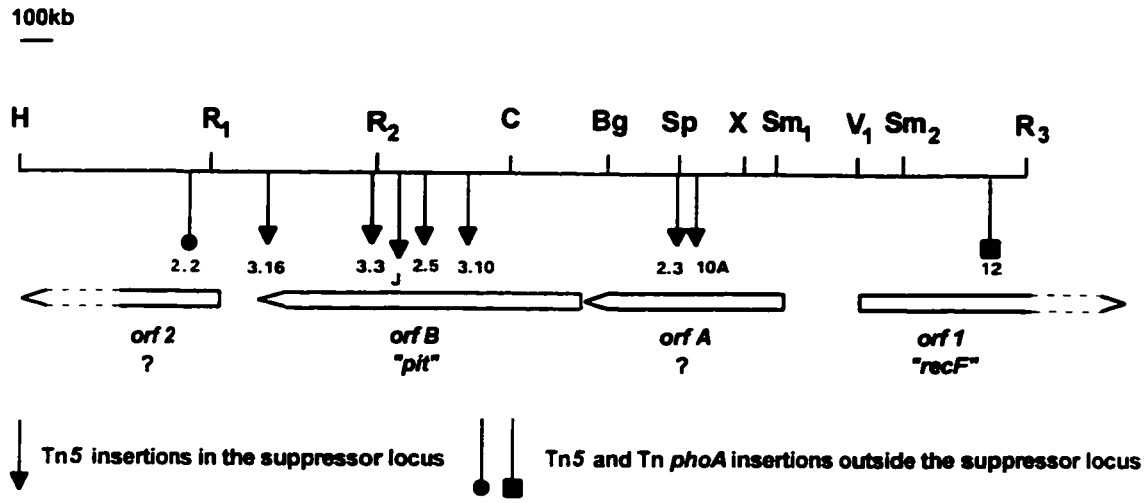

Fig. 4-4a: Map showing the position and size of the two complete and two partial open reading frames deduced from the sequence of the fragment between *Eco*RI(3) and insertion Ω2.2 of pTH90. Homology of *orfB* for *pit* and *orf1* for *recF* are indicated. Also indicated is the position of seven T*n5* insertions that disrupted the *sfx1* locus (▼) as well as one Tn*5* (●) and one Tn*phoA* (■) insertion located outside the suppressor locus. The restriction sites indicated are Bg: *Bgl*II; C: *Cla*I; H: *Hin*dIII; R: *Eco*RI; Sm: *Sma*I; Sp: *Sph*I; V: *Eco*RV and X: *Xho*I.

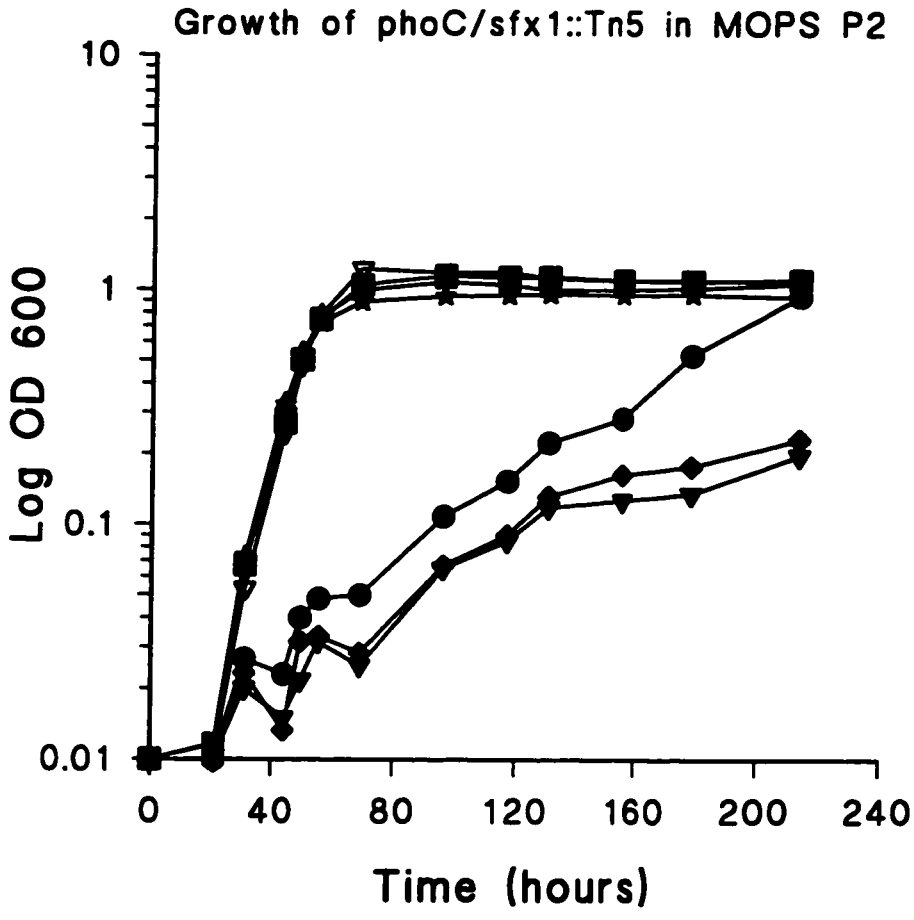

Fig. 4-4b: Growth of Rm1021 (wt, ■), RmG490 (*phoC*Ω490, ●), RmG762 (*phoC*Ω490, *sfx1*, ★), RmG821 (*phoC*Ω490, *sfx1*Ω2.2::Tn*5*, Δ), RmG822 (*phoC*Ω490, *sfx1*Ω2.3::Tn*5*, ◆), RmG830 (*phoC*Ω490, *sfx1*Ω3.10::Tn*5*, ▼) and RmH842 (*phoC*Ω490, *sfx1*Ω12::Tn*phoA*, ∇) in MOPS-buffered minimal media supplemented with 2mM Pi. Each time point represents the average of triplicate values.

Note: the growth phenotypes of *phoC*Ω490, *sfx1*::Tn5Ω 3.16; 3.3; J; 2.5, and 10A were similar to RmG822 and RmG830. These results are not included in this figure.

Disruption of the *sfx1* locus not only failed to suppress the growth phenotype of the *phoC*Ω490 mutant, it reduced its growth rate to 75.4 hours between OD_{600} of 0.1 to 0.6 (Fig. 4-4b). This locus in RmG490 appeared then to encode one of the alternative low affinity phosphate transport systems that allowed slow growth of the *phoC*Ω490 mutant in MOPS P2. Because some growth was still observed when both the sfx1 locus and PhoCDET systems were not functional, other alternative phosphate transporter(s) are probably present in the cell.

3- Nucleotide sequence of *sfx*1

The 2828bp nucleotide sequence from the *Eco*RI(3) restriction site to the Tn*5* insertion Ω2-2 was determined (Fig. 4-4a). Both strands were sequenced by the dideoxy-chain termination method using overlapping fragments (see Appendix B-2 and 3 for strategy of sequencing and sequence). Sequence analysis revealed the presence of two complete (*orfA* and *pit*) and two partial (*recF* and *orf2*) open reading frames (ORF) (Fig. 4-4a). *orfA* and *pit* were transcribed in the same direction and encoded proteins of 214 (23.8 kD, pI: 4.57) and 334 (35.2 kD, pI: 8.89) amino acid, respectively. The adenosine nucleotide from the *orfA* stop codon (TGA) and the *pit* start codon (ATG) was common to the two genes suggesting that both genes were transcribed as a single transcript. In both cases, the ATG was preceded by a potential ribosome binding

site (GATGGA-N6-ATG for *orfA* and GAGA-N7-ATG for *pit*). A cruciform-type stem-loop structure (GC-rich) followed by seven AT-rich residues downstream of the *pit* stop codon (TGA) suggested the presence of a *rho*-independent terminator. Analysis of the region upstream from the *orfA* start codon revealed a potential Pribnow box, TACAAT (consensus sequence TAtAaT (Pribnow, 1975; Schaller et al. 1975)) located 40 nucleotides away from the ATG site. The -35 region, whose consensus sequence reads tcTTGACat (Takanami et al., 1976; Seeburg et al., 1977), was not found 17 residues upstream from the TATA box. However we found a modified Pho Box-like sequence 35 nucleotides upstream from the putative TATA box (Fig. 4-5). This Pho Box-like sequence contained 7 mismatches compared to the *E. coli* consensus sequence CTGTCATAa(/t)At(/a)CTGTCAc(/t) (Wanner, 1993). Analysis of the promoter region of the *E. coli pit* gene, suggested to Sofia et al. (1994) that *pit* expression may be σ^{54} (*ntrA*)-dependent. To investigate whether expression of the *orfA pit* locus of *R. meliloti* was *ntrA*-dependent, pTH376 *(pit::lacZ* fusion) and pTH378 (*orfA::lacZ* fusion) were mated into RmH808 (*ntrA*, Lac$^-$ strain) and assayed for β-galactosidase activity after 38 hours growth in MOPS P0 and MOPS P2. *pit* and *orfA* expression in this background showed no difference with their expression in a wild type background (data not shown). Thus, the *orfA* and *pit* genes do not require *ntrA* for expression.

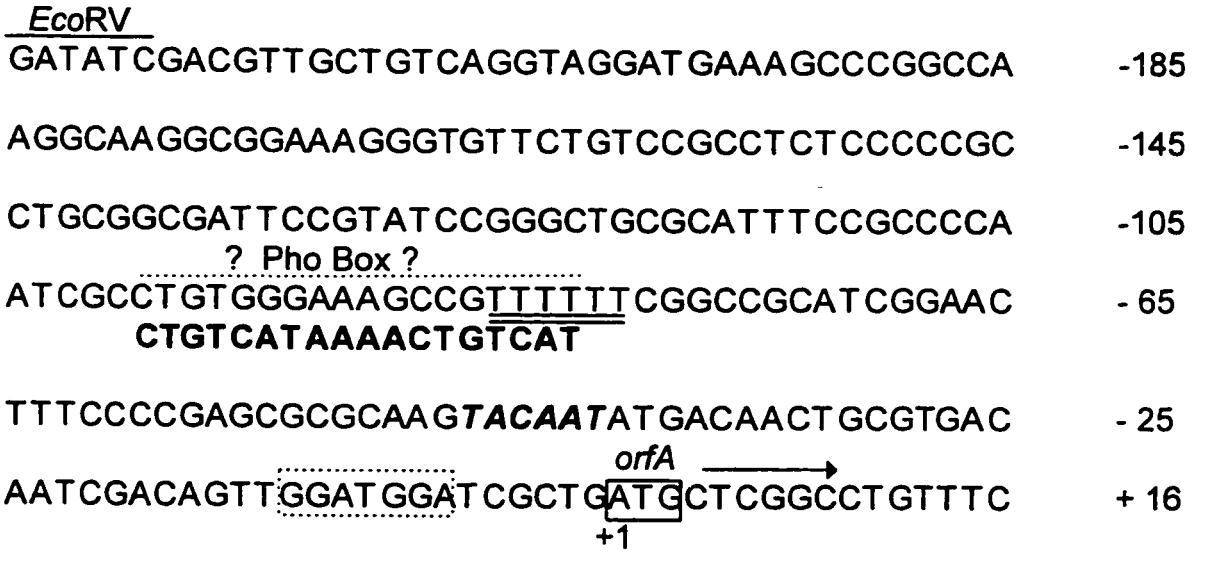

Fig. 4-5: *sfx1-orfA* promoter region. Indicated are the *orfA* ATG codon (boxed, with A numbered as +1), the direction of translation (arrow), the ribosome binding site (dashed box), the potential TATA Box (bold italic) and the potential Pho box (dashed overline) beneath which the consensus Pho Box of an *E. coli* promoter is reported (bold). The *Eco*RV site is also indicated as well as the hexa-thymidine region of an *sfx1* sequence (double underline).
Note; in the wild type sequence, this region is made of seven thymidines.

Both *orfA* and *pit* had a high G + C content (61.8% for *orfA* and 63.9% for *pit*) with a strong bias for G and C at the third position (82.7% for *orfA* and 87.1% for *pit*) as expected for G+C rich organisms (Muto and Osawa, 1987). Comparison of the *orfA* and *pit* deduced proteins with the *Rhizobium* codon usage obtained from the analysis of 126 genes (Wada et al., 1992) revealed that few rare codons were present in these proteins, suggesting that these genes are probably expressed in *R. meliloti.*

recF was located 233 residues upstream from *orfA* and was transcribed in the opposite direction relative to *orfA-pit*. *orf2* located 113 residues downstream from the *pit* stop codon was transcribed in the same direction as *orfA-pit*. A potential ribosome binding site was found upstream from both partial open reading frames; a TCGGA sequence was found 6 residues upstream from the ATG of *recF* and a GGAGG sequence was located 5 nucleotides away from the ATG codon of *orf2*. Neither *recF* nor *orf2* were part of the *sfx1* locus because *recF* laid upstream from the *Eco*RV restriction site and was disrupted by the Tn*phoA*(12) insertion and *orf2* overspanned the *Eco*RI (2) restriction site and was disrupted by the Tn*5* (2-2) insertion.

4- Analysis of the deduced proteins

The analyses of the 2828bp sequence encompassing the *sfx1* locus, revealed the presence of two complete genes, *orfA* and *pit*, and parts of two genes designated *recF* and *orf2*.

a) The Pit protein

BlastX GenBank searches (Gish and States, 1993) revealed the Pit protein was similar to:

- the low-affinity Pit phosphate transport protein of *E. coli* (EcPitA) (Sofia et al., 1994). The Pit protein also showed similarity to numerous uncharacterized proteins homologous to EcPitA; these included EcPitB of *E. coli* (Bollinger et *al.*, 1995) whose gene is located at 67 min on the chromosomal map and shares 81.0 % amino acid identity with EcPitA , and the putative low-affinity inorganic phosphate transporter of *Streptomyces halstedii* (Blanco et *al.*, 1993).
- the phosphate-repressible phosphate permease, of *Neurospora crassa* (NcPho-4^{+}) (Mann et al., 1989) and homologous proteins such as several retrovirus receptors in human (vanZeijl et al., 1994), mice (Johann et al., 1992), hamster (Wilson et al., 1994) and rat (Miller et al., 1994).
- the *glvr-1* deduced protein of *Mycobacterium leprae* (Smith, unpublished).

- the *HI1604* deduced protein of *Haemophilus influenza* (a purple bacteria of the gamma subdivision; Fleischmann et *al.*, 1995).
- a putative phosphate permease of *Arabidopsis thaliana* (Quigley et *al.*, 1996).

A *pit*-like gene product appears to be widespread among both prokaryotic and eukaryotic organisms. Its function as a phosphate transporter has been characterized for EcPitA (Rosenberg et al., 1982), NcPho-4$^+$ (Mann et al., 1989), and some of the retrovirus receptors (see for review, Kavanaugh and Kabat, 1996).

Pairwise alignments revealed that EcPitA (499 aa), NcPho-4$^+$ (590 aa) and HI1604 (420 aa) shared 34%, 32% and 27% amino acid identity with the *sfx1*-Pit protein, respectively (Fig. 4-6a). Multiple alignment between these proteins (Fig. 4-6b) showed greatest similarity in the N and the C-terminal regions, whereas the central, mostly hydrophilic domain present in EcPitA and NcPho-4$^+$ and mostly hydrophobic domain of HI1604 was absent from RmPit . The strongest identity to Pit was obtained with the *glvr-1* (*pit*) deduced protein of *Mycobacterium leprae* (414 aa) (39% identity, 61% conserved; Fig. 4-6a). Similarity was seen throughout these proteins except MlPit which carried an additional hydrophilic C-terminal extension 81 amino acids long. Alignment of these two genes revealed 63% identity at the nucleic acid level (Fig. 4-6c).

Hydropathy plot determined by the Tmpred and TopPred II programs and the positive-inside rule (von Heijne, 1986) confirmed the homology data in that

```
RmPit       ---MDATLAFP---LLVGLIAVALFFDFLNGLHDAANSIATIVSTRVLRPQYAVFWAAFF
EcPitA      MLHLFAGLDLHTGLLLLLALAFVLFYEAINGFHDTANAVATVIYTRAMRSQLAVVMAAVF
               . * *       **.  .*  **.. .** **.**..**.. ** .* * **  ** *

RmPit       NFIAFLFFGLHVAETLGTGIIDPGIVTP------QVIFAALMGAITWNIVTWVFGIPSSS
EcPitA      NFLGVLLGGLSVAYAIVHMLPTDLLLNMGSSHGLAMVFSMLLAAIIWNLGTWYFGLPASS
            **.  *  ** ** ..  .  ...        ..*. *. ** **. ** **.*.**

RmPit       SHALIGGLVGAGLA---KTGFSSIVWQGLLKTA---GAIVMSPGIGFVLA--LLLVLIVS
EcPitA      SHTLIGAIIGIGLTNALMTGTSVVDALNIPKVLSIFGSLIVSPIVGLVFAGGLIFLLRRY
            **.*** ..* **.    ** * .  .. *     *....** .* * *  *. .*

RmPit       WLFVRQ------TPFAVDST---------FRVLQFVSASLYSLGHGGNDAQKTMGIIAVL
EcPitA      WSGTKKRARIHLTPAEREKKDGKKKPPFWTRIALILSAIGVAFSHGANDGQKGIGLVMLV
            *   ..      **   .             *.  .**   . ** ** ** .*.. ..

RmPit       LF------------SQGYLGS----------------------------------------
EcPitA      LIGVAPAGFVVNMNATGYEITRTRDAINNVEAYFEQHPALLKQATGADQLVPAPEAGATQ
            *             . **  .

RmPit       --EF------------------------------------------------------------
EcPitA      PAEFHCHPSNTINALNRLKGMLTTDVESYDKLSLDQRSQMRRIMLCVSDTIDKVVKMPGV
              **

RmPit       --------------------YVPFWVVITCQAAIALGTLFGGWRIVHTMGSKITK--LNP
EcPitA      SADDQRLLKKLKSDMLSTIEYAPVWIIMAVALALGIGTMIGWRRVATTIGEKIGKKGMTY
                              * * *....  *. .**. *  *.  *.* ** *  ..

RmPit       MQGFCAETGGAITLFAATWLGIPVSTTHTITGAIIGVGAARRVSAVRWGLAGNIVVAWVI
EcPitA      AQGMSAQMTAAVSIGLASYTGMPVSTTHVLSSSVAGTMVVD-GGGLQRKTVTSILMAWVF
              ** .*.   *... *.  *.****** .. .. *          ..      *..***

RmPit       TMPAAALISALCYFAADLVA
EcPitA      TLPAAVLLSGGLYWLSLQFL
            *.*** *.*   *  .
```

```
RmPit       MDATLAFPLLVGLIAVALFFDFLN-GLHDAANSIATIVSTRVLRPQYAVFWAAFFNFIAF
NcPho4      -MVLHQFDYLLAIGTIFAALDAWNIGANDVANSWATSVAARSVTYLQAMILGSIMEFAGS
                  *  *. . ..    *  * * .* *** ** *..*  .   *.   .   *

RmPit       LFFGLHVAETLGTGIID-------PGIVTPQVIFAALMGAITWNIVTWVFGIPSSSSHAL
NcPho4      VGVGARVADTIRTKVVDTTLFADDPALLMLGMVCAVVASSIYLTMATR-FGLPVSTTHSI
            .  * .**.*. * ..*       * ..   .. * .  .*  .. *  **.* *..*..

RmPit       IGGLVGAGLAKTGFSSIVWQGLLKTAGAI------VMSPGIG-------FVLALLLVLIV
NcPho4      MGGVIGMGIAAVGADGVQWVGSSINDGVVSVFLAWVIAPGLAGAFASIIFLVTKYGVLLR
            .**..* *.*  *   . * *   . * .       *..**.        *...   **.

RmPit       S-------------------------W------------------------------
NcPho4      SNPVYKAFVMVPIYFGITAALLCMLLLWKGGSYKVTLTNPEIAGTIIGVGAAWALLVTIF
            *                         *

RmPit       ------------------------LFVRQ---TPFAVDST------------------
NcPho4      LMPWLYRIVILEDWQLRFWHIPLGPLLLRRGEVPPPPADGSGVVQDFYAGRLTKEQLAAR
                                    * .*.   *   * .

RmPit       ------------------------------------------------------------
NcPho4      RAAQNGDSEMAAGAVTSSTSNPSAPTDGEKGATITKDDSSYSHDHSEPAQAAQPQIKTMV

RmPit       ----------------------FR------------------------------------
NcPho4      GPRPAGPWHSGAVLFWYVKWALFRGVDQDVLSSQQEKSVISSDVEELHAHATHYDNKTEY
                                 **

RmPit       ---VLQFVSASLYSLGHGGNDAQKTMG--IIAVLLFSQGYLG--SEFYVPFWVVITCQAA
NcPho4      MYSFLQIMTAAAASFTHGANDIANAIGPYATVFQLWKDGALPEKGKADVPVWILVFGASC
                 ** ..*.  *  ** **   ..*       *   * *        ** *...   ..

RmPit       IALGTLFGGWRIVHTMGSKITKLNPMQGFCAETGGAITLFAATWLGIPVSTTHTITGAII
NcPho4      LVIGLWTYGYNIMRNLGNRITLQSPSRGFSMELGSAVTVILATRLKLPVSTTQCITGATV
            . .*    *  *....* .**   * .**. * * *.*.  ** * .*****..**** .

RmPit       GVGAARRVS-AVRWGLAGNIVVAWVITMPAAALISALCYFAADLVA-------
NcPho4      GVGLCSGTWRTINWRLVAWIYMGWFITLPVAGIISG-CLMGIIINAPRWGYSG
            *** .     .. * *   * . * **.* * .**  *     . *
```

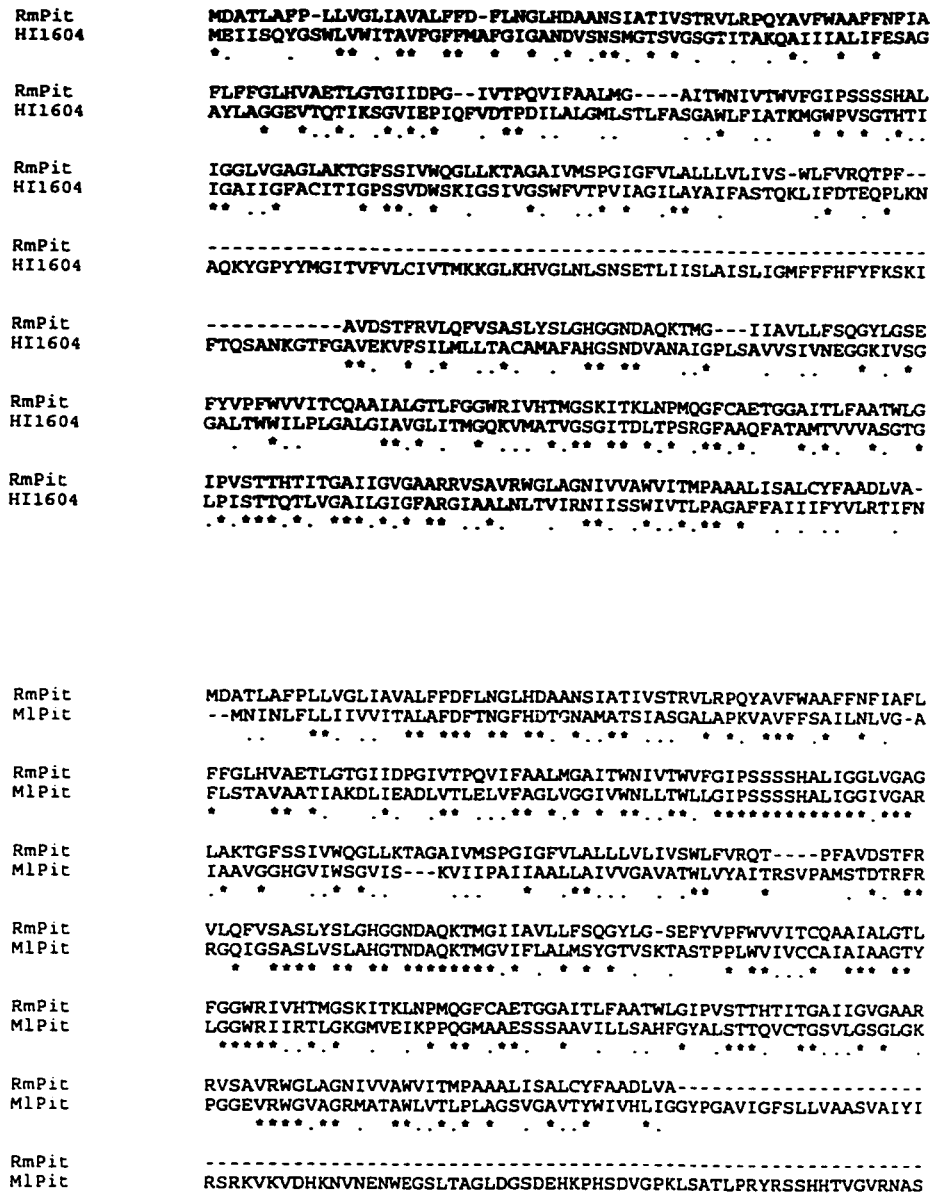

Fig. 4-6a: Pairwise alignments between the *pit* deduced protein of *R. meliloti* (RmPit) and, the *pitA* deduced protein of *E. coli* (EcPitA), the *pho-4*$^{+}$ deduced protein of *N. crassa* (NcPho4), the *HI1604* deduced protein of *H. influenza* (HI1604) *and the glvr-1* deduced protein of *M. leprae* (MlPit). (★) and (.) indicates amino acid identity and conserved, respectively.

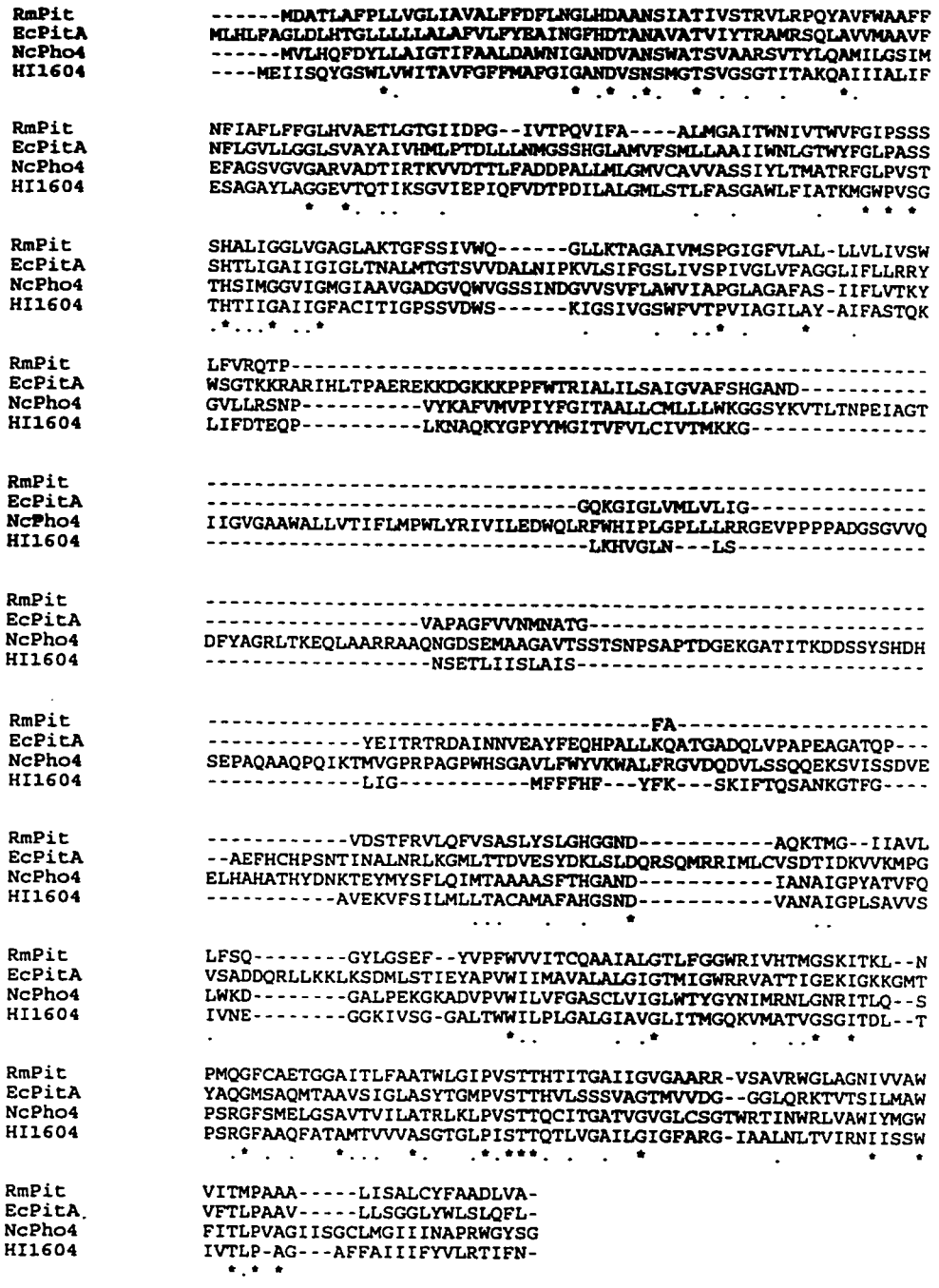

Fig. 4-6b: CLUSTAL W alignment between the *pit* deduced protein of *R. meliloti* (RmPit), the *pitA* deduced protein of *E. coli* (EcPitA), the *pho-4*$^{+}$ deduced protein of *N. crassa* (NcPho4) and the *HI1604* deduced protein of *H. influenza* (HI1604). (★) and (.) indicates amino acid identity and conserved, respectively.

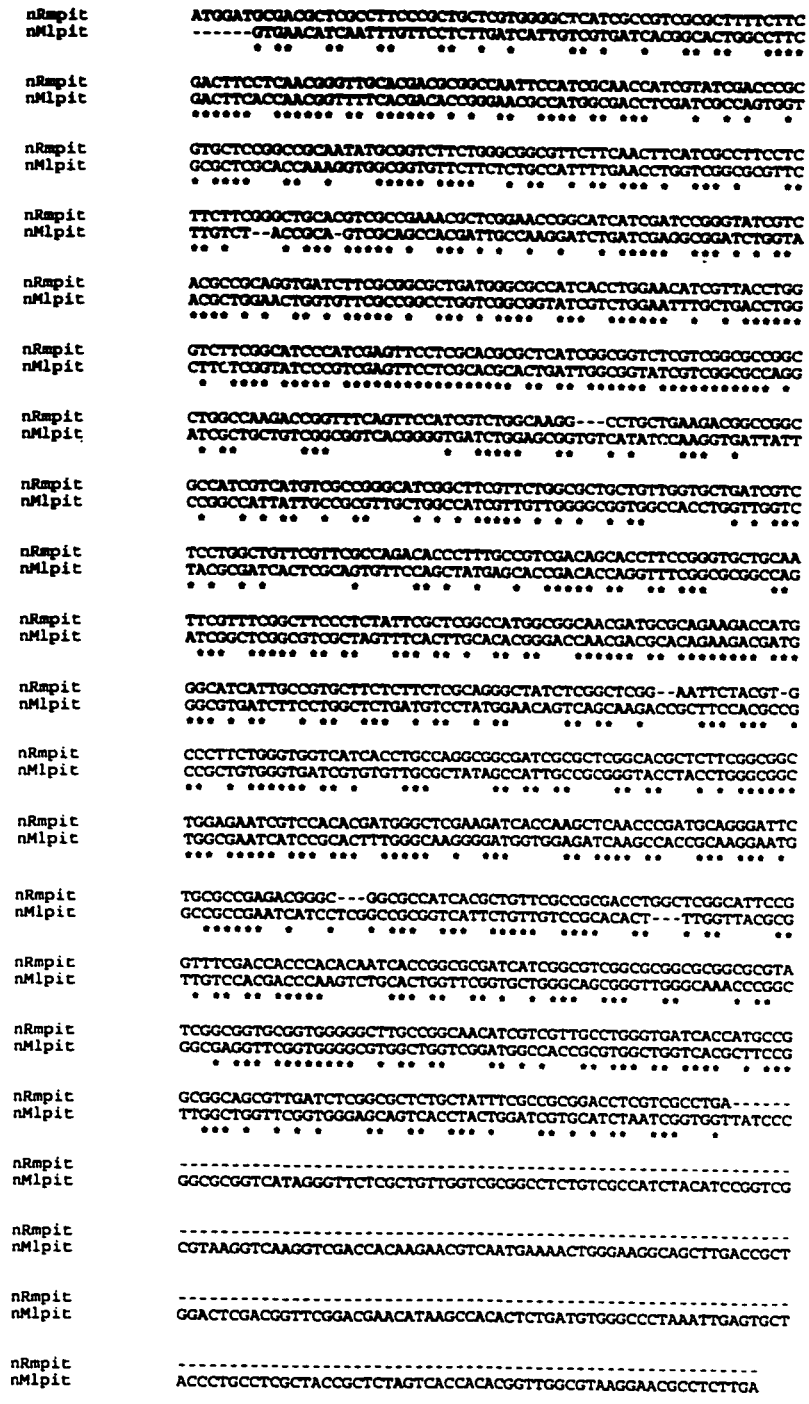

Fig. 4-6c: Pairwise alignments between the *pit* nucleotide sequences of *R. meliloti* (nRmpit) and *M. leprae* (nMlpit). (★) indicates identical nucleotides.

the protein encodes a membrane protein. Nine "certain" membrane-spanning domains were determined by the TopPred II program and a model for the secondary structure of the deduced protein is presented in Fig. 4-7. If RmPit acts as a secondary transporter with a 6+6 transmembrane helices construction (Nikaido and Saier, 1992) as Ncpho-4^{+} and EcPitA are suggested to be (Mann et al., 1989; Wanner, 1996), an active RmPit protein may require the formation of a dimer.

b) The OrfA protein

A GenBank search revealed that the OrfA protein (214 aa) was similar to the deduced protein of *Haemophilus influenza HI1603* open reading frame (226 aa). Alignment of these proteins revealed 21% amino acid identity and 39% conserved (Fig. 4-8a). This result was particularly interesting as this gene was located just upstream from the *pit*-like *HI1604* gene of *H. influenza*. Protein HI1604 shared 27% amino acid identity with the Pit protein (see above). In addition, the *HI1603* and *HI1604* genes were separated by 25bp and thus probably transcribe on a single transcript as appeared to be the case with the *orfA/pit* genes of *R. meliloti*. No *orfA*-like open reading frame was detected upstream from *mlglvr-1* and *EcpitA* and, except for *HI1603*, no other *orfA*-like gene was detected in GenBank searches.

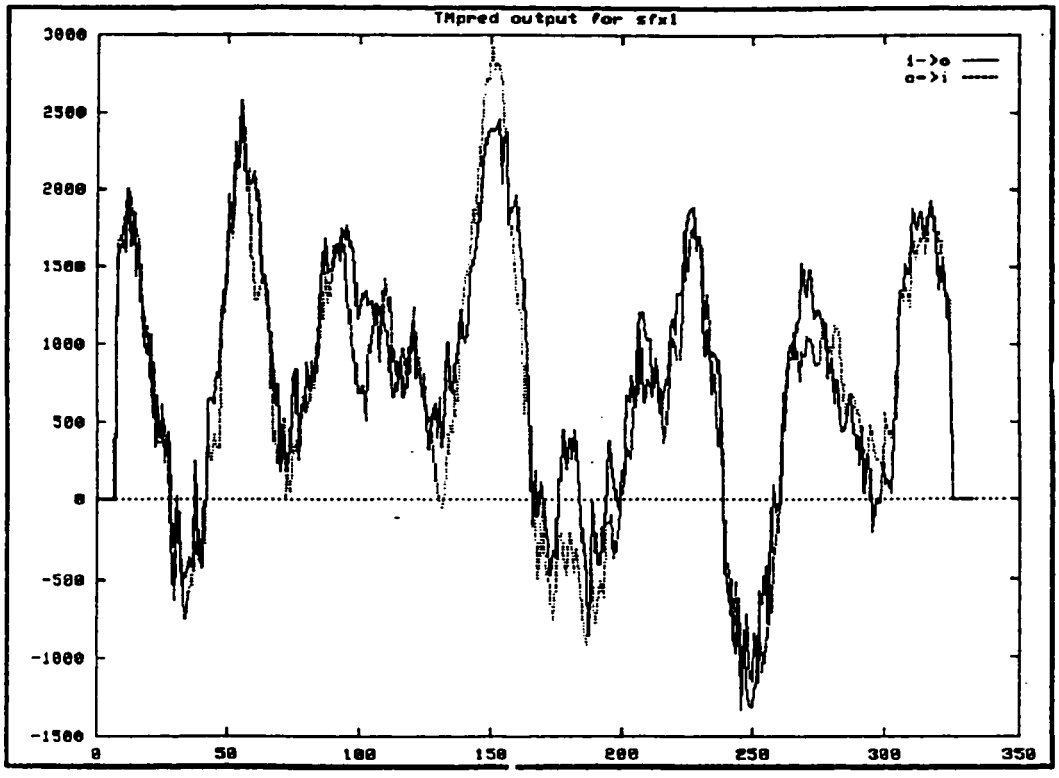

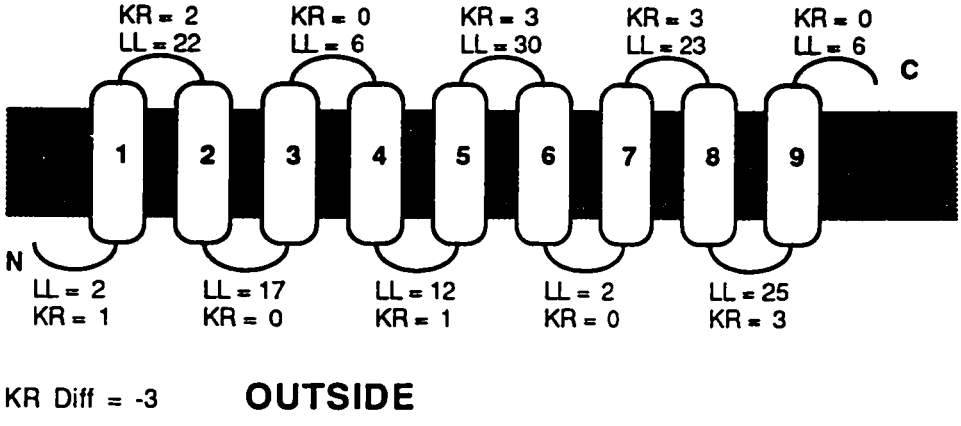

Fig. 4-7: Top; Hydropathy plot generated by the Tmpred program (Hofmann and Stoffel, 1993). Bottom; Drawing created by the TopPred II program (Claros and von Heijne, 1994) representing the secondary structure for the *pit* deduced protein. KR represent the number of Lys and Arg; LL, the loop length and KR Diff, the positive charge difference.

```
OrfA        MLGLFRKLLPREDRFFDLFADHSRTVMGAAEALNALLAG-----GPDIESHCDRIVALEN
HI1603      -MAMNNILGLFAHSPLKPLQKHSEKVTECSDLLIPFFQTTFSKNWEQAEEKRLEISQCER
             . .   *              **  *  ... *                 * .   *   *

OrfA        EADEITREVLLAVRRSFITPFDRGDIKDLIQSMD----DAIDMMHKTVK---TIRLYEQK
HI1603      EADSLKREIRLKLPRGLFLPIDRTDLLELVTQQDKLANYAKDIAGRMIGRQFGIPEEMQE
            *** . **. * . *    * ** *. .*.   *     * *.  . .     *    *

OrfA        SFDPGMQAMGAAVVEAAHLVAEAIPLLSRIGANAHRLSAI---AEEVTHVEDRSDQLHEQ
HI1603      EFLH-YVKRSLDAIHQAHRVIEEMDKLLETGFKGRELKLVNDMIQELDSIEDDTDQMQIK
             *          . ** * * .  *   *   . * .    .*.  .** .**.. .

OrfA        GLKDLFQRHGASNPMAYIIGSEIYGELEKVVDRFEDVANEISGIVIENV
HI1603      LRKMLYTIESRYNPIDVMFLYKIIEWVGVLADQAQRVGSRIELMLARS-
              * *.      **.  .    *   . . *. . *   *  ..
```

>pOrfA

MLGLFRKLLPREDRFFDLFADHSRTVMGAAEALNALLAGGPDIESHCD

RIVALENEADEITREVLLAVRRSFITPFDRGDIKDLIQSMDDAIDMMHKT

VKTIRLYEQKSFDPGMQAMGAAVVEAAHLVAEAIPLLSRIGANAHRLSA

IAEEVTHVEDRSDQLHEQGLKDLFQRHGASNPMAYIIGSEIYGELEKV

VDRFEDVANEISGIVIENV

Fig. 4-8: Top (a); Pairwise alignment between the *orfA* deduced protein of *R. meliloti* (OrfA) and the *HI1603* deduced protein of *H. influenza* (HI1603). (★) and (.) indicates amino acid identity and conserved, respectively.

Bottom (b); OrfA protein sequence showing the potential secretory signal (boxed) and a putative transmembrane domain (underlined).

Analysis of the deduced-protein sequence of *orfA* predicted a secretory signal sequence with a potential cleavage site between position 28 and 29 (Fig.4-8b) which conformed to the (-3, -1) rule (Oliver, 1985), suggesting that the protein may be periplasmic. A search for a potential membrane spanning domains using the Tmpred method suggested the presence of a putative transmembrane helix from amino acid 116 to 135 implying that the protein may be membrane bound. The *HI1603* deduced protein did not show any potential secretory signal sequence in its N-terminal region, nor did it possess any potential membrane spanning domain. This suggests that secondary structure and cell localization of these two proteins may be different and thus may have distinct functions.

c) The RecF and Orf2 proteins

GenBank searches with the DNA upstream of *orfA* revealed a partial open reading frame which was homologous to many RecF proteins In *E. coli*, RecF is required for the resumption of the replication at DNA replication forks (Courcelle et al., 1997; Kogoma, 1997). The highest homology was with the RecF protein of *Caulobacter crescentus* (388aa; Rizzo et al., 1993), where the deduced 176 amino acids of the R. meliloti RecF-like protein shared 43.2% identity; 57.4% conserved with the *C. crescentus* RecF protein (Fig 4-9). The homology

```
RmRecF          MPHKVFLTRLKLSDFRNYATLALDLDQRHVVLTGENGAGKTNLMEGVSFLSPGRGLRRAA
CcRecF          MASAALLS-LTLADFRSYERARLETGGRSVYLFGANGAGKTNLLEAISLLSPGKGLRGVS
                *     *. * *.*** *    *.   * * * * ********.* .* ****.***  .

RmRecF          YADVAR----VGAPDGFSVFAAVD-GMEGSVEIGTGTQGTEEGQSRR-LRINGTAARTVD
CcRecF          LAEVGRRLPGEAVGRAWAVAAEVQSGEDAPVRIGTGVEQG--GAARRTVRLEGETVPPG-
                 *.* *           .* * *  * .  * **** .    * .** .*. * .

RmRecF          ELTDHLRVLWLTPAMDGLFTGPSADRRRFLDRLVLSLDPEHGRRASEFDRAMRSATG---
CcRecF          RLADHVRPIWLTPAQDRLFLEAASERRRFFDRLVFAGEPAHAANANGYDKAQRRAYAPAC
                 *.**.* .***** * **   ...**** **** . .* *   *  .*.* * *

RmRecF          -FSRN-----------------------------------------------------
CcRecF          RRRRNGRAPADAAWLTALEARLAEFGALLAQARARTLLALQAEIDGRGDRPFPLARLGLT
                   **          . .

RmRecF          ------------------------------------------------------------
CcRecF          GEWERMAVEGAPFAEIELKLAQALASARARDGAAGRALTGPHRGDLAIFHVEKDRPAAEC

RmRecF          ------------------------------------------------------------
CcRecF          STGEQKALILNLVLAQAARLSRAESAPNPVILLDEVAAHLDLTRRAALADELTALKLQAF

RmRecF          --------------------------------
CcRecF          LTGTDESLFDHLKGRALGVRVGDAGLTTLEDE
```

Fig. 4-9: Pairwise alignment between the *recF* deduced protein of *R. meliloti* (RmRecF) and the *recF* deduced protein of *C. crescentus* (CcRecF). (★) and (.) indicates amino acid identity and conserved, respectively.

extended over the N-terminus of RecF and hence this gene is transcribed divergently from the *orfA pit* genes.

In GenBank searches with the partial *orf2* region, located downstream from *pit*, we failed to detect *orf2*-like genes.

5- Subcloning of the *sfx1* wild type locus

To investigate the nature of the *sfx1* mutation, we cloned the *orfA pit* region from the wild type strain. As the 4.8kb *Hin*dIII-*Sac*I fragment contained the entire *sfx1* locus (see above) and was present in the wild type strain (see Fig. 4-1b), Rm1021 (wild type) genomic DNA was digested with the *Hin*dIII and *Sac*I restriction enzymes. The resulting fragments were subcloned into the pUC118 vector digested with the same enzymes. *E. coli* DH5α competent cells were transformed with the religated DNA and the 2000 to 3000 Ap^r transformants obtained per plate were screened by colony hybridization using pTH276, the 4.8kb *Hin*dIII-*Sac*I fragment of pTH90, as probe. Plasmid DNA from two clones which hybridized to the probe were further examined by restriction with the *Eco*RI, *Sac*I, *Hin*dIII and *Sac*I/*Hin*dIII enzymes. Only clone #1 carried a 4.8kb *Hin*dIII-*Sac*I fragment similar to the one found in pTH90 (data not shown). This clone, designated pTH354, contains the wild type *sfx1* locus.

6- Localization of the *sfx1* mutation

To determine whether the *sfx1* mutation lay in the *orfA-recF* intergenic region (Fig. 4-4a), *Xho*I/*Eco*RI (3) and *Eco*RV(1)/*Eco*RI (3) fragments from the *sfx1* locus were cloned, together with a Nm^r marker, into pBR322 to give pTH396 and pTH397 respectively (see Material and Methods). The two plasmids were transferred into RmG490 (*phoC*Ω490) and the Nm^r recombinants arising via a Campbell-type single crossover in the RmG490 genome were isolated. These colonies were screened on GYM medium, where *phoCDET* mutants generate a mucoid colony phenotype as opposed to the dry colony phenotype of the wild type and *phoC*Ω490 *sfx1* strains. Suppression of the *phoC*Ω490 mucoid phenotype in these recombinants was dependent on: (i) the presence and location of the *sfx1* mutation in the cloned fragment and (ii) the location of the recombination event. 12 out of the 70 (17%) pTH396 recombinants formed dry colonies on GYM medium and thus suppressed the mucoid phenotype of RmG490. Also, these twelve recombinants grew similarly to the wild type in MOPS medium containing 2mM phosphate (data not shown). All 70 pTH397 recombinants tested formed mucoid colonies on GYM. Together these data indicate that the *sfx1* mutation lay between the *Xho*I and *Eco*RV(1) restriction sites of pTH276 (*orfA-recF* intergenic region).

The *Xho*I/*Eco*RV(1) fragments from the *sfx1* locus in pTH380 and the wild type locus in pTH354 were subcloned in pUC118. The DNA sequence of each

```
WTEVX       GATATCGACGTTGCTGTCAGGTAGGATGAAAGCCCGGCCAAGGCAAGGCGGAAAGGGTGT
SFX1EVX     GATATCGACGTTGCTGTCAGGTAGGATGAAAGCCCGGCCAAGGCAAGGCGGAAAGGGTGT
            ************************************************************

WTEVX       TCTGTCCGCCTCTCCCCCGCCTGCGGCGATTCCGTATCCGGGCTGCGCATTTCCGCCCCA
SFX1EVX     TCTGTCCGCCTCTCCCCCGCCTGCGGCGATTCCGTATCCGGGCTGCGCATTTCCGCCCCA
            ************************************************************

WTEVX       ATCGCCTGTGGGAAAGCCGTTTTTTTCGGCCGCATCGGAACTTTCCCCGAGCGCGCAAGT
SFX1EVX     ATCGCCTGTGGGAAAGCCGTTTTTT-CGGCCGCATCGGAACTTTCCCCGAGCGCGCAAGT
            *************************** ************************************

WTEVX       ACAATATGACAACTGCGTGACAATCGACAGTTGGATGGATCGCTGATGCTCGGCCTGTTT
SFX1EVX     ACAATATGACAACTGCGTGACAATCGACAGTTGGATGGATCGCTGATGCTCGGCCTGTTT
            ************************************************************

WTEVX       CGCAAGCTCCTCCCCCGGGAAGACCGTTTCTTCGACCTCTTCGCCGATCATTCGCGCACC
SFX1EVX     CGCAAGCTCCTCCCCCGGGAAGACCGTTTCTTCGACCTCTTCGCCGATCATTCGCGCACC
            ************************************************************

WTEVX       GTCATGGGTGCGGCGGAGGCACTGAACGCGTTGCTTGCCGGCGGCCCGGACATCGAAAGC
SFX1EVX     GTCATGGGTGCGGCGGAGGCACTGAACGCGTTGCTTGCCGGCGGCCCGGACATCGAAAGC
            ************************************************************

WTEVX       CATTGCGACCGCATCGTCGCGCTCGAG
SFX1EVX     CATTGCGACCGCATCGTCGCGCTCGAG
            ***************************
```

Fig. 4-10: Pairwise alignment of the wild type and *sfx1* *Xho*I-*Eco*RV sequences. (★) indicates nucleotide identity. Only one mismatch is observed; deletion of a thymidine residue in the hepta-thymidine region of the *sfx1* sequence.

fragment was determined. Both sequences were identical, except for a missing T in a hepta-thymidine region of the wild type sequence (i.e.: 7Ts in wild type sequence versus 6Ts in the sequence from the *sfx1* locus; Fig. 4-10). This region is centered 81 residues upstream from the *orfA* start codon.

In summary, these data confirmed that the *sfx1* mutation is located within the *XhoI/EcoRV*(1) fragment of pTH276 and provide strong evidence that the thymidine deletion in the *sfx1* sequence is responsible for the phenotypic differences between the wild type and the *sfx1 orfA pit* locus.

7- Effect of *sfx1* on *orfA* and *pit* expression

To investigate whether the genotypic difference between the *sfx1* and wild type locus resulted in differences in *orfA pit* expression, we constructed transcriptional *lacZ* fusions to *orfA* and *pit* from both the wild type and *sfx1* locus. The fusions, which included the *recF-orfA* intergenic region, were made by subcloning the 2.1kb *EcoRI* and the 1kb *EcoRI/SphI* fragments of pTH380 (sfx1) and pTH354 (wild type) into the broad host range plasmid pMP220 (see Materials and Methods). In addition, chromosomal *pit* fusions in both wild type and *sfx1* strains were constructed in which a cassette (*lacZ*mobSp) was inserted immediately following the *pit* gene such that *lacZ* was transcriptionally fused to *pit* (see Materials and Methods).

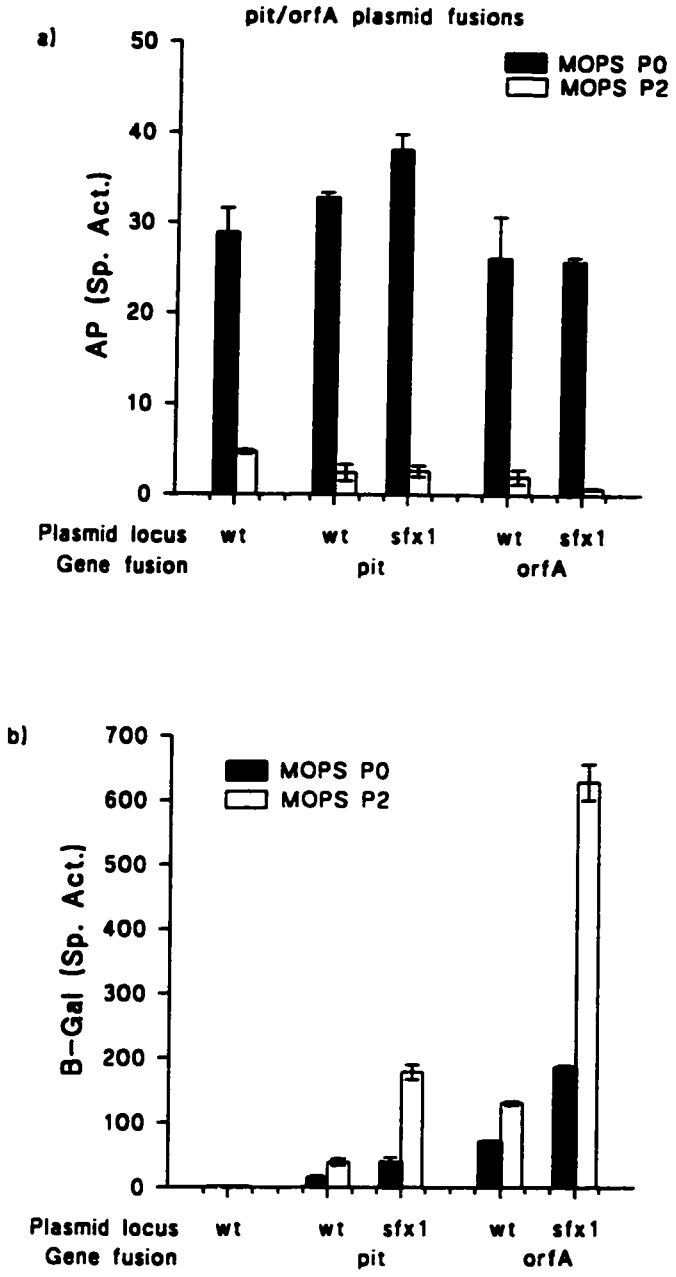

Fig. 4-11: Histogram showing the alkaline phosphatase (a) and β-galactosidase activities (b) of the *pit* and *orfA*::*lacZ* plasmid fusions containing strains after 38 hours growth in MOPS-buffered minimal media with no phosphate added (■) and supplemented with 2mM phosphate (□). The plasmid fusions were made by subcloning the *pit* and *orfA* genes from both wild type (wt) and *sfx1* loci in pMP220. Each data point represents the average of triplicate values ± S.E. (error bars).

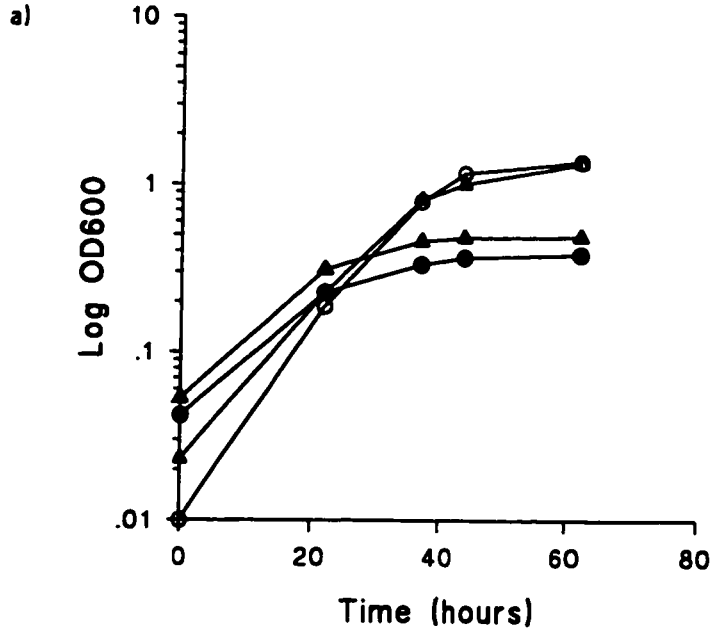
a)
10
1
.1
.01
Log OD600
0
20
40
60
80
Time (hours)

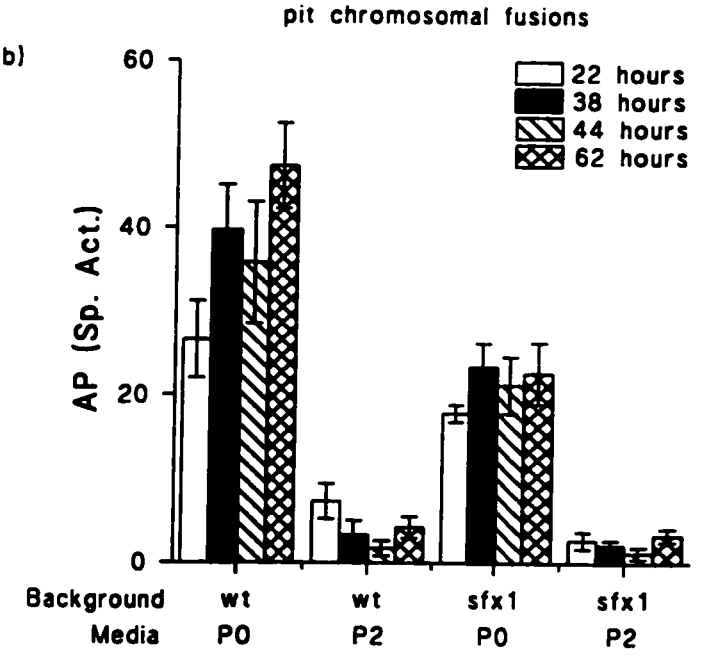
pit chromosomal fusions
b)
60
40
20
0
AP (Sp. Act.)
22 hours
38 hours
44 hours
62 hours
Background
Media
wt
P0
wt
P2
sfx1
P0
sfx1
P2

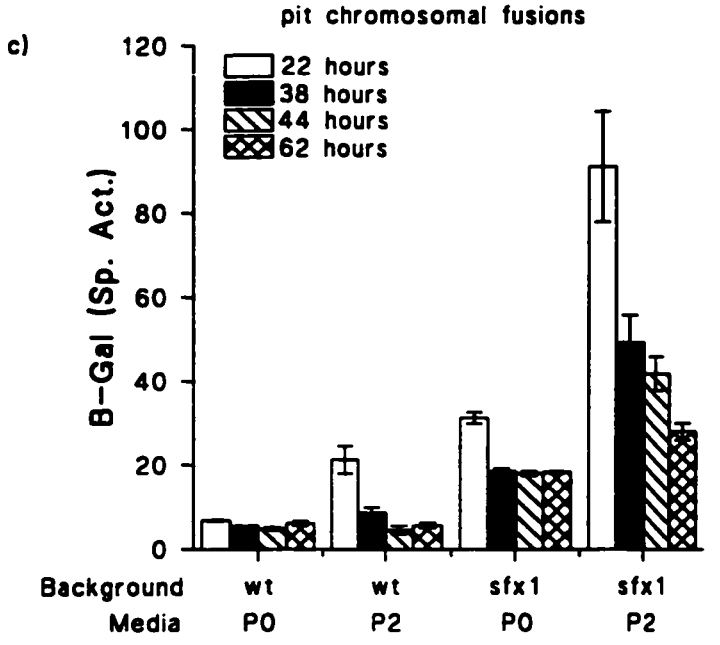

Fig. 4-12: Growth (a), alkaline phosphatase (b) and β-galactosidase activities (c) of *pit*::*lacZ* chromosomal fusions from wild type and *sfx1* strains after 22, 38, 44 and 62 hours growth. (a); ●, ○: *pit* fusion from a wild type background; ▲, Δ: *pit* fusion from a *sfx1* background. ●, ▲: cells grown in MOPS P0; ○, Δ: cells grown in MOPS P2. (b and c); pit chromosomal fusions from wild type (wt) or sfx1 background strains grown in MOPS P0 or P2 media. The β-galactosidase activities presented are corrected from the activity obtained when the *lacZ* gene was fused in the opposite orientation relative to *pit*. This activity was about 10 units whatever the growth conditions. Each data point represents the average of triplicate values ± S.E. (error bars).

Expression of the wild type and *sfx1 orfA pit* fusions were tested after 38 hours growth in MOPS-buffered media with no phosphate (P0) or 2mM phosphate (P2) added. High and low alkaline phosphatase (AP) activities confirmed that the cells were grown under phosphate deficient and phosphate sufficient conditions respectively (Fig. 4-11a and 4-12b). The expression of *sfx1-pit*, as measured by the level of β-galactosidase activity of plasmid-borne fusions, was 3 and 5 times higher than the wild type-*pit* fusion following growth in MOPS P0 and MOPS P2, respectively (Fig. 4-11b). Similarly, expression of the *sfx1-orfA* fusion was about 3-fold higher than the wild type-*orfA* fusion. Higher levels of expression for all the plasmid born fusions were obtained when the cells were grown in MOPS P2 as opposed to MOPS P0 suggesting that *orfA pit* expression increased when the cells were grown under phosphate sufficient conditions. In all backgrounds and whatever the growth condition of the cells containing the fusions, the level of *orfA* expression was 3- to 5-fold higher than the level of *pit* expression.

The chromosomal fusions showed lower levels of expression than the plasmid fusions as expected due to the lower copy number of the genes. (As in the case of the plasmid fusions, the chromosomal *pit* fusions showed 3- to 5-fold more expression in the *sfx1* than in the wild type background (Fig. 4-12c). Analyzing the expression of the fusions at various stages of growth revealed a higher level of *pit* expression in the exponential phase of growth (22 hours).

When reaching the saturation phase of growth, *pit* expression decreased to a constitutive low level of expression that remained more than 3-fold higher in the *sfx1* than in the wild type background. Thus, consistent with the results of the plasmid fusions, the *sfx1* mutation led to at least 3-fold increase in *pit* expression. Phosphate regulation was observed, after 22 hours growth (exponential phase), in both the wild type and *sfx1* background with 3 times more expression for the cells grown in MOPS P2 than in MOPS P0. This regulation was however not observed in the wild type background and was gradually reduced in the *sfx1* background as the cells settled in saturation phase suggesting a growth phase regulation of the locus. This apparent lack of phosphate regulation in the wild type background may reflect the very low level of expression (limit of detection) measured from these fusions.

In summary, our results show increased *orfA pit* expression due to the *sfx1* mutation. The *orfA pit* expression appears to be under the influence of the phosphate content of the media with increased expression of *orfA pit* in response to high external phosphate concentration. This phosphate-induced regulation was the reverse of what was observed for the genes of the Pho regulon.

8- Effect of the *phoC*Ω490 mutation on *orfA* and *pit* expression

Using plasmid-borne fusions, we also investigated whether the *phoCDET* mutation affected *orfA pit* expression. The plasmids from both wild type and *sfx1*

locus were mated into RmH667 (Lac$^-$; *phoC*Ω490) and assayed for β-galactosidase expression after 38 hours growth in MOPS P0 or MOPS P2. The alkaline phosphatase activity was as expected; with the *phoCDET* derived strains showing high alkaline phosphatase activity when the cells were grown in MOPS P0 and MOPS P2 (Fig. 4-13a; see also Bardin et al., 1996, Fig. 5). The *phoC*Ω490 mutation reduced the expression of *orfA pit* from a wild type promoter so that the level of expression of the fusions was the same whether they were from MOPS P0 or MOPS P2 grown cells (Fig. 4-13b). An identical result was obtained when the *phoC*Ω490 mutation was transduced in the chromosomal pit::lacZ fusion strain (Fig. 4-13d). This provides additional evidence that *phoCDET* cells behave as if they were phosphate starved. The level of *sfx1-pit::lacZ* chromosomal fusion in a *phoC*Ω490 background was identical to the level of expression in a wild type background. This result, together with the lack of AP activity from MOPS P2 grown cells (Fig. 4-13c), confirmed that the *sfx1-orfA pit* is functional in these constructs. Expression of the *sfx1-orfA* and *sfx1-pit* plasmid fusions from MOPS P2 grown cells was reduced by 23 to 30% in a *phoCDET* background. However, their level of expression was still 2 to 3 times higher than the level of the wild type fusions in a wild type background grown in MOPS P2. A 2- to 3-fold increase in *orfA pit* expression, due to the *sfx1* mutation, appeared here again to be sufficient to allow suppression of the *phoCDET* phenotypes.

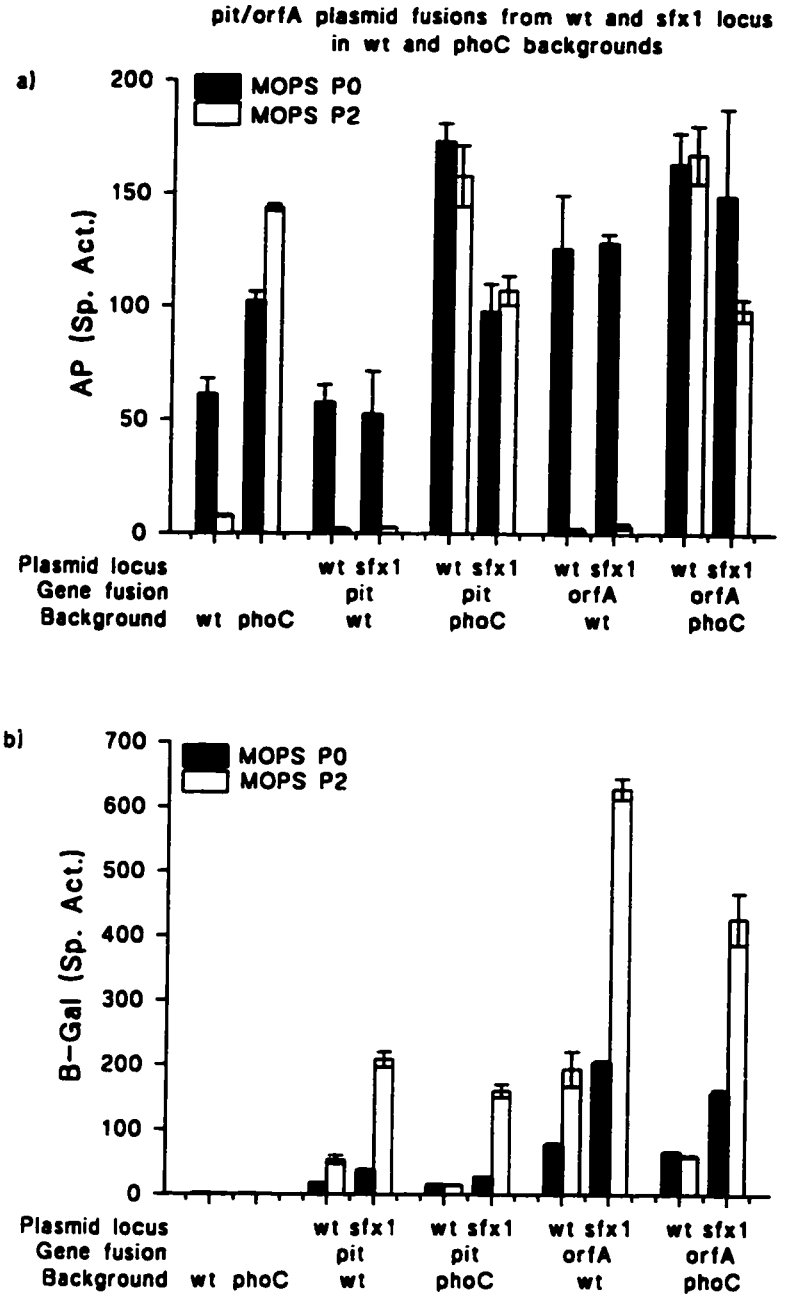

Fig. 4-13: Histogram showing the alkaline phosphatase (a) and β-galactosidase activities (b) of the *pit* and *orfA*::*lacZ* plasmid fusions containing strains after 38 hours growth in MOPS-buffered minimal media with no phosphate added (■) and supplemented with 2mM phosphate (□). The plasmid fusions, made by subcloning the *pit* and *orfA* genes (Gene fusion) from both wild type (wt) and sfx1 loci (Plasmid locus), were mated in both wild type (wt) and H667 (*phoC*Ω490) backgrounds. Each data point represents the average of triplicate values ± S.E. (error bars).

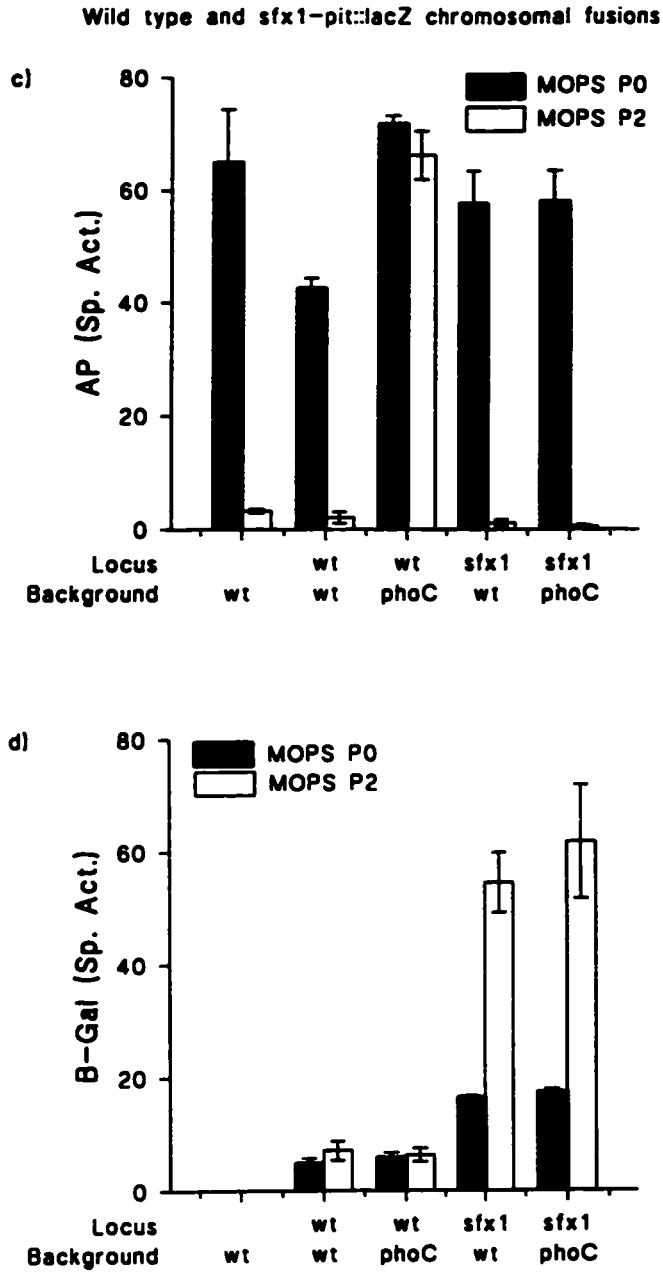

Fig. 4-13: Histogram showing the alkaline phosphatase (c) and β-galactosidase activities (d) of the wild type- and *sfx1-pit*::*lacZ* chromosomal fusions after 32 hours growth in MOPS-buffered minimal media with no phosphate added (■) and supplemented with 2mM phosphate (□). The fusions were tested in both wild type and *phoC*Ω490 backgrounds. The β-galactosidase activities presented are corrected from the activity obtained when the *lacZ* gene was fused in the opposite orientation relative to *pit*. This activity was about 10 units whatever the growth conditions. Each data point represents the average of triplicate values ± S.E. (error bars).

It is interesting that *sfx1*-derived fusions were still phosphate regulated in the *phoC*Ω490 background. As these cells are phosphate starved even when they are grown in MOPS P2 media, as indicated by the high level of AP measured, we would have expected *sfx1-pit* and *sfx1-orfA* expression to be the same in both MOPS P0 and MOPS P2 *phoC* grown cells. High expression of the fusions in MOPS P2 suggested that the *sfx1* promoter mutation enabled the locus to be induced by the high external phosphate concentration probably by enhancing the binding of a phosphate-dependent transcriptional activator. The mechanism by which this occurred and the protein(s) involved in this regulation remain to be characterized.

9- Increasing the wild type *orfA pit* copy number suppresses the *phoC*Ω490 growth phenotype

The data obtained from the above expression studies suggested that a small increase (3x) in orfA *pit* expression was sufficient to suppress the phenotypes associated with the *phoCDET* mutation. We therefore cloned the wild type *orfA pit* locus as a partial 2.6kb *Eco*RI fragment from pTH354 into the broad host range vector pRK7813. The resulting plasmid, pTH391 was mated into RmG490 (*phoC*Ω490). As a control experiment, we also mated plasmid pTH348, carrying the *sfx1* region, into RmG490. Both of these transconjugants grew like the wild type in MOPS media containing 2mM phosphate (Fig. 4-14).

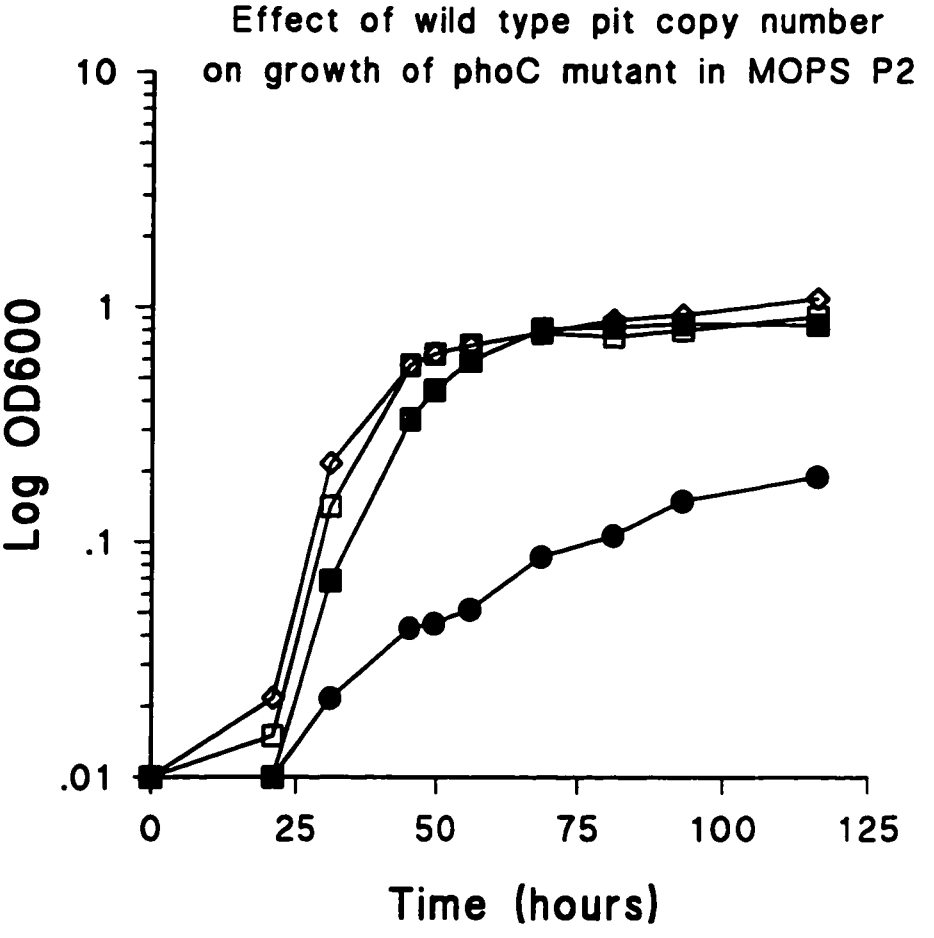

Fig. 4-14: Growth of Rm1021 (wt, ■), RmG490 (*phoC*Ω490, ●), RmH607 (*phoC*Ω490 / pTH348,✧) and RmH841 (*phoC*Ω490 / pTH391, □) in MOPS-buffered minimal media supplemented with 2mM Pi. Each time point represents the average of triplicate values.

This observation confirmed that increasing the copy number of the wild type *orfA pit* locus was sufficient to allow wild type growth of the *phoCΩ*490 mutant in media containing 2mM phosphate.

10- Role of *orfA pit* in divalent cation assimilation

Van Veen et al. (1994a and b; 1993b) showed that a metal-phosphate ($MeHPO_4$, with Me being either Ca^{2+}; Mg^{2+}; Mn^{2+} or Co^{2+}) but not Pi was translocated via the Pit system in *E. coli* and *A. johnsonii.* Preliminary experiments were performed to address whether the orfA *pit* locus of *R. meliloti*, characterized in this study, was influenced by the Ca^{2+} and/or Mg^{2+} divalent cations present in the MOPS-buffered minimal medium. Growth of the wild type strain Rm1021, RmG490 (*phoCΩ*490), RmG762 (*phoCΩ*490, *sfx1*) and RmG591 (*sfx1*) was examined in MOPS P2 media in the presence or absence of either Ca^{2+}, Mg^{2+} or both of these cations (Fig. 4-15). The absence of Mg^{2+} dramatically reduced the final growth yield of all cultures (OD_{600} of 0.3 at 0mM Mg^{2+} vs OD_{600} of 1.0 in 2mM Mg^{2+}). The yield was even more reduced when both Ca^{2+} and Mg^{2+} were withdrawn from the media (reaching an OD_{600} of 0.25 for the wild type strain). The absence of either Ca^{2+} or Mg^{2+} from the media did not result in any growth phenotype of the *sfx1* containing strains. However, in cultures lacking both Ca^{2+} and Mg^{2+} the yield of RmG591 and RmG762 cultures was reduced when compared to the wild type strain. Strain RmG762 in which phosphate

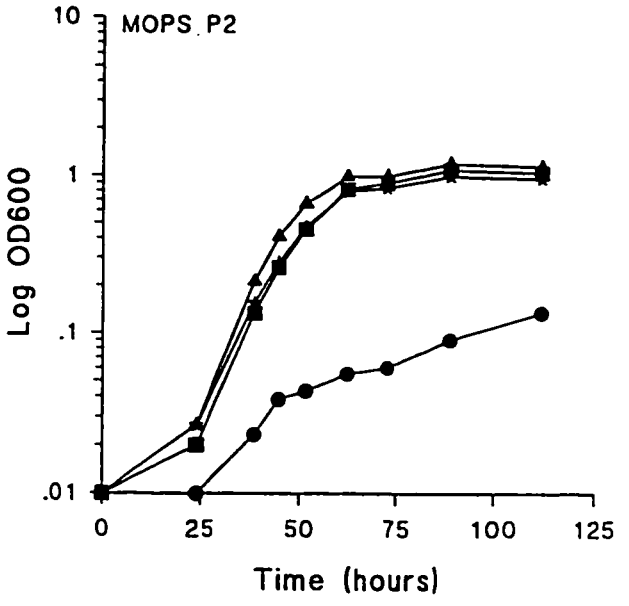
MOPS P2
10
1
.1
.01
Log OD600
0
25
50
75
100
125
Time (hours)

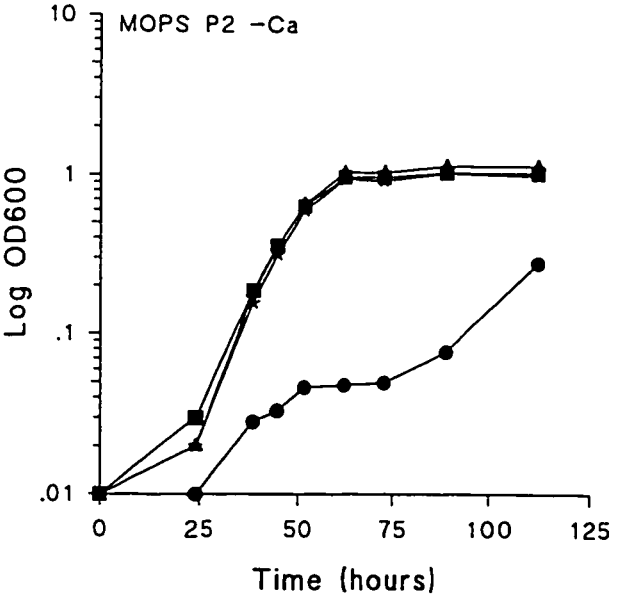
MOPS P2 -Ca
10
1
.1
.01
Log OD600
0
25
50
75
100
125
Time (hours)

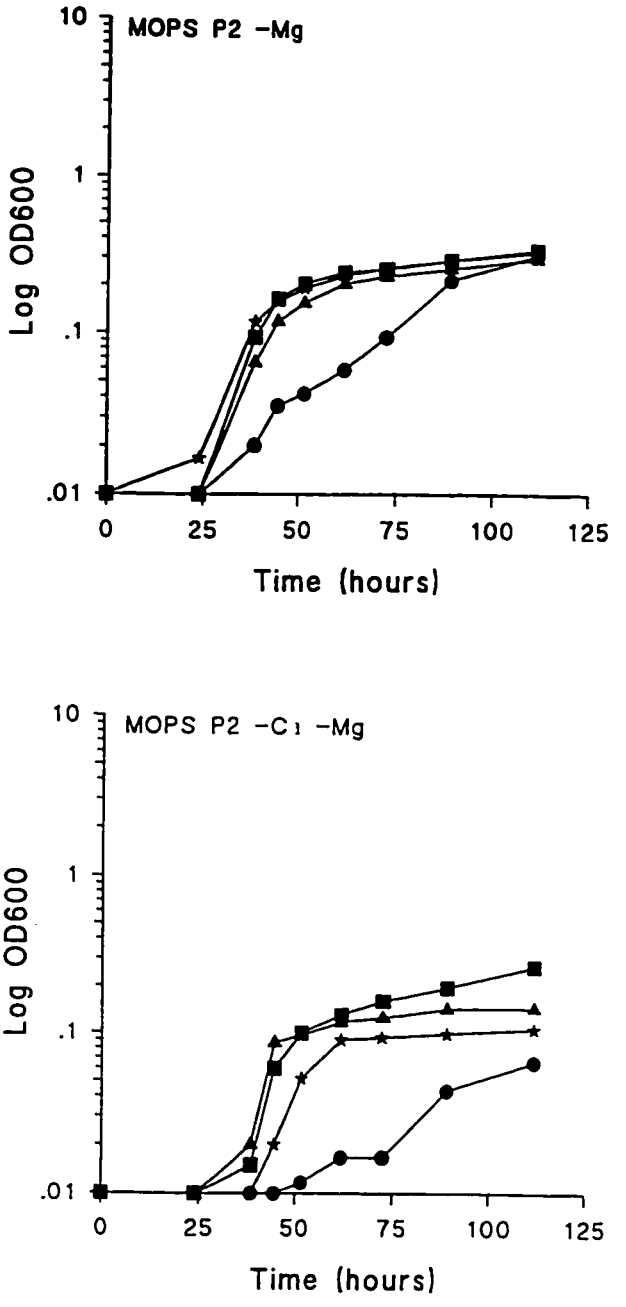

Fig. 4-15: Growth of Rm1021 (wt, ■), RmG490 (*phoC*Ω490, ●), RmG762 (*phoC*Ω490, *sfx1*, ★) and RmG591 (*sfx1*, ▲) in MOPS-buffered minimal media supplemented with 2mM Pi (MOPS P2) and lacking $CaCl_2$ (MOPS P2 -Ca), $MgSO_4$ (MOPS P2 -Mg) or lacking both divalent cations ($CaCl_2$ and $MgSO_4$; MOPS P2 -Ca -Mg). Each time point represents the average of triplicate values.

uptake appears to occur primarily via the Pit system still grew significantly more than RmG490 (*phoC*Ω490), suggesting that even though the Pit system may preferably translocate metal phosphate, it is able to take up ortho-phosphate as well. The levels of *pit* expression in wild type or *sfx1* backgrounds, as determined by the level of β-galactosidase expression from *lacZ* plasmid fusions, was not affected by the absence of divalent cations in the growth media (data not shown).

Our experiments demonstrated that Mg^{2+} cations are required for growth. *R. meliloti* strains, dependent on the Pit transport system for phosphate uptake, show a slight growth reduction in media lacking both Ca^{2+} and Mg^{2+} divalent cations. We note however that further experiments will have to be done in order to directly address the substrate specificity of the Pit system.

D- Discussion

The *sfx1* locus of *R. meliloti* was previously identified through the genetic analysis of second-site mutations which suppress the symbiotic Fix$^-$ phenotype of *ndvF* mutants (Oresnik et al., 1994). The *ndvF* locus contains four genes, *phoCDET*, which encode a phosphate transport system (Chapter III; Bardin et al., 1996).

This chapter reports a genetic characterization of the *sfx1* suppressor mutation. The locus, localized in a 2kb *Eco*RI-*Eco*RV fragment, contains two open reading frames designated *orfA* and *pit*. Because the two genes partially overlap and showed the same type of regulation, they probably constitute an operon in the order, *orfA-pit*. The predicted *R. meliloti* Pit protein is homologous to phosphate transport proteins previously identified in *E. coli* and *Neurospora crassa* (Sofia et al., 1994, Mann et al., 1989). Suppression of the symbiotic and growth phenotypes associated with mutation in the *ndvF* (*phoCDET*) locus by *sfx1* suggests that the loss of one phosphate transport system (*phoCDET*) was rescued by mutation in a second phosphate transporter (*orfA pit*). Evidence that *sfx1* was dependent upon a functional *orfA-pit* locus included (1) Tn*5* mutations in *pit* and/or *orfA* abolished suppression of both the symbiotic and growth phenotype of a *phoCDET* strain and (2) Pi uptake of a *phoCDET* mutant strain

could not be restored when the *pit* gene was interrupted by a Tn*5* insertion (Dr. Voegele, personal communication).

In the absence of the major phosphate transport system encoded by *phoCDET*, the wild type *orfA pit* allele was not able to assimilate enough phosphate to sustain the metabolic functions of the cell (even when the cells were grown in a media containing high phosphate concentration). This raises questions concerning the regulation of expression of this locus.

The work presented here strongly suggests that the low level of *orfA pit* expression is responsible for the lack of phosphate assimilation in the *phoCDET* mutant strains. Employing chromosomal and plasmid-borne transcriptional *lacZ* gene fusions, we found that the *orfA pit* expression from the *sfx1* locus was 3 to 5 times higher than *orfA pit* expression from the wild type locus. In addition, increasing the expression of the wild type *orfA pit* locus by subcloning it in a multicopy plasmid (like pRK7813) was sufficient to suppress the growth phenotype of a *phoCDET* mutant. Preliminary results also indicated that this plasmid restored some Pi uptake of *phoCΩ*490 strain (data not shown). Suppression by the wild type *orfA pit* locus cloned on a low copy number plasmid vector (pLAFR1, that contained 2 to 4 copies per cell; data not shown), as well as the 3- to 5-fold increase in expression of the locus by the *sfx1* mutation suggests that as little as 3 extra copies of the wild type locus may be sufficient to assimilate enough phosphate to support normal cell growth for *phoCDET*

mutants in MOPS P2 and to fix nitrogen efficiently when inoculated on alfalfa plants.

orfA pit expression, whether in a wild type or *sfx1* background is also under phosphate regulation. Higher levels of expression were measured when the cells containing the *orfA* and *pit*::*lacZ* plasmid-borne fusions were grown under phosphate sufficient conditions (2mM Pi) than phosphate limiting conditions (0mM Pi). Similar results were obtained when exponentially growing cells containing the *pit* chromosomal fusions in both the wild type and *sfx1* backgrounds were examined. *orfA pit* is then phosphate regulated in an opposite manner than the genes of the Pho regulon. Pit may then be the main Pi transporter under phosphate sufficient conditions while *phoCDET* would take up phosphate mainly when Pi concentrations in the environment are reduced. The inability of the *orfA pit* wild type locus to assimilate enough phosphate, under Pi sufficient conditions, to allow growth of a *phoCDET* mutant can be explained by the repression of the locus in these phosphate-starved cells. This suggested that *pit* expression may depend upon the internal, rather than external Pi concentration. Alternatively, the PhoCDET transport system may be involved in sensing the environmental Pi concentration and thus be indirectly involved in regulating *pit* expression. The involvement of PstSCAB, the high affinity phosphate transport system in *E. coli*, in sensing environmental phosphate has also been suggested (Wanner, 1996). It is interesting the locus directed by a

sfx1 mutation was still expressed and was phosphate regulated under these conditions.

The biochemical characteristics of the Pit transport system are currently being examined in our laboratory by Dr. Voegele. He has confirmed that *pit* encodes a low-affinity phosphate transport system that constitutes the main phosphate transporter in a phosphate sufficient environment. On this basis, RmPit is similar to the PitA system of *E. coli*; Muda et al. (1992) postulated that Pit is the major phosphate transporter under high phosphate conditions, with Pst, the high-affinity phosphate transport system in *E. coli*, participating to only 30% of the Pi uptake. RmPit however differs from EcPitA as far as its regulation is concerned; *EcpitA* was shown to be constitutively expressed in *E. coli* (Willsky and Malamy, 1980a) while we presented evidence that it is phosphate regulated in *R. meliloti*.

The *sfx1* suppressor mutation was located in the promoter region of the *orfA* gene and was characterized as a deletion of a thymidine residue in an hepta-thymidine sequence located about 80 nucleotides upstream from the start codon of *orfA*. As this deletion appears to increase expression of the *orfA-pit* locus, the point mutation likely affected the binding site or destabilized a repressor component of the system. Alternatively, it may increase the stability of a phosphate-dependent activator/σ-factor/RNA polymerase complex to the promoter region leading to an increased level in *orfA pit* expression. In this

respect, Scholten and Tommassen (1993) showed that the level of *phoE* expression could be increased in cells grown under phosphate sufficient conditions by modifying the Pribnow box of the promoter toward a more optimal consensus sequence.

Analysis of the promoter region revealed the presence of a putative Pho Box just upstream from the thymidine deletion suggesting that PhoB may regulate the locus. In *E. coli*, PhoB transcriptionally activates the genes of the Pho regulon under phosphate limiting conditions (Wanner, 1996). As *R. meliloti orfA pit* expression is repressed under these conditions, PhoB or a PhoB-dependent protein appears to negatively regulate the locus. PhoB has never been shown to act as a negative regulator in *E. coli*, although Smith and Payne (1992) postulated that PhoB may negatively regulate, in response to a low phosphate environment, the expression of the periplasmic binding proteins involved in peptide transport in *E. coli*. Analysis of *phoB* mutants of *Rhizobium meliloti* revealed its role as repressor of the *orfA-pit* locus (see Chapter V). The *sfx1* mutation, however, did not affect the PhoB repression as *phoB* mutations affected *orfA pit* expression in a similar manner whether fusions from the wild type or *sfx1* locus were considered. The mechanism by which the *sfx1* point mutation in the promoter region of *orfA pit* leads to increased expression of the locus as well as the proteins involved in this induction are still unknown.

The role and function of *orfA* is unclear. The gene shows no homology with the GenBank data base except with the *HI1603* gene of *Haemophilus influenza* (Fleischmann et al., 1995). *HI1603* is itself located upstream from a *pit*-like gene in this organism. However it appears that these two proteins are structurally different and hence may have distinct functions. Because of its weak (if any) association with the membrane, it is unlikely that OrfA is involved in the transport itself and may rather be involved in regulating *pit* expression.

The PitA transporter in *E. coli* as well as the low affinity phosphate transport system of *A. johnsonii* have been shown to transport divalent metal-phosphate instead of Pi (Van Veen et al., 1994b; Van Veen et al., 1993b). Experiments in which the divalent cations were withdrawn from the growth media reduced the growth of cells depending on the Pit system for phosphate assimilation. The Pit system of *R. meliloti* may then have a similar substrate specificity to the Pit systems of *A. johnsonii* and *E. coli* (Van Veen et al., 1993b; Van Veen et al., 1994b). Additional experiments are however required to confirmed this observation.

In summary, suppression of the symbiotic phenotype of the *phoCDET* mutants occurred by increasing the level of expression of a locus, *orfA pit*, likely to encode a second phosphate transport system in *R. meliloti*. This provides additional evidence that it was the failure of *phoCDET* to take up phosphate that was responsible for the symbiotic phenotype of this strain. The mechanism by

which *sfx1* increases *orfA pit* expression remains unclear. However, the point mutation (deletion of a thymidine in the hepta-thymidine region of what is believed to be the *orfA pit* promoter region) seems to be specific for suppression of the phenotypes associated with *phoCDET* mutations. It was indeed found that *sfx4* and *sfx5*, other Class I suppressor mutations, isolated from independent inoculation experiments, possess the same deletion (N. Falcioni, personal communication).

Appendix B

pTH61 is a pUC18 derived plasmid containing the 12kb *Hin*dIII fragment of pTH90 (*sfx1* locus). In addition to the global restriction map, the sites for a given restriction enzyme are shown on individual maps and the distances between the sites are indicated (in kb). *Bgl*II (Bg); *Eco*RI (R), *Eco*RV (V), *Sac*I (Sc), *Sma*I (Sm) and *Xho*I (X).

Drawing showing the overlapping fragments used to determine the 2828bp sequence containing the *sfx1* mutation. The sequence is presented from the *Eco*RI (3) (see Fig. 4-4a) restriction site (nucleotide 1) to the Tn*5* insertion Ω2-2 (nucleotide 2828).

Nucleotide sequence from the *Eco*RI (3) (see Fig. 4-4a) restriction site (1) to the Tn*5* insertion Ω2-2 (2828). The deduced amino acid sequence of each open reading frame is indicated and the arrow indicates the direction of translation. Also indicated are the location of the following restriction enzymes (over-line): *Bgl*II (Bg); *Cla*I (C), *Eco*RI (ER), *Eco*RV (V), *Sac*II (ScII), *Sma*I (Sm), *Sph*I (Sp) and *Xho*I (X).

Appendix B-1: Restriction map of pTH61

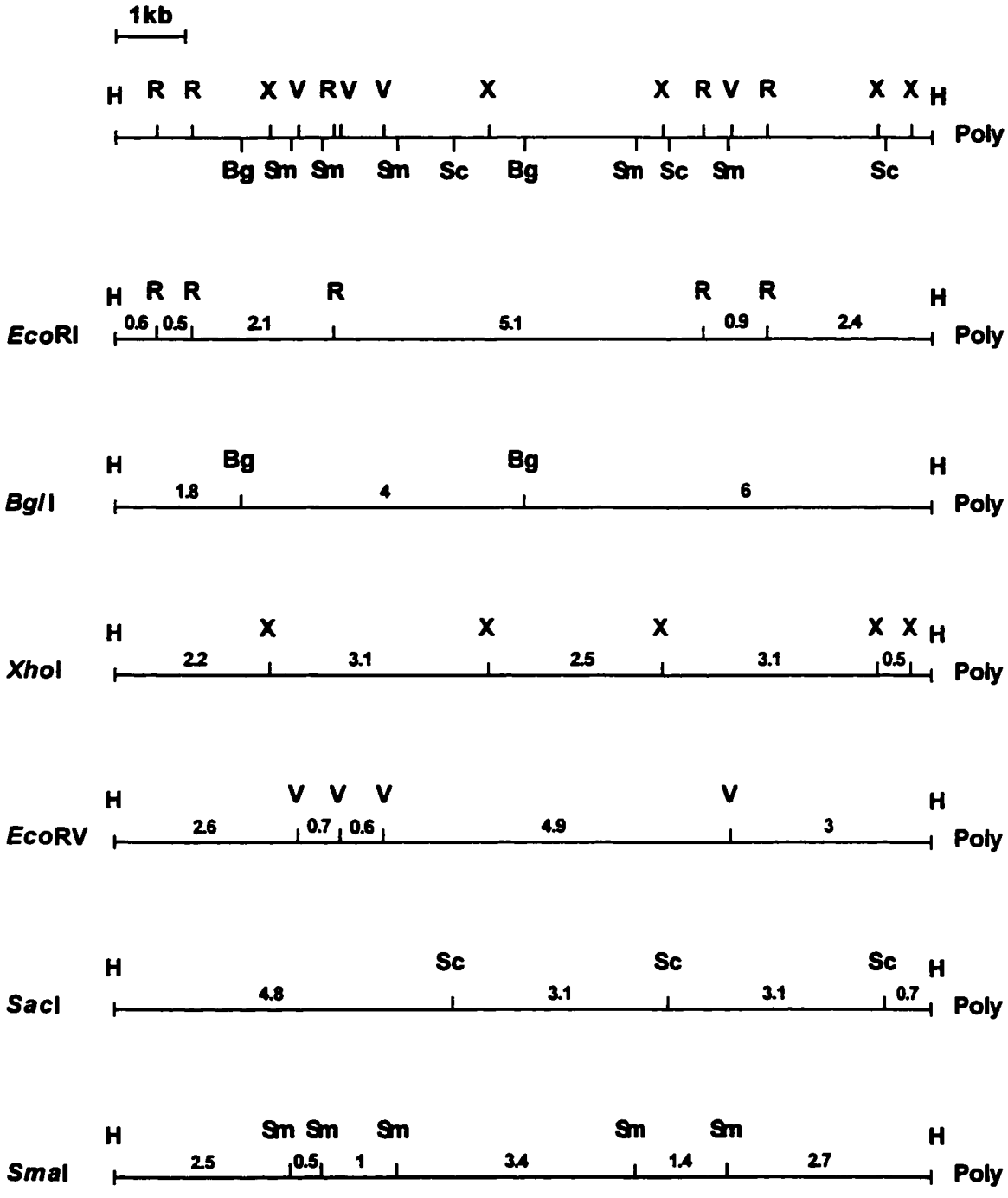

Appendix B-2: Strategy of sequencing of the *sfx1* locus

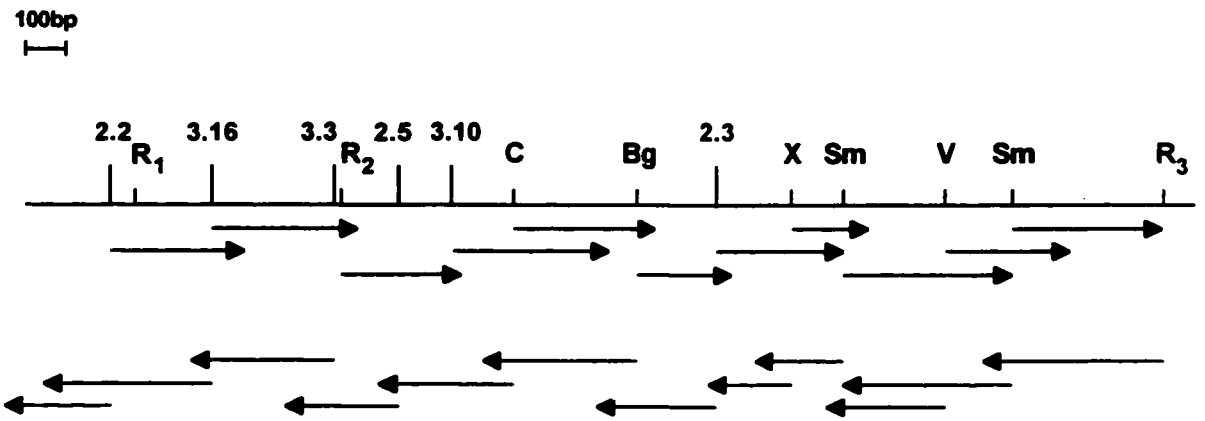

Appendix B-3: Sequence of the *sfx1* locus

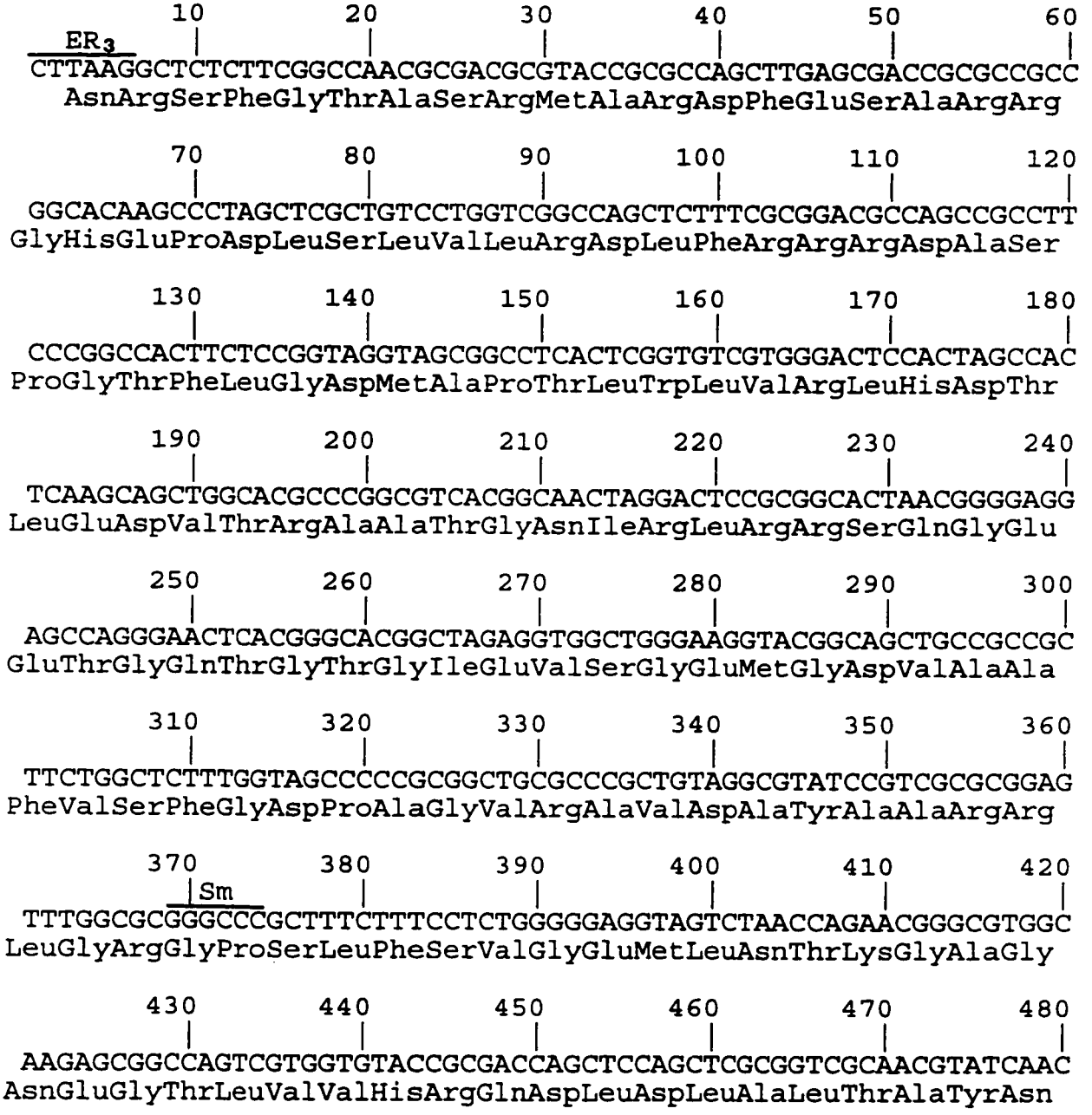

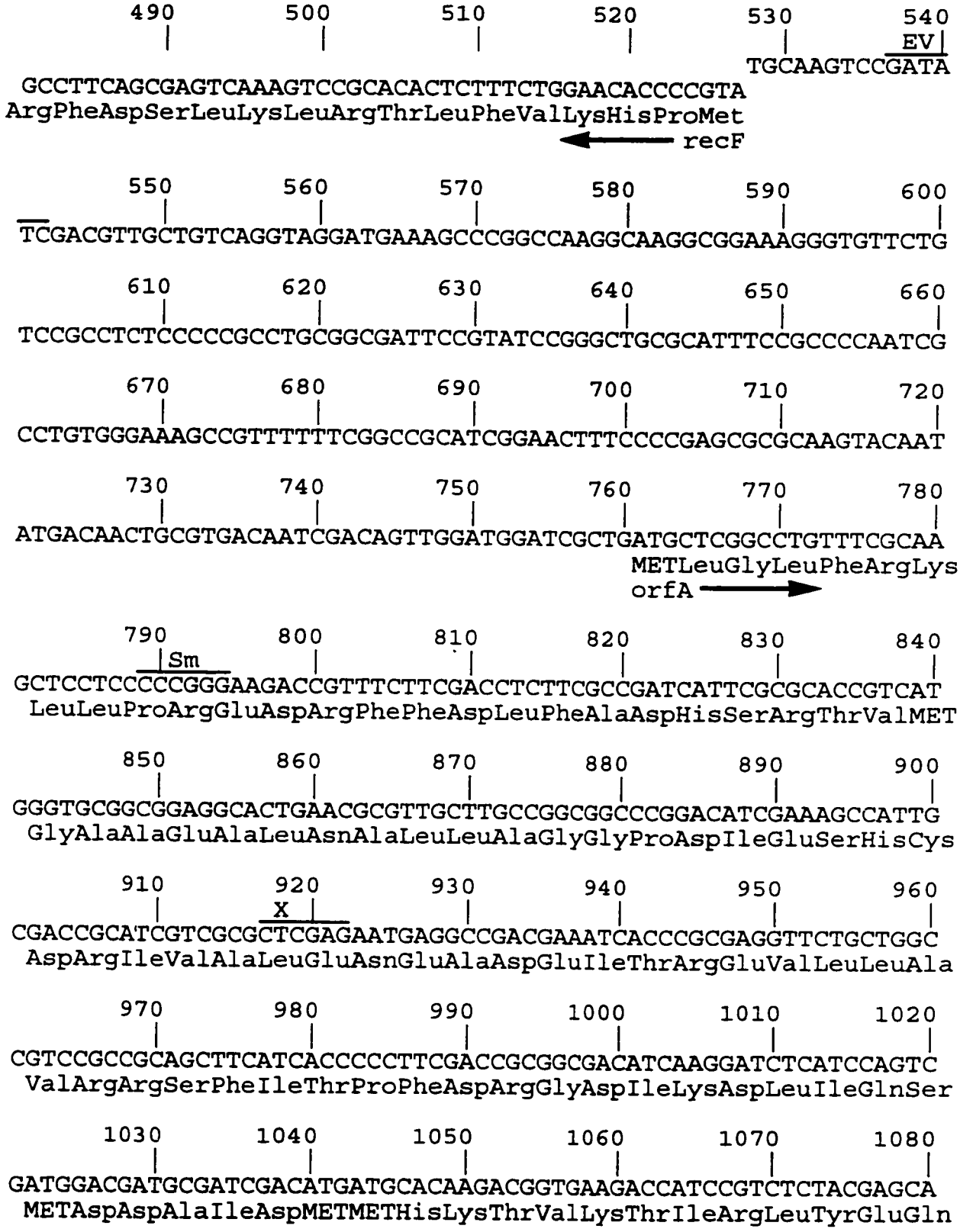
490 500 510 520 530 540
EV
TGCAAGTCCGATA
GCCTTCAGCGAGTCAAAGTCCGCACACTCTTTCTGGAACACCCCGTA
ArgPheAspSerLeuLysLeuArgThrLeuPheValLysHisProMet
recF
550 560 570 580 590 600
TCGACGTTGCTGTCAGGTAGGATGAAAGCCCGGCCAAGGCAAGGCGGAAAGGGTGTTCTG
610 620 630 640 650 660
TCCGCCTCTCCCCCGCCTGCGGCGATTCCGTATCCGGGCTGCGCATTTCCGCCCCAATCG
670 680 690 700 710 720
CCTGTGGGAAAGCCGTTTTTTCGGCCGCATCGGAACTTTCCCCGAGCGCGCAAGTACAAT
730 740 750 760 770 780
ATGACAACTGCGTGACAATCGACAGTTGGATGGATCGCTGATGCTCGGCCTGTTTCGCAA
METLeuGlyLeuPheArgLys
orfA
790 800 810 820 830 840
Sm
GCTCCTCCCCCGGGAAGACCGTTTCTTCGACCTCTTCGCCGATCATTCGCGCACCGTCAT
LeuLeuProArgGluAspArgPhePheAspLeuPheAlaAspHisSerArgThrValMET
850 860 870 880 890 900
GGGTGCGGCGGAGGCACTGAACGCGTTGCTTGCCGGCGGCCCGGACATCGAAAGCCATTG
GlyAlaAlaGluAlaLeuAsnAlaLeuLeuAlaGlyGlyProAspIleGluSerHisCys
910 920 930 940 950 960
X
CGACCGCATCGTCGCGCTCGAGAATGAGGCCGACGAAATCACCCGCGAGGTTCTGCTGGC
AspArgIleValAlaLeuGluAsnGluAlaAspGluIleThrArgGluValLeuLeuAla
970 980 990 1000 1010 1020
CGTCCGCCGCAGCTTCATCACCCCCTTCGACCGCGGCGACATCAAGGATCTCATCCAGTC
ValArgArgSerPheIleThrProPheAspArgGlyAspIleLysAspLeuIleGlnSer
1030 1040 1050 1060 1070 1080
GATGGACGATGCGATCGACATGATGCACAAGACGGTGAAGACCATCCGTCTCTACGAGCA
METAspAspAlaIleAspMETMETHisLysThrValLysThrIleArgLeuTyrGluGln

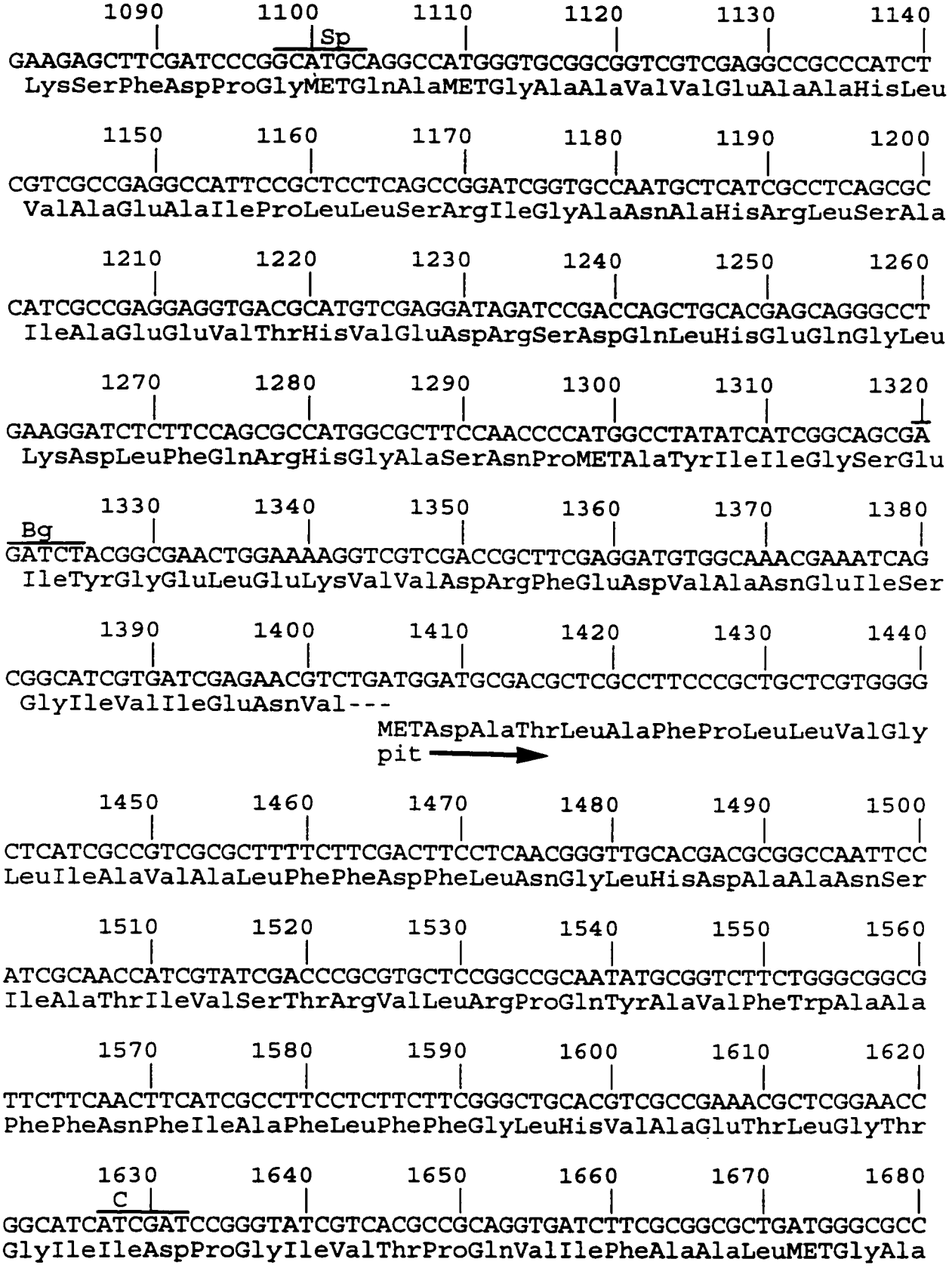
1090 1100 1110 1120 1130 1140
Sp
GAAGAGCTTCGATCCCGGCATGCAGGCCATGGGTGCGGCGGTCGTCGAGGCCGCCCATCT
LysSerPheAspProGlyMETGlnAlaMETGlyAlaAlaValValGluAlaAlaHisLeu
1150 1160 1170 1180 1190 1200
CGTCGCCGAGGCCATTCCGCTCCTCAGCCGGATCGGTGCCAATGCTCATCGCCTCAGCGC
ValAlaGluAlaIleProLeuLeuSerArgIleGlyAlaAsnAlaHisArgLeuSerAla
1210 1220 1230 1240 1250 1260
CATCGCCGAGGAGGTGACGCATGTCGAGGATAGATCCGACCAGCTGCACGAGCAGGGCCT
IleAlaGluGluValThrHisValGluAspArgSerAspGlnLeuHisGluGlnGlyLeu
1270 1280 1290 1300 1310 1320
GAAGGATCTCTTCCAGCGCCATGGCGCTTCCAACCCCATGGCCTATATCATCGGCAGCGA
LysAspLeuPheGlnArgHisGlyAlaSerAsnProMETAlaTyrIleIleGlySerGlu
1330 1340 1350 1360 1370 1380
Bg
GATCTACGGCGAACTGGAAAAGGTCGTCGACCGCTTCGAGGATGTGGCAAACGAAATCAG
IleTyrGlyGluLeuGluLysValValAspArgPheGluAspValAlaAsnGluIleSer
1390 1400 1410 1420 1430 1440
CGGCATCGTGATCGAGAACGTCTGATGGATGCGACGCTCGCCTTCCCGCTGCTCGTGGGG
GlyIleValIleGluAsnVal---
METAspAlaThrLeuAlaPheProLeuLeuValGly
pit
1450 1460 1470 1480 1490 1500
CTCATCGCCGTCGCGCTTTTCTTCGACTTCCTCAACGGGTTGCACGACGCGGCCAATTCC
LeuIleAlaValAlaLeuPhePheAspPheLeuAsnGlyLeuHisAspAlaAlaAsnSer
1510 1520 1530 1540 1550 1560
ATCGCAACCATCGTATCGACCCGCGTGCTCCGGCCGCAATATGCGGTCTTCTGGGCGGCG
IleAlaThrIleValSerThrArgValLeuArgProGlnTyrAlaValPheTrpAlaAla
1570 1580 1590 1600 1610 1620
TTCTTCAACTTCATCGCCTTCCTCTTCTTCGGGCTGCACGTCGCCGAAACGCTCGGAACC
PhePheAsnPheIleAlaPheLeuPhePheGlyLeuHisValAlaGluThrLeuGlyThr
1630 1640 1650 1660 1670 1680
C
GGCATCATCGATCCGGGTATCGTCACGCCGCAGGTGATCTTCGCGGCGCTGATGGGCGCC
GlyIleIleAspProGlyIleValThrProGlnValIlePheAlaAlaLeuMETGlyAla

```
      1690        1700        1710        1720        1730        1740
ATCACCTGGAACATCGTTACCTGGGTCTTCGGCATCCCATCGAGTTCCTCGCACGCGCTC
IleThrTrpAsnIleValThrTrpValPheGlyIleProSerSerSerSerHisAlaLeu

      1750        1760        1770        1780        1790        1800
ATCGGCGGTCTCGTCGGCGCCGGCCTGGCCAAGACCGGTTTCAGTTCCATCGTCTGGCAA
IleGlyGlyLeuValGlyAlaGlyLeuAlaLysThrGlyPheSerSerIleValTrpGln

      1810        1820        1830        1840        1850        1860
GGCCTGCTGAAGACGGCCGGCGCCATCGTCATGTCGCCGGGCATCGGCTTCGTTCTGGCG
GlyLeuLeuLysThrAlaGlyAlaIleValMETSerProGlyIleGlyPheValLeuAla

      1870        1880        1890        1900        1910        1920
CTGCTGTTGGTGCTGATCGTCTCCTGGCTGTTCGTTCGCCAGACACCCTTTGCCGTCGAC
LeuLeuLeuValLeuIleValSerTrpLeuPheValArgGlnThrProPheAlaValAsp

      1930        1940        1950        1960        1970        1980
AGCACCTTCCGGGTGCTGCAATTCGTTTCGGCTTCCCTCTATTCGCTCGGCCATGGCGGC
SerThrPheArgValLeuGlnPheValSerAlaSerLeuTyrSerLeuGlyHisGlyGly

      1990        2000        2010        2020        2030        2040
AACGATGCGCAGAAGACCATGGGCATCATTGCCGTGCTTCTCTTCTCGCAGGGCTATCTC
AsnAspAlaGlnLysThrMETGlyIleIleAlaValLeuLeuPheSerGlnGlyTyrLeu

      2050        2060        2070        2080        2090        2100
      ER2
GGCTCGGAATTCTACGTGCCCTTCTGGGTGGTCATCACCTGCCAGGCGGCGATCGCGCTC
GlySerGluPheTyrValProPheTrpValValIleThrCysGlnAlaAlaIleAlaLeu

      2110        2120        2130        2140        2150        2160
GGCACGCTCTTCGGCGGCTGGAGAATCGTCCACACGATGGGCTCGAAGATCACCAAGCTC
GlyThrLeuPheGlyGlyTrpArgIleValHisThrMETGlySerLysIleThrLysLeu

      2170        2180        2190        2200        2210        2220
AACCCGATGCAGGGATTCTGCGCCGAGACGGGCGGCGCCATCACGCTGTTCGCCGCGACC
AsnProMETGlnGlyPheCysAlaGluThrGlyGlyAlaIleThrLeuPheAlaAlaThr

      2230        2240        2250        2260        2270        2280
TGGCTCGGCATTCCGGTTTCGACCACCCACACAATCACCGGCGCGATCATCGGCGTCGGC
TrpLeuGlyIleProValSerThrThrHisThrIleThrGlyAlaIleIleGlyValGly
```

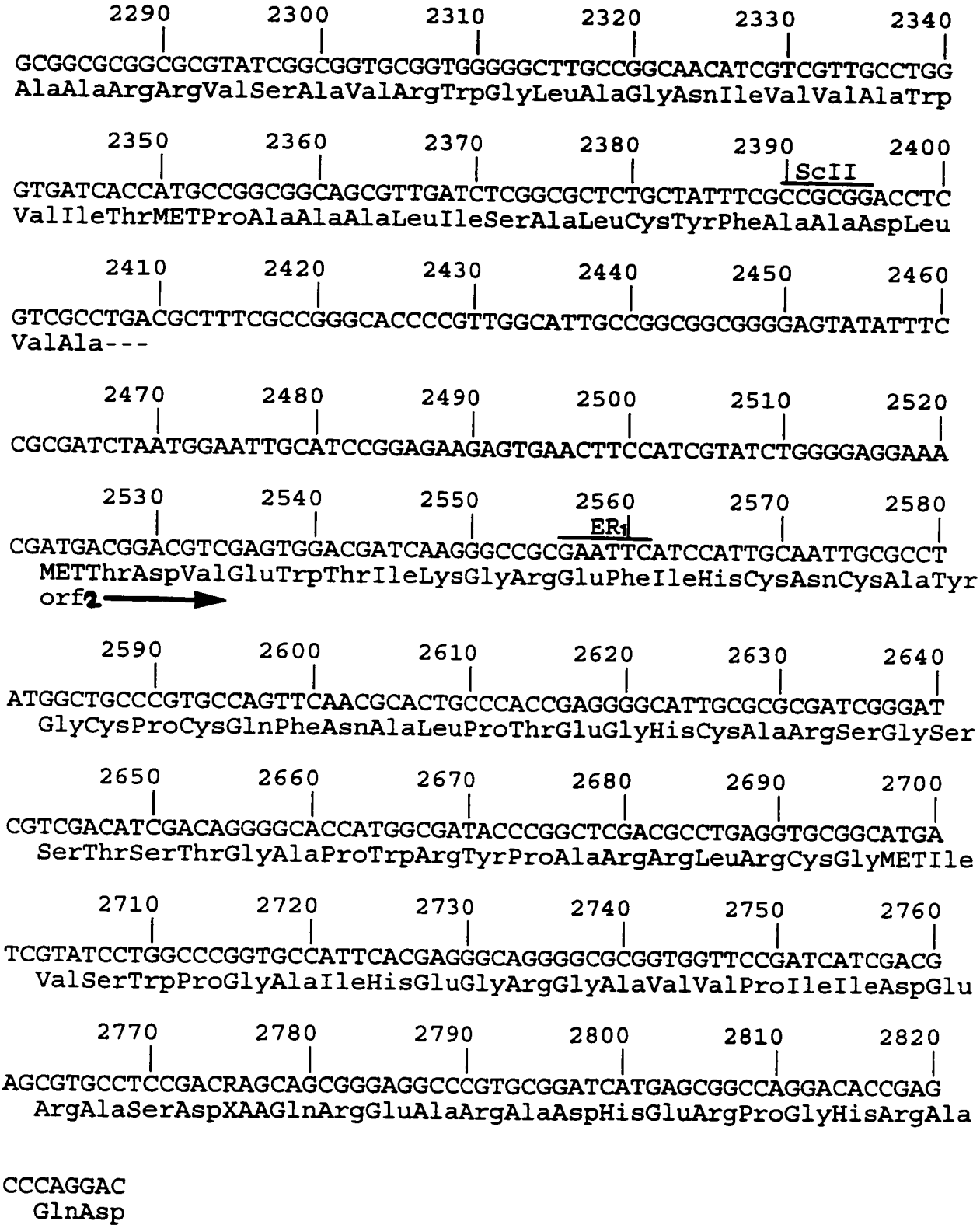
2290 2300 2310 2320 2330 2340
GCGGCGCGGCGCGTATCGGCGGTGCGGTGGGGGCTTGCCGGCAACATCGTCGTTGCCTGG
AlaAlaArgArgValSerAlaValArgTrpGlyLeuAlaGlyAsnIleValValAlaTrp
2350 2360 2370 2380 2390 2400
ScII
GTGATCACCATGCCGGCGGCAGCGTTGATCTCGGCGCTCTGCTATTTCGCCGCGGACCTC
ValIleThrMETProAlaAlaAlaLeuIleSerAlaLeuCysTyrPheAlaAlaAspLeu
2410 2420 2430 2440 2450 2460
GTCGCCTGACGCTTTCGCCGGGCACCCCGTTGGCATTGCCGGCGGCGGGGAGTATATTTC
ValAla---
2470 2480 2490 2500 2510 2520
CGCGATCTAATGGAATTGCATCCGGAGAAGAGTGAACTTCCATCGTATCTGGGGAGGAAA
2530 2540 2550 2560 2570 2580
ER1
CGATGACGGACGTCGAGTGGACGATCAAGGGCCGCGAATTCATCCATTGCAATTGCGCCT
METThrAspValGluTrpThrIleLysGlyArgGluPheIleHisCysAsnCysAlaTyr
orf2
2590 2600 2610 2620 2630 2640
ATGGCTGCCCGTGCCAGTTCAACGCACTGCCCACCGAGGGGCATTGCGCGCGATCGGGAT
GlyCysProCysGlnPheAsnAlaLeuProThrGluGlyHisCysAlaArgSerGlySer
2650 2660 2670 2680 2690 2700
CGTCGACATCGACAGGGGCACCATGGCGATACCCGGCTCGACGCCTGAGGTGCGGCATGA
SerThrSerThrGlyAlaProTrpArgTyrProAlaArgArgLeuArgCysGlyMETIle
2710 2720 2730 2740 2750 2760
TCGTATCCTGGCCCGGTGCCATTCACGAGGGCAGGGGCGCGGTGGTTCCGATCATCGACG
ValSerTrpProGlyAlaIleHisGluGlyArgGlyAlaValValProIleIleAspGlu
2770 2780 2790 2800 2810 2820
AGCGTGCCTCCGACRAGCAGCGGGAGGCCCGTGCGGATCATGAGCGGCCAGGACACCGAG
ArgAlaSerAspXAAGlnArgGluAlaArgAlaAspHisGluArgProGlyHisArgAla
CCCAGGAC
GlnAsp

• **Appendix B-4:** Tentative to determinate the transcriptional start site upstream of *orfA* by primer extension. The primer extension experiment was performed as stated in Bardin et al. (1996) using wild type (Rm1021) and *sfx1* (RmG591) RNA extracted from LB grown cells. The primer used is boxed in the sequence below with the 5' and 3' direction indicated. This experiment was not successful as many bands appeared on the autoradiograph and were very faint. The nucleotides at which the main bands appeared are indicated by ↓. Also indicated are the orfA translational start codon (+1), downstream of a putative TATA box (bold), the hexa-thymidine sequence (from an *sfx1* promoter, underlined) and the putative Pho Box (hatched over-line). The location of the *Eco*RV and *Sma*I restriction sites are over-lined.

*Eco*RV ↓↓

GATATCGACGTTGCTGTCAGGTAGGATGAAAGCCCGGCCA -185

AGGCAAGGCGGAAAGGGTGTTCTGTCCGCCTCTCCCCCGC -145

CTGCGGCGATTCCGTATCCGGGCTGCGCATTTCCGCCCCA -105

? Pho Box ?

ATCGCCTGTGGGAAAGCCGTTTTTTCGGCCGCATCGGAAC - 65

↓ ↓ ↓

TTTCCCCGAGCGCGCAAG***TACAAT***ATGACAACTGCGTGAC - 25

orfB →

AATCGACAGTTGGATGGATCGCTGATGCTCGGCCTGTTTC + 16

*Sma*I +1

GCAAGCTCCTCCCCCGGGAAGACCGTTTCTTCGACCTCTT + 56

CGCCGATCATTCGCGCACCGTCATGGGTGCGGCGGAGGCA + 96

3' 5'

PRIMER

CHAPTER V

Characterization of the sfx2 locus

A- Introduction

N_2-fixing root nodules result from a complex interaction between bacteria of the family *Rhizobiaceae* and leguminous plants. We recently characterized the symbiotic *ndvF* locus of *R. meliloti* and showed that it consists of four genes *phoCDET* which encode an ABC-type phosphate transport system (Bardin et al., 1996). Strains carrying insertion mutations in any of the *phoCDET* genes grew poorly in media containing 2mM inorganic phosphate and formed nodules which contained few bacteria and failed to fix N_2 (Fix^- phenotype). Occasionally, we observed pink Fix^+ root-nodules on the plants inoculated with *phoCDET* mutants. Genetic analysis of isolates from these nodules revealed that they carried second-site mutations which suppressed the *phoCDET* Fix^- phenotype. Two suppressor classes (I and II) were distinguished according to phenotypic characteristics and their position on *the R. meliloti* chromosome (Oresnik et al., 1994). In chapter IV of this thesis, we described the subcloning and sequencing

of the class I suppressor locus carrying the *sfx1* mutation. The sequence revealed the presence of two open reading frames, designated *orfA and pit*, that probably form an operon. The deduced *pit* protein is homologous to phosphate transport proteins, including the low-affinity phosphate transport protein (Pit) of *E. coli* (Wanner, 1996). The *orfA* gene shows similarity to an open reading frame in *H. influenza* which also lay upstream from a *pit*-like gene but no homologous gene was present upstream of the *pit* gene of *E. coli*. Expression of *orfA-pit* at the *R. meliloti sfx1* locus was found to be at least three times higher than expression in a wild-type background. We hypothesized that the increased *orfA-pit* expression results in increased phosphate uptake via the Pit-like protein and hence suppresses the phosphate and symbiotic phenotypes associated with *phoCDET* mutations.

In this chapter we report that the Class II suppression mutation, *sfx2*, maps to the *phoUB* locus of *R. meliloti*. We show that *phoUB* insertion mutants suppress the symbiotic, growth and mucoid phenotypes of *phoC*Ω490 mutation. Suppression by these mutants appears to occur by derepression of the *orfA-pit* genes thus allowing increased Pi uptake via the Pit transport system of *R. meliloti*.

B- Results

1- Strains carrying the *sfx2* mutation are deficient in alkaline phosphatase expression.

The levels of alkaline phosphatase (AP) activity detected in wild type cells cultured in MOPS-buffered minimal media with no added phosphate (MOPS P0) are ten to twenty fold higher than the AP activity found in cells grown in the same media containing 2mM inorganic phosphate (MOPS P2) (Fig. 5-1 and Bardin et al., 1996). Therefore, as is the case for many bacteria, measurements of alkaline phosphatase activity in *R. meliloti*, can be used to monitor the cell physiological status with respect to phosphate availability.

Experiments with the *R. meliloti phoCΩ*490 mutant, RmG490 (mutant representative of the different *phoCDET* mutants studied, see Chapter III), revealed a high AP activity when cultured either in the absence of added phosphate or in media containing 2mM Pi (Fig. 5-1). Thus even in the presence of 2mM Pi, RmG490 cells appeared to be starved for phosphate and this phenotype is consistent with the observation that RmG490 grows poorly in media containing 2mM Pi (Fig. 6; Bardin et al. 1996; see also Appendix A in Chapter III). As we had previously found that *R. meliloti phoCDET* mutants grew like the wild type in MOPS media containing 2mM aminoethylphosphonate (AEP) as a P source, we measured AP activity in cultures of RmG490 and the wild-type

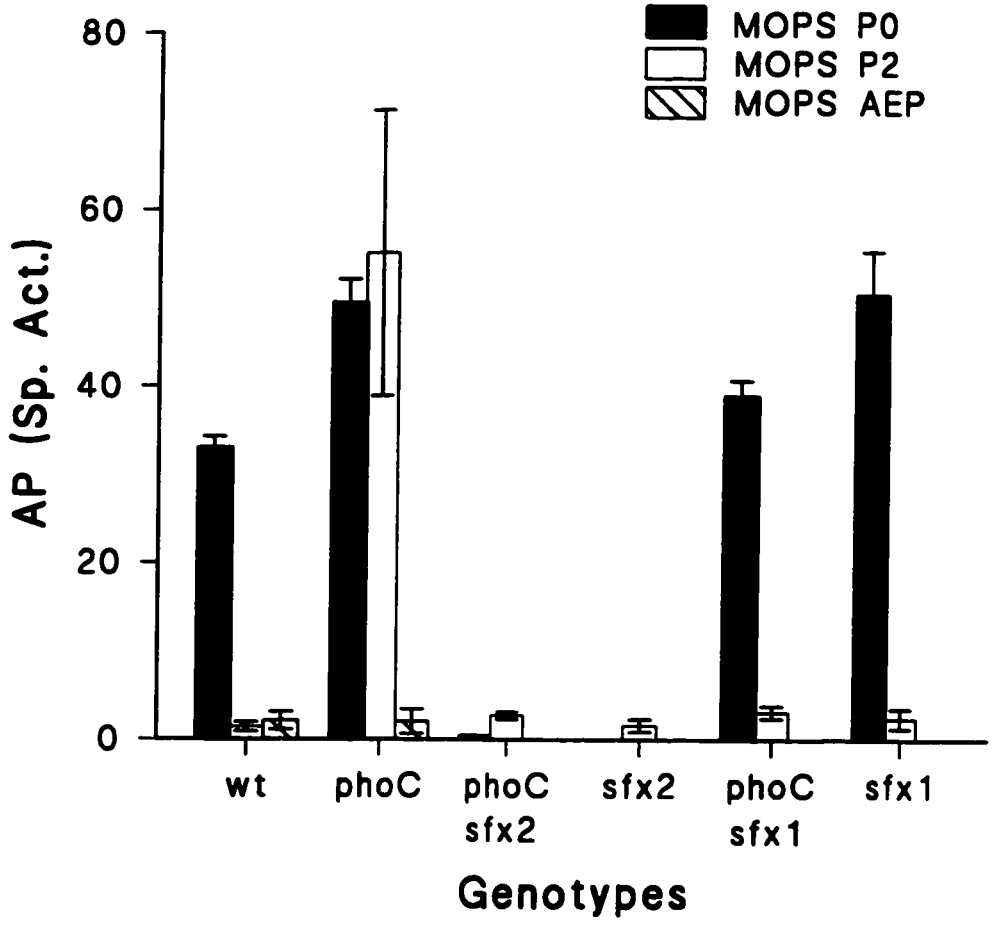

Fig. 5-1: Alkaline phosphatase (AP) activity of Rm1021 (wt), RmG490 (*phoC*), *sfx2* strains in *phoC*Ω490 or wild type backgrounds (phoC/sfx2 or sfx2, respectively) and *sfx1* strains in *phoC*Ω490 or wild type backgrounds (phoC/sfx1 or sfx1, respectively) after 60 hours growth in MOPS-buffered minimal media with no phosphate added (MOPS P0, solid box) or containing 2mM inorganic phosphate (MOPS P2, open box). The AP activity of Rm1021 and RmG490 was also determined after 80 hours growth in MOPS-buffered minimal media containing 2mM aminoethylphosphonate (MOPS AEP, hatched box). Each activity represents the average of triplicate values ± S.E..

Rm1021 following growth in this medium (Fig. 5-1). Both RmG490 and wild-type strains contained low background AP activities after growth in 2mM AEP. Thus, unlike what is observed with *E. coli* where mutants defective in the high affinity transport system (*pstSCAB*) showed constitutive AP expression (Cox et al., 1989), AP expression in the *R. meliloti phoCΩ*490 mutant was repressed when a readily assimilated phosphorus source like AEP was provided in the growth media.

To examine the effect of the previously isolated *ndvF* (*phoCDET*) symbiotic suppressor mutations on alkaline phosphatase expression, the class I and class II suppressor mutations, *sfx1* and *sfx2* respectively, were introduced into a *phoCΩ*490 mutant to generate the strains RmG762 and RmH363, respectively. AP activity in these strains was repressed in the presence of 2mM Pi (Fig. 5-1). Unexpectedly however, no alkaline phosphatase activity was detected when RmH363 (*phoC sfx2*) was grown in MOPS medium with no Pi added (P0). This result was in contrast with what we observed with the wild type (wt), RmG591 (*sfx1*) and RmG762 (*phoC sfx1*) strains. Subsequent analysis revealed that RmG497 cells which carry the *sfx2* mutation in an otherwise wild-type background also lacked alkaline phosphatase activity (AP^- phenotype) (Fig. 5-1, see also Appendix C-1). The other Class II suppressor, *sfx3*, in a Δ*phoCDET* background, also showed no AP activity when grown in MOPS P0 (see Appendix C-1). The AP^- phenotype of strains carrying Class II mutation,

together with suppression of the mucoid colony and symbiotic phenotypes associated with the *phoCDET* (*ndvF*) mutations (Oresnik et al., 1994) suggested that *sfx2/3* probably affects regulatory gene(s) involved in phosphorus assimilation similar to the *phoBR* genes of *E. coli* (see Wanner, 1993).

Using the AP^- phenotype of the *sfx2/3* containing strains, we employed a screening method for identifying these mutants by plating the cells on LB media supplemented with 60μg/ml of 5-bromo-4-chloro-3-indolyl phosphate (X-$Phos^{60}$). As the *sfx2/3* mutants were unable to hydrolyze the chromogenic compound the colonies remained white, while blue colonies were obtained with the wild type strain Rm1021.

2- Mapping of the *sfx2* locus

Tn*5* and Tn*5*-233 insertions linked to *sfx2* were previously isolated as follows: lysates made from a pool of 6000 random Tn*5* insertions (Bank NM1) and a pool of 2000 random Tn*5*-233 insertions (Bank GS2) were transduced into RmF346 (Δ*phoCDET sfx2*, deoxycholate sensitive; Oresnik *et al.*, 1994). Individual Nm^r and Gm^r-Sp^r transductants were screened for loss of sensitivity to deoxycholate. Three Tn*5* insertions, designated RmG549 (Ω5256), RmG551 (Ω5258) and RmG552 (Ω5259) and three Tn*5*-233 insertions, designated RmG639 (Ω5262), RmG640 (Ω5263) and RmG641 (Ω5264) showed linkage to the deoxycholate sensitivity phenotype of the mutant strain. Here we determined

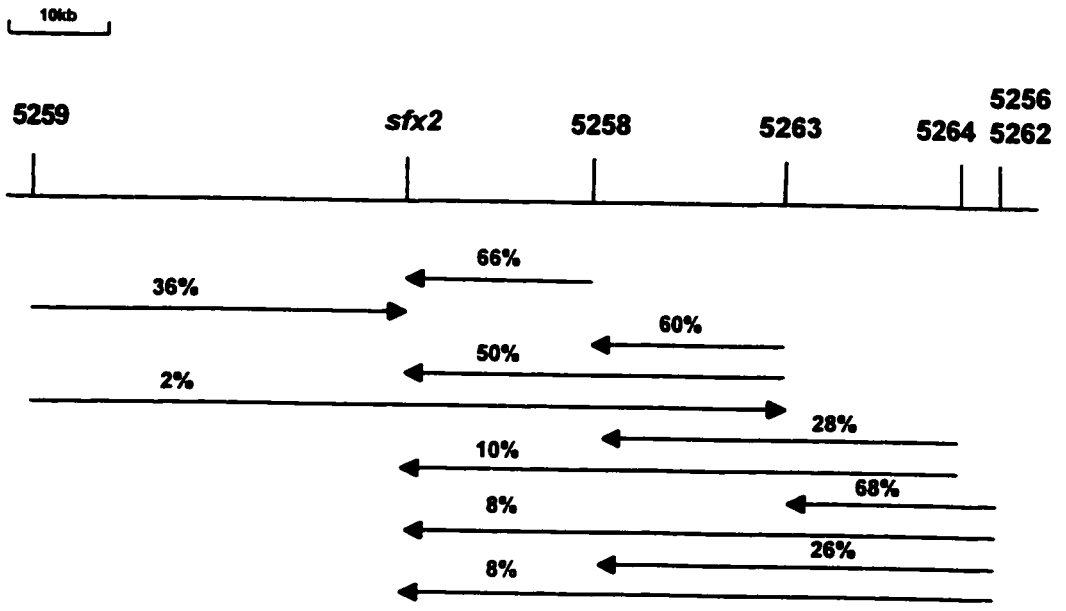

Fig. 5-2 Genetic linkage map showing the location of *sfx2* relative to three Tn*5* insertions (Ω5256, Ω5258 and Ω5259) and three Tn*5*-233 insertions (Ω5262, Ω5263 and Ω5264). The cotransduction frequency is represented in %.

Table 5.1: Two (a) and three (b) factor crosses used to calculate the linkage between the markers shown in Fig. 5-2. Linkages were determined by patching 50 transductant colonies on appropriate media. Linkages of Ω5262, Ω5263 and Ω5264 to Ω5258 are not reported in these tables as they were previously determined by I. Oresnik . Abbreviation used: (B): blue colonies on LBX-Phos^{60}; (W): white colonies on LBX-Phos^{60}; wt: wild type; G: Gm; S: Sp, (^{s}) and (^{r}) meaning sensitive and resistant, respectively.

Table 5-1a: Two factor crosses

Donor		recipient		% linkage to sfx2
strain	**insertion**	**strain**	**genotype**	
RmG551 (B)	Ω5258:: Tn*5*	RmG479 (W)	*sfx2* Ω5033::Tn*5*	33 (B) / 50 → 66%
RmG639 (W)	Ω5262:: Tn*5*-233	Rm1021 (B)	wt	4 (W) / 50 → 8%
RmG640 (W)	Ω5263:: Tn*5*-233	Rm1021 (B)	wt	25 (W) / 50 → 50%
RmG641 (B)	Ω5264:: Tn*5*-233	RmG479 (W)	*sfx2* Ω5033::Tn*5*	5 (B) / 50 → 10%

Table 5-1b: Three factor crosses

Donor		Recipient		Classes			
strain	**insertion**	**strain**	**genotype**	**B G^sS^s**	**B G^rS^r**	**W G^sS^s**	**W G^rS^r**
RmG549 (B)	Ω5256:: Tn*5*	RmG640 (W)	*sfx2* Ω5263:: Tn*5*-233	4	0	30	16
RmG552 (B)	Ω5259:: Tn*5*	RmG640 (W)	*sfx2* Ω5263:: Tn*5*-233	1	17	0	32

<u>% linkage:</u>

Φ G549 → G640: 4 (B) /50 → 8% linked to *sfx2*
34 Gm^s-Sp^s /50 → 68% linked RmG640
Φ G552 → G640: 18 (B) /50 → 36% linked to *sfx2*
1 Gm^s-Sp^s /50 → 2% linked RmG640

the genetic linkage of these insertions to *sfx2* using the alkaline phosphatase phenotype of the *sfx2* mutation. The Nm^r or Gm^r-Sp^r of the insertions were transduced into the *sfx2* strain RmG497 or the wild type strain Rm1021 and individual transductants were screened for the presence of blue or white colonies respectively on LBX-Phos[60] plates. The linkages of these insertions to *sfx2* and to one another is reported in Fig. 5-2 and Table 5-1a and b. Insertion Ω5258 was the closest to the *sfx2* locus with a linkage of 66% (about 21kb away from *sfx2*, as determined from the Wu equation (Wu, 1966)). This linkage value was similar to the 70% linkage value obtained when Ω5258 was transduced into RmF346 and the transductants were checked for resistance to deoxycholate (Oresnik et al., 1994).

The location of *sfx2* on the *R. meliloti* genome was determined using seven Tn*5-mob* insertion strains as described in Oresnik et al. (1994). The Tn*5-mob* insertions were transduced into strain RmG640 (Ω5263, 50% linked to *sfx2*; see Fig. 5-2). The highest frequency of Gm^r-Sp^r colonies was obtained from the strain transferring clockwise from *trp-33*.

3- Isolation of alkaline phosphatase deficient mutations linked to *sfx2*.

In an attempt to clone the wild type *sfx*2 locus, we transferred a wild type *R. meliloti* clone bank into the *sfx2* mutant RmG497 and screened the transconjugants for complementation of the AP^- phenotype on LBX-Phos plates.

No blue colonies were obtained. As an alternate strategy, we sought to isolate additional *sfx*2-like mutations by screening pools of insertion mutants for AP^- colonies. A pool of random Tn*5*-132 (oxytetracycline resistant; Bank OT1) insertions in Rm1021 and a pool of random Tn*5* insertions in Rm1021 (Bank NM1) were plated on LBX-Phos[60]. One AP^- Tn*5* insertion mutant (RmH405, *pho27*), and twenty six AP^- Tn*5*-132 mutants were identified and purified. Linkage of the Tn*5*-132 mutations to the *sfx*2 locus was examined by transducing Nm^r from strain RmG551, carrying the Ω5258::Tn*5* insertion (see Fig. 5-2), into these strains and screening for the presence of blue transductant colonies on X-Phos[60] plates. Three Tn*5*-132 insertion mutations, designated *pho10*, *pho8* and *pho3* (in which the Tn5-132 was replaced by Tn*5*-233), showed 60%, 64% and 66% linkage to Ω5258::Tn*5* respectively (Table 5-2). These linkage values were similar to the 66% and 62% linkage obtained of *sfx2* and *sfx3* with Ω5258::Tn*5*, suggesting that the *pho10*, *pho8* and *pho3* insertions probably map to the sfx2-*sfx3* locus. The other 23 white Tn*5*-132 insertion mutants showed no linkage to Ω5258::Tn*5*, however these were 100% linked in transduction to the Tn*5* insertion in *pho27* (strain RmH405). We also determined the linkage of *pho10*, *pho8* and *pho3* to Ω5259::Tn5 which maps on the opposite side of *sfx2* (see Fig. 5-2). Nm^r was transduced from strain RmG552 into the *pho10*, *pho8*, *pho3*, *sfx2* and sfx3 recipient strains, and similar numbers of AP^+

Donor		Recipient		
strain	**insertion**	**strain**	**genotype**	**% linkage**
RmG551 (B)	Ω5258:: Tn*5*	RmG497 (W)	*sfx2* Ω5033::Tn*5*-233	33 (B) / 50 → 66%
		RmG425 (W)	*sfx3* ΔΩ5033-5064:: Tn*5*-233	31 (B) / 50 → 62%
		RmH850 (W)	*phoU10*:: Tn*5*-233	30 (B) / 50 → 60%
		RmH851 (W)	*phoB8*:: Tn*5*-233	32 (B) / 50 → 64%
		RmH852 (W)	*phoB3*:: Tn*5*-233	33 (B) / 50 → 66%
RmG552 (B)	Ω5259:: Tn*5*	RmG497 (W)	*sfx2* Ω5033::Tn*5*-233	20 (B) / 50 → 40%
		RmG425 (W)	*sfx3* ΔΩ5033-5064:: Tn*5*-233	22 (B) / 50 → 44%
		RmH850 (W)	*phoU10*:: Tn*5*-233	24(B) / 50 → 48%
		RmH851 (W)	*phoB8*:: Tn*5*-233	22 (B) / 50 → 44%
		RmH852 (W)	*phoB3*:: Tn*5*-233	21 (B) / 50 → 42%

Table 5-2: Linkage of *sfx2*, *sfx3*, *phoU10*, *phoB8* and *phoB3* to the Tn*5* insertions Ω5258 and Ω5259. The linkage was determined by patching 50 Nm^r transductants on LBX-$Phos^{60}$ and LBGm^{20}-Sp^{100} plates. For *phoU10*, *phoB8* and *phoB3*, all the blue colonies on LBX-$Phos^{60}$ were also Gm^s-Sp^s while the white one were Gm^r-Sp^r, as expected. The linkage was determined by recording the number of blue (Gm^s-Sp^s) colonies. (B): blue colonies on LBX-$Phos^{60}$; (W): white colonies on LBX-$Phos^{60}$.

recombinants were obtained in the five crosses (40 to 48%; Table 5-2). Together these data suggest that *pho10*, *pho8*, *pho3* and *sfx2/3* map close to each other at a locus between Ω5259 and Ω5258.

Following the transfer of the pLAFR1 wild type *R. meliloti* clone bank into the *pho10* mutant (RmH399) we identified three cosmid clones (pTH282, pTH284 and pTH286) able to complement the AP^- phenotype of the mutant strain. Restriction analysis suggest that these clones shared common 20 and 24kb *Eco*RI as well as 10 and 26kb *Hin*dIII fragments. These cosmids, transferred into the *pho8*, *pho3* and *sfx3* mutants (RmH428, RmH430 and RmG425, respectively) also complemented the AP^- phenotype of these strains. When these plasmids were transferred into *sfx2* mutants RmG497 and RmH318, no complementation of the AP^- phenotype was observed. This result together with the inability to isolate *sfx2* complementing clone from the wild type Rm1021 clone bank (above) indicates that *sfx2* may be a dominant mutation.

4- *pho10, pho8* and *pho3* map to the *phoUB* locus of *R. meliloti*

In order to identify the gene(s) in which the *pho10*, *pho8* and *pho3* insertions were located, we replaced the Tn*5*-132 insertions in these mutants with the Tn*V* transposon. Tn*V* possesses the gene encoding NptII (Km^r) and the pSC101 origin of vegetative replication (able to replicate in *E. coli* but not in *R. meliloti*), flanked by the inverted repeats $IS50_L$ and $IS50_R$ (Furuichi et al., 1985).

The genomic DNA of these Tn*V* containing strains was digested with *Sal*I, religated and the ligation mixture was used to transform DH5α competent cells. As Tn*V* does not possess any *Sal*I restriction site, the religated plasmid will contain flanking genomic DNA. The Km^r plasmids obtained this way were named pTH292, pTH311 and pTH287 for *pho10*, *pho8* and *pho3* insertions, respectively. Subclones of these plasmids were sequenced using the IS50 primer (5'- TCACATGGAAGTCAGATCCT -3'). Blast searches revealed that *pho10* was located in the *phoU* gene and *pho3* and *pho8* in the *phoB* gene of *R. meliloti* (Fig. 5-3a and Appendix C-2). The DNA sequence of the *R. meliloti phoB* and part of *phoU* have been previously determined (accession number M96261; Cannon's group, unpublished data). The sequence revealed that these genes were adjacent to one another in the *phoU-phoB* order. The deduced PhoB protein was 47.6% identical (70% conserved) with the PhoB protein of *E. coli*, while the deduced C-terminal 117 amino acids from PhoU were 36% identical (52% conserved) with the corresponding region of the *E. coli* PhoU protein (see Fig 5-3b for alignments). The *pho10* insertion was located 28 amino acids away from the end of the partial sequence of PhoU as determined from sequence alignment to the PhoU protein sequence of *E. coli*. Insertions *pho3* and *pho8* were located at position 157 aa and 188 aa of the *R. meliloti* PhoB sequence, respectively.

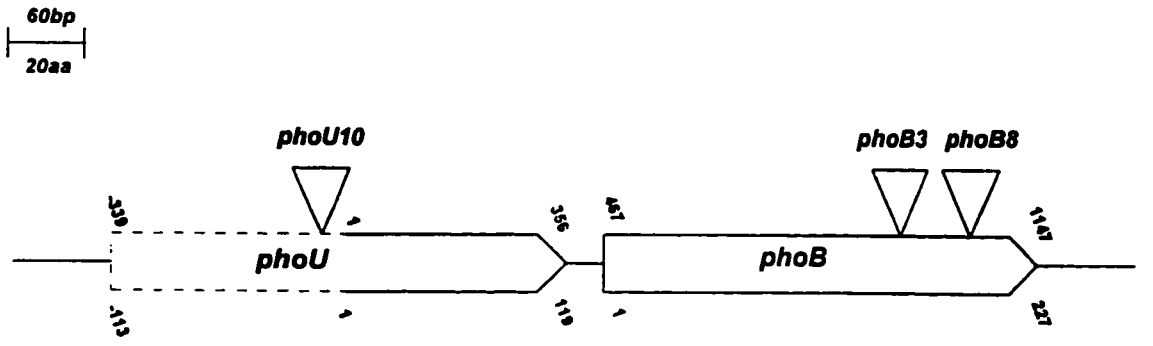

Fig. 5-3a Map of the *phoU-phoB* locus of *R. meliloti* showing the location of the *phoU10*, *phoB3* and *phoB8* insertions. The complete sequence of *phoB* and partial sequence of *phoU* have been deposited in the Data Bank by Cannon's group (accession number M96261; unpublished). The hatched part of the *phoU* gene represents the putative remaining portion of the gene determined from its alignment to the *phoU* gene of *E. coli*. A 276 nucleotide sequence of this portion has been sequenced in our laboratory (see Appendix C-2).
The numbers above the figure correspond to the number of base pairs, while the amino acid numbers are indicated below the figure.

```
pRmphoB         MLPKIAVVEDEEALSVLLRYNLEAEGFEVDTILRGDEAEIRLQERLPDLLILDWMLPGVS
pEcphoB         MARRILVVEDEAPIREMVCFVLEQNGFQPVEAEDYDSAVNQLNEPWPDLILLDWMLPGGS
                *  .* *****  .  .. . **  **.  .     * *  .*.*  ***..******* *

pRmphoB         GIELCRRLRQRPETERLPIIMLTARGEESERVRGLATGADDYVVKPFSTPELMARVKAML
pEcphoB         GIQFIKHLKRESMTRDIPVVMLTARGEEEDRVRGLETGADDYITKPFSPKELVARIKAVM
                **.  ..*..   *  .*..******** .***** ******. ****  **.**.**..

pRmphoB         RRAKPEVLSTLLRCGDIELDRETHRVHRRSREVRLGPTEFRLLEFLMSSPGRVFSRSQLL
pEcphoB         RRISPMAVEEVIEMQGLSLDPTSHRVMAGEEPLEMGPTEFKLLHFFMTHPERVYSREQLL
                **  *  .  ..    . **  .***      . .*****.** * *. * **.** ***

pRmphoB         DGVWGHDIYVDERTVDVHVGRLRKALNFSNMPDVIRTVRGAGYSLES--
pEcphoB         NHVWGTNVYVEDRTVDVHIRRLRKALEPGGHDRMVQTVRGTGYRFSTRF
                  ***  .**..******. ******   .   ...****.**   .
```

```
pRmphoU         ------------------------------------------------------------
pEcphoU         MDSLNLNKHISGQFNAELESIRTQVMTMGGMVEQQLSDAITAMHNQDSDLAKRVIEGDKN

pRmphoU         ------------------------------------------------------------
pEcphoU         VNMMEVAIDEACVRIIAKRQPTASDLRLVMVISKTIAELERIGDVADKICRTALEKFSQQ

pRmphoU         ---LARGLEHLAELALVQLKEVLDVYASRSPEKANSIRERDEEIDAIYTSLFRELLTYMM
pEcphoU         HQPLLVSLESLGRHTIQMLHDVLDAFARMDIDEAVRIYREDKKVDQEYEGIVRQLMTYMM
                   *   ** *   ..  *..*** .*    . * *   *  .*  *  . *.*.****

pRmphoU         EDPRNITPCTHLLFCAKNIERIGDHATNIAETIYYMATGAQPQGERPKDDMTSTLGSVTD
pEcphoU         EDSRTIPSVLTXLFCARSIERIGDRCQNICEFIFYYVKGQDFRHVGGDELDKLLAGKDSD
                ** *.*      ****. ******.. **.* *.*   *   .     .      *  .*

pRmphoU         -
pEcphoU         K
```

Fig.5-3b Protein alignments between the PhoU and PhoB protein sequences of *R. meliloti* (pRm), deduced from the sequence deposited in the Data Bank, and the PhoU and PhoB protein sequences of *E. coli* (pEc). ★ and · indicates amino acid identity and conserved, respectively.

In view of these results the *pho10*, *pho8* and *pho3* alleles were designated *phoU10*, *phoB8* and *phoB3*, respectively. The linkage of sfx2/3 to *phoU10*, *phoB8* and *phoB3*, and the AP^- phenotype of these five mutants suggests that the *sfx2* and *sfx3* mutations are located in the phoUB locus of *R. meliloti*.

The Tn*5*-132 of pho27 was also replaced by a Tn*V* transposon and the religated Tn*V* containing plasmid was subcloned and sequenced. The sequence shows no significant homology with proteins deposited in the Data Bank.

5- *phoB* and *phoU* are required for growth on phosphonates.

The PhoB protein of *E. coli* is a transcriptional activator of the many genes expressed under phosphate deprivation, including the phosphonate uptake and degradation genes (Wackett et al., 1987). In order to investigate whether the *phoB*-like gene of *R. meliloti* also plays a central role in P assimilation, the ability of the *phoB* (and *phoU*) mutants to utilize various sources of phosphorus was determined and compared to the growth of the wild type, the *phoC*Ω490 and *pho27* mutants. Growth experiments were performed in MOPS-buffered minimal media containing the phosphonates aminoethylphosphonate (AEP), ethylphosphonate (EP), aminomethylphosphonate (AMP) and methylphosphonate (MP) as well as the phosphorus compounds glycerol-3-phosphate (G3P), glucose-6-phosphate (Glc6P) and phosphoserine (PSer) at a

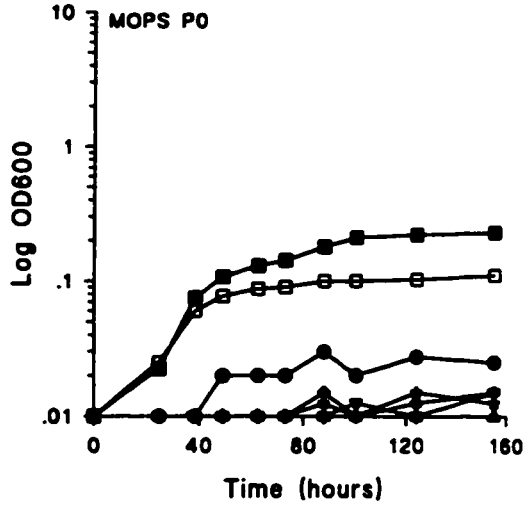
MOPS P0
Log OD600
10
1
.1
.01
0
40
80
120
160
Time (hours)

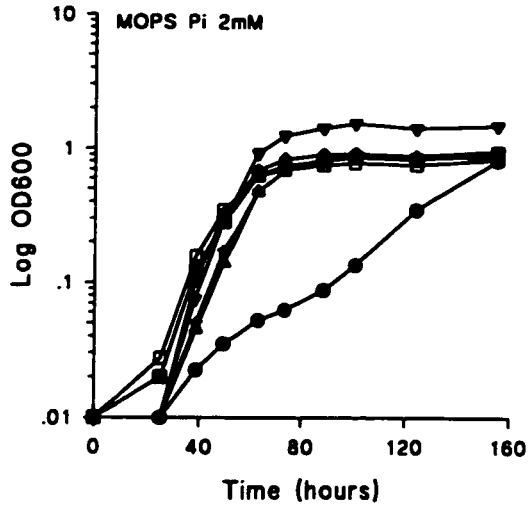
MOPS Pi 2mM
Log OD600
10
1
.1
.01
0
40
80
120
160
Time (hours)

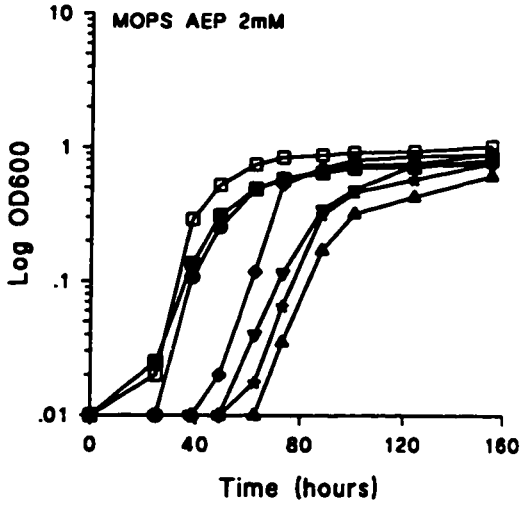
MOPS AEP 2mM
Log OD600
10
1
.1
.01
0
40
80
120
160
Time (hours)

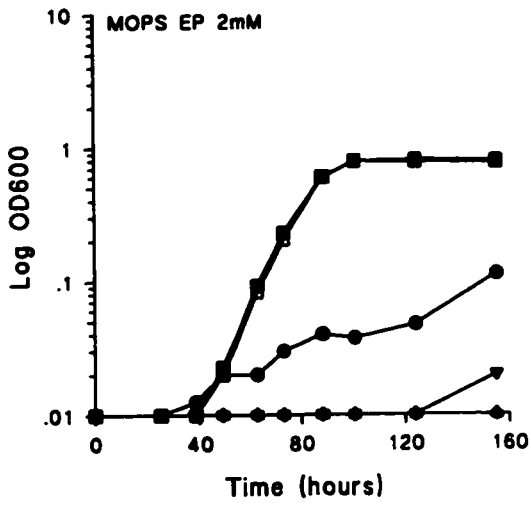
MOPS EP 2mM
Log OD600
10
1
.1
.01
0
40
80
120
160
Time (hours)

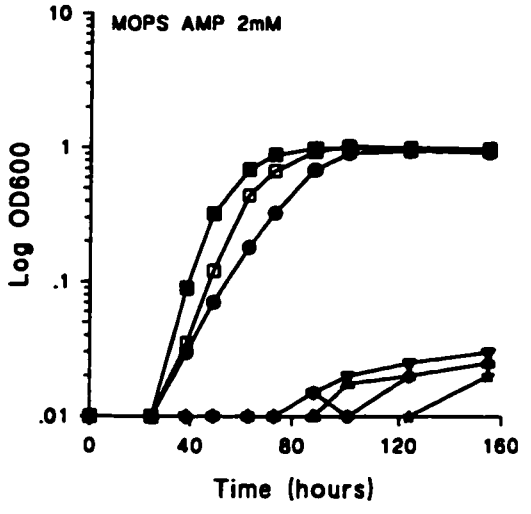
MOPS AMP 2mM
Log OD600
10
1
.1
.01
0
40
80
120
160
Time (hours)

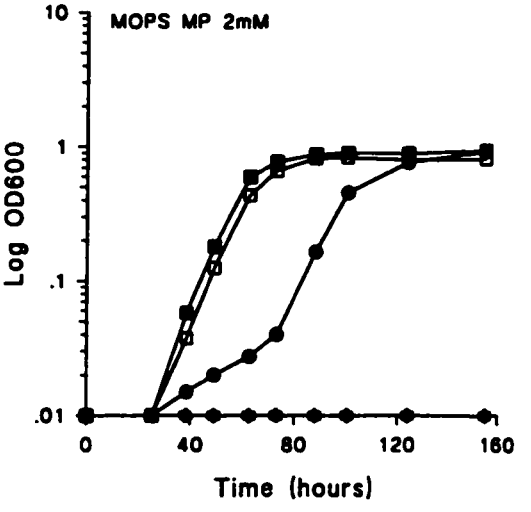
MOPS MP 2mM
Log OD600
10
1
.1
.01
0
40
80
120
160
Time (hours)

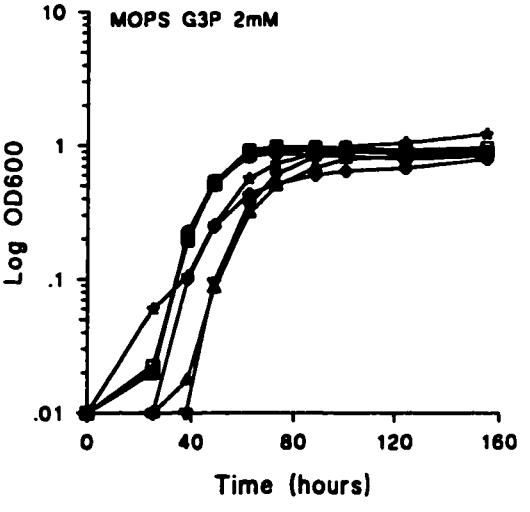
MOPS G3P 2mM
Log OD600
10
1
.1
.01
0
40
80
120
160
Time (hours)

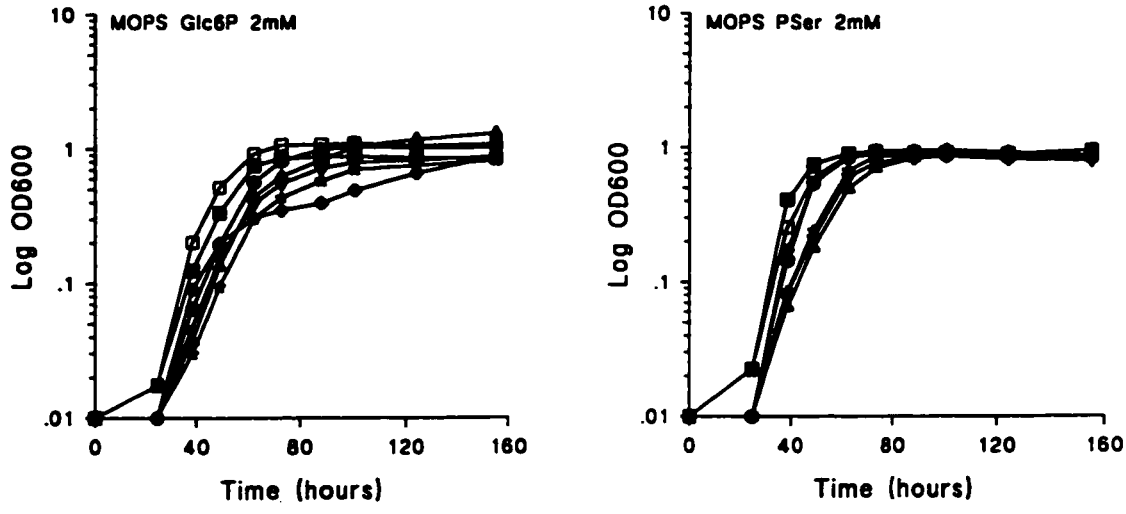

Fig. 5-4 Growth of *sfx2*, *phoU* and *phoB* mutants in MOPS-buffered minimal media with no phosphate added (MOPS P0), or containing 2mM of, inorganic phosphate (MOPS Pi), aminoethylphosphonate (MOPS AEP), ethylphosphonate (MOPS EP), aminomethylphosphonate (MOPS AMP), methylphosphonate (MOPS MP), glycerol-3-phosphate (MOPS G3P), glucose-6-phosphate (MOPS Glc6P) and phosphoserine (MOPS PSer). The growth of these mutants was compared to the growth of the wild type strain Rm1021, RmG490 (*phoC*Ω490) and *pho27*. The symbols are as follows: Rm1021 (wt, ■), RmG490 (*phoC*Ω490, ●), RmH610 (*pho27*::Tn*V*, □) RmH836 (*phoU10*::Tn*V*, ▼), RmH837 (*phoB8*::Tn*V*, ◆), RmH838 (*phoB3*::Tn*V*, ★) and RmG497 (*sfx2*, ▲). Each data point represents the average of triplicate values.

concentration of 2mM. Growth was compared with that obtained in phosphate-free media (MOPS P0) and in media containing 2mM Pi (MOPS Pi 2mM) (Fig. 5-4).

The *sfx2*, *phoB* and *phoU* mutants grew poorly on EP, MP and AMP indicating that the genes involved in the uptake and/or degradation of these compounds were under phosphate regulation and required functional PhoU and /or PhoB proteins for expression in *R. meliloti*. These growth phenotypes were clearly different to the one obtained using the *phoC*Ω490 mutant. The slow growth of *phoC*Ω490 was significantly higher than the growth of the *phoUB* mutants in EP while in MP and AMP *phoC*Ω490 grew to the level of the wild type with a delay of about 30 hours in MP. This suggested that the growth impairment of *sfx2*, *phoB* and *phoU* mutants in media containing EP, MP and AMP as sole phosphorus source was not due to lack of expression of the *phoCDET* phosphate transport system in these mutants (see below).

Following a lag of about 20-30 hours, both the *phoU* and *phoB* mutants grew at a growth rate comparable to the wild type in medium containing AEP. The growth lag in MOPS AEP suggests that an alternative system was induced in the *phoUB* mutants to assimilate this compound. In *Enterobacter aerogenes* (Lee et al., 1992) and *Salmonella typhimurium* (Jiang et al., 1995) the phosphonatase pathway that specifically assimilates and degrades AEP is Pho regulated and requires the PhoB protein for transcription. The system for uptake

and/or metabolism of AEP, induced in a *phoUB* mutant background in *R. meliloti*, was similar to the phosphonatase pathway as far as the specificity was concerned but did not require PhoB for expression. This may constitute a novel PhoB-independent pathway for utilization of AEP as phosphorus source.

Except for a slight delay of 4 to 6 hours, the *phoUB* mutants grew as well as the wild type on the organophosphates glycerol-3-phosphate (G3P), glucose-6-phosphate (Glc6P) and phosphoserine (PSer), suggesting that the assimilation and degradation of these compounds is unlikely to be Pho regulated (Fig. 5-4).

The growth of the mutant strains in MOPS medium containing 2mM Pi was similar to the growth of the wild type, although a slight growth delay (3 to 4 hours) was observed in the mutant cultures. In the absence of added phosphate, a small residual level of growth was usually observed in cultures inoculated with the wild type strain. We attribute this residual growth to the utilization of phosphate reserves such as polyphosphate. No residual growth was observed for any of the *phoUB/sfx2* mutant strains, suggesting that a very limited phosphate reserve was present in these mutants. This correlates well with the finding that in *Klebsiella aerogenes* the *ppk* gene encoding the polyphosphate kinase enzyme which catalyzes polyphosphate formation is part of the Pho regulon (Kato et al., 1993) and that the *E. coli ppk* gene promoter possesses two putative Pho Boxes (Akiyama et al., 1992).

The *pho27* mutation, disrupting an open reading frame showing no significant homology with protein of the Data Bank, showed no growth phenotype and the mutant grew as well as the wild type strain in the various phosphorus media.

We note that in all media, the *R. meliloti phoU* mutant had an identical phenotype to the *phoB* mutant. This differs considerably from the phenotypes of the *E. coli phoU* mutants that constitutively express the genes of the Pho regulon. A simple explanation for this result may lie in the fact that the *R. meliloti phoU* Tn*5* insertion is likely to be polar on *phoB* (see discussion).

6- *phoB* is required for *phoCDET* expression

The induction (over 10 fold) of *phoD::lacZ* and *phoE::lacZ* gene fusions in response to phosphate starvation and the presence of two Pho-like Boxes in the promoter region upstream of the *phoC* gene suggested that *phoCDET* expression required a PhoB-like protein as transcriptional activator (Bardin et al., 1996). To investigate whether the *phoB*-like gene of *R. meliloti* characterized in this study was required for *phoCDET* expression, plasmid-borne *lacZ* fusions to *phoD* (insertion 7A) and *phoE* (insertion 19) (described in Bardin et al., 1996) were transferred into the Lac$^-$ *phoB3* and *phoB8* strains, RmH615 and RmH616 respectively. β-Galactosidase activity in these strains was measured after 38 hours growth in a MOPS-buffered minimal media with no phosphate added

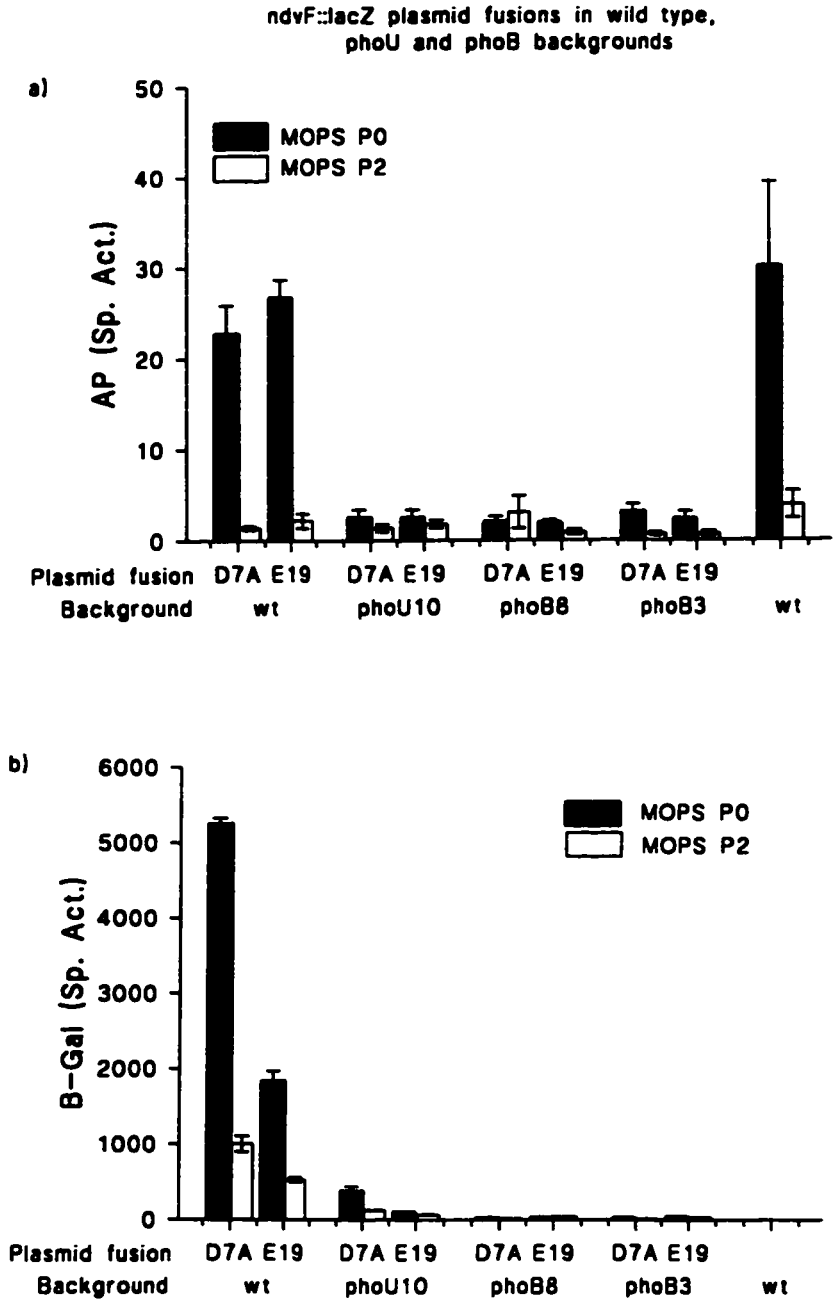

Fig. 5-5 Alkaline phosphatase (a) and β-galactosidase (b) activities of plasmid-borne *ndvF::lacZ* fusions in Lac$^-$, wild type (wt), *phoU10*, *phoB8* and *phoB3* backgrounds after 38 hours growth in MOPS-buffered minimal media with no phosphate added (MOPS P0, solid box) or containing 2mM inorganic phosphate (MOPS P2, open box). The transcriptional *lacZ* fusions were due to *Tn5*-B20 insertions in the *phoD* (D7A) and *phoE* (E19) genes. Each data point represents the average of triplicate values ± S.E..

(MOPS P0) and media supplemented with 2mM Pi (MOPS P2). Alkaline phosphatase activity was also measured to verify the phosphate physiological state of the cells. As expected the Lac$^-$ but otherwise wild type strain (wt) showed high AP activity when grown in MOPS P0 and low AP activity when grown in MOPS P2 while the *phoB3*, *phoB8* and *phoU10* derivatives showed low AP activity regardless of the growth medium (Fig. 5-5a). In the wild type background, both the *phoD::lacZ* and *phoE::lacZ* directed β-galactosidase activity was 4 to 5 times higher under P limiting conditions (MOPS P0) than P sufficient conditions (MOPS P2). In the *phoB3* and *phoB8* backgrounds β-galactosidase activity was not detected from either fusion even from cells grown in MOPS P0 (Fig 5-5b). The same phenotype was obtained when these fusion plasmids were mated into an *sfx2* strain (strain RmH693; data not shown). In the *phoU10* background (strain RmH617), *phoD* and *phoE* directed β-galactosidase activity was also dramatically repressed, with very little activity detected. It therefore appears that *phoB* (and perhaps *phoU*) are required for *phoCDET* expression.

7- *phoB* and *phoU* mutations are able to suppress the growth, mucoidy and Fix$^-$ phenotypes of *phoCDET* mutants.

The *phoU10*, *phoB8* and *phoB3* mutations had phenotypic effects which were similar to the suppressor mutation *sfx*2. As the *sfx2* mutation was originally identified as a suppressor of the Fix$^-$ phenotype of *phoCDET* (*ndvF*) mutants we

Strain	Genotype	ARA ± S.E. (nmol/plant/ hour)	% wt ARA	Dry Weight (mg/plant) ± S.E.	% wt Dry weight
Rm1021	wt	1359.4 ± 146.0	100.0	39.4 ± 4.7	100.0
RmG490	*phoC*Ω490	19.6 ± 8.6	1.4	7.7 ± 0.1	19.5
RmG497	*sfx2*	1428.5 ± 297.1	105.1	35.5 ± 6.4	90.1
RmH363	*phoC*Ω490 *sfx2*	1711.7 ± 148.6	125.9	33.2 ± 4.1	84.3
RmH836	*phoU10*::Tn*V*	1919.6 ± 696.5	141.0	38.7 ± 3.0	98.2
RmH623	*phoC*Ω490 *phoU10*::Tn*V*	1315.7 ± 397.2	96.8	39.5 ± 2.7	100.2
RmH837	*phoB8*::Tn*V*	1627.5 ± 301.5	119.7	45.4 ± 6.6	115.2
RmH624	*phoC*Ω490 *phoB8*::Tn*V*	1480.0 ± 261.5	108.9	35.4 ± 3.7	89.8
RmH838	*phoB3*::Tn*V*	775.7 ± 109.3	57.1	39.5 ± 1.5	100.2
RmH625	*phoC*Ω490 *phoB3*::Tn*V*	1115.7 ± 121.1	82.1	38.5 ± 3.8	97.7
UI		0	0	6.8 ± 0.6	17.2

Table 5-3: Symbiotic phenotype of *sfx2*, *phoU10*, *phoB8* and *phoB3* mutants in wild type and *phoC*Ω490 backgrounds. The acetylene reduction activity (ARA) was determined on 28 day old alfalfa root systems from three plants. Values are the mean of three independent measurements (total of nine roots) ± S.E.. The shoot dry weight represents the average of 3 times 10 plants ± S.E.. The percentages were calculated relative to the wild strain (Rm1021) values (set at 100%). UI: uninoculated.

tested the *phoB* and *phoU* insertion mutations for their ability to suppress the symbiotic as well as other phenotypes associated with the *phoCDET* mutations. The latter included the poor growth phenotype of *phoCDET* mutants in MOPS media containing 2mM Pi and their mucoidy colony morphology on low osmolarity media (GYM plates). The *phoUB-phoC*Ω490 strains were constructed by transducing the *phoU10, phoB8* and *phoB3::*Tn*V* (Nm^r) insertion alleles from strains RmH399, RmH428 and RmH430 into RmG490 (*phoC*Ω490) to create strains RmH623, RmH624 and RmH625, respectively.

Plants inoculated with the *ndvF* mutant *phoC*Ω490 were small and chlorotic 28 days after inoculation and showed little evidence of N_2-fixation as measured by acetylene reduction and plant dry weight (Table 5-3). In the presence of *phoU10, phoB8* and *phoB3* mutations the Fix^- phenotype of the *phoC*Ω490 mutant strain was suppressed to Fix^+ with shoot dry weight and acetylene reduction values comparable to the wild type strain Rm1021 (Table 5-3). We also noted that the individual *phoB* and *phoU* mutants appeared to show no reduction in symbiotic effectiveness compared to the wild type strain.

In MOPS-buffered minimal media containing 2mM Pi, the *phoC*Ω490 mutant grew poorly, however the double mutants carrying *phoC*Ω490 together with *phoU10*, *phoB8* , *phoB3* or the *sfx2* alleles grew as well as the wild type strain Rm1021 (Fig. 5-6). This result is consistent with the finding that strains carrying *phoB*, *phoU* and *sfx2* mutations in an otherwise wild type background

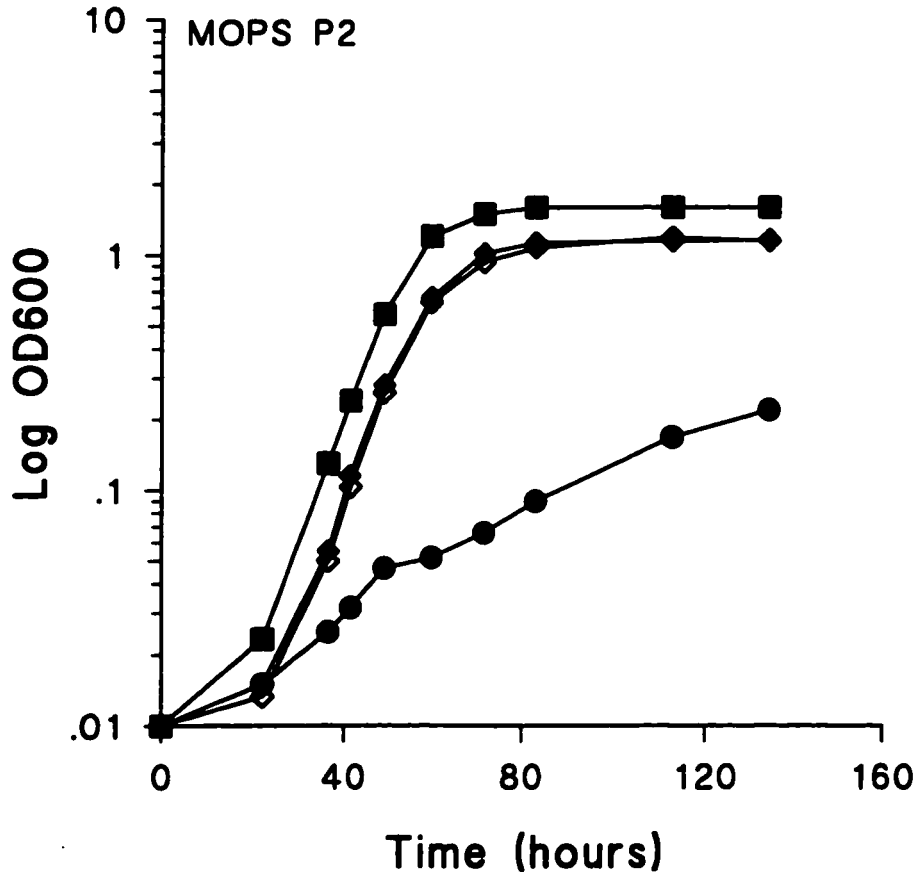

Fig. 5-6 Growth experiment showing suppression of the growth phenotype of *phoC* mutant in MOPS-buffered minimal media containing 2mM Pi by *R. meliloti phoUB* mutants. The strains presented are Rm1021 (wt, ■), RmG490 (*phoC*Ω490, ●), RmH625 (*phoB3*, *phoC*Ω490, ✧) and RmH838 (*phoB3*, ◆). The growth characteristics of RmH623 (*phoU10*, *phoC*Ω490), RmH624 (*phoB8*, *phoC*Ω490) and RmH363 (*sfx2*, *phoC*Ω490) were similar to those of RmH625 and are not presented here to simplify the figure. Each data point represents the average of triplicate values.

grew like the wild type strain in media containing 2mM Pi (Fig. 5-4), despite the fact that the *phoCDET* encoded phosphate transport system is not expressed in these strains (Fig. 5-5b). The system allowing Pi transport into *phoU/B* mutants could also be responsible for allowing the *phoU/B-phoC*Ω490 double mutants to grow normally in media containing 2mM phosphate (Fig. 5-6).

Oresnik et al., (1994) observed that *phoCDET* (*ndvF*) mutants form mucoid colonies when plated on low osmolarity GYM medium whereas the wild type formed non-mucoid (dry) colonies on this medium. The mucoid phenotype is dependent upon genes required for synthesis of the exopolysaccharide II (EpsII) of *R. meliloti* and these genes were known to be expressed under phosphate starvation conditions (Zhan et al., 1991). This mucoid colony phenotype was also reversed by increasing the osmolarity of the media by adding 100mM of various salt, such as NaCl, KCl or $MgSO_4$. In addition *phoCDET sfx1* or *phoCDET sfx2* double mutants generated a dry wild type phenotype (Oresnik et al., 1994). We investigated whether the *phoUB* mutations were able to suppress the mucoid phenotype of *phoCDET* mutants by plating RmH623 (*phoC*Ω490 *phoU10*), RmH624 (*phoC*Ω490 *phoB8)* and RmH625 (*phoC*Ω490 *phoB3)* on GYM agar. In all cases a dry colony morphology comparable to that of the wild type was obtained (Table 5-4). Moreover when the *phoC*Ω490 mutant RmG490 was plated on GYM agar supplemented with 2mM AEP (a Pi source the mutant strain was able to utilize), the colonies had a dry wild type morphology. These data

Strain	Genotype		GYM	GYM / NaCl	GYM / AEP2
Rm1021	wt		D	D	D
RmG490	*phoC*Ω490		M	D	D
RmG497	*sfx2*		D	D	_
RmH363	*phoC*Ω490 *sfx2*		D	D	_
RmH836	*phoU10*::Tn*V*		D	D	_
RmH623	*phoC*Ω490 *phoU10*::Tn*V*		D	D	_
RmH837	*phoB8*::Tn*V*		D	D	_
RmH624	*phoC*Ω490 *phoB8*::Tn*V*		D	D	_
RmH838	*phoB3*::Tn*V*		D	D	_
RmH625	*phoC*Ω490 *phoB3*::Tn*V*		D	D	_

Table 5-4: Colony morphologies of *sfx2*, *phoU10*, *phoB8* and *phoB3* mutants in wild type and *phoC*Ω490 backgrounds on low osmolarity plates (GYM; glutamate / yeast / mannitol) and GYM plates supplemented with 100mM NaCl. Rm1021 and RmG490 were also tested on GYM media containing 2mM aminoethylphosphonate (AEP2). D and M indicate a dry-type and a mucoid-type colony morphology, respectively.

provide evidence that the mucoid phenotype of *phoCDET* mutants is a direct consequence of the phosphate starvation state of the cells.

In summary, mutations at the *phoUB* locus were phenotypically similar to the *sfx2* suppressor mutation and suppressed all of the known phenotypes associated with mutations in the *phoCDET* locus.

8- *phoUB* and *sfx2* mutations lead to increase in *orfA pit* expression

In view of above results, we suspected *phoB* and/or *phoU* mutations to increase expression of the recently characterized *orfA-pit* locus which appears to encode an alternate phosphate transport system in *R. meliloti* (see Chapter IV). To investigate this possibility, we transduced *phoB*, *phoU* and *sfx2* mutations into the chromosomal-borne transcriptional *lacZ* fusion, to the wild type-*pit* (strain RmH754 (*phoU10*), RmH755 (*phoB8*), RmH756 (*phoB3*) and RmH765 (*sfx2*)) and to the *sfx1-pit* locus (strain RmH861 (*phoU10*), RmH862 (*phoB8*), RmH863 (*phoB3*) and RmH860 (*sfx2*)). The level of *pit* expression (β-galactosidase activity) was measured after 32 hours growth in MOPS P0 and MOPS P2. The results from these experiments are shown in Figure 5-7a and b. As previously reported (Chapter IV): i) the overall levels of *pit* expression were higher when directed from the *sfx1* promoter than when directed from the wild type *pit* promoter; ii) in the wild type background, *pit* expression directed from both wild type and *sfx1* promoters was phosphate regulated as shown by the β-

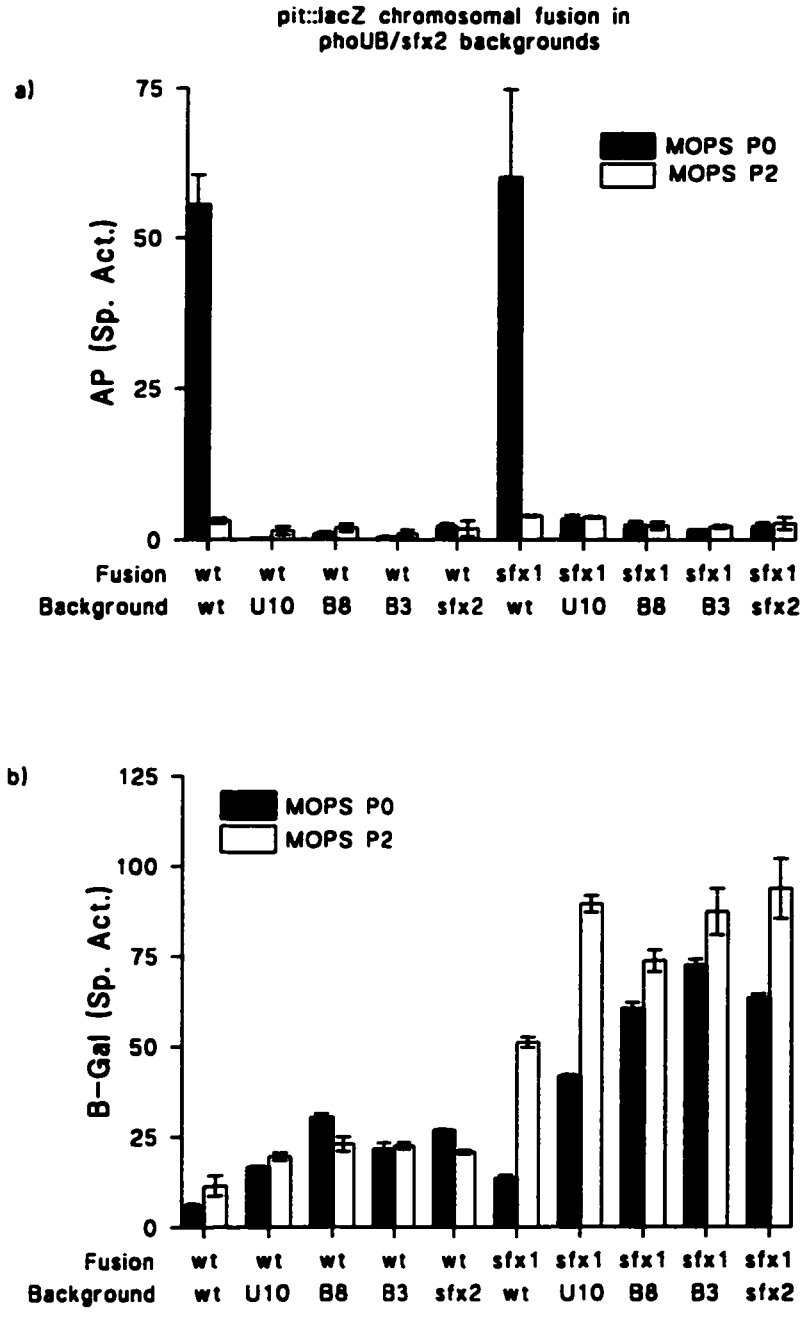

Fig. 5-7 Alkaline phosphatase (a) and β-galactosidase (b) activities of wild type- and *sfx1-pit::lacZ* chromosomal fusion in Lac$^-$, wild type (wt), *phoU10* (U10), *phoB8* (B8), *phoB3* (B3) and sfx2 backgrounds. The assay was performed after 32 hours growth in MOPS-buffered minimal media with no phosphate added (MOPS P0, solid box) or in media supplemented with 2mM Pi (MOPS P2, open box). Each value represents the average of triplicate values ± S.E..

galactosidase activity which was 3- to 4-fold higher in cells grown with 2mM phosphate compared to phosphate limited cells (P0). The results also demonstrate: iii) in the *phoU/phoB/sfx2* backgrounds, *pit* expression was increased 4.5- to 5.5-fold when the cells were grown in MOPS P0 and 1.5- to 2-fold when the cells were grown in MOPS P2 compared to its expression in a wild type background suggesting that *phoB* (*phoU*) is negatively regulating *pit* expression; iv) in the *phoU/phoB/sfx2* backgrounds the phosphate dependent regulation of *pit* expression from a wild type promoter was dramatically reduced with the expression of *pit* in MOPS P0 nearly reaching the expression in MOPS P2 grown cells, suggesting that phosphate regulation of *pit* expression was probably mediated via PhoB (PhoU). The same tendency was also observed in a *sfx1-pit::lacZ* fusion but not as clearly.

A similar regulation was observed when the plasmid fusions were mated into (1) *phoUB*(*sfx2*) backgrounds (data not shown) and (2) *phoCΩ490/phoUB* (*sfx2*) backgrounds (Fig. 5-7c and d) suggesting that the increase of *pit* expression in *phoUB/sfx2* mutant strains was independent of *phoCDET*. Suppression of *phoCDET* mutations by *phoUB* and *sfx2* then appear to be due to a 7- to 10-fold increase in *pit* expression (determined by comparing the difference in *pit* expression between *phoC* and *phoC phoUB/sfx2* mutants from MOPS P2 grown cells). The higher level of *pit* repression in cells grown under phosphate limiting conditions is believed to be due to the larger amount of

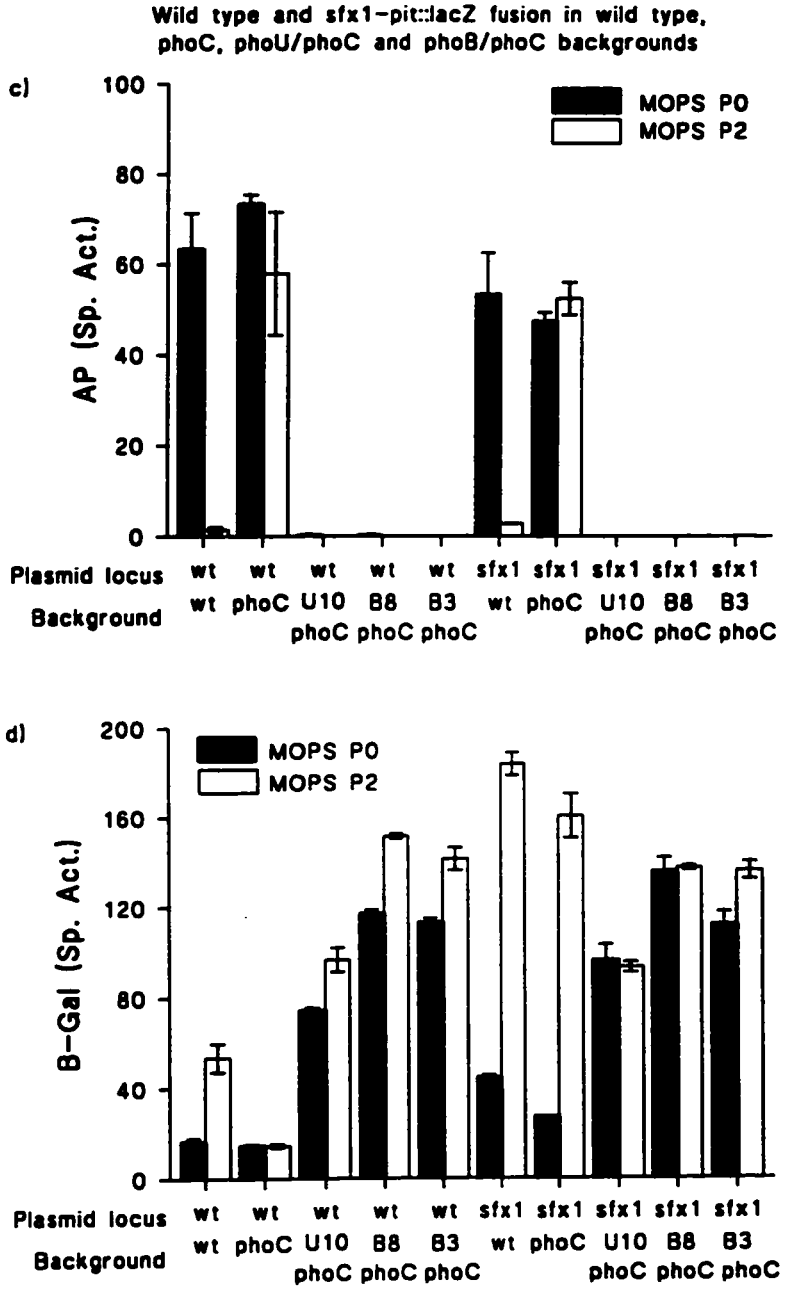

Fig. 5-7 Alkaline phosphatase (c) and β-galactosidase (d) activities of *pit::lacZ* plasmid fusion in Lac⁻, wild type (wt), *phoCΩ*490 (phoC), *phoU10/phoCΩ*490, *phoB8/phoCΩ*490, *phoB3/phoCΩ*490 and sfx2/*phoCΩ*490 backgrounds. The assay was performed after 38 hours growth in MOPS-buffered minimal media with no phosphate added (MOPS P0, solid box) or in media supplemented with 2mM Pi (MOPS P2, open box). Each value represents the average of triplicate values ± S.E..

activated PhoB protein present in these cells. A non-negligible level of activated PhoB (PhoU) protein appeared to be present in MOPS P2 grown cells as PhoB was able to repress expression of the *pit* locus to up to two fold.

Expression of the wild type and *sfx1-pit* alleles showed homologous response to the *phoUB-sfx2* mutations suggesting that the *sfx1* mutation did not affect the possible PhoB binding site in the promoter region of the *orfA-pit* locus. Although, *sfx1* on one hand and *sfx2/phoUB* on the other hand suppressed phenotypes associated with mutation in the *phoCDET* locus by increasing *pit* expression the mechanism by which this occurred appeared to be distinct.

9- *orfA-pit*::Tn*5 phoB/sfx2* double mutations are lethal

The absence of a functional PhoCDET transport system in a *phoUB* mutant suggested that phosphate was assimilated via an alternative transport system such as Pit. The genetic evidence above is consistent with this hypothesis. Here, we present further evidence which stems from our finding that we were unable to construct a *phoB3 orfA/pit*::Tn*5* or *sfx2 orfA/pit*::Tn*5* double mutants (Table 5-5). Strains RmG765 (*orfA*Ω2.3::Tn5) and RmG774 (*pit*Ω3.10::Tn5) were used as donors to transduce the *orfA pit* alleles into RmH406 (*phoB3*) and RmG497 (*sfx2*) strains. Transductants were selected on LB medium containing 200 μg/ml neomycin. Both *orfA/pit*::Tn*5* alleles were

Table 5-5 Viability of *sfx2* and *phoB3* strains after transducing lysates made from two *sfx1*::Tn*5* insertions strains in the absence or the presence of pTH90 (sfx1) or pTH38 (*phoCDET*). Viable counts of the transduction mixtures were determined to ascertain that the number of recipient cells were equivalent for every transduction. The number (#) of Nm^r transductant was determined after plating 0.1ml of the transduction mixture on selective plates. ND: not determined.

Donor		Recipient			
strain	**insertion**	**strain**	**genotype**	**viable counts** ($x10^6$ cells)	**# of Nm^r transductants** (per 0.1ml)
RmG765	*orfA*Ω2.3::Tn*5*	Rm1021	wt	131	167.5 ± 3.5
		RmH852	*phoB3*::Tn*5*-233	ND	0
		RmH856	*phoB3*::Tn*5*-233 / pTH90 (*sfx1*)	138	74.0 ± 3
		RmH855	*phoB3*::Tn*5*-233 / pTH38 (*phoCDET*)	113	0
		RmG497	*sfx2*, Ω5033::Tn*5*-233	ND	0
		RmH503	*sfx2*, Ω5033::Tn*5*-233 / pTH90 (*sfx1*)	69	26.5 ± 6.5
		RmH502	*sfx2*, Ω5033::Tn*5*-233 / pTH38 (*phoCDET*)	124	0
RmG774	*pit*Ω3.10::Tn*5*	Rm1021	wt	64	210.5 ± 0.7
		RmH852	*phoB3*::Tn*5*-233	ND	0
		RmH856	*phoB3*::Tn*5*-233 / pTH90 (*sfx1*)	156	90.0 ± 4
		RmH855	*phoB3*::Tn*5*-233 / pTH38 (*phoCDET*)	194	0
		RmG497	*sfx2*, Ω5033::Tn*5*-233	ND	0
		RmH503	*sfx2*, Ω5033::Tn*5*-233 / pTH90 (*sfx1*)	51	40.0 ± 3
		RmH502	*sfx2*, Ω5033::Tn*5*-233 / pTH38 (*phoCDET*)	136	0

readily transduced into the wild type strain Rm1021, however no transductants were obtained with the *phoB* or *sfx2* recipient strains unless these strains were made meridiploid for the *orfA pit* locus by first introducing the pTH90 plasmid. Making the *phoB* or *sfx2* mutants meridiploid for the *phoCDET* locus by transferring pTH38 had no effect, presumably because *phoCDET* expression occurs neither in a *phoB* or *sfx2* background. The requirement of a functional Pit protein for the survival of *phoB* and *sfx2* mutants suggests that the alternate Pi transport system which must be operative in these mutants is Pit protein dependent.

C- Discussion

Genetic analysis of the *sfx2* suppressor mutation resulted in the isolation of one *phoU* and two *phoB* transposon insertion mutants of *R. meliloti*. The precise location of the insertions within the *phoB* and *phoU* structural genes were established by DNA sequencing. The three mutants were identified on the basis of their alkaline phosphatase negative (AP^-) phenotypes and their linkage to the *sfx2* locus. In the case of the *phoB* mutants, the AP^- phenotype was expected as PhoB is required for AP expression in other bacteria (Lee et al., 1989; Anba et al., 1990). On the other hand, the AP^- phenotype of the *phoU* mutant was unusual as *phoU* mutants of both *E. coli* and *P. aeruginosa* were constitutive for alkaline phosphatase activity (Steed et Wanner, 1993; Kato et al., 1994, respectively). In *R. meliloti* the *phoB* gene is located downstream from *phoU* (accession # M96261 Cannon et al., unpublished). Given the *phoUB* gene order and the relatively small (111 bp) intergenic region, it is possible that in *R. meliloti*, *phoUB* are transcribed as a single mRNA, in which case *phoU* insertion mutants would also be genotypically $phoB^-$. If this is the case, elucidation of the role of *phoU* in *R. meliloti* will require the construction of defined $phoU^- phoB^+$ strains. It is worth noting the *E. coli phoU* mutants grow poorly in MOPS P2 and M63 media containing a variety of carbon sources as well as in complex media (Steed

and Wanner, 1993). We haven't observed analogous phenotypes with the *phoU* insertion mutant we isolated in *R. meliloti*.

Analysis of the sequence downstream of *phoB* revealed no *phoR*-like open reading frame, suggesting that *phoR*, if present in this strain, does not form an operon with *phoB* as observed in various organisms (Lee et al., 1989; Anba et al., 1990 and Lee and Hulett, 1992). We also note that our screening experiment did not result in the isolation of any *phoR* mutants. It is, however, possible that one would not detect *phoR* mutants as AP^- colonies if PhoB can be activated by kinases other than PhoR; thus leading to PhoR-independent transcriptional activation of genes of the Pho regulon. Kinases other than PhoR are known to activate PhoB in *E. coli* (Amemura et al., 1990; Wanner, 1996).

Our data showing that *phoD* and *phoE::lacZ* gene fusions are not expressed in a *phoB* mutant background (Fig. 5-5) is consistent with the presumed role of the *R. meliloti* PhoB protein as the central transcriptional activator of genes whose expression is responsive to low levels of extracellular phosphate. We previously identified two *E. coli* "Pho Box"-like sequences overlapping the -35 region of the *phoC* promoter (Bardin et al., 1996). By analogy to what is known in *E. coli*, it is likely that the *R. meliloti* PhoB protein binds the "Pho Box" elements at the *phoC* promoter to activate its transcription.

The observation that *sfx2* and *phoUB* insertion mutants behaved like a wild type strain when inoculated in plants or when grown in 2mM Pi, despite the

lack of *phoCDET* expression, suggested that an alternative Pi transport system was induced in these mutants. In addition, the loss of viability of *phoUB/sfx2 orfA/pit*::Tn5 double mutants prompted us to monitor *pit* expression in a *phoUB/sfx2* mutated background. In a wild type background, *pit* expression, from chromosomal *lacZ* fusions, was higher (although weakly; 2-fold) under conditions of excess Pi than under conditions of phosphate starvation (Fig. 5-7, see also Chapter IV). In the *phoB* background, however, *pit* expression showed little to no regulation by the phosphate concentration of the media (similar level of *pit* expression whether the cells were grown in MOPS P0 or MOPS P2), and the overall level of *pit* expression was higher in this background than in a wild type background. Thus, in contrast to *phoCDET* transcription, our data employing *pit::lacZ* gene fusions suggest that PhoB, or a PhoB-dependent gene product is a negative regulator of *pit* expression. PhoB-dependent regulation of *pit* expression therefore contrasts with the constitutive expression of the Pit transport system of *E. coli* (Rosenberg, 1987). It is interesting that expression of *pit* and *phoCDET* encoded Pi transport systems show opposite patterns of expression in response to concentration of available phosphate. It is likely that the pattern of *phoCDET* and *pit* expression reflects different physiological characteristics of the two transport systems. Indeed, we have recently obtained evidence that the Pit system is a low-affinity Pi transporter, whereas, the

PhoCDET system has a high-affinity for Pi (Voegele, Bardin and Finan, 1997 in preparation).

Most studies of the Pho regulon have focused on genes whose expression increases in response to Pi limitation. VanBogelen et al. (1996) recently published a survey of *E. coli* proteins whose synthesis was influenced by the extracellular phosphate concentrations. These authors estimated that the synthesis rate of 413 proteins was modified under phosphate limitation, of these 208 were induced and 205 repressed. These authors noted that the promoter regions of three repressed genes, *ompF*, *pfl* and *ssb* contain putative PhoB boxes, however other than that observation we are not aware of any reports where the actual mechanism of repression of these genes has been examined. Smith and Payne (1992) suggested that PhoB may repress expression of periplasmic peptide transport binding proteins under low phosphate conditions. They also identified a putative PhoB Box that seemed to overlap with the RNA polymerase binding sites of normal promoters. The work presented here then provides the first genetic evidence of a PhoB or a PhoB-dependent protein acting as phosphate-dependent repressor of gene expression. The mechanism by which available Pi regulates *orfA pit* expression will require further analysis of the promoter region; in this respect it is interesting that the *sfx1* mutation increases the basal rate of *pit* transcription, yet *pit* expression from the *sfx1* locus is still regulated by the concentration of available phosphate. PhoB inactivation

abolishes phosphate regulation of the wild type- but not of *sfx1-orfA pit* locus. The *sfx1* mutation then "creates" a new phosphate regulation of the locus which is not PhoB-dependent. The increase in *pit* expression by *sfx1* and *sfx2/phoUB* mutations therefore occur via two different mechanisms.

It is worth mentioning that a significant amount of activated PhoB protein seems to be present in cells grown under phosphate sufficient conditions as *pit* expression under these growth conditions was repressed up to two fold compared to its expression in a *phoB*$^-$ background. As a *pit* mutant showed no growth or symbiotic phenotypes (data not shown), we argue that the level of *phoCDET* expression in MOPS P2 may be sufficient to assume normal functioning of the cells.

PhoB was required for growth of *R. meliloti* in MOPS-buffered minimal media containing various phosphonates as the sole source of P (Fig. 5-4). In *E. coli* the uptake and/or degradation of aminomethylphosphonate, methylphosphonate and ethylphosphonate by the C-P lyase pathway is under Pho regulon control (Wackett et al., 1987). Thus the requirement of a functional PhoB protein for growth on these compounds was expected with *R. meliloti* as well. It was however surprising that the *phoU/B* mutants grew as well as the wild type (after a slight delay) when aminoethylphosphonate (AEP) was the sole P source (Fig. 5-4). This compound can be taken up and metabolized by the C-P lyase pathway in *E. coli* and the phosphonatase pathway in *Enterobacter*

aerogenes and *S. typhimurium*. In these last two organisms, expression of the phosphonatase pathway was also activated by PhoB (Lee et al, 1992; Jiang et al, 1995). Our study clearly demonstrates that *R. meliloti* can transport and metabolize AEP via a PhoB-independent pathway.

sfx1 and *sfx2* were originally identified as mutations which suppressed the symbiotic Fix$^-$ phenotype of *ndvF (phoCDET)* mutants. The *sfx1* mutation was previously shown to result in increased expression of the *orfA pit* operon. As *pit* is homologous to many phosphate transport proteins (see Chapter IV), we hypothesize that the increased expression of *pit* results in increased phosphate transport and hence suppression of the growth and symbiotic phenotypes of the *ndvF (phoCDET)* mutants. Our findings that *sfx2* and *phoU/B* mutations result in increased *pit* expression are also consistent with the idea that increased expression of *pit* is responsible for the suppression of the symbiotic and free-living phenotypes associated with *phoCDET* (*ndvF*) mutations. The dominance of the *sfx2* mutation may be attributed to the fact that this mutation leads to the formation of a modified protein that impairs with the functioning of the wild type protein. The modified protein may have increased affinity for the promoters of genes of the Pho regulon, preventing access of the wild type protein and thus transcriptional activation of the genes. Another possible explanation may lay in the structure of the protein; if the protein is active as a dimer, the formation of an

hetero-oligomeric structure made of wild type and modified peptides could form an inactive protein, here again preventing expression of the Pho genes.

Appendix C

- Appendix C-1: Alkaline phosphatase activity of *sfx2* and *sfx3* strains.

The strains tested were 1021 (wt), RmG439 (*ndvF*ΔG439), RmG514 (*ndvF*ΔG439, *sfx2*, Ω5025::Tn*5*), RmF114 (ΔΩ5033-5064::Tn*5*-233; megaplasmid deletion removing the *phoCDET* locus (Fig. 1-2, Top)), RmF346 (ΔΩ5033-5064::Tn*5*-233, *sfx2*; strain isolated from Fix$^+$ nodules) and RmG425 (ΔΩ5033-5007::Tn*5*-233, *sfx3*, strain isolated from Fix$^+$ nodules).

⇒ No AP activity in *sfx2* and *sfx3* containing strains.

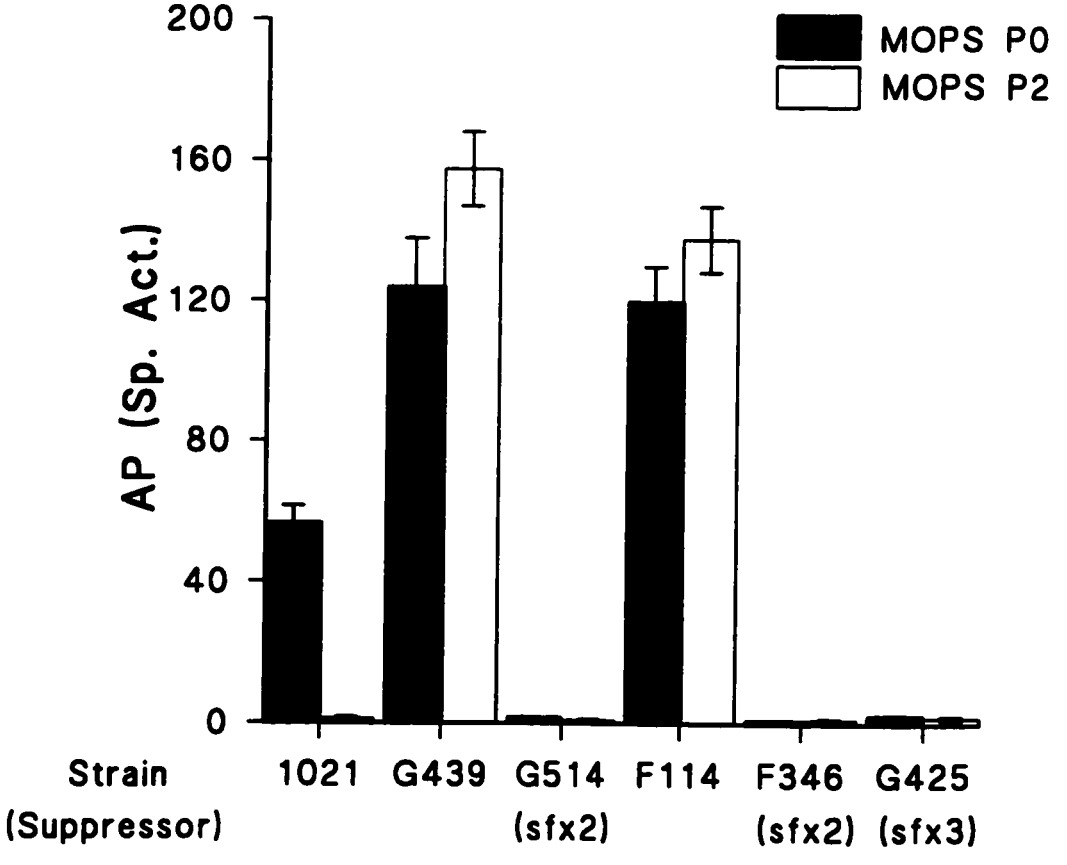

- Appendix C-2: Map of The *phoUB* locus of *Rhizobium meliloti* showing the Tn*V* subclone of *phoU10* (pTH292), *phoB3* (pTH287) and *phoB8* (pTH311).The four sequenced fragments are indicated:

Sequence 1; determined from pTH301 (pTH292 subclone (*phoU10*))

Sequence 2; determined from pTH328 (pTH292 subclone(*phoU10*))

Sequence 3; determined from pTH302 (pTH287 subclone (*phoB3*))

Sequence 4; determined from pTH331 (pTH311 subclone(*phoB8*))

Restriction sites indicated: *Hin*dIII (H); *Sal*I (Sl).

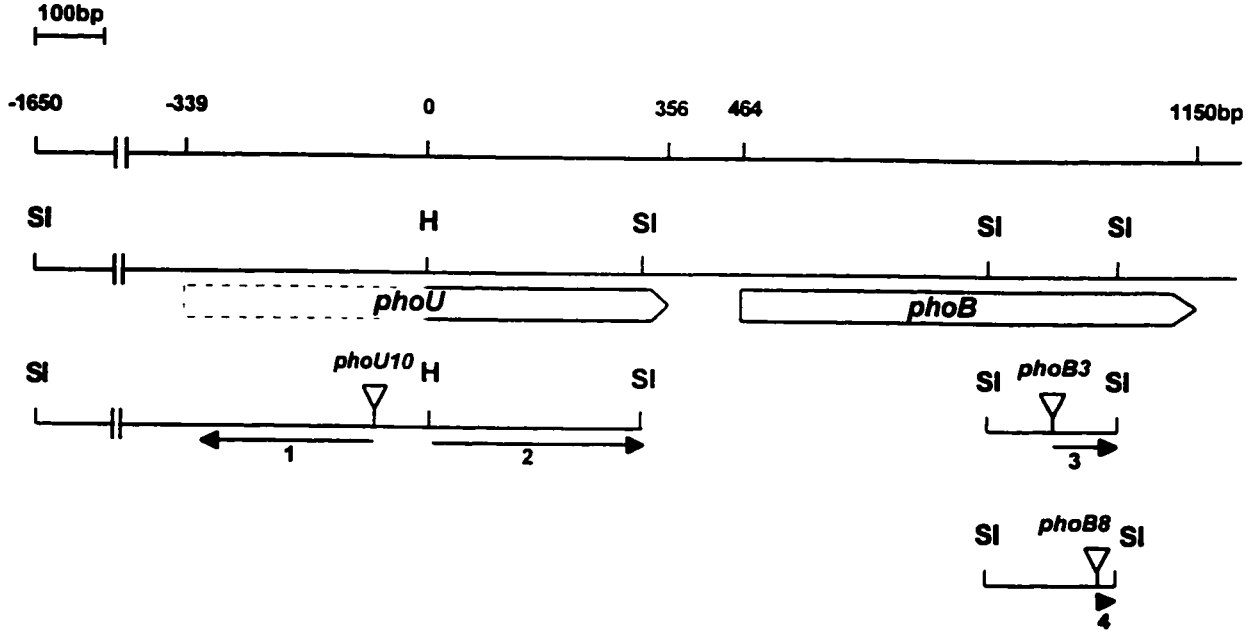

- Appendix C-3: Phenotypes associated with the RmF222 mutant.

RmF222 is a Rm1021 strain mutated with ethyl methanesulfonate which showed reduced AP activity (Long et al., 1988). In LB, the mutant strain grew as well as the wild type parent strain (Rm1021) and was able to effectively nodulate alfalfa plants. As it is believed that this mutant probably affects a regulatory gene of the Pho regulon, we investigated whether it was linked to the *phoUB* locus.

- Linkage experiments:

We transduced the Nm^r of Ω5258::Tn*5* (blue on X-Phos) into RmF222 and obtained a 56.5% linkage (26 blue colonies out of 46 colonies patched); a linkage similar to the one obtained when Ω5258::Tn*5* was transduced into *phoUB/sfx2* mutants. In addition, pTH282 and pTH284, plasmids complementing the AP phenotype of *phoUB/sfx3* mutants, were also able to complement the AP phenotype of RmF222.

- In contrast with *phoUB/sfx2* mutants, F222 mutation did not suppress the phoCDET symbiotic phenotype and exhibit a different growth pattern than *phoUB/sfx2* mutants when grown in media containing various phosphorus:

The growth over time of RmF222 (✧) in, MOPS P0, and 2mM of Pi, AEP, EP, AMP, MP, G3P, Glc6P and PSer, is compared to the wild type strain Rm1021 (■) and the *phoC*Ω490, RmG490 strain (●).

* In MOPS P0, after delay, F222 reached the wild type growth background. In the same media, *phoUB/sfx2* mutants showed no growth.
* In MOPS Pi, F222 showed intermediate growth between the wild type strain and the *phoC* mutant. In the same media, *phoUB/sfx2* mutants grew as well as the wild type strain.
* In MOPS AEP, F222 showed delayed growth compared to the wild type and *phoC* mutant as observed for the *phoUB/sfx2* mutants.
* In MOPS EP, F222 started growing 50 hours after the wild type strain; very little growth was observed in this media for the *phoUB/sfx2* mutants.
* In MOPS AMP, F222 reached the wild type growth after 30 hours delay; very little growth was observed in this media for the *phoUB/sfx2* mutants.
* In MOPS MP, F222 started growing 75 hours after the wild type strain; no growth was observed in this media for the *phoUB/sfx2* mutants.
* In MOPS G3P, F222 like the *phoUB/sfx2* mutants showed growth delay (about 5 hours) compared to the wild type strain.
* In Glc6P, F222 showed a slight growth delay compared to the wild type strain as observed for the *phoUB/sfx2* mutants.
* In MOPS PSer, the growth of F222 strain was slower that the *phoUB/sfx2* mutants.

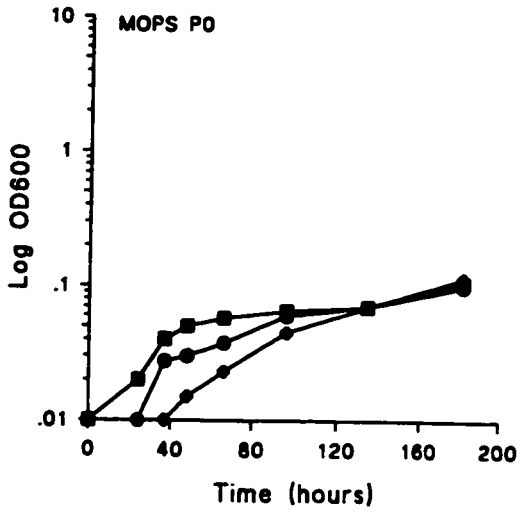
MOPS P0
Log OD600
10
1
.1
.01
0
40
80
120
160
200
Time (hours)

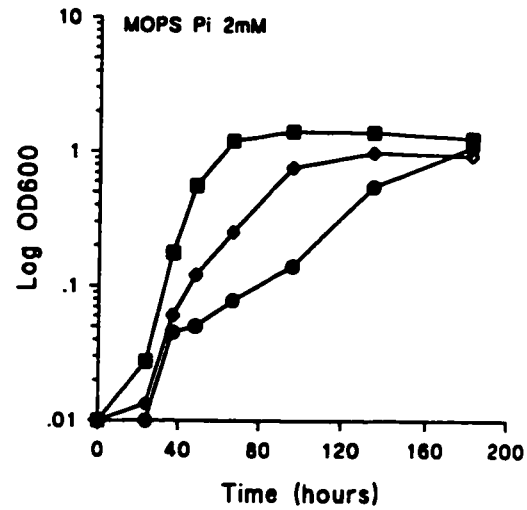
MOPS Pi 2mM
Log OD600
10
1
.1
.01
0
40
80
120
160
200
Time (hours)

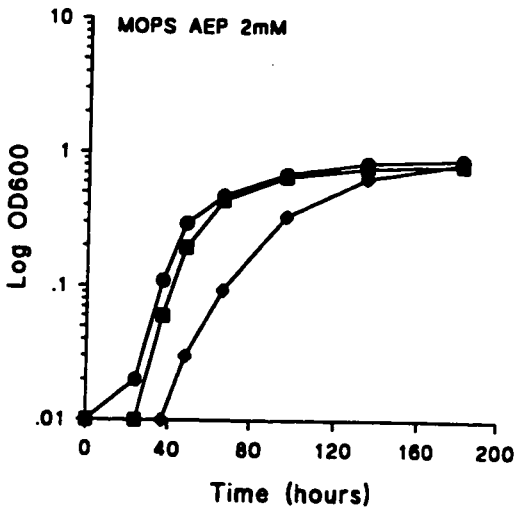
MOPS AEP 2mM
Log OD600
10
1
.1
.01
0
40
80
120
160
200
Time (hours)

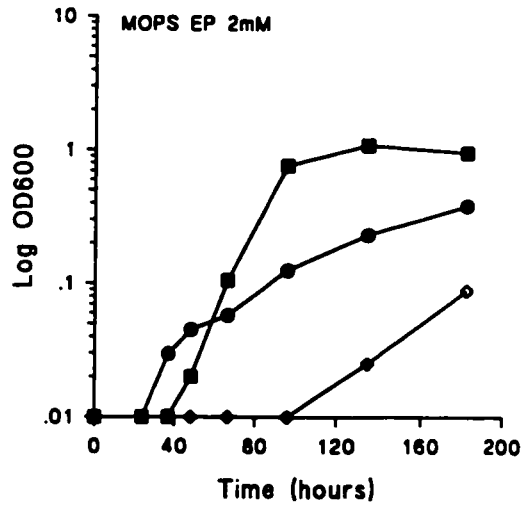
MOPS EP 2mM
Log OD600
10
1
.1
.01
0
40
80
120
160
200
Time (hours)

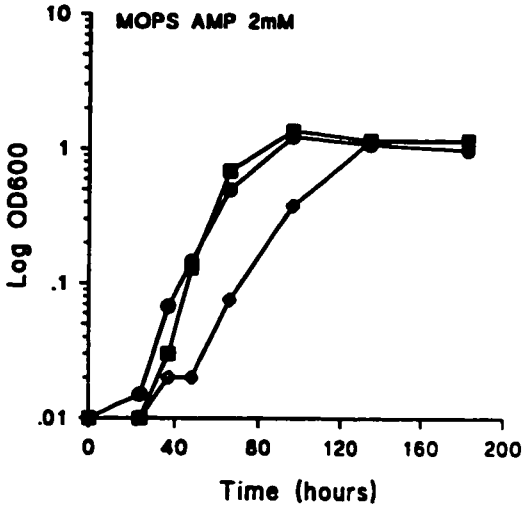
MOPS AMP 2mM
Log OD600
10
1
.1
.01
0
40
80
120
160
200
Time (hours)

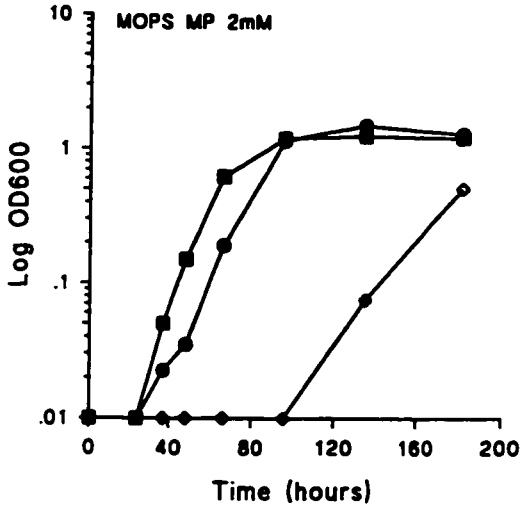
MOPS MP 2mM
Log OD600
10
1
.1
.01
0
40
80
120
160
200
Time (hours)

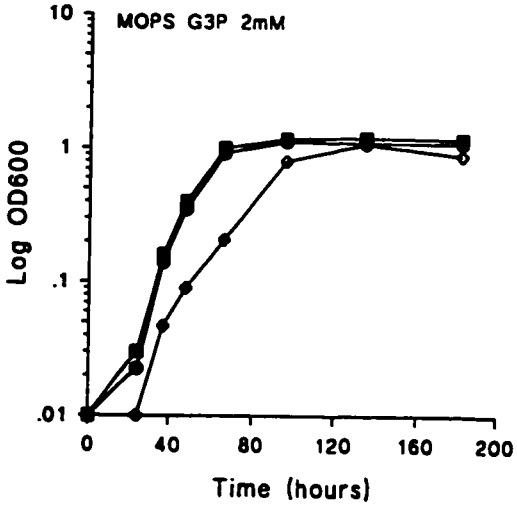
MOPS G3P 2mM
Log OD600
10
1
.1
.01
0
40
80
120
160
200
Time (hours)

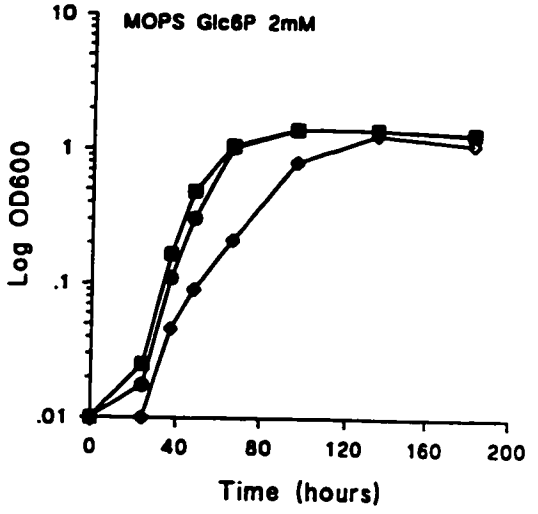
MOPS Glc6P 2mM
Log OD600
10
1
.1
.01
0
40
80
120
160
200
Time (hours)

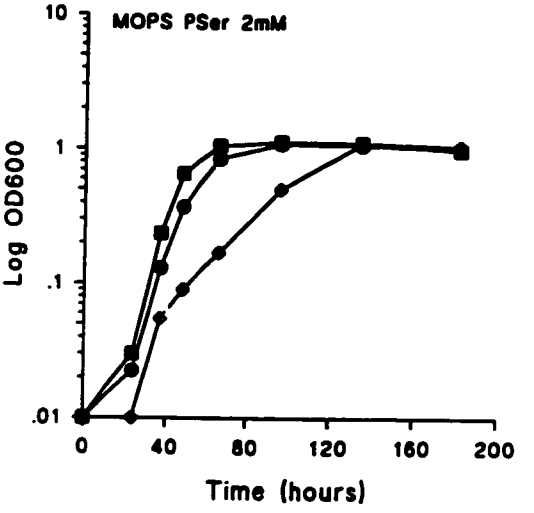
MOPS PSer 2mM
Log OD600
10
1
.1
.01
0
40
80
120
160
200
Time (hours)

- Appendix C-4: Sequences of *pho27* from both side of the Tn*V* insertion.

Note: J111 and J112 correspond to the E. coli strain numbers containing the two subclones.

>J111

CCATCGATGCCGAAgGCCGTCTCTGGGTCTCGACCGACGGCAACAACGAAAAGGACACGG
GACGCACCGACGGGGTCTGGGCCGTCGAGACCGAAgGCGAAGGCCGCGGCACCTCGAAGC
TGTTCTTCCGCGTGCCGGTCGGCGCCGAAATGTGCGGCCCGAGCTTCAACCCGACGAGCG
ACACCTTCTTCCTCGCGGTTCAGCATCCGGGCGATGCCGGTCTCGCAACCTACGAAAAGC
CGGCGACGCGCTGGCCGGATTTCCGCGACgACATGCCGGTGCGCCCGGcCGTCGTCGCCG
TGACCAgGCAGGGTGGCGGCAAgATCGGCTGAAcCAAGCCTCAgAgTTCGGAGCGCGGCG
CTGGCGCACGCgCTCCGGCAAGCCTCGTTGGTCGCGGTGTAgCGGTGCCCTTTCCTCTGC
TCGGTCGTCCCTGTGCTCGTCACagGGATCCAGCCAgACCagGTCCTnGAGCTGAAaAGA
TTtCCCCGCGCCGCAgACGCGGnGCTGCTCTCaTCTCTGTgCCagCACAgAgATGATGAA
GGGGAGAANACAGTCCTTNCCCCTACCGGANTTATCNCTACGCCACCCTCCCTTCTNCTG
CNCCCGTCNCNGGATNGAANCACCTTNANCCCCACATCNGATTCCCTCTCTCNTCNCNTG
ACAACTNTCNTGGTCATNCGCTCCACCCCCTGGTNTNACTTGCGGTNAGANTAGCCTNAA
CGAGGCCGTAAGNTCTTNNCCCTCTCNTTCCCNAGCTTCGAANNCACTTTATGTTTGNCN
CTTTCCCTTTNCCCCNTTCC

>j112

CATCGATGGCGCAATTGTCCGGCATGCCGAACCAgCCGTTCCTGGTCGTCGCGGTGGAGA
AgGAgGCACCGACCTCGGCGACGCTCGGATCGCCGCACTTCAGCAGTACGTCCCAGCGGG
ATTTCGTCGAGGCGAAGTCGCCGTCCGTTTCCGAAATCTCGACGATGTGGCCGAAGCATT
CTTGGCACGCGGATTGGCGGCGTCGATCTCGTCCTCCTTGCGCTTCGTGTTGTTGGTCAG
CATGACATAGACCTTGCCGGTCTTCGGGTTGGGCTGGACGTCTTCCGGCCGGTCCATCTT
GGTCGCGCCGAGCGCATCGGCGGCAAGACGGGTGTCgATCAGCACGTCGGCCTGGGAGGC
GAAGCCGTTCTCGGCCGTCAGCGGACCTTCGCCATGGACGAGAGGCATCCAgGTGACCGt
GCCGTCCTCGTCGAACTTGGCCACGTAgAGCGTGCCTTCATCGAAgAGATCCATATTCgC
gGCGCGGTCgTCaGGGTTGTAgGTGCCTTTCGTCACgAACTTGTAgACATAgTCgTAACG
CTCGTCGTCgCCGCTATaTAgGAgANCCCNCCCGTCCCTGTTGANNATCNACTCCACCCT
CCGTGCTTGAAACGTCTNATCCCGTGCGCTTCTCCNGAACGGAGGTGGGGTTCNNCNGAT
CAACTCAACACCCNCCCAAACGGTTGNTTCTNCGCTCTTGGAAAGTCAACCGCCTNAAAT
TCNACANTCTNCTGCCCCCCGGNTCCNAGGCTTTCCCTGNTAATTCTCACCTNTCCTACT
NTTCCCNTTNNANTNTNTNCGCCNCANTCCCCNCNCTCAACCGNAACTCNCTCC

Chapter VI

General Discussion

A) The new symbiotic locus *ndvF* encodes a phosphate transport system in *Rhizobium meliloti.*

The *ndvF* locus consists of four genes, *phoCDET* which encode an ABC-type transporter homologous to the *phnCDE* phosphonate transport system of *Escherichia coli* (Metcalf and Wanner, 1991). The PhoC protein is homologous to PhnC, the ATPase component of the transporter. PhoD is similar to PhnD, the putative periplasmic substrate-binding protein. The hydrophobic nature of PhoE and PhoT, both homologous to PhnE, make them likely to constitute the transmembrane components of the transporter. Evidence suggesting that *phoCDET* encodes a phosphate transporter include:

- *phoCDET* mutants grow poorly in MOPS-buffered minimal media containing 2mM Pi.
- *phoCDET* mutants fail to transport phosphate at low concentration.

In addition, all the phenotypes associated with the *phoCDET* mutations were shown to be the result of phosphate deprivation in those strains:

1. The high level of alkaline phosphatase (AP) activity measured in *phoCDET* mutants cells, even when the cells were cultured under phosphate sufficient conditions (conditions that repress AP expression in wild type cells), was attributed to the phosphate-starvation state of these cells. AP expression was indeed repressed when these mutants strains were grown in media supplemented with phosphorus sources they can utilize (such as AEP (Fig. 5-1), G3P, Glc6P and PSer; data not shown).
2. The mucoid phenotype of *phoCDET* mutants when plated on the low osmolarity media (GYM) is dependent on the expression of the *exp* genes encoding for the synthesis of exopolysaccharide II (Oresnik et al., 1994). Induction of these genes under phosphate limitation (Zhan et al., 1989; 1991) as well as reversion of the mucoid phenotype of *phoCDET* mutants to a dry (wild type) phenotype by adding 2mM AEP to the GYM plate also pointed to the phosphate starved behavior of these cells. It is interesting to mention that increasing the osmolarity of the GYM media by adding 100mM of various salts also reverted *phoCDET* mutants to a dry phenotype. This effect is likely due to the repression of the *esp* genes synthesis rather than a direct effect of the salt concentration on the phosphate transport system; the 100mM NaCl present in the MOPS P2 media did not prevent the growth phenotype of these mutants.

3. The symbiotic phenotype of *phoCDET* mutants was suppressed by spontaneous second site mutations in two distinct chromosomal loci both of which increased expression of an alternative phosphate transport system homologous to *pit*, the low-affinity phosphate transport system in *E. coli* (Sofia et al., 1994). The two types of suppressor mutations named *sfx1* and *sfx2*, also suppressed all the phenotypes associated with the *phoCDET* mutations. This provides definite evidence that the Fix$^-$ phenotype of *phoCDET* mutants was the result of the inability of these mutants to assimilate phosphate.

Kinetic experiments suggest that PhoCDET is a high-affinity, low-velocity transport system. The nature of the phosphate uptake inhibition in presence of phosphonates and arsenate has not been characterized yet. A competitive inhibition would suggest that these compounds are transported into the cell by the PhoCDET system. This would imply that PhoCDET has a wide substrate-specificity which contrasts with the high-specificity for phosphate of Pst, the high-affinity phosphate transporter of *E. coli*. Bacteria may have evolved such a transport system to cope with the soil environment where compounds like phosphonates may provide an alternative source of phosphorus.

Many bacteria have high-affinity phosphate transport systems and genetic characterization of some of these transporters indicates that they are ABC-type homologous to the *pst* system of *E. coli* (Nikata et al., 1996, Takemaru et al.,

1996). The ABC-type transporter appears to provide the best mechanism to assimilate a solute against a very high gradient.

B) An alternative phosphate transport system in *R. meliloti.*

Subcloning and sequencing of the *sfx1* suppressor locus revealed the presence of two open reading frames which partially overlap and thus likely form an operon. The deduced protein of the first gene, o*rfA*, showed no significant homology with proteins deposited in data banks while the second gene was homologous to *pit*, the low-affinity phosphate transport system of *E. coli* as well as other phosphate transporters found in both prokaryotic and eukaryotic organisms (see results section of Chapter IV). Suppression of the *phoCDET* associated phenotypes by the *sfx1* mutation resulted from a thymidine deletion in a seven T stretch lying 80 nucleotides upstream of the presumed start codon of *orfA*. This mutation seems to be responsible for increased expression of the *orfA-pit* genes. Increased expression of *orfA pit*, either via the *sfx1* mutation or by increasing the copy number of the wild type allele (by subcloning the locus on a multicopy plasmid), was sufficient to allow enough phosphate uptake (Dr. Voegele, personal communication) to restore normal growth in MOPS P2 and

the symbiotic capability to the *phoCDET* mutant strains. The role and function of *orfA* remains unknown.

The presence of two phosphate transporters in *R. meliloti* 1021 conflicts with the results previously reported which indicated that various *Rhizobium* strains carried only a single phosphate transport system (Smart et al., 1984a). *E. coli* (Willsky and Malamy, 1980a), *Acinetobacter johnsonii* (Van Veen et al., 1993a), *Acinetobacter lwooffi* (Yashphe et al., 1992) and *Bacillus cereus* (Rosenberg et al, 1969), however, possess two main Pi transport systems that differ in their affinity and specificity for phosphate as well as for the type of phosphate species they transport (as observed in *E. coli* and *A. johnsonii*, Van Veen et al., 1993b and 1994b). This suggests that these organisms have evolved two Pi transport systems in order to adjust to the phosphate species found in their environment. While the PhoCDET transport system appears to be essential for the growth of *R. meliloti* in the low-phosphate soil environment and nodule induction, the use of a Pit-like system in this bacteria remains to be defined.

C) Regulation of the phosphate transport systems.

Both *phoCDET* and *pit* expression appeared to be phosphate regulated via the PhoB (and possibly PhoU) protein but in opposite manners. Expression of *phoCDET* is induced and *pit* expression is repressed under phosphate-starvation conditions by PhoB or a PhoB-dependent protein. Regulation of the phosphate transport systems in *R. meliloti* 1021 is proposed in the following model (Fig. 6-1): When the cells are grown under phosphate deprivation, the PhoB protein, probably activated by phosphorylation, induces expression of the Pho regulon, including *phoCDET*, and represses either directly or indirectly expression of the *orfA-pit* locus. High phosphate conditions on the other hand, either prevent PhoB expression or deactivates PhoB leading to derepression of the *orfA-pit* locus with a concomitant decrease in *phoCDET* expression. This model is supported by the recent finding that Pit appears to be the main phosphate transport system in wild type cells grown in MOPS media containing 2mM Pi (Dr. Voegele, personal communication).

In accordance with the proposed model, the slow growth phenotype of *phoCDET* mutants in MOPS-buffered minimal media containing 2mM Pi can be interpreted by the fact that in these mutants the high content of activated PhoB, as suggested by the high AP activity, results in *pit* repression (as seen by the decrease in pit expression in a *phoCDET* mutant background; Fig. 5-7d). The

Fig. 6.1: Model showing the regulation of *phoCDET* and *orfA pit* loci under low and high phosphate conditions. Under low phosphate conditions, we believe that expression of the *phoUB* operon is induced. The PhoB protein produced is probably activated by phosphorylation (as shown in *E. coli*) and the activated protein ($PhoB^A$) induces *phoCDET* expression. PhoB, either directly or indirectly (via a protein X), also represses *orfA pit* expression. Under high phosphate conditions, $PhoB^A$ is not produced due to either to:
1) repression of the *phoUB* operon by the high Pi environment; or
2) the activated PhoB protein is not produced.
In any case, this results in the absence of *phoCDET* expression and in the derepression of *orfA pit* leading to the expression of these genes.

Low Pi conditions

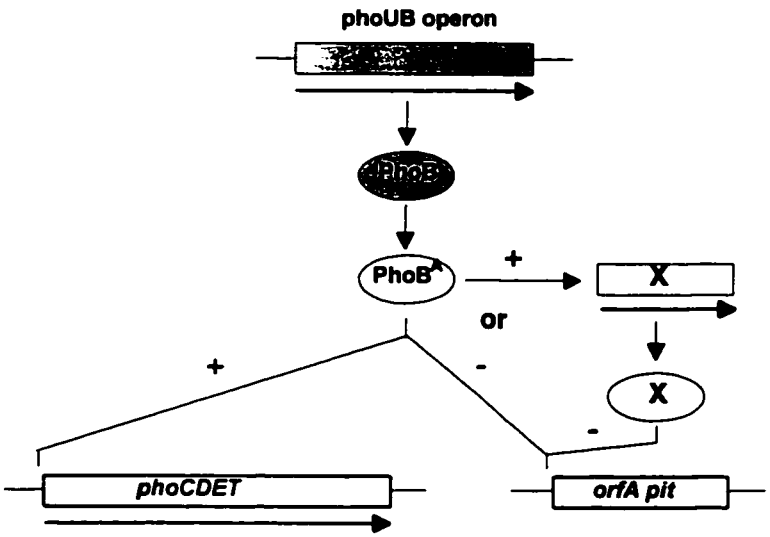

High Pi conditions

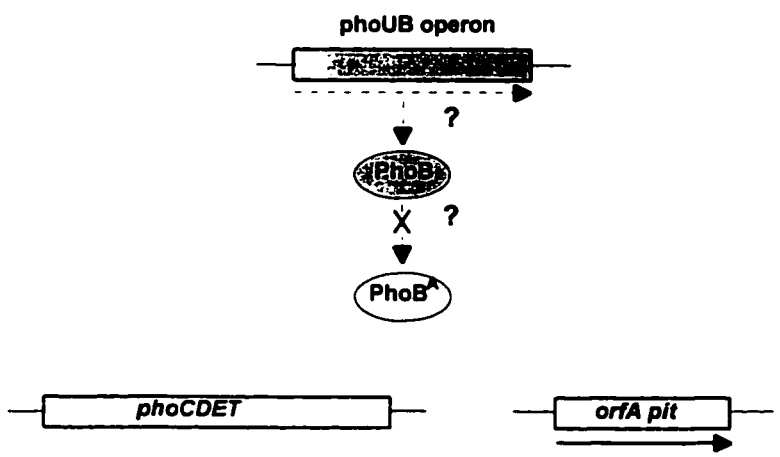

PhoCDET system then appears to be required for Pi signaling. A similar role has been proposed for the PstSCAB Pi transport system of *E. coli* (Wanner, 1996) The slow growth of these mutants is then indicative of slow phosphate uptake which is partially due to residual activity of Pit but also to alternative low-affinity phosphate transporter(s) as the double mutant (*phoCDET*, *pit::*Tn*5*) still grew but at a slower rate than a *phoCDET* mutant (Fig. 4-4b). In *E. coli*, alternative phosphate uptake systems include the phosphonate, the glycerol-3-phosphate and the glucose-6-phosphate transport systems (Metcalf and Wanner, 1991; Maloney et al., 1990). Systems similar to some of these phosphorus transporters are likely to be present in *R. meliloti*. These alternative phosphate transport systems appear to be PhoB regulated because the *phoB/pit* double mutation (in which *phoCDET* is not expressed) was lethal while *phoCDET/ pit* double mutants were not.

Regulation of the phosphate transport systems in *R. meliloti* contrasts with the ones in *E. coli*, *A. johnsonii* and *P. aeruginosa* (Willsky and Malamy, 1980a; Van Veen et al., 1993a; Poole and Hancock, 1984) as far as the expression of the low-affinity phosphate transport system is concerned. We demonstrated that the *pit* system of *R. meliloti* is phosphate regulated by a PhoB-dependent mechanism while the low-affinity transporters are believed to be constitutively expressed in these organisms.

D) Importance of the phosphate transport systems for the establishment of an efficient symbiosis.

Because of the competition between microorganisms for nutritional resources in the soil, bacteria equipped with an efficient uptake system for an essential compound which is present in low concentrations in soil, such as phosphate, will certainly have an advantage over strains with a less efficient uptake system. Growth efficiency is however not the only factor influencing the establishment of an efficient symbiosis. An increasing number of articles suggests a probable effect of P deficiency on the release of Nod factors and modification of molecules (lipopolysacharides) that are at the base of the communication between the plant host and rhizobia for the establishment of an efficient symbiosis (Mckay and Djordjevic, 1993; Howieson et al., 1993; Tao et al., 1992). Strains deficient in phosphate uptake may then have the dual disadvantage of growing poorly in the soil environment and be impaired in the release of Nod factors or in the synthesis of molecules essential for initiation of the infection process. In the case of the *phoCDET* mutants, reduction in phosphate uptake primarily affects the infection process as numerous small white nodules were present on the root of alfalfa plants inoculated with these mutant strains, although after delay. Due to the importance of a high affinity phosphate transport system for viability in the soil environment and the

establishment of an efficient symbiotic interaction with the plant host, it is not surprising that bacteria carrying second-site mutations which activate an alternative Pi transport system are readily selected for by the plant host.

Although, we are not able to investigate whether the high-affinity phosphate transport system is required in the nodule environment, it is rather unlikely due to the very high phosphate content as confirmed by, the presence of polyphosphate granules in the nodules and the low level of phosphate uptake measured in snake bean bacteroids (Smart et al., 1984a). Mutations in the *pit* locus show no effect on either the efficiency of nodule infection or acetylene reduction activity (data not shown). This suggests that *pit* is not required in the nodule or that the low level of *phoCDET* expression in this high phosphate environment was sufficient to take over *pit* deficiency. Phosphate uptake by *phoCDET* was indeed increased when cells lacking the Pit system were grown in MOPS 2mM Pi (Dr. Voegele, personal communication). It is interesting that Smart et al. (1984a) noted that AP activity in the bacteroid was significantly higher than in free-living bacteria grown under phosphate-rich conditions. This activity may however be due to factors independent of the phosphate concentration in, or surrounding the bacteroids.

References

Akiyama, M., E. Crooke, and A Kornberg.1992. The polyphosphate kinase gene of *Escherichia coli*. J. Biol. Chem. **267**:22556-22561.

Allen, N.S., M.N. Bennett, D.N. Cox, A. Shipley, D.W. Ehrhardt, and S.R. Long. 1994. Effects of Nod factors on alfalfa root hair Ca^{2+} and H^{+} currents and on cytoskeleton behavior, p 107-114. *In*, M.G. Daniels, J.A. Downie, and A.E. Osbourne, eds. Advances in Molecular Genetics of Plant-Microbe Interactions, vol. 3. Dordrecht: Kluwer Academic Publishers.

Ambudkar, S.V., T.J. Larson, and P.C. Maloney. 1986a. Reconstitution of sugar phosphate transport systems of *Escherichia coli*. J. Biol. Chem. **261**:9083-9086.

Ambudkar, S.V., L.A. Sonna, and P.C. Maloney. 1986b. Variable stoichiometry of phosphate-linked anion exchange in *Streptococcus lactis*: implications for the mechanism of sugar phosphate transport in bacteria. Proc. Natl. Acad. Sci. USA **83**:280-284.

Amemura, M., K. Makino, H. Shinagawa, and A. Nakata. 1990. Cross talk to the phosphate regulon of *Escherichia coli* by PhoM protein: PhoM is a histidine protein kinase and catalyzes phosphorylation of PhoB and PhoM-open reading frame 2. J. Bacteriol. **172**:6300-6307.

Anba, J., M. Bidaud, M.L. Vasil, and A. Lazdunski. 1990. Nucleotide sequence of the *Pseudomonas earuginosa phoB* gene, the regulatory gene for the phosphate regulon. J. Bacteriol. **172**:4686-4689.

Argast, M. 1978. A second transport system for sn-glycerol 3-phosphate in *Escherichia coli*. J. Bacteriol. **136**:1070-1083.

Argast, M. and W. Boos. 1980. Coregulation in *Escherichia coli* of a novel transport system for sn-glycerol 3-phosphate an outer membrane protein Ic (e, E) with alkaline phosphatase and phosphate-binding protein. J. Bacteriol. **143**:142-150.

Banfalvi, Z., E. Kondorosi, and A. Kondorosi. 1985. *Rhizobium meliloti* carries two megaplasmids. Plasmid **13**:129-138.

Banfalvi, Z., V. Sakanyan, C. Koncz, A. Kiss, A. Dusha, and A. Kondorosi. 1981. Location of nodulation and nitrogen fixation genes on a high molecular weight plasmid of *R. meliloti*. Mol. Gen. Genet. **184**:318-325.

Bardin, S.D., D. Dan, M. Osteras, and T.M. Finan. 1996. A phosphate transport system is required for symbiotic nitrogen fixation by *Rhizobium meliloti*. J. Bacteriol. **178**:4540-4547.

Beck, D.P., and D.N. Munns. 1984. Phosphate nutrition of *Rhizobium* spp. Appl. Environ. Microbiol. **47**:278-282.

Beck, D.P., and D.N. Munns. 1985. Effect of calcium on the phosphorus nutrition of *Rhizobium meliloti*. Soil Sci. Soc. Am. J. **49**:334-337.

Bennett, R.L., and M.H. Malamy. 1970. Arsenate resistant mutants of *Escherichia coli*. Biochem. Biophys. Res. Commun. **40**:496-503.

Berg, C.M. , and D.E. Berg. 1987. Uses of transposable elements and map of known insertions, p 1071-1107. *In*, F.C. Niedhardt, J.L. Ingraham, K.B. Low, B. Magasanik et al. (eds). *Escherichia coli* and *Salmonella typhimurium* Cellular and Molecular Biology. American Society for Microbiology, Washington, D.C.

Beringer, J.E., J.L. Beynon, A.V. Buchanan-Wollaston, and A.W.B. Johnston. 1978. Transfer of the drug resistance transposon Tn*5* to *Rhizobium*. Nature (London) **276**:633-634.

Bethenfalvay, G., and J.F. Yoder. 1981. The *Glycine-Glomus-Rhizobium* symbiosis. I. Phosphorus effect on nitrogen fixation and mycorrhizal infection. Physiol. Plant. **52**:141-145.

Bieleski, R.L. 1973. Phosphate pools, phosphate transport, and phosphate availability. Ann. Rev. Plant. Physiol. **24**:225-252.

Blanco, G., A. Preda, P. Brian, C. Mendez, K.F. Charter, and J.A. Salas. 1993. A hydroxylase-like gene product contributes to synthesis of a polyketide spore pigment in *Streptomyces halstedii*. J. Bacteriol. **175**:8043-8048.

Bollinger, J.M. Jr., D.S. Kwon, G.W. Huisman, R. Kolter, and C.T. Walsh. 1995. Glutathionylspermidine metabolism in Escherichia coli. Purification, cloning, overproduction, and characterization of a bifunctional glutathionylspermidine synthetase/amidase. J. Biol. Chem. **270**:14031-14041.

Bradford, M.M. 1976. A rapid and sensitive method for the quantitation of microgram quantities of protein utilizing the principle of protein-dye binding. Anal. Biochem. **72**:248-254.

Breedveld, M.W., A.L. Benesi, M.L. Marco, and K.J. Miller. 1995. Effect of phosphate limitation on synthesis of periplasmic cyclic β- (1,2)-glucans. Appl. Environ. Microbiol. **61**:1045-1053.

Bromfield, E.S.P., N.P. Thurman, S.T. Whitwill, and L.R. Barran. 1987. Plasmids and symbiotic effectiveness of representative phage types from two indigenous populations of *Rhizobium meliloti*. J. Gen. Microbiol. **133**:3457-3466.

Bullock, W.O., J.M. Fernandez, and J.M. Short. 1987. XL1-Blue: a high efficiency plasmid transforming *recA Escherichia coli* strain with β-galactosidase selection. BioTechniques **5**:376-378.

Burkardt, B., and H.J. Burkardt. 1984. Visualization and exact molecular weight determination of a *Rhizobium meliloti* symbiotic megaplasmid. J. Mol. Biol. **175**:213-218.

Burkardt, B., D. Schillik, and A. Puhler. 1987. Physical characterization of *Rhizobium meliloti* megaplasmids. Plasmid **17**:13-25.

Carlson, R.W., N.P.J. Price, and G. Stacey. 1995. The biosynthesis of rhizobial lipo-oligosaccharide nodulation signal molecules. Mol. Plant-Microbe Interact. **7**:684-695.

Cassman, K.G., N.D., D.N. Munns, and D.P. Beck. 1981a. Phosphorus nutrition of *Rhizobium japonicum*: strain differences in phosphate storage and utilization. Soil Sci. Soc. Am. J. **45**:517-520.

Cassman, K.G., N.D., D.N. Munns, and D.P. Beck. 1981b. Growth of *Rhizobium* strains at low concentrations of phosphate. Soil Sci. Soc. Am. J. **45**:520-523.

Cebolla, A., and A.J. Palomares. 1994. Genetic regulation of nitrogen fixation in *Rhizobium meliloti*. Microbiologia **10**:371-384.

Chan, F.Y., and A. Torriani. 1996. PstB protein of the phosphate-specific transport system of *Escherichia coli* is an ATPase. J. Bacteriol. **178**:3974-3977.

Charles, T.C., and T.M. Finan. 1991. Analysis of a 1600-kilobase *Rhizobium meliloti* megaplasmid using defined deletions generated *in vivo*. Genetics **127**:5-20.

Charles, T.C., and T.M. Finan. 1990. Genetic map of *Rhizobium meliloti* pRmSU47b. J. Bacteriol. **172**:2469-2476.

Charles, T.C., W. Newcomb, and T.M. Finan. 1991. *ndvF*, a novel locus located on megaplasmid pRmeSU47b (pEXO) of *Rhizobium meliloti*, is required for normal nodule development. J. Bacteriol. **173**:3981-3992.

Charles, T.C., R.S. Singh, and T.M. Finan. 1990. Lactose utilization and enzymes encoded by megaplasmids in *Rhizobium meliloti* SU47: implications for population studies. J. Gen. Microbiol. **136**:2497-2502.

Clarkson, D.T., P.C. Kerridge, D.W. Sherriff, and M.J. Fisher. 1983. Effects of phosphorus deficiency on photosynthesis and stomacal function in the tropical legume, Sratro. Annu. Report ARC Letcombe Lab. **1982**:65-66.

Claros, M.G., and G. von Heijne. 1994. TopPred II: an improved software for membrane protein structure predictions. Comput. Appl. Biosci. **10**:685-686.

Coleman, J.E. 1992. Structure and mechanism of alkaline phosphatase. Annu. Rev. Biophys. Biomol. Struct. **21**: 441-483.

Cook, D., D. Dreyer, D. Bonnet, M. Howell, E. Nomy, and K. VandenBosch. 1995. Transient induction of a peroxidase gene in *Medicago truncatula* precedes infection by *0*. Plant cell **7**:215-225.

Copper, J.B., and S.R. Long. 1994. Morphogenetic rescue of *Rhizobium meliloti* nodulation mutants by *trans*-zeatin secretion. Plant Cell **6**:215-225.

Courcelle, J., C. Carswell-Crumpton, and P.C. Hanawalt. 1997. *recF* and *recR* are required for the resumption of replication at DNA replication forks in *Escherichia coli*. Proc. Natl. Acad. Sci. USA. **94**:3714-3719.

Cox, G.B., D. Webb, J. Godovac-Zimmermann, and H. Rosemberg. 1988. Arg-220 of the PstA protein is required for the phosphate transport through the phosphate-specific transport system in *Escherichia coli* but not for alkaline phosphatase repression. J. Bacteriol. **170**:2283-2286.

Cox, G.B., D. Webb, and H. Rosenberg. 1989. Specific amino acid residues in both the PstB and the PstC proteins are required for phosphate transport by the *Escherichia coli* Pst system. J. Bacteriol. **171**:1531-1534.

David, M., O. Domergue, P. Pognonec, and D. Kahn. 1987. Transcription patterns of *Rhizobium meliloti* symbiotic plasmid pSym: identification of a *nifA*-independent *fix* genes. J. Bacteriol. **169**:2239-2244.

Dazzo, F.B., G.L. Truchet, R.I. Hollingsworth, E.M. Mrabak, H.S. Pankratz, S. Philip-Hollingsworth, J.L. Salzwedel, K. Chapman, L. Appenzeller, A. Squartini, D. Gerhold, and G. Orgambide. 1991. *Rhizobium* lipo-oligosaccharide modulates infection thread development in white clover root hairs. J. Bacteriol. **173**:5371-5384.

de Faria, S.M. H.T. Hay, and J.L. Sprent. 1988. Entry of rhizobia into the roots of *Mimosa scabrella* Bentham occurs between epidermal cells. J. Gen. Microbiol. **134**:2291-2296.

De Vos, G.F., G. Walker, and E.R. Signer. 1986. Genetic manipulations in *Rhizobium meliloti* utilizing two new transposon Tn*5* derivatives. Mol. Gen. Genet. **204**:485-491.

Debelle, F., C. Rosenberg, J. Vasse, F. Maillet, J. Denarie, and G. Truchet. 1986. Assignment of symbiotic developmental phenotypes to common and specific nodulation (*nod*) genetic loci of *Rhizobium meliloti*. J. Bacteriol. **168**:1075-1086.

Dénarié, J., and J. Cullimore. 1993. Lipo-oligosaccharide nodulation factors: A new class of signaling molecules mediating recognition and morphogenesis. Cell **74**:951-954.

Dénarié, J., F. Debellé, and C. Rosenberg. 1992. Signaling and host range variation in nodulation. Annu. Rev. Microbiol. **46**:497-531.

Dietz, G.W. 1976. The hexose phosphate transport system of *Escherichia coli*. Adv. Enzymol. **44**:237-259.

Dreyfus, B.L., J.L Garcia, and M. Gillis. 1988. Characterization of *Azorhizobium caulinodans* gen. nov., sp. nov., a stem-nodulating nitrogen-fixing bacterium isolated from *Sesbania rostrata*. J. Syst. Bacteriol. **38**:89-98.

Dylan, T., D.R. Helinski, and G.R. Ditta. 1990. Hypoosmotic adaptation in *Rhizobium meliloti* requires β-(1,2)-glucan. J. Bacteriol. **172**:1400-1408.

Dylan, T., L. Ielpi, S. Stanfield, L. Kashyap, C. Douglas, M. Yanofsky, E. Nester, D.R. Helinski, and G. Ditta. 1986. *Rhizobium meliloti* genes required for nodule development are related to chromosomal virulence genes in *Agrobacterium tumefaciens*. Proc. Natl. Acad. Sci. USA **83**:4403-4407.

Eardly, B.D., L.A. Materon, N.H. Smith, D.A. Johnson, M.D. Rumbaugh, and R.K. Selander. 1990. Genetic structure of natural populations of nitrogen-fixing bacterium *Rhizobium meliloti*. Appl. Environ. Microbiol. **56**:187-194.

Ehrhardt, D.W., E.M. Atkinson, and S.R. Long. 1992. Depolarization of alfalfa root hair membrane potential by *Rhizobium meliloti* Nod factors. Science **256**:998-1000.

Eiglmeier, K. W. Boos, and S.T. Cole. 1987. Nucleotide sequence and transcriptional strartpoint of the *glpT* gene of *Escherichia coli*: extensive sequence homology of the G3P transport protein with components of the H6P transport system. Mol. Microbiol. **1**:251-258.

Elvin, C.M., N.E. Dixon, and H. Rosenberg. 1986. Molecular cloning of the phosphate (inorganic) transport (*pit*) gene of *Escherichia coli* K12. Identification of the *pit*$^+$ gene product and physical mapping of the *pit-gor* region of the chromosome. Mol. Gen. Genet. **204**:477-484.

Figurski, D.H., and D.R. Helinski. 1979. Replication of an origin-containing derivative plasmid of RK2 dependent on a function provided in *trans*. Proc. Natl. Acad. Sci. USA **76**:1648-1652.

Finan, T.M., E. Hartwieg, K. Lemieux, K. Bergman, G.C. Walker, and E.R. Signer. 1984. General transduction in *Rhizobium meliloti*. J. Bacteriol. **159**:120-124.

Finan, T.M., A.M. Hirsch, J.A. Leigh, E. Johansen, G.A. Kuldau, S. Deegan, G.C. Walker, and E.R. Signer. 1985. Symbiotic mutants of *Rhizobium meliloti* that uncouple plant from bacteria differentiation. Cell **40**:869-877.

Finan, T.M., B. Kunkel, G.F. De Vos, and E.R. Signer. 1986. Second symbiotic megaplasmid in *Rhizobium meliloti* carrying exopolysaccharide and thiamine synthesis genes. J. Bacteriol. **167**:66-72.

Finan, T.M., I. Oresnik, and A. Bottacin. 1988. Mutants of *Rhizobium meliloti* defective in succinate metabolism. J. Bacteriol. **170**:3396-3403.

Fisher. H.M. 1994. Genetic regulation of nitrogen fixation in rhizobia. Microbiol. Rev. **58**:352-368.

Fisher, R.F., and S.R. Long. 1992. *Rhizobium*-plant signal exchange. Nature **357**:655-660.

Fleischmann, R.D., M.D. Adams, O. White, R.A. Clayton, E.F. Kirkness, A.R. Kerlavage, C.J. Bult, J.-F. Tomb, B.A. Dougherty, J.M. Merrick, K. Mckenney, G. Sutton, W. Fitzhugh, C.A. Fields, J.D. Gocayne, J.D. Scott, R. Shirley, L.-I. Liu, A. Glodek, J.M. Kelley, J.F. Weidman, C.A. Phillips, T. Spriggs, E. Hedblom, M.D. Cotton, T.R. Utterback, M.C. Hanna, D.T. Nguyen, D.M. Saudek, R.C. Brandon, L.D. Fine, J.L. Fritchman, J.L. Fuhrmann, N.S.M. Geoghagen, C.L. Gnehm, L.A. Mcdonald, K.V. Small, C.M. Fraser, H.O. Smith, and J.C. Venter. 1995. Whole-genome random sequencing and assembly of *Haemophilus influenza* Rd. Science **269**:496-512.

Fortin, M.G., M. Zechelowska, and D.P.S. Verma. 1985. Specific targeting of membrane nodulins to the bacteroid-enclosing compartment in soybean nodules. EMBO J. **4**:3141-3046.

Franssen, H., P. Mylona, K. Pawlowski, K. Vandesande, R. Heidstra, R. Geurts, A. Kozik, M. Matvienko, W.C. Yang, A.E. Hadri, F. Martinezabarca, and T. Bisseling. 1995. Plant genes involved in root-nodule development on legumes. Philosophical Transactions of the Royal Society of London - Series B: Biological Sciences **350**:101-107.

Friedberg, I. 1977. Phosphate transport in *Micrococcus lyzodeikticus*. Biochim. Biophys. Acta **466**:451-465.

Friedman, A.M., S.R. Long, S.E. Brown, W.J. Buikema, and F.M. Ausubel. 1982. Construction of a broad host range cloning vector and its use in the genetic analysis of *Rhizobium* mutants. Gene **18**:189-196.

Furuichi, T., M. Inouye, and S. Inouye. 1985. Novel one-step cloning vector with a transposable element: application to the *Myxococcus xanthus* genome. J. Bacteriol. **164**:270-275.

Galinier, A., A.M. Garnerone, J.M. Reyrat, D. Kahn, J. Batut, and P. Boistard. 1994. Phosphorylation of the *Rhizobium meliloti* FixJ protein induces its binding to a regulatory region at the *fixK* promoter. J. Biol. Chem. **269**:23784-23789.

Gish, W., and D.J. States. 1993. Identification of protein coding region by database similarity search. Nat. Genet. **3**:266-272.

Glazebrook, J., and G.C. Walker. 1989. A novel exopolysaccharide can function in place of the calcofluor-binding exopolysaccharide in nodulation of alfalfa by *Rhizobium meliloti*. Cell **56**:661-672.

Glucksmann, M.A., T.L. Reuber, and G.C. Walker. 1993. Family of glycosyl tranferases needed for the synthesis of succinoglycan by *Rhizobium meliloti*. J. Bacteriol. **175**:7033-7044.

Goethals, K., M. Van Montagu, and M. Holsters. 1992. Conserved motifs in a divergent *nod* box of *Azorhizobium caulinadans* ORS571 reveals a common structure in promoters regulated by LysR-type proteins. Proc. Natl. Acad. Sci. USA **89**:1646-1650.

Haldimann, A., M.K. Prahalad, S.L. Fisher, S.-K. Kim, C.T. Walsh, and B.L. Wanner. 1997. Altered recognition mutants of the response regulator PhoB: a new genetic strategy for studying protein-protein interactions. Proc. Natl. Acad. Sci. USA. In Press.

Hancock, R.E., R. Siehnel, and N. Martin. 1990. Outer membrane proteins of *Pseudomonas*. Mol. Microbiol. **4**:1069-1075.

Harold, F.M., and J.R. Banda. 1966. Interaction of arsenate with phosphate transport system in wild type and mutant *Streptococcus faecalis*. J. Bacteriol. **91**:2257-2262.

Harold, F.M., R.L. Harold, and A. Abrams. 1965. A mutant of *Streptococcus faecalis* defective in phosphate uptake. J. Biol. Chem. **240**:3145-3153

Harold, F.M., and E. Spitz. 1975. Accumulation of arsenate, phosphate and arsenate by *Streptococcus faecalis*. J. Bacteriol. **122**:266-277.

Hawker, S. 1985. Sucrose, p 1-51. *In*, P.M. Dey, and R.A. Dixon, eds. Biochemistry of Storage Carbohydrates in Green Plants. London: Academic Press.

Heidstra, R., R. Geurts, H. Franssen, H.P. Spaink, A. van Kammen, and T. Bisseling. 1994. Root hair deformation activity of nodulation factors and their fate on *Vicia sativa*. Plant Physiol. **105**:787-797.

Higgins, C.F. 1992. ABC transporters: from microorganisms to man. Annu. Rev. Cell Biol. **8**:67-113.

Hirsch, A.M., T.V. Bhuvaneswari, J.G. Torrey, and T. Bisseling. 1989. Early nodulin genes are induced in alfalfa root outgrowths elicited by auxin transport inhibitors. Proc. Natl. Acad. Sci. USA **86**:1244-1248.

Hofmann, K., and W. Stoffel. 1993. Tmbase- a data base of membrane spanning proteins segments. Biol. Chem. Hoppe-Seyler **347**:166.

Holt, J.G., N.R. Krieg, P.H.A. Sneath, J.T. Staley and S.T. Williams. 1994. Genus *Rhizobium*, p 95; 169. *In*, Bergey's manual of determinative bacteriology. Ninth Edition. Williams and Wilkins.

Horvath, B. R. Heidstr, M. Lados, M. Moerman, H.P. Spaink, J.-C. Promé, A. van Kammen, and T. Bisseling. 1993. Lipo-oligosaccharides of *Rhizobium* induce infection-related early nodulin gene expression in pea root hairs. Plant J. **4**:727-733.

Howieson, J.G., A.D. Robson, and M.A. Ewin. 1993. External Pi and calcium concentrations and pH but not the product of rhizobial nodulation genes affect the attachment of *Rhizobium meliloti* to roots of annual medics. Soil Biol. Biochem. **25**:567-573.

Hulett, F.M. 1995. The signal-transduction network for Pho regulation in *Bacillus subtilis*. Mol. Microbiol. **19**:933-939.

Hynes, M.F., R. Simon, P. Muller, K. Niehaus, M. Labes, and A. Puhler. 1986. The two megaplasmids of *Rhizobium meliloti* are involved in effective nodulation of alfalfa. Mol. Gen. Genet. **202**:356-362.

Israel, D.W. 1987. Investigation of the role of phosphorus in symbiotic dinitrogen fixation. Plant Physiol. **84**:835-840.

Israel, D.W. 1993. Symbiotic dinitrogen fixation and host plant growth during development of and recovery from phosphorus deficiency. Physiol. Plant. **88**:294-300.

Jakobsen, I. 1985. The role of phosphorus in nitrogen fixation by young pea plants (*Pisum sativum*). Physiol. Plant. **64**:190-196.

Jarvis, B.D.W., C.E. Pankhurst, and J.J. Patel. 1982. *Rhizobium loti*, a new species of legume root nodule bacteria. Int. J. Syst. Bacteriol. **32**:378-380.

Jiang, W., W.W. Metcalf, K.-S. Lee, and B.L. Wanner. 1995. Molecular cloning, mapping, and regulation of Pho regulon genes for phosphonate breakdown by the phosphonatase pathway of *Salmonella typhimurium* LT2. J. Bacteriol. **177**:6411-6421.

Johann, S.V., J.J. Gibbons, and B. O'Hara. 1992. Glvr-1, a receptor for gibbon ape leukemia virus, is homologous to a phosphate permease of *Neurospora crassa* and is expressed at high levels in the brain and thymus. J. Virol. **66**:1635-1640.

Jones, J.D.G., and N. Gutterson. 1987. An efficient mobilizable cosmid vector, pRK7813, and its use in a rapid method for marker exchange in *Pseudomonas fluorescens* strain HV37a. Gene **61**:299-306.

Jordan, D.C. 1984. Family III. *Rhizobiaceae* Conn 1938. 321^{AL}, p234-254. *In*, N.R. Krieg and J.G. Holt (ed.), Bergey's manual of systematic Bacteriology, vol. 1. Williams and Wilkins, Baltimore.

Jourmet, E.P., M. Pichon, A. Dedieu, F. de Billy, G. Truchet, and D.G. Barker. 1994. *Rhizobium meliloti* Nod factors elicit cell-specific transcription of the *ENOD12* gene in transgenic alfalfa. Plant J. **6**:241-249.

Kaback, H.R. 1990. Lac permease of *Escherichia coli*: on the path of the proton. Philosophical Transactions of the Royal Society of London- Series B: Biological Sciences. **326**:425-436.

Kato, J., A. Ito, T. Nikata, and H. Ohtake. 1992. Phosphate taxis in *Pseudomonas aeroginosa*. J. Bacteriol. **174**:5149-5151.

Kato, J., Y. Sakai, T. Nikata, and H. Ohtake. 1994. Cloning and characterization of a *Pseudomonas aeroginosa* gene involved in the negative regulation of phosphate taxis. J. Bacteriol. **176**:5874-5877.

Kato, J., T. Yamamoto, K. Yamada, and H. Ohtake. 1993. Cloning, sequence and characterization of the polyphosphate kinase-encoding gene (*ppk*) of *Klebsiella aerogenes*. Gene **137**:237-242.

Kavanaugh, M.P., and D. Kabat . 1996. Identification and characterization of a widely expressed phosphate transporter/retrovirus receptor family. Kidney International **49**:959-63.

Kijne, J.W. 1992. The *Rhizobium* infection process, p 349-398. *In*, G. Stacey, R.H. Burris, and H.J. Evans, eds. Biological Nitrogen Fixation. New York: Chapman and Hall.

Kim, S.-K., K. Makino, M. Amemura, H. Shinagawa, and A. Nakata. 1993. Molecular analysis of the *phoH* gene, belonging to the phosphate regulon in *Escherichia coli*. J. Bacteriol. **175**:1316-1324.

Kimura, S., K. Makino, H. Shinagawa, M. Amemura and A. Nakata. 1989. Regulation of the phosphate regulon of *Escherichia coli*: characterization of the promoter of the *pstS* gene. Mol. Gen. Genet. **215**:374-380.

Kogoma, T. 1997. Is RecF a DNA replication protein? Proc. Natl. Acad. Sci. USA. **94**:3483-3484.

Larson, T.J., S. Ye, D.L. Weissenborn, H.J. Hoffmann, and H. Schweizer. 1987. Purification and characterization of the repressor for the sn-glycerol 3-phosphate regulon of *Escherichia coli*. J. Biol. Chem. **262**:15869-15874.

Lee, J.W., and F.M. Hulett. 1992. Nucleotide sequence of the *phoP* gene encoding PhoP, the response regulator of the phosphate regulon of *Bacillus subtilis*. Nucleic Acids Res. **20**:58-48.

Lee, T.-Y, K. Makino, H. Shinagawa, M. Amemura, and A. Nakata. 1989. Phosphate regulon members of the family *Enterobacteriaceae*: comparison of the *phoB-phoR* operons of *Escherichia coli*, *Shigella dysenteriae*, and *Klebsiella pneumoniae*. J. Bacterio l. **171**:6593-6599.

Lee, K.-S., W.W. Metcalf, and B.L. Wanner. 1992. Evidence for two phosphonate degradative pathways in *Enterobacter aerogenes*. J. Bacteriol. **174**:2501-2510.

Lerouge, P., P. Roche, C. Faucher, F. Maillet, G. Truchet, J.C. Promé, and J. Dénarié. 1990. Symbiotic host-specificity of *Rhizobium meliloti* is determined by a sulfated and acylated glucosamine oligosaccharide signal. Nature **344**:781-784.

Leung, K., and P.J. Bottomley. 1987. Influence of phosphate on the growth and nodulation characteristics of *Rhizobium trifolii*. Appl. Environ. Microbiol. **53**:2098-2105.

Lin, E.C.C. 1976. Glycerol dissimilation and its regulation in bacteria. Ann. Rev. Microbiol. **30**:535-578.

Lin, E.C.C., and S. Iuchi. 1991. Regulation of gene expression in fermentation and respiratory systems in *Escherichia coli* and related bacteria. Annu. Rev. Genet. **25**:361-387.

Lindström, K. 1989. *Rhizobium galegae*, a new species of legume root nodule bacteria. Int. J. Syst. Bacteriol. **39**:365-367.

Liu, C.-M., P.A. McLean, C.C. Sookdeo, and F.C. Cannon. 1991. Degradation of the herbicide glyphosate by members of the family *Rhizobiaceae*. Appl. Environ. Microbiol. **57**:1799-1804.

Long, S. 1996. *Rhizobium* symbiosis: nod factors in perspective. Plant Cell **8**:1885-1898.

Long, S., S. McCurre, and G.C. Walker.1988. Symbiotic loci of *Rhizobium meliloti* identified by random Tm*phoA* mutagenesis. J. Bacteriol. **170**:4257-4265.

Makino, K., M. Amemura, T. Kawamoto, S. Kimura, H. Shinagawa, A. Nakata, and M. Suzuki. 1996. DNA binding of PhoB and its interaction with RNA polymerase. J. Mol. Biol. **259**:15-26.

Makino, K., M. Amemura, S.-K. Kim, A. Nakata, and H. Shinawaga. 1994. Mechanism of transcriptional activation of the phosphate regulon in *Escherichia coli*, pp. 5-12. *In* A. Torriani-Gorini, E. Yagil, and S. Silver (eds.), Phosphate in Microorganisms: Cellular and Molecular Biology. ASM Press, Washington, D.C.

Makino, K., M. Amemura, S.-K. Kim, A. Nakata, and H. Shinawaga. 1993. Role of the σ^{70} subunit of RNA polymerase in transcriptional activation by activator protein PhoB in *Escherichia coli*. Genes Dev. **7**:149-160.

Makino, K., M. Amemura, S.-K. Kim, H. Shinawaga, and A. Nakata. 1992. Signal transduction of the phosphate regulon in *Escherichia coli* mediated by phosphorylation, p. 191-200. *In* S. Papa, A. Azzi, and J.M. Tager (eds.), Adenine Nucleotides in Cellular Energy Transfer and Signal Transduction. Birkäuser Verlag, Basel.

Makino, K., H. Shinawaga, M. Amemura, T. Kawamoto, M. Yamassa, and A. Nakata. 1989. Signal transduction in the phosphate regulon of *Escherichia coli* involves phosphotransfer between PhoR and PhoB proteins. J. Mol. Biol. **210**:551-559.

Makino, K., H. Shinawaga, M. Amemura, and A. Nakata. 1986a. Nucleotide sequence of the *phoB* gene, the positive regulatory gene for phosphate regulation of *Escherichia coli* K-12. J. Mol. Biol. **190**:37-44.

Makino, K., H. Shinawaga, M. Amemura, and A. Nakata. 1986b. Nucleotide sequence of the *phoR* gene, a regulatory gene for the phosphate regulon of *Escherichia coli* K-12. J. Mol. Biol. **192**:549-556.

Maloney, P.C., S.V. Ambudkar, V. Anantharam, L.A. Sonna, and A. Varadhachary. 1990. Anion-exchange mechanisms in bacteria, Microbiol Rev. **54**:1-17.

Mann, B.J., B.J. Bowman, J. Grotelueschen, and R.L. Metzenberg. 1989. Nucleotide sequence of *pho-4*$^+$, encoding a phosphate-repressible phosphate permease of *Neurospora crassa*. Gene **83**:281-289.

Manoil, C. and J. Beckwith. 1985. Tn*phoA*, a transposon probe for protein export signals. Proc. Natl. Acad. Sci. USA **82**:8129-8133.

Martin, F., N.E. Tolbert. 1983. Factors which affect the amount of inorganic phosphate, phosphorylcholine, and phosphorylethanolamine in xylen exudate of tamato plants. Plant physiol. **73**:464-470.

McKay, I.A., and M.A. Djordjevic. 1993. Production and excretion of *nod* metabolites by *Rhizobium leguminosarum* bv. *trifolii* are disrupted by the same environmental factors that reduces nodulation in the field. Appl. Environ. Microbiol. **59**:3385-3392.

Meade, H., S. Long, G. Ruvkin, S. Brown, and F. Ausubel. 1982. Physical and genetic characterization of symbiotic and auxotrophic mutants of *Rhizobium meliloti*. J. Bacteriol. **149**:114-122.

Medveczky, N., and H. Rosenberg. 1971. Phosphate transport in *Escherichia coli*. Biochim. Biophys. Acta **241**:494-506.

Metcalf, W.W., and B.L. Wanner. 1993. Evidence of a fourteen-gene, *phnC* to *phnP*, locus for phosphonate metabolism in *Escherichia coli*. Gene **129**:27-32.

Mergaert, P., M. van Montagu, J.-C. Promé, and M. Holsters. 1993. Three unusual modifications, a D-arabinose, an *N*-methyl, and a carbomoyl group are present on Nod factors of *Azorhizobium caulinodans* strain ORS571. Proc. Natl. Acad. Sci. USA **90**:1551-1555.

Metcalf, W.W., and B.L. Wanner. 1991. Involvement of the *Escherichia coli phn* (*psiD*) gene cluster in assimilation of phosphorus in the form of phosphonates, phosphite, Pi esters, and Pi. J. Bacteriol. **173**:587-600.

Miller, D.G., R.H. Edwards, and A.D. Miller. 1994. Cloning of the cellular receptor for amphotropic murine retroviruses reveals homology to that of gibbon ape leukemia virus. Proc. Natl. Acad. Sci. U.S.A. **91**:78-82.

Minchin, F.R., J.E. Sheehy, and J.F. Witty. 1986. Further errors in the acetylene reduction assay: effect of plant disturbance. J. Exp. Bot. **37**:1581-1591.

Mosse, B., C.L. Powell, and D.S. Hayman. 1976. Plant growth responses to vesicular arbuscular mycorrhiza. IX. Interactions between VA mycorrhiza, rock phosphate, and symbiotic nitrogen fixation. New Phytol. **76**:331-342.

Muda, M., N.N. Rao, and A. Torriani. 1992. Role of PhoU in phosphate transport and alkaline phosphatase regulation. J. Bacteriol. **174**:8057-8064.

Mullen, M.D., D.W. Israel, and A.G. Wollum II. 1988. Effects of *Bradyrhizobium japonicum* and soybean (*Glycine max* (L.) Merr.) Phosphorus nutrition on nodulation and dinitrogen fixation. Appl. Environ. Microbiol. **54**:2387-2392.

Muto, A., and S. Osawa. 1987. The guanine and cytosine content of genomic DNA and bacterial evolution. Proc. Natl. Acad. Sci. USA **84**:166-169.

Nap, J.-P., and T. Bisseling. 1990. Developmental biology of a plant-prokaryote symbiosis: The legume root nodule. Science **250**:948-954.

Ndoye, I., F. de Billy, J. Vasse, B. Dreyfus, and G. Truchet. 1994. Root nodulation of *Sesbania rostrata*. J. Bacteriol. **176**:1060-1068.

Newcomb, W. 1981. Nodule morphologenesis and differentiation. Int. Rev. Cyt. Suppl. **13**:246-298.

Niehaus, K. D. Kapp, and A. Pühler. 1993. Plant defense and delayed infection of alfalfa pseudonodules induced by an exopolysaccharide (EPS I)-deficient *Rhizobium meliloti* mutant. Planta **190**:415-425.

Nikaido, H., and M.H.Jr. Saier. 1992. Transport proteins in bacteria: common themes in their design. Science **258**:936-942.

Nikata, T., Y. Sakai, K. Shibata, J. Kato, A. Kuroda and H. Ohtake. 1996. Molecular analysis of the phosphate-specific transport (*pst*) operon of *Pseudomonas aeroginosa*. Mol. Gen. Genet. **250**:692-698.

O'Brian, MR. 1996. Heme synthesis in the *Rhizobium*-legume symbiosis: a palette for bacterial and eukaryotic pigments. J. Bacteriol. **178**:2471-2478.

O'Gara, F., and K.T. Shanmugan. 1976. Regulation of nitrogen fixation by rhizobia. Export of fixed N_2 as NH_4^+. Biochim. Biophys. Acta **437**:313-321.

Oliver, D. 1985. Protein secretion in *Escherichia coli*. Annu. Rev. Microbiol. **39**:615-648.

Oresnik, I.J., T.C. Charles, and T.M. Finan. 1994. Second site mutation specifically suppress the Fix$^-$ phenotype of *Rhizobium meliloti ndvF* mutations on alfalfa: Identification of a conditional *ndvF*-dependent mucoid colony phenotype. Genetics **136**:1233-1343.

Overbeeke, N., H. Bergmans, F. Van Mansfeld, and B. Lugtenberg. 1983. Complete nucleotide sequence of *phoE*, the structural gene for the phosphate limitation inducible outer membrane pore protein of *Escherichia coli* K-12. J. Mol. Biol. **163**:513-532.

Parkinson, J.S. 1993. Signal transduction schemes in bacteria. Cell **73**:857-871.

Perotto, S., N. Donovan, B.K. Drøback, and N.J. Brewin. 1995. Differential expression of a glycosyl inositol phospholipid antigen an the peribacteroid membrane during pea nodule development. Mol. Plant-Microbe Interact. **8**:560-568.

Pongsakul, P., and E.S. Jensen. 1991. Dinitrogen fixation and soil N uptake by soybean as affected by phosphorus availability. J. Plant Nutr. **14**:809-823.

Poole, K., and R.E.W. Hancock. 1984. Phosphate transport in *Pseudomonas aeroginosa*: involvement of a periplasmic phosphate-binding protein. Eur. J. Biochem. **144**:607-612.

Poolman B., R.M.J. Nijssen, and W.N. Konings. 1987. Dependence of *Streptococcus lactis* phosphate transport on internal phosphate concentration and internal pH. J. Bacteriol. **169**:5373-5378.

Pribnow, D. 1975. Nucleotide sequence of an RNA polymerase binding site at an early T7 promoter. Proc. Natl. Acad. Sci. U.S.A. **72**:784-788.

Price, N.P.J., B. Relic, F Talmont, A Lewin, D. Promé, S.G. Pueppke, F. Maillet, J Dénarié, J.-C. Promé, and W.J. Broughton. 1992. Broad-host-range *Rhizobium* species strain NGR234 secretes a family of carbomylated, and fucosylated, nodulation signals that are *O*-acylated or sulfated. Mol Microbiol. **6**:3575-3584.

Quigley, F., P. Dao, A. Cottet, and R. Mache.1996. Sequence analysis of an 81kb contig from *Arabidopsis thaliana* chromosome III. Nucleic Acids Res. **24**:4313-4318.

Rao, N.N., M. F. Roberts, A. Torriani, and J. Yashphe. 1993. Effect of *glpT* and *glpD* mutations on expression of the *phoA* gene in *Escherichia coli.* J. Bacteriol. **175**:74-79.

Reyrat, J.M., M. David, C. Blonski, P. Boistard, and J. Batut. 1993. Oxygen-regulated *in vitro* transcription of *Rhizobium meliloti nifA* and *fixK* genes. J. Bacteriol. **175**:6867-6872.

Ribet, J., and J.-J. Drevon. 1995a. Increase in permeability to oxygen and in oxygen uptake of soybean nodules under limiting phosphorus nutrition. Physiol. Plant. **94**:198-304.

Ribet, J., and J.-J. Drevon. 1995b. Phosphorus deficiency increases the acetylene-induced decline in nitrogenase activity in soybean (Glycine max (L.) Merr.). J. Exp. Botany **46**:1479-1486.

Rizzo, M.F., L. Shapiro, and J.W. Gober. 1993. Asymmetric expression of the gyrase B gene from the replication-competent chromosome in the *Caulobacter crescentus* predivisional cell. J. Bacteriol. **175**:6970-6981.

Robson, A.D., G.W. O'Hara, and K. Abott. 1981. Involvement of phosphorus in nitrogen fixation by subterranean clover (*Trifolium subterraneum* L.). Aust. J. Plant Physiol. **8**:427-436.

Rolfe, B., and P.M. Gresshoff. 1988. Genetic analysis of legume nodule initiation. Annu. Rev. Plant Physiol. **39**:297-319.

Rolin, D.B., P.E. Pfeffer, R.T. Boswell, J.H. Schmidt, and S.I. Tu. 1989. In *vivo* ^{31}P NMR spectroscopic studies of soybean *Bradyrhizobium* symbiosis. FEBS lett. **254**:203-206.

Ronson, C.W.P., P. Lyttleton, and J.G. Robertson. 1981. C_4-dicarboxylate transport mutants of *Rhizobium trifolii* form ineffective nodules on *Trifolium repens*. Proc. Natl. Acad. USA **78**:4284-4288.

Rosenberg, C., P. Boistard, J. Dénarié, and F. Casse-Delbart. 1981. Genes controlling early and late functions in symbiosis are located on a megaplasmid in *Rhizobium meliloti*. Mol. Gen. Genet. **184**:326-333.

Rosenberg, C., F. Casse-Delbart, I. Dusha, M. David, and C. Boucher. 1982. Megaplasmids in the plant-associated bacteria *Rhizobium meliloti* and *Pseudomonas solanacearum*. J. Bacteriol. **150**:402-406.

Rosenberg, H. 1987. Phosphate transport in prokaryotes, p.205-248. *In* B.P. Rosen and S. Silver (ed.), Ion transport in prokaryotes. Academic Press, Inc., San Diego, Calif.

Rosenberg, H., R.G. Gerdes, and K. Chegwidden. 1977. Two systems for the uptake of phosphate in *Escherichia coli*. J. Bacteriol. **131**:505-511.

Rosenberg, H., N Medveczky, and J.M. La Nauze. 1969. Phosphate transport in *Bacillus cereus*. Biochim. Biophys. Acta **193**:159-167.

Rosenberg, H., L.M. Russell, P.A. Jacomb, and K. Chegwidden. 1982. Phosphate exchange in the pit transport system in Escherichia coli. J. Bacteriol. **149**:123-30.

Sa, T.M. and D.W. Israel. 1991. Energy status and functioning of phosphorus-deficient soybean nodules. Plant Physiol. **97**:928-935.

Sambrook, J., E.F. Fritsch, and T Maniatis. 1989. Molecular cloning. A laboratory manual. Second edition. Cold Spring Harhor Laboratory Press, New York.

Sanjuan, J., R.W. Carlson, H.P. Spaink, R. Bhat, W. Mark Barbour, J. Glushka, and J. Stacey. 1992. A 2-O- methylfucose moiety is present in the lipopolysaccharide nodulation signal of *Bradyrhizobium japonicum*. Proc. Natl. Acad. Sci. USA. **89**:8789-8793.

Schaller, H., C. Gray,and K. Herrmann. 1975. Nucleotide sequence of an RNA polymerase binding site from the DNA of bacteriophage fd. Proc. Natl. Acad. Sci. USA. **72**:737-741.

Scholla, M.H., and G.H. Elkan. 1984. *Rhizobium fredii* sp. nov., a fast-growing species that effectively nodulates soybeans. Int. J. Syst. Bacteriol. **34**:484-486.

Scholten, M., and J. Tommassen. 1993. Topology of the PhoR protein of *Escherichia coli* and functional analysis of internal deletion mutants. Mol. Microbiol. **8**:269-275.

Schubert, K.R. 1986. Products of biological nitrogen fixation in higher plants: Synthesis, transport, and metabolism. Annu. Rev. Plant Physiol. **37**:539-574.

Schultze, M., B. Quiclet-Sire, E. Kondorosi, H. Virelizier, J.N. Glushka, G. Endre, S.D. Géro, and A. Kondorosi. 1992. *Rhizobium meliloti* produces a family of sulfated lipo-oligosaccharides exhibiting different degrees of plant host specificity. Proc. Natl. Acad. Sci. USA **89**:192-196.

Schweizer, H., M. Argast, and W. Boos. 1982. Characteristics of a binding protein-dependent transport system for sn-glycerol 3-phosphate in *Escherichia coli* that is part of the Pho regulon. J. Bacteriol. **150**:1154-1163.

Seeburg, P.H., C. Nusslein, and H. Schaller. 1977. Interaction of RNA polymerase with promoters from bacteriophage fd. Eur. J. Biochem. **74**:107-113.

Seki, T., H. Yoshikawa, H. Takahashi, and H. Saito. 1988. Nucleotide sequence of the *Bacillus subtilis phoR* gene. J. Bacteriol. **170**:5935-5938.

Seki, T., H. Yoshikawa, H. Takahashi, and H. Saito. 1987. Cloning and nucleotide sequence of *phoP*, the regulatory gene for alkaline phosphatase and phosphodiesterase in *Bacillus subtilis*. J. Bacteriol. **169**:2913-2916.

Shaw, V.K., and W.J. Brill. 1977. Isolation of an iron-molybdenum cofactor from nitrogenase. Proc. Natl. Acad. Sci. USA. **74**:3249-3253.

Shortridge, V., A. Lazdunski, and M.L. Vasil. 1992. Osmoprotectants and phosphate regulate expression of phospholipase C in *Pseudomonas aeroginosa*. Mol. Microbiol. **6**:863-871.

Smart, J.B., M.J. Dilworth, and A.D. Robson. 1984a. Effect of phosphorus supply on phosphate uptake and alkaline phosphatase activity in rhizobia. Arch. Microbiol. **140**:281-286.

Smart, J.B., A.D. Robson, and M.J. Dilworth. 1984b. A continuous culture study of the phosphorus nutrition of *Rhizobium trifolii* WU95, *Rhizobium* NGR234 and *Bradyrhizobium* CB756. Arch. Microbiol. **140**:276-280.

Smit, G., T.A.N. van Brussel, and J.W. Kijne. 1992. Inactivation of a root factor by ineffective *Rhizobium*: A molecular key to autoregulation of nodulation in *Pisium sativum*, p 371. *In*, R. Palacios, J. Mora, and W.E. Newton, eds. New Horizons in Nitrogen Fixation. Dordrecht: Kluwer Academic Publishers.

Smith, M.W. and J.W. Payne. 1992. Expression of periplasmic binding proteins for peptide transport is subject to negative regulation by phosphate limiting condition in *Escherichia coli*. FEMS Microbiology letters. **79**:183-190.

Sofia, H.J., V. Burland, D.L. Daniels, G. Plunkett III, and F.R. Blattner. 1994. Analysis of the *Escherichia coli* genome. V. DNA sequence of the region from 76.0 to 81.5 minutes. Nucleic Acids Res. **22**:2576-2586.

Soupène, E., M. Foussard, P. Boitard, G. Truchet, and J. Batut. 1995. Oxygen as a key developmental regulator of *Rhizobium meliloti* N2-fixation gene expression within the alfalfa root nodule. Proc. Natl. Acad. Sci USA. **92**:3759-3763.

Spaink, H.P., R.J.H. Okker, C.A. Wijffelman, E. Pees, and B.J.J. Lugtenberg. 1987. Promoters in the nodulation region of the *Rhizobium leguminosarum* Sym plasmid pRL1J1. Plant Mol. Biol. **9**:27-39.

Spaink, H.P., D.M. Sheely, A.A.N. van Brussel, J. Glushka, W.S. York, T. Tak, O. Geiger, E.P. Kennedy, V.N. Reinhold, and B.J.J. Lugtenberg. 1991. A novel highly unsaturated fatty acid moiety of lipo-oligosaccharide signals determines host specificity of *Rhizobium*. Nature **354**:125-130.

Steed, P.M., and B.L. Wanner. 1993. Use of the *rep* technique for allele replacement to construct mutants with deletions of the *pstSCAB-phoU* operon: evidence of a new role for the PhoU protein in the phosphate regulon. J. Bacteriol. **175**:6797-6809.

Surin, B.P., H. Rosenberg, and G.B. Cox. 1985. Phosphate-specific transport system of *Escherichia coli*: nucleotide sequence and gene-polypeptide relationships. J. Bacteriol. **161**:189-198.

Takanami, M. K. Sugimoto, H. Sugisaki, and t. Okamoto. 1976. Sequence of promoter for coat protein of bacteriophage fd. Nature (London) **319**:121-126.

Takemaru, K.-I., M. Mizuno, and Y. Kobatashi. 1996. A *Bacillus subtilis* gene cluster similar to the *Escherichia coli* phosphate-specific transport (*pst*) operon: evidence for a tandemly arranged *pstB* gene. Microbiol. **142**:2017-2020.

Tao, H., N. Brewin, and K.D. Noel. 1992. *Rhizobium leguminosarum* CFN42 lipopolysaccharide antigenic changes induced by environmental conditions. J. Bacteriol. **174**:2222-2229.

Thiel, T. 1988. Phosphate transport and arsenate resistance in the cyanobacterium *Anabaena variabilis*. J. Bacteriol. **170**:1143-1147.

Thompson, J.D., D.G. Higgins, and T.J. Gibson. 1994. Clustal W: improving the sensitivity of progressive multiple sequence alignment trough sequence weighting, position-specific gap penalties and weight matrix choice. Nucleic Acids Res. **22**:4673-4680.

Trinick, M.J. 1988. Biology of the *Parasponia-Bradyrhizobium* symbiosis. Plant Soil **110**:177-185.

Truchet, G., P. Roche, P. Lerouge, J. Vasse, S. Camut, F. de Billy, J.C. Promé, and J. Dénarié. 1991. Sulphated lipo-oligosaccharide signals from *Rhizobium meliloti* elicit root nodule organogenesis in alfalfa. Nature **351**:670-673.

VanBogelen, R.A., E.R. Olson, B.L. Wanner, and F.C. Neidhardt. 1996. Global analysis of proteins synthesized during phosphorus restriction in *Escherichia coli*. J. Bacteriol. **178**:4344-4366.

van Heijne, G. 1986. The distribution of positively charged residues in bacterial inner membrane proteins correlates with the trans-membrane topology. EMBO J. **5**:3021-3027.

Van Kammen, A. 1984. Suggested nomenclature for plant genes involved in nodulation and symbiosis. Plant Mol. Biol. Rep. **2**:43-45.

Van Spronsen, P.C., R. Bakhuizen, A.A.N. van Brussel, and J.W. Kijne. 1994. Cell wall degradation during infection thread formation by the root nodule bacterium *Rhizobium leguminosarum* is a two-step process. Eur. J. Cell Biol. **64**:88-94.

Van Veen, H.W., T. Abee, G.J.J. Kortstee, W.N. Konings, and A.J.B. Zehnder. 1994a. Substrate specificity of the two phosphate transport systems of *Acinetobacter johnsonii* 210A in relation to phosphate speciation in its aquatic environment. J. Biol. Chem. **269**:16212-16216.

Van Veen, H.W., T. Abee, G.J.J. Kortstee, W.N. Konings, and A.J.B. Zehnder. 1994b. Translocation of metal phosphate via the phosphate inorganic transport system of *Escherichia coli*. Biochemistry **33**:1766-1770.

Van Veen, H.W., T. Abee, G.J.J. Kortstee, W.N. Konings, and A.J.B. Zehnder. 1993a. Characterization of two phosphate transport systems in *Acinetobacter johnsonii* 210A. J. Bacteriol. **175**:200-206.

Van Veen, H.W., T. Abee, G.J.J. Kortstee, W.N. Konings, and A.J.B. Zehnder. 1993b. Mechanism and energetics of the secondary phosphate transport system of *Acinetobacter johnsonii* 210A. J. Biol. Chem. **268**:19377-19383.

van Zeijl, M., S.V. Johann, E. Closs, J. Cunningham, R. Eddy, T.B. Shows, and B. O'Hara. 1994. A human amphotropic retrovirus receptor is a second member of gibbon ape leukemia virus receptor family. Proc. Natl. Acad. Sci. U.S.A. **91**:1168-1172.

Vasse, J., F. de Billy, S Camut, and G. Truchet. 1990. Correlation between ultrastructural differentiation of bacteroids and nitrogen fixation in alfalfa nodules. J. Bacteriol. **172**:4296-4306.

Verma, D.P.S. 1992. Signals in root nodule organogenesis and endocytosis of *Rhizobium*. Plant Cell **4**:373-382.

Verma, D.P., and Z. Hong. 1996. Biogenesis of the peribacteroid membrane in root nodules. Trends Microbiol. **4**:364-368.

Versaw, W.K., and R.L. Metzenberg. 1995. Repressible cation-phosphate symporters in *Neurospora crassa*. Proc. Nalt. Acad. Sci. USA. **92**:3884-3887.

Vieira, J. and J. Messing. 1987. Production of single-stranded plasmid DNA. Methods Enzymol. **153**:3-34.

von Heijne, G. 1986. The distribution of positively charged residues in bacterial inner membrane proteins correlates with the trans-membrane topology. EMBO J. **5**:3021-3027.

Wackett, L.P., B.L. Wanner, C.P. Venditti and C.T. Walsh. 1987. Involvement of the phosphate regulon and the *psiD* locus in the cabon-phosphorus lyase activity of *Escherichia coli* K-12. J. Bacteriol. **169**:710-717.

Wada, K.-N., Y. Wada, F. Ishibashi, T. Gojobori, and T. Ikemura. 1992. Codon usage tabulated from the GenBank genetic sequence data. Nucleic Acids Res. **20**:2111-2118.

Wanner, B.L. 1996. Phosphorus assimilation and control of the phosphate regulon, p 1357-1381. *In* Neidhardt ed., Second Edition. *Escherichia coli* and *Salmonella*: Cellular and Molecular Biology. ASM Press.

Wanner, B.L. 1993. Gene regulation by phosphate in enteric bacteria. J. Cell. Biochem. **51**: 47-54.

Wanner, B.L. 1992. Minireview. Is cross regulation by phosphorylation of two-component response regulator proteins important in bacteria? J. Bacteriol. **174**:2053-2058.

Wanner, B.L. 1983. Overlapping and separate controls on the phosphate regulon in *Escherichia coli* K-12. J. Mol. Biol. **166**:283-308.

Wanner, B.L., and J.A. Boline. 1990. Mapping and molecular cloning of the *phn* (*psiD*) locus for phosphonate utilization in *Escherichia coli*. J. Bacteriol. **172**:1186-1196.

Wanner, B.L., and M. R. Wilmes-Riesenberg. 1992. Involvement of phosphotransacetylase, acetate kinase, and acetyl phosphate synthesis in the control of the phosphate regulon in *Escherichia coli*. J. Bacteriol. **174**:2124-2130.

Wanner, B.L., M.R. Wilmes, and D.C. Young. 1988. Control of bacterial alkaline phosphatase synthesis and variation in an *Escherichia coli* K-12 *phoR* mutant by adenyl cyclase, the cyclic AMP receptor protein, and the *phoM* operon. J. Bacteriol. **170**:1092-1102.

Watson, R.J., Y.-K. Chan, R. Wheatcroft, A.-F. Yang, and S. Han. 1988. *Rhizobium meliloti* genes required for C4-dicarboxylate transport and symbiotic nitrogen fixation are located on a megaplasmid. J. Bacteriol. **170**:927-934.

Webb, D.C., and G.B. Cox. 1994. Proposed mechanism for phosphate translocation by the phosphate-specific transport (Pst) system and role of the Pst system in phosphate regulation, p.37-42. *In* A. Torriani-Gorini, E. Yagil, and S. Silver (eds.), Phosphate in Microorganisms: Cellular and Molecular Biology. ASM Press, Washington, D.C.

Werner, D. 1992. Physiology of nitrogen-fixing legume nodules: Compartments and functions, p 399-431. *In*, G. Stacey, R.H. Burris, and H.J. Evans, eds. Biological Nitrogen Fixation. New York: Chapman and Hall.

Weston, L.A., and R.J. Kadner. 1988. Role of *uhp* genes in expression of the *Escherichia coli* sugar-phosphate transport system. J. Bacteriol. **170**:3375-3383.

Willsky, G.R., and M.H. Malamy. 1980a. Characterization of two genetically separable inorganic phosphate transport system in *Escherichia coli*. J. Bacteriol. **144**:356-365.

Willsky, G.R., and M.H. Malamy. 1980b. Effect of arsenate on inorganic phosphate transport in *Escherichia coli*. J. Bacteriol. **144**:366-374.

Wilson, C.A., K.B. Fanell, and M.V. Eiden. 1994. Proprieties of a unique form of the murine amphotropic leukemia virus receptor expressed on hamster cells. J. Virol. **68**:7697-7703.

Witty, J.F., F.R. Minchin, L. Skøt, and J.E. Sheely. 1986. Nitrogen fixation and oxygen in legume root nodules. Oxford Surv. Plant Cell Biol. **3**:275-315.

Wu, T.T. 1966. A model for 3 points analysis of random general transduction. Genetics **54**:405-410.

Xavier, K.B., M. Kossmann, H. Santos, and W. Boos. 1995. Kinetic analysis by *in vivo* ^{31}P Nuclear Magnetic Resonance of internal Pi during uptake of sn-glycerol-3-phosphate by the Pho regulon-dependent Ugp system and the *glp* regulon-dependent GlpT system. J. Bacteriol. **177**:699-704.

Yanisch-Perron, C., J. Vieira and J. Messing. 1985. Improved M13 phage cloning vectors and host strains: nucleotide sequences of the M13mp18 and pUC19 vectors. Gene **33**:103-119.

Yarosh, O.K., T.C. Charles, and T.M. Finan. 1989. Analysis of C_4-dicarboxylic acid transport genes in *Rhizobium meliloti*. Mol. Microbiol. **3**:813-823.

Yashphe, J., H. Chikarmane, M. Iranzo, and H.O. Halvorson. 1992. Curr. Microbiol. **24**:275-280.

Young, J.P.W. 1992. Phylogenetic classification of nitrogen-fixing organisms, p 43-86. *In* G. Stacey, R.H. Burris and H.J Evans; Biological nitrogen fixation. Chapman and Hall.

Zhan, H., C.C. Lee and J.A. Leigh. 1991. Induction of the second exopolysaccharide (EPSb) in *Rhizobium meliloti* SU47 by low phosphate concentrations. J. Bacteriol. **173**:7391-7394.

Zhan, H., S.B. Levery, C.C. Lee and J.A. Leigh. 1989. A second exopolysaccharide of *Rhizobium meliloti* strain SU47 that can function in root nodule invasion. Proc. Natl. Acad. Sci. USA **86**:3055-3059.

IMAGE EVALUATION TEST TARGET (QA-3)

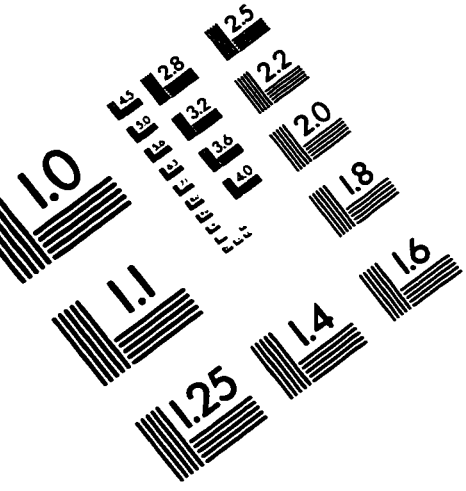

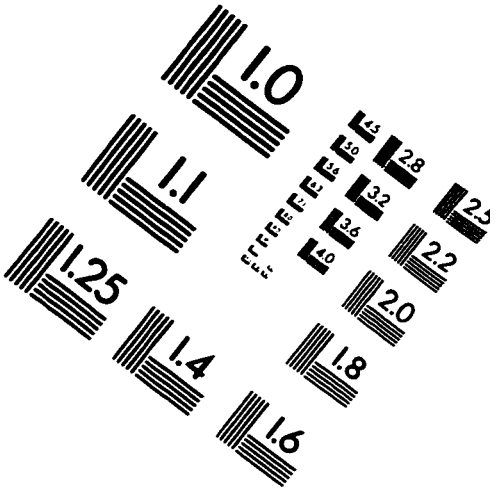

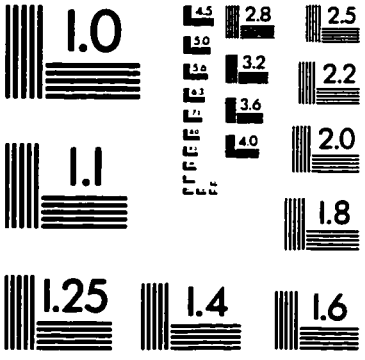

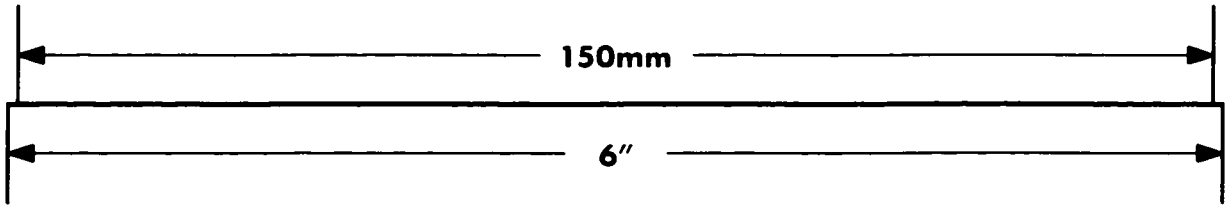

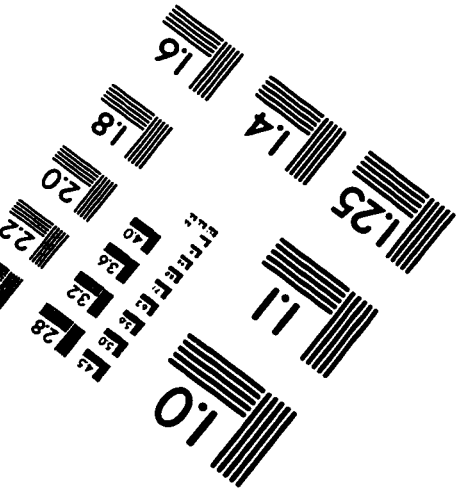

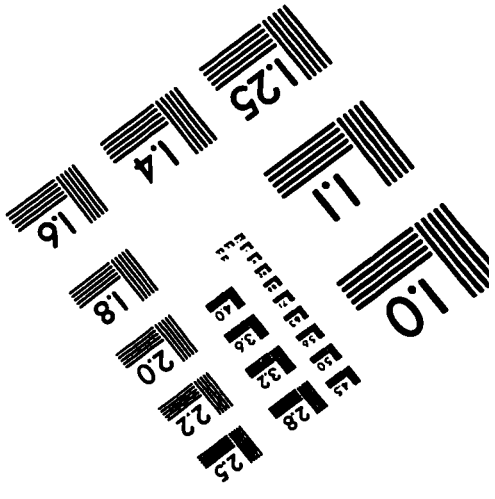

APPLIED IMAGE, Inc
1653 East Main Street
Rochester, NY 14609 USA
Phone: 716/482-0300
Fax: 716/288-5989